Interactions of Endogenous and Exogenous Molecules with the Human Blood–Brain Barrier

Watson, Christopher

Awarding institution:
King's College London

Interactions of Endogenous and Exogenous Molecules with the Human Blood–Brain Barrier

Christopher P. Watson

KING'S College LONDON

A thesis submitted to King's College London for the degree of

Doctor of Philosophy

2012

Abstract

The BBB is a biological firewall that carefully regulates the cerebral microenvironment by acting as a physical, metabolic and transport barrier to molecules bound for the brain. This selectively permeable interface was modelled in this thesis using the recently established immortalised human cerebral microvascular endothelial cell line (hCMEC/D3) to investigate interactions with endogenously and exogenously derived molecules of clinical significance.

The endogenous molecules in question are the cationic amino acids (CAA) L-arginine, the precursor for nitric oxide (NO), and asymmetric dimethylarginine (ADMA), an endogenously derived analogue of L-arginine that acts as a potent inhibitor of NO production. As well as being an important vasodilator, NO has regulatory roles in the brain and on the BBB itself. Transport mechanisms utilised by L-arginine are known, but are not fully understood for ADMA – particularly so at the BBB. This is of clinical significance giving the emerging role of ADMA in many brain and cerebrovascular diseases. Understanding these transport mechanisms and other interactions of ADMA with the BBB is therefore very important for the study of disease emergence, detection and progression. We discovered in the hCMEC/D3s that high concentrations of ADMA could induce endothelial dysfunction in a BBB permeability model, leading to an increase in paracellular permeability to the paracellular marker FITC-dextran (40kDa). We also illustrated interactions of ADMA with a variety transport proteins, basing the study design on our observed L-arginine interactions. The CAA transport system y^+ was heavily implicated for both molecules through the use of established inhibitors. Furthermore, the expression of CAT-1, the best known protein from this group was confirmed in the hCMEC/D3s. We also found evidence of an efflux transport system for ADMA (but not L-arginine), implicating the neutral and CAA transporter $ATB^{0,+}$. The protein expression of $ATB^{0,+}$ was also confirmed in the cells. Intracellular ADMA was even shown to induce *trans*-stimulation of extracellular L-arginine, providing evidence for a role of ADMA in the 'L-arginine paradox', a phenomenon observed *in vivo* that administered L-arginine can alleviate the effects of NO reduction (such as vasoconstriction), despite there being 20-30 times the amount of L-arginine present to saturate the NO producing enzyme.

In summary, our endogenous molecule findings from this thesis identify the likely transport mechanisms used by ADMA and implicate ADMA in endothelial dysfunction as well as the 'L-arginine paradox'. These data are not only important with regards to the brain, but apply to

other microvascular endothelia such as those found in peripheral cardiovascular system, where ADMA remains a major area of investigation.

The exogenous molecules studied during this PhD are drugs currently used to treat the second-stage of human African Trypanosomiasis (HAT). HAT is a neglected parasitic disease that continues to persist in sub-Saharan Africa. It is fatal if untreated. Recently, it has been described that eflornithine and nifurtimox combination therapy (NECT), improves the efficacy of both drugs compared to their monotherapy, although why this happens remains unclear. We hypothesised that it may be due to improved CNS delivery, although we failed to show improvements in accumulation of either eflornithine or nifurtimox with NECT or when the individual drugs were in combinations with the other anti-HAT drugs. Interestingly, the combination of eflornithine and pentamidine caused a decrease in eflornithine accumulation, implicating an unidentified pentamidine-sensitive transport system – possibly an adenosine-sensitive influx transporter. The cellular influx transport mechanisms used by eflornithine has been suggested to be those used by CAA due to the structural similarity of eflornithine with the CAA ornithine and so this was studied. We revealed in the hCMEC/D3s that eflornithine had degrees of sensitivity to a variety of transport mechanisms, in which system y^+ appears to be the principal influx mechanism. Similar anti-HAT drug combination therapy studies with nifurtimox were performed and also illustrated a significant interaction with pentamidine; although conversely to eflornithine we demonstrated an increase in nifurtimox accumulation as a result of nifurtimox-pentamidine combination. Previous *in situ* observations by our group suggested nifurtimox was a substrate for efflux transport systems at the BBB that are separate from P-gp and this too was investigated, identifying the well known drug efflux pump BCRP as the principal nifurtimox efflux transporter.

With regards to exogenous molecules, we provide evidence of CAA influx mechanisms for the anti-HAT drug eflornithine and an efflux system for nifurtimox, principally involving BCRP. We also found that NECT and combination therapy of eflornithine or nifurtimox with the other anti-HAT drugs did not improve eflornithine or nifurtimox accumulation when compared to controls – except when pentamidine was combined with nifurtimox. This finding suggests that nifurtimox-pentamidine combination may improve efficacy of nifurtimox in the field.

Collectively, these data further demonstrate of the suitability of the hCMEC/D3 cell line as a powerful tool for human *in vitro* BBB investigation across a range of study areas.

Table of Contents

Table of Figures

Table of Tables

List of Abbreviations

2-DG – 2-deoxy-D-glucose

AAs – amino acids

AD – Alzheimer's disease

ADMA – N^G,N^G-dimethylarginine or asymmetric dimethylarginine

ADP – adenosine diphosphate

AMT – adsorptive-mediated transcytosis

ATP – adenosine triphosphate

BAT – broad-scope amino acid transporter

BBB – blood-brain barrier

BCA – bicinchoninic acid

BCSFB – blood-cerebrospinal fluid barrier

BCRP – breast cancer resistance protein

BECs – brain endothelial cells

bFGF – basic fibroblast growth factor

BMECs – brain microvascular endothelial cells

BRB – blood-retinal barrier

BSA - bovine serum albumin

CAA – cationic amino acids

CAT – cationic amino acid transporter

CATT – card agglutination test for trypanosomiasis

CDE – clathrin-dependent endocytosis

cGMP – 3',5'-cyclic guanosine monophosphate

CIE – clathrin-independent endocytosis

CNS – central nervous system

CSF – cerebrospinal fluid

CT – combination therapy

DDAH – N^G,N^G – (or asymmetric) dimethylarginine dimethylaminohydrolase

DDI – drug-drug interactions

DMSO – dimethyl sulfoxide

DPBS+ – Dulbecco's phosphate buffered saline with calcium and magnesium

DPBS- – Dulbecco's phosphate buffered saline without calcium and magnesium

DNDi – Drugs for Neglected Diseases initiative

DMEM – Dulbecco's modified Eagle's medium

eNOS – endothelial nitric oxide synthase

FITC – Dex - fluorescein isothiocyanate labelled dextran

GJs – gap junctions

GTPases - guanosine triphosphatases

GTP – guanosine triphosphate

HAT – human African trypanosomiasis

HD – Huntington's disease

hCMEC/D3 – human cerebral microvascular endothelial cells D3

HRP – horseradish peroxidise

HUVEC – human umbilical vein endothelial cells

IF – immunofluorescence

iNOS – inducible/immune nitric oxide synthase

IFN-γ – interferon gamma

LAT1 – large neutral amino acid transporter 1

LDL – low-density lipoprotein

L-NAME – N^G-nitro-L-arginine methyl ester

L-NIO – N-iminoethyl-L-ornithine

L-NMMA – N^G-monomethyl-L-arginine

MARCD – microangiopathy-related cerebral damage

MECT – melarsoprol eflornithine combination therapy

MDR – multidrug resistance

MRP – multidrug resistance-associated protein

mRNA – messenger ribonucleic acid

Na^+ – sodium ion

NAA – neutral amino acids

NECT – nifurtimox eflornithine combination therapy

NMDA – N-methyl-D-aspartate

NMCT – nifurtimox melarsoprol combination therapy

nNOS – neuronal nitric oxide synthase

NO – nitric oxide

NVU – neurovascular unit

PBS – phosphate buffered saline

PBS-T – phosphate buffered saline TWEEN

PD – Parkinson's disease

P-gp – p-glycoprotein

PKG – protein kinase G

PNGase F – N-linked-glycopeptide-(N-acetyl-beta-D-glucosaminyl)-L-asparagine amidohydrolase

P_i – inorganic phosphate

PVDF – polyvinylidene fluoride

RMT – receptor mediated transcytosis

RT – room temperature

S1 – stage 1 of human African trypanosomiasis

S2 – stage 2 of human African trypanosomiasis

SDS-PAGE – sodium dodecyl sulphate polyacrylamide gel electrophoresis

siRNA – small interfering ribonucleic acid

T. b. gambiense – *Trypanosoma brucei gambiense*

T. b. rhodesiense – *Trypanosoma brucei rhodesiense*

TEER – transendothelial electrical resistance

TNF-α – tumour necrosis factor alpha

VEGF – vascular endothelial growth factor

WB – western blot

wt – wild-type

Acknowledgements

Firstly, I wish to thank my primary supervisor Dr. Sarah A. Thomas for her continued supervision, advice and guidance throughout my PhD. Without her it would not have been possible and I will miss her company. I also wish to thank fellow PhD student Mehmet Fidanboylu and lab technician Murat Dogruel for their help, support and friendship during this journey. I will also miss their company!

Next I wish to thank my father Peter, mother Carolyn and brothers Tom and Rich for their support and belief. A special mention goes to my parents for putting up with me while I wrote the thesis!

I would like to say a special thank you to my beautiful girlfriend Rebecca Goldberg for her love, friendship and support during the ups and downs of my PhD.

I also acknowledge my good friends and former flatmates Evangelos Pazarentzos and Enrico Cristante for their help, advice and support with tricky aspects of my PhD including molecular biology and the permeability assays.

The help I received from the rest of the BBB group at King's College London will not be forgotten and I wish to also thank them. This is especially true for Dr. Larisa Mihoreanu for her help at the beginning of my PhD; Ana Georgian for her help and advice; Dr. Siti Yusof for her support and advice with the permeability assays; Dr. Svetlana Drndarski and Dr. Diana Dolman for her general help and guidance; Dr Charlie Pontikis for his help at the beginning of my PhD; Professor N. Joan Abbott for her wisdom and experience; Dr. David Begley for his support as my second supervisor; Dr. Rachel Brown for her help with the molecular biology, and Dr. Jane Preston for her kindness in letting me use her equipment and for her general advice.

I also would like to thank Dr. Dom Spina for his help and support as my postgraduate coordinator and for being on the interview panel that gave me the opportunity to do a PhD at KCL. I also thank Professor Giovanni Mann for his knowledge of *trans*-stimulation and for reading my transfer report and Professor Robert Hider for his help and opportunity he gave to collaborate. Ralph Wilson and John Chesson get a special mention for their help with equipment during my time at Guy's campus. I also thank Dr. Maria de Castro Vasconcelos Goncalves for her help and support with the confocal microscopy in the Wolfson CARD.

Dr. Ignacio Romero and Miguel Alejandro Lopez-Ramirez get a special mention for their help, expertise and advice with the hCMEC/D3 cell line, particularly for teaching me the permeability assay.

I also wish to thank my good friends Dara Mohammadi, Myrsini Tsimon, Jackie Lighten, Alex Papadopoulos, Dr. Paul Tisdale, Daniel Watson, Jennifer Adlington, James Peacock, Matthew Harwood, Wale Oyeleye, Tom Cwik, Will Goodliffe, George Hare, Rong Yang and anyone else I have forgotten to write here that have helped me through my PhD with their friendship and advice!

'It seems to me that the natural world is the greatest source of excitement; the greatest source of visual beauty; the greatest source of intellectual interest. It is the greatest source of so much in life that makes life worth living.'

- Sir David Attenborough

Chapter 1. Introduction

1.1. The need for brain barriers

As the central component to the nervous system in vertebrates and most invertebrates, the brain is the most complex organ in the body. It processes a huge array of information and controls activities all over the body, and as such is very metabolically active. Due to the brains limited ability to store energy a constant supply is essential, most of which comes in the form of glucose which is converted to adenosine-triphosphate (ATP) to maintain neuronal function (Liu et al., 2009). Despite being only 2% of the body mass, the human brain metabolises about 50% of total body glucose and receives 15% of cardiac output under basal conditions (Fehm et al., 2006).

On top of needing a high amount of energy, the brain also requires a carefully controlled microenvironment for proper functioning of sensitive neuronal and brain processes. This homeostasis can only be achieved by separating the central nervous system (CNS) from the milieu of the periphery and carefully regulating the molecular traffic between the two interfaces. Furthermore, the CNS and peripheral separation interfaces must also be effective enough to block the entry of pathological agents and microorganisms in to the brain. Thus a variety of selectively permeable barriers have evolved at different areas of the CNS-blood interfaces. These barriers are the blood-cerebrospinal fluid barrier (BCSFB), blood-retinal barrier (BRB), blood-nerve barrier, blood-labyrinth barrier and the focus of this thesis, the blood-brain barrier (BBB) (please see (Neuwelt et al., 2011) for further descriptions of these barriers).

The resultant separation of the CNS from the periphery is done to the extent that the brain is virtually isolated from the peripheral immune system under normal healthy conditions. This immune-privileged status held by the brain is not entirely accurate however as we now know a small number of peripheral surveillance immune cells are able to scan just inside the CNS, interacting with the highly sensitive microglial cells which constantly scan the CNS for potential infectious agents. The interactions between immune cells and pathological agents are extremely rapid in the CNS to reduce the potential damage both an infection and immune reaction could have on the highly sensitive brain tissue (see (Engelhardt and Coisne, 2011) for a recent review).

1.2. Cirumventricular organs

The BCSFB, formed by epithelial cells between the choroid plexus (CP) blood vessels and cerebrospinal fluid and the second largest CNS-blood interface barrier, plays important roles in regulating the brains molecular traffic, such as ascorbic acid transport (Spector, 2009). The CP belongs to specialized brain regions collectively called the cirumventricular organs (CVOs). The CVOs form an interacting network of organs which have leaky barriers allowing neurons to detect substances such as peptide hormones across the tissue and blood, but are separated from the rest of the brain by the BCSFB and the BBB (Abbott et al., 2006). The other CVOS fall into two categories – sensitive organs or secretory organs – depending on their functions. The sensitive organs are the vascular organ of the lamina terminalis, the subfornical organ, and the area postrema and are involved in fluid regulation and peptide detection, with the latter involved in vomit control following detection of noxious substances (Duvernoy and Risold, 2007). The secretory organs are the neurohypophysis, which secrete hormones made in the hypothalamus, and the pineal gland which produces hormones such as melatonin (Ganong, 2000). The reader is directed to (Siso et al., 2010) for an overview of the CVOs, which are not the focus of this thesis. Please also see (Redzic, 2011) for a recent detailed overview of the BCFSB.

1.3. Historical observations

The existence of a BBB was first empirically observed by the German Nobel laureate Paul Ehrlich in the late 1890s. He designed a series of experiments to compare the oxygen consumptions of various organs by using intravital dyes, the colours of which change with their redox state. He noted that some of the dyes following injection into peripheral veins, arteries or subcutaneously, poorly stained the brain and CNS tissues despite heavily staining other organs. Ehrlich and others incorrectly concluded from these early observations that the dyes had organ-specific affinities (Banks, 2008).

Further experimental work by Ehrlich's student, Edwin Goldman, and Max Lewandowski shed light on this phenomenon. They injected brains directly with dyes and observed that the brain was stained heavily, but the peripheral tissues were unstained. As a result they came up with a new theory that the brain must hold back certain molecules and coined the term 'Bluthirnschranke' ('blood-brain barrier' in German), but the location of actual barrier eluded these early BBB pioneers. The crude light microscopy techniques of the time failed to show any

difference between brain and peripheral vasculatures. As a result, the concept of the BBB didn't gain widespread acceptance until scanning electron microscopes and systemic injection of horseradish peroxidise were used to visualize the BBB in the 1960s (Bechmann et al., 2007). These techniques started to reveal a complex arrangement of different cell types around the BBB and that a complex network of tight junctions (TJs) also existed between the cells. It is a combination of these features that give the brain vasculature their greater physical barrier properties over their peripheral equivalents.

Thus it became clear that the BBB proper is localised at the cerebral capillary endothelium and acts as a biological firewall, carefully regulating the flow of molecular traffic whilst simultaneously blocking microbial entry to the brain.

1.4. Components of the blood-brain barrier

The features of the barrier exist due to a group of interacting cellular components that are not only crucial for the development of the structure, but also crucial for its continued activity.

1.4.1. The Neurovascular unit

A single layer of brain microvascular endothelial cells (BMECs) of the BBB, together with the surrounding basal lamina, neighbouring pericytes, and the endfeet of glial cells called astrocytes (which cover >98% of the BBB vascular wall) are the integral components of a structure called the neurovascular unit (NVU, see figure 1.1 a) (Abbott et al., 2006, Neuwelt et al., 2011). The NVU encompasses all components of the BBB, maintaining structural integrity and allowing a link between neuronal activity and the oxygen and nutrient supply from the blood. It also helps to regulate BBB permeability through modulation of cellular substrate specific membrane transporters, transcytotic vesicles, and BMEC paracellular permeability (Neuwelt et al., 2011).

The NVU even regulates the blood flow to the BBB by interacting with surrounding smooth muscle cells upstream of the BBB (Saunders et al., 2008). Endothelial vasoactive substances such as nitric oxide (NO) (discussed later in section 1.9) are released from brain endothelial cells (BECs) by agonists that activate specific receptors on the cell surface, or by changes in shear stress produced by alternations in the rate of blood flow. Gap junctions (GJs) between adjacent BECs, connect the cytoplasm of cells together and so permit intracellular responses to be transmitted between BECs, invoking a large chemo-responses which are converted by smooth muscle cells and pericytes into changes in vascular diameter (Iadecola, 2004). These

signals constrict or relax smooth muscle cells by inducing changes in concentrations of intracellular Ca^{2+} and altering the phosphorylation state of light chain myosin. These processes result in regulation of blood flow to the brain microvasculature, crucial to homeostasis of the cerebral microenvironment (Iadecola, 2004, Hawkins and Davis, 2005, Abbott et al., 2006). Please see (Attwell et al., 2010) for a recent detailed review of the control components of the NVU have on brain blood flow.

Studies are revealing the true dynamic role the NVU plays in using its specialised cell groups and complex signalling processes to both serve and protect the brains interests. See (Abbott et al., 2006, Neuwelt et al., 2011) for in-depth reviews of the NVU.

1.4.2. BBB endothelium

Compared to peripheral capillary endothelium, BMECs have reduced non-specific endocytosis and transcytosis to hydrophobic molecules, meaning they can almost only cross the BBB via the selective transport proteins or by specialised receptor mediated transcytosis events (figure 1.1 b) (Abbott et al., 2006, Abbott et al., 2010). BMECs of the BBB also have more ATP-producing mitochondria than peripheral endothelium to power the energy dependent transport mechanisms (e.g. ABC-transporters) that are abundant at the BBB (Oldendorf and Brown, 1975, Oldendorf et al., 1976).

As well as these features, BMECs have the most complex cell-cell junction components of all the endothelium in the body that almost completely block the paracellular flow of molecules, sealing the cells together; essentially forming a continuous single-cell-wide membrane. These junctional components are discussed in section 1.6.

1.4.3. Astrocytes

Astrocytes are glial cells and one of the most numerous cell classes in the CNS. They have a wide variety of roles in the brain including maintenance of ion homeostasis of the extracellular space, neurotransmitter uptake and processing, and pH regulation (Sofroniew and Vinters, 2010). In the context of the BBB, astrocytes interact with BMECs and pericytes to form the tube-like structures of capillaries *in vitro* and are believed to play key roles in gliovascular signalling by inducing perivascular release of vasoactive agents (Ramsauer et al., 2002). Due to their physical association with the BBB endothelium, astrocyte end-feet have long been associated with proper BBB functioning (Davson and Oldendorf, 1967, Abbott, 2002, Abbott et al., 2006). There is much evidence from *in vitro* studies that astrocytes upregulate BBB features

such as TJs, drug metabolising enzyme expression and transport protein polarisation (Dehouck et al., 1990, Haseloff et al., 2005).

Despite the importance of astrocytes in maintaining the BBB, the precise mechanisms by which this is achieved remain poorly understood. The temporal correlation between astrocyte differentiation and maturation of the BBB during early development also suggests functional roles for astrocytes in the early establishment as well as regulation of the BBB, and it is believed that Wnt signalling pathways are involved (Liebner et al., 2011).

1.4.4. Pericytes

The role of pericytes in the maintenance and induction of the BBB has, until recently, been poorly understood. Pericytes are contractile cells that abluminally surround endothelial cells, sharing the extracellular matrix layer known as the basal lamina. They are found in high amounts at the BRB and the BBB (Frank et al., 1987, Shepro and Morel, 1993) and were originally believed to only support the vascular endothelium, helping to regulate local blood flow (Balabanov and Dore-Duffy, 1998). This belief was supported by the discovery that pericytes contain receptors for a variety of vasoactive mediators such as angiotensin II (Healy and Wilk, 1993) and vasopressin (van Zwieten et al., 1988).

However, by using viable pericyte-deficient murine models it was discovered that pericytes actually help regulate BBB permeability through modulation of transcytosis, which resulted in permeability of the BBB to normally impenetrable immunoglobulins (Armulik et al., 2010). It has also recently emerged that pericytes have integral roles in maintaining astrocyte end-feet polarisation around the cerebral microvasculature and also regulating BBB-specific gene expression (Armulik et al., 2011).

As with astrocytes, pericytes have also been implicated in BBB development during embryogenesis. Data analysing genetically modified mice deficient for pericyte formation (mice with null and hypomorphic alleles of *Pdgfrb*) revealed that pericyte distribution during BBB development directly determined BBB permeability *in vivo* (Daneman et al., 2010). In their paper, Daneman et al., also demonstrated that pericytes regulated BBB specific features such as complex TJ formation *in vitro*, increasing the transendothelial electrical resistance (TEER – a measurement of ionic paracellular flow) 4-fold in co-culture with BMECs when compared to BMEC culture alone. The authors also discovered that astrocytes do not extend processes to contact the early BBB until the first postnatal week, meaning that if astrocytes were

responsible for BBB formation, these would not be acquired until after birth. Their findings provided compelling evidence that pericytes in fact are more crucial than astrocytes during BBB development by strengthening the TJs, reducing transcytosis and inhibiting leukocyte adhesion molecule expression in endothelial cells, to help them maintain a BBB phenotype into adulthood, where astrocytes then play roles in maintaining and regulating BBB function (Daneman et al., 2010).

1.5. Functions of the blood-brain barrier

With a surface area of 12 to 18 m^2 per average adult human brain, the largest CNS-blood interface by far is the BBB and therefore it plays the predominant role in regulating the cerebral microenvironment (Abbott et al., 2010).

The BBB supplies the brain with nutrients whilst allowing efflux of brain waste into the blood. It also protects the brain from ionic composition fluctuations that occur after metabolic events or exercise which could disturb synaptic and axonal signalling events in the brain (Abbott et al., 2006). The BBB separates peripheral and CNS pools of neurotransmitters and other neuroactive molecules, stopping interference between the two systems (Bernacki et al., 2008, Abbott et al., 2010).

The collective influence of the NVU has not only allowed the BBB to evolve a highly specialised phenotype, but it continues to regulate and maintain the BBB's crucial physical, metabolic and transport barrier functions (see figure 1.1 b for overview schematic).

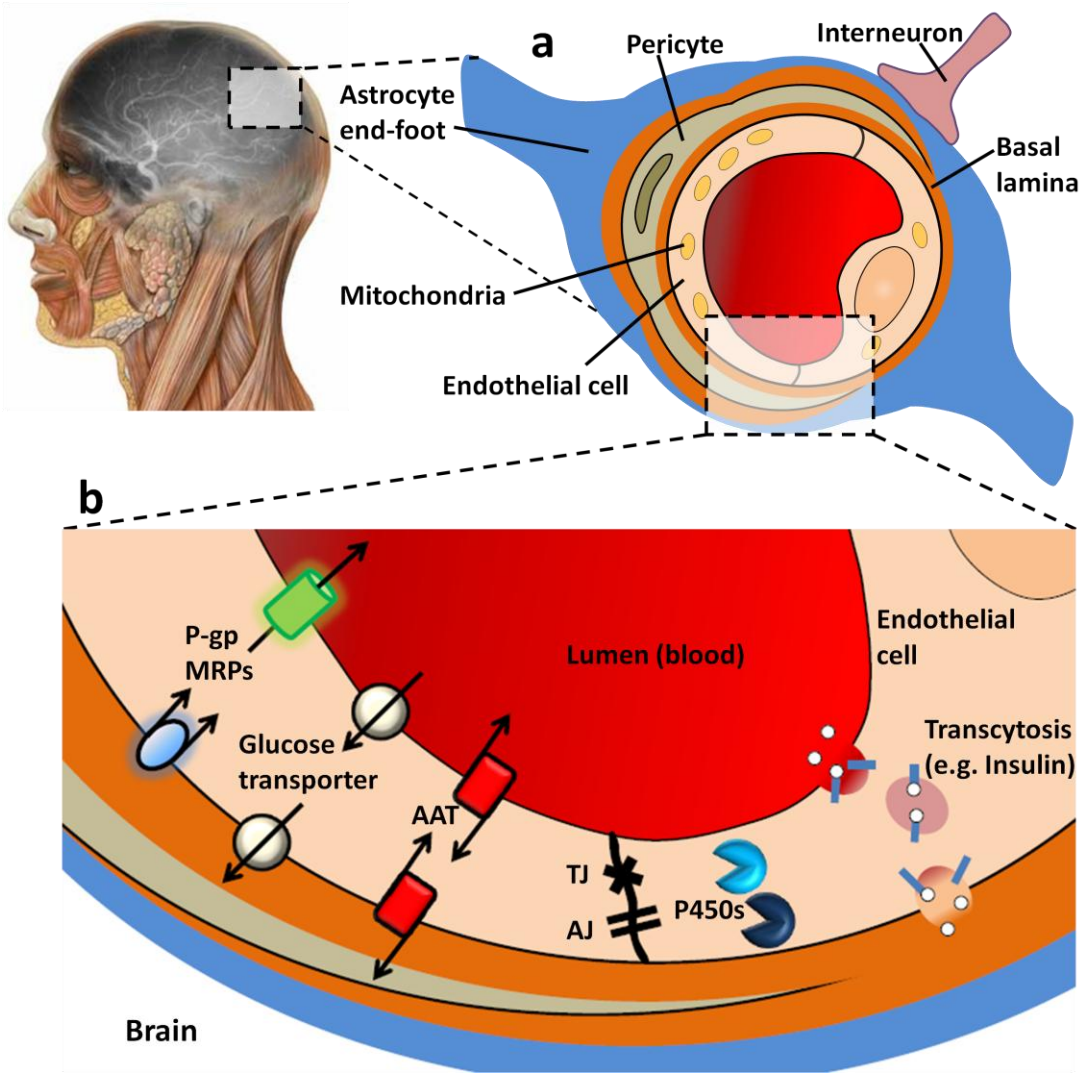

Figure 1.1. The neurovascular unit (NVU) and the blood-brain barrier (BBB). **a|** The NVU constituents are the basal lamina, pericytes, astrocyte end-feet, and perivascular neurons (Interneuron) that all interact with the mitochondria-rich cerebromicrovascular endothelial cells giving them unique properties over the peripheral endothelium. This forms the BBB. **b|** The phenotype of the BBB gives it three barrier functions; a physical barrier formed by the tight junctions (TJ) and adherens junctions (AJ) eliminating paracellular flow of molecules (see section 1.4.1), a metabolic barrier consisting of drug metabolising enzymes such as cytochrome P450s (P450s) and a transcellular substrate specific transport barrier that regulates the traffic of polar molecules through the transmembrane proteins such as ATP-binding cassette (ABC) transporters P-glycoprotein (P-gp) and multi-drug resistance associated proteins (MRPs), amino-acid transporters (AAT) and glucose transporters. Some larger molecules such as peptides and antibodies can cross the BBB by compartmentalisation via receptor mediated transcytosis (e.g. insulin) or non-specific absorptive-mediated transcytosis. Figure based on (Cecchelli et al., 2007).

1.6. Physical barrier

As a type of continuous capillary system, the BMECs of the BBB are sealed together by a combination of junctional complexes, which collectively form a physical barrier to the brain. The junctional complexes are GJs, adherens junctions (AJs) and TJs.

1.6.1. Gap junctions

The cytoplasm connecting GJs (mentioned previously in 1.4.1) promote signalling and molecular exchange between adjacent cells (of molecules up to 1kDa in molecular weight) and can also be responsible for perpetuating adverse conditions and disease (Eugenin et al., 2011). However, GJs do little in the way of maintaining structural integrity (Nagasawa et al., 2006).

1.6.2. Adherens junctions

AJs are formed by a variety of different molecules that interplay with TJs to form a dynamic barrier that regulates specific functional properties. They therefore indirectly contribute to the physical barrier of the BMECs. Through AJs, cellular adhesion is mediated by transmembrane proteins which promote homophilic interactions and form a paracellular zipper-like structure along the cell border (Dejana, 2004). Through the transmembrane adhesion protein vascular endothelial cadherin (VE-cadherin), AJs are believed to connected to the cell actin cytoskeleton via α- and β- catenins, which stabilises the junction (Niessen, 2007), although the precise components involved are unclear.

AJs are crucial for proper TJ formation and blocking aspects of their arrangement can inhibit correct organisation of TJs. This was demonstrated recently when AJ transmembrane adhesion protein vascular endothelial cadherin (VE-cadherin) was shown to mediate regulation of TJ protein claudin-5, modulating permeability *in vitro* (Taddei et al., 2008).

1.6.3. Tight junctions

Whereas the compositional organisation of AJs is ubiquitous along the vasculature, TJ composition varies greatly depending on the location and role of the endothelium. In areas such as post-capillary venules where rapid interchanges between blood and tissue are required, TJs are poorly organised and permeable, but in the BMECs they are the most complex and restrictive of the body, conferring the physical barrier properties to the BBB (Dejana, 2004, Niessen, 2007). Such is the effectiveness of the restriction, even the paracellular movement of small ions such an Cl^- and Na^+ are significantly restricted, giving the BMECs a

TEER measurement of >1000 ohm.cm^2 *in vivo*, compared to the 20 ohm.cm^2 of peripheral equivalents (Abbott et al., 2006).

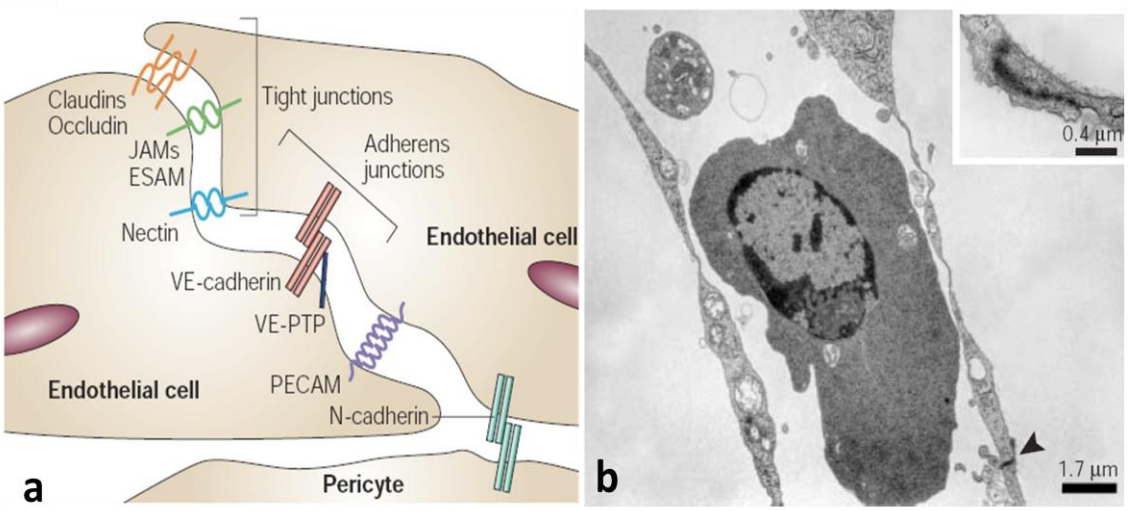

Figure 1.2. Adherens junction and tight junction organisation. a| At adherens junctions, cell adhesion is promoted by VE-cadherin which closely associates with the actin cytoskeleton. Through its extracellular domain, VE-cadherin is complexed with vascular endothelial protein tyrosine phosphatase (VE-PTP) and so is involved in endothelial proliferation and differentiation signalling processes. At tight junctions, cell adhesion is maintained by claudins, occludin, junction adhesion molecules (JAMs) and endothelial cell selective adhesion molecule (ESAM). Nectin is involved in the organisation of both adherens junctions and tight junctions. **b|** A transmission electron microscopy image of a small blood vessel containing a monocyte, complete with a visible endothelial junction (arrow). Cells partially overlap at the point of junctional formation (insert). Diagram adapted from (Dejana, 2004).

Claudins are the main constituents the TJ backbone and bind homotypically to other claudins on adjacent cells. This produces the primary seal of the junction (Huber et al., 2001, Bernacki et al., 2008). Some claudins expressed in the TJs of the BBB endothelium are very rarely found in the peripheral endothelium and attribute to the tightness of the BBB TJs (Wolburg et al., 2009). These include claudin-1, -3, -5 and -12, although due to cross-reactivity of antibodies, there is some controversy as to which claudins are more specific to the BMECs of the BBB (Lippoldt et al., 2000, Wolburg et al., 2003). There are currently 24 members of the claudin family (Erickson et al., 2007) which share their overall organisation of four transmembrane domains with two extracellular loops with another transmembrane protein called occludin.

Although it was the first TJ protein found at the BBB (Furuse et al., 1993), the precise function of occludin in TJs is not yet fully understood but it has been shown to regulate the physical barrier and have a signalling role (Dejana, 2004, Niessen, 2007). Although occludin is not required for the formation of TJs, it may be necessary to regulate barrier properties (Wolburg et al., 2009). What is clear is that it is the combined presence of claudins and occludins that give TJs their proper function.

Other transmembrane proteins such as members of the junctional adhesion molecule (JAM) family and the endothelial cell selective adhesion molecule (ESAM) play contributing roles the cell-cell adhesion by interacting with one another and with cytoplasmic proteins such as zonula occludens (ZOs) which link with the cellular actin skeleton (Bazzoni, 2003). ZOs are junctional components able to associate with many transmembrane proteins as well as other ZOs to form effective scaffolding structures. JAMs also play roles in monocyte migration through the BBB during inflammation and immune responses (Palmeri et al., 2000).

The complexity of the BMEC TJs come down to the not only the transmembrane adhesion protein components, but where they are associated in the membrane and how they are regulated by the microenvironment. Freeze-fracture electron microscopy, the method of choice when investigating TJ morphology, has allowed comparisons to be made between the component complexity of different TJs of different cell types and locations (Wolburg et al., 2009). The two fracture faces (the interior view of membranes exposed by freeze fracturing) are termed the P-face and E-face (the fractured membrane halves adjacent to the **P**rotoplasm and **E**xtracellular space respectively (Robenek and Severs, 2008). TJs from brain and non-brain endothelial cells show that their components are not only different but they associate with different areas of the membrane. In BMECs, the TJ molecules associate with both membranes equally (or slightly more to the P-face) whereas in non-brain endothelium, the TJ components almost completely associate with the E-face alone (Wolburg et al., 2009). Interestingly, freeze-fracture analysis of *in vitro* BBB endothelium gives a TJ component association of non-brain endothelium, suggesting the quality of the barrier offered by the TJ is under the control of the brain microenvironment and NVU (Wolburg et al., 2009).

Furthermore, tight junctions are also a crucial factor in development of luminal-abluminal cell polarity (Dejana, 2004, Schneeberger and Lynch, 2004). Mutual exclusion during cellular membrane formation between two evolutionarily conserved protein complexes, Crumbs (CRB)

and partitioning defective (Par) complexes, expressed at TJs allows establishment and maintenance of luminal and abluminal polarity of epithelial and endothelial cells, (covered is great detail in (Shin et al., 2006)). The establishment of cell polarity also requires growth and motility inhibition at cell confluency (*in vitro* and *in vivo*) in which both AJ and TJ components are implicated alongside growth factors such as vascular endothelial growth factor (VEGF) (Dejana, 2004).

1.7. The metabolic barrier

Metabolism is a crucial process in the body where molecules such as amino acids, lipids and carbohydrates are constructed (anabolised) or destructed (catabolised) to allow proper cellular function. Drug metabolism is the pharmacological and toxicological inactivation and elimination of toxic compounds, including drugs and xenobiotics, which could have adverse effects on the body. It is an essential factor in overall drug disposition to body regions and the rate of which it occurs has a huge impact on the action and intensity of pharmacological agents (Strazielle and Ghersi-Egea, 2005).

Although drug metabolism is essentially a hepatic responsibility, it also occurs (to a lesser extent) in the brain. Metabolizing enzymes at the BBB act as a 'metabolic barrier' for the CNS. These metabolic processes act to filter unwanted blood-derived compounds and change the bioavailability of drugs to the brain. Both phase I enzymes (such as epoxide hydrolyses and cytochrome P450s, see figure 1.1 b) and phase II enzymes, (e.g. UDP-glucuronosyltransferase, glutathione S-transferase or sulfotransferase), have been identified in human and rodent BBBs (Strazielle and Ghersi-Egea, 2005). Although not 'classical' drug-metabolizing enzymes, purine and pyrimidine metabolizing enzymes may also play a role in the delivery of nucleoside derivatives to the CNS. High specific activities of purine nucleoside phosphorylase and adenosine deaminase have been measured in bovine brain endothelial cells (Johnson and Anderson, 1996).

1.8. Transport barrier

With the paracellular route to the brain virtually unavailable to water-soluble compounds in a healthy BBB system, a variety of transcellular and transport-mediated pathways remain the only means for entry (see figure 1.3). The majority of these pathways are substrate specific and give the BBB its selectable 'gate' properties. Small non-polar gaseous molecules such as O_2 are able to freely diffuse through the lipid membranes, and this route is also an entry point for other small lipophilic agents such as ethanol (Abbott et al., 2006). The levels of non-specific endocytosis (i.e. pinocytosis) are low in cerebral endothelia due to a lack of vesicles, compared to peripheral endothelium, but receptor mediated transport and substrate specific transporter proteins (transporters) are prominent at the BBB and most hydrophilic substrates have to use these to cross the brain endothelium (Hawkins and Egleton, 2008).

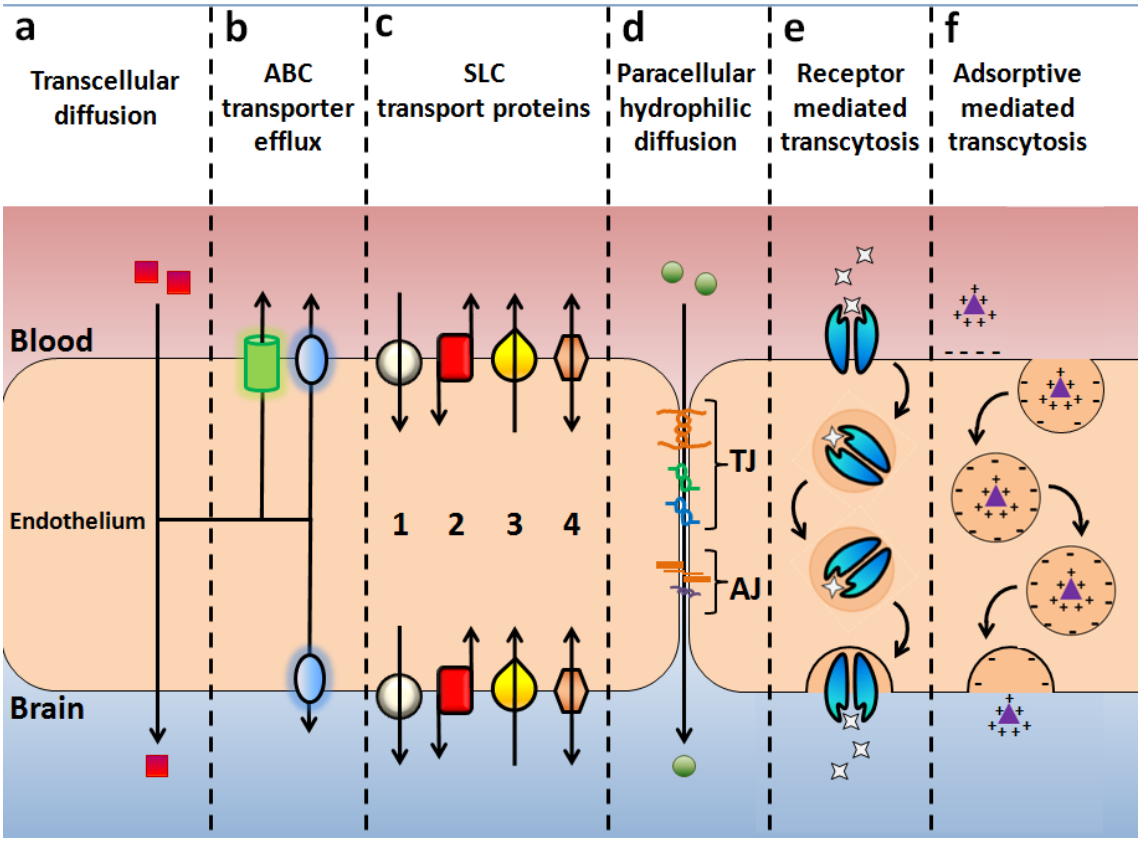

Figure 1.3. Molecular pathways across the blood-brain barrier. **a|** Some small lipid-soluble molecules are able to passively diffuse across the large membrane surface area of the BBB endothelium. These include drugs such as barbiturates and alcohols. **b|** ATP-binding cassette (ABC) transport pumps such as p-glycoprotein (P-gp), breast cancer resistance protein (BCRP) and multi-drug resistance associated proteins (MRPs), actively efflux some of these lipid-soluble molecules against their concentration gradient, out of the brain endothelium into the blood. Most are luminally (blood) located, but some are found at the abluminal (brain) side. **c|** A huge variety of substrate specific transport proteins are expressed on both the luminal and abluminal membranes of the BBB. The vast majority of these are solute carrier (SLCs) which are either passive or secondarily active which transport essential polar molecules including amino acids and glucose. This can be done using unidirectional pumps into the CNS (1), by an exchange of one substrate for another or be driven by ionic gradients (transport using this method is bidirectional depending on electrochemical gradients) (2), unidirectional out of the CNS (3) or bidirectional pumps which depend on substrate concentration gradient (4). **d|** Under healthy conditions, the tight junctions (TJ) and adherens junctions (AJ) of the BBB severely restrict paracellular movement of hydrophilic molecules so only a small percentage can cross this route. Some immune cells and pharmacological agents are able modulate the TJs to partially or fully open the paracellular route for entry to the brain. **e|** Receptor mediated transcytosis and endocytosis allows large proteins such as insulin to bind to a specific receptor and cross the BBB. **f|** Cationic (+) molecules can attract to the anionic (-) membrane or glycocalyx, internalise and cross the BBB by adsorptive mediated endocytosis and transcytosis. Both of these transcytosis/endocytosis methods involve vesicular pathways through the BBB cells. Figure redrawn based on figures from (Abbott et al., 2006, Abbott et al., 2010).

1.8.1. Endocytosis at the BBB

Most solutes with large molecular weights such as proteins and peptides are only able to cross the healthy BBB whole via endocytotic mechanisms which internalises them forming vesicles and then traffics them across the BBB endothelium via transcytosis (Abbott et al., 2010). There are at least two forms of endocytotic events for these molecules at the BBB, depending on their properties; clathrin-dependent endocytosis (CDE) or clathrin-independent endocytosis (CIE). Clathrin is a protein with structural properties that has crucial roles in shaping and lining cellular vesicles with a variety of specialised accessory proteins (Mousavi et al., 2004). BMECs are characterised by a high density of clathrin-coated pits (Simionescu et al., 1988) and so CDE is believed to be the more prominent method of endocytosis at the BBB. It is also interesting to note that clathrin-coated pits have been found more abundantly at the luminal membrane in rat BMECs, indicating a unidirectional blood-brain pathway (Simionescu et al., 1988).

CIE often involves lipid-rafts, highly ordered lipid microdomains in the lipid bilayer of eukaryote plasma membranes that are involved in endocytosis (Kirkham and Parton, 2005). One abundant type of lipid raft involved in CIE is caveolae, formed by complexes of integral membrane proteins called caveolins which bind to other transmembrane proteins, inducing their endocytosis upon stimulus. Therefore, caveolae internalisation is a highly regulable process and has been shown to be a key mediator of claudin-5 and occludin internalisation following chemokine stimulus, that alter TJ integrity during pro-inflammatory events (Kirkham and Parton, 2005, Stamatovic et al., 2009). However, there are less caveolae at the BBB in comparison to peripheral endothelium, suggesting that this form of endocytosis is less accessible to molecules than the abundant clathrin-coated pits (Herve et al., 2008). One form of CIE – macropinocytosis – has been demonstrated to be the method of BBB entry used by HIV-1 when ICAM-1 molecules line the macropinosome as it invaginates (Liu et al., 2002).

1.8.2. Transcytosis at the BBB

As well as two major forms of endocytosis, there are two methods of transcytosis at the BBB. These are receptor-mediated transcytosis (RMT) and adsorptive mediated transcytosis (AMT, see figure 1.3 for schematic). RMT involves the binding of a molecules ligand to its specific receptor on the cell surface, before internalisation of the receptor and subsequent transcytosis via vesicular transport pathways (Jones and Shusta, 2007). This transport method has been well demonstrated with the iron binding glycoprotein transferrin at the blood-brain

barrier *in vitro* and *in vivo* (Roberts et al., 1993, Descamps et al., 1996). RMT often involves the presence of receptors in clathrin-coated pits, which are either expressed in the pits before or after ligand binding, although caveolae can also have specific receptor expression (Herve et al., 2008).

AMT is believed to be non-specific, and without the influence of receptors, and in most cases requires the molecule to have a net positive charge which will bind to negative charges on the cell membrane or glycocalyx which can be absorbed and internalised as a vesicle before transcytosis (Jones and Shusta, 2007). It is important to note that the transcytosis trafficking pathways through the cells used by cationic substrates are not well defined. AMT has also recently been suggested to be the method of BBB traversal used by the bacterium species *Cronobacter in vitro*, with the authors demonstrating presence of the bacterium inside vacuoles in primary human BMVECs and below the filters following transcytotic events (Giri et al., 2012).

For thorough reviews of endocytosis and transcytosis across the BBB see (Herve et al., 2008, Smith and Gumbleton, 2006).

1.8.3. Transport proteins

The continuous membrane of BMECs, essentially formed by the physical barrier of the BBB, allows polar molecules unable to cross the membrane to utilise a huge variety of transporters. The polarised structure of the BBB, created by the physical barrier, creates a situation where substrate concentration gradients can exist between brain and blood which is exploited by the transporters to regulate the brain's molecular traffic. These transport processes can be facilitated or active transport mechanisms (see figure 1.4). Certain transporters move polar substrates down their concentration gradient from high to low in an energy-independent process termed facilitated diffusion, using carrier proteins. It is thought that these carrier proteins undergo conformational changes to transfer bound substrate across the membrane down their concentration gradient (Alberts et al., 1994).

Ions such as Na^+ use gated transmembrane channel proteins that open and close to rapidly regulate ion and substrate flow and intracellular concentration, along concentration gradients. In active transport, energy expenditure is required to move solutes from one side of the membrane to the other against concentration gradients. This form of transport can be divided into secondary and primary. Primary active transport require the hydrolysis of ATP at the

nucleotide binding domains of the transport proteins themselves to release energy for substrate transport (Leslie et al., 2005). Secondary active transport however uses the electrochemical gradient of ions to power solute exchange through antiport proteins (exchangers) where the driving ion and solute move in opposite directions, or symport proteins (a.k.a. cotransporters) where the driving ion and solute move in the same direction (Alberts et al., 1994).

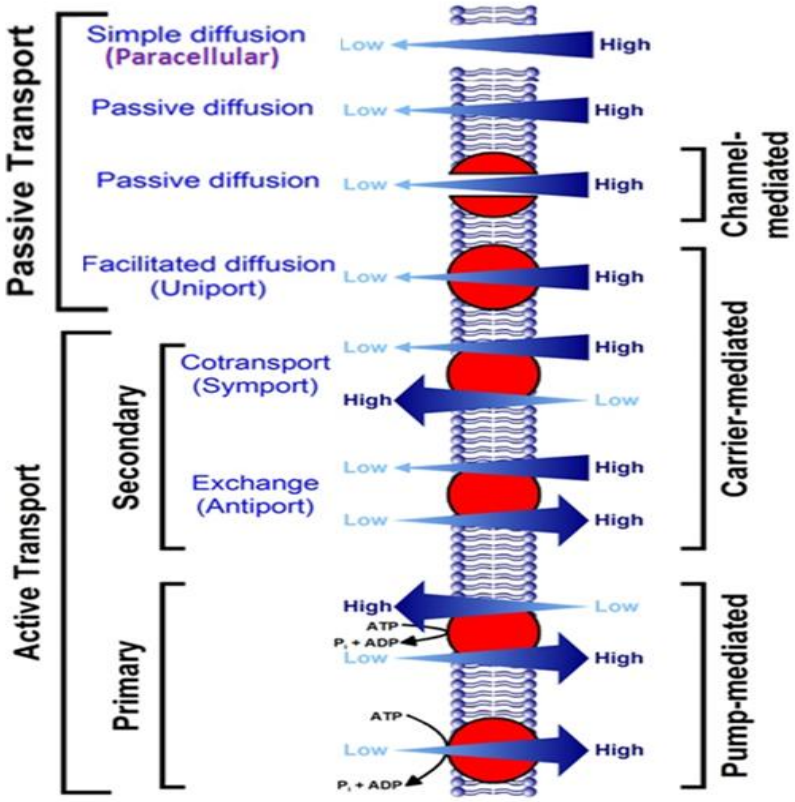

Figure 1.4. Membrane transport processes. Only a limited number of solutes can cross cell membranes without the aid of transport proteins (simple and passive diffusion). The great majority of biologically relevant solutes must use membrane transport proteins thorough passive or active transport mechanisms to cross cell membranes. Passive transporters are either channel-mediated proteins for passive diffusion, or carrier-mediated for facilitated diffusion. Active transport can be divided into secondary or primary. Secondary requires ion electrochemical gradient exchange with solutes for movement with or against concentration gradients and can be either symport or antiport. Primary active transport requires the hydrolysis of adenosine triphosphate (ATP) to adenosine diphosphate (ADP) and inorganic phosphate (P_i) to move substrates against concentration gradients. Big arrows depict movement of substrate against concentration gradients (low to high) and small arrows depict movement down concentration gradients (high to low). Figure adapted from physiologyweb.com (http://www.physiologyweb.com/lecture_notes/membrane_transport/membrane_transport_processes_summary.html)

1.8.4. ABC transporters

Protecting the brain and CNS from potentially harmful substances are a superfamily of transport proteins known as ABC transporters, most of which export their substrates from BMECs of the BBB into the blood (Begley, 2004). These active transport systems hydrolyse ATP to adenosine diphosphate (ADP) and inorganic phosphate (P_i) to induce conformational changes in their transmembrane domains. This allows transport of their substrates which vary from lipids and drug solutes to toxins and steroids (Begley, 2004). Because of their roles in exporting therapeutic drugs from cells, several members of the 48-member ABC-transporter superfamily are collectively known as multidrug resistance (MDR) proteins and these have a huge impact on the distribution of drugs into the CNS (Leslie et al., 2005).

The best-known representative of the MDR ABC transporters and the first shown at the human BBB is P-glycoprotein (P-gp) (also known as MDR1 in humans and mdr1a and mrd1b in mice) which is coded by the gene ABCB1 in humans and *abcb1a* and *abcb1b* in mice (Cordon-Cardo et al., 1989, Begley, 2004). MDR1 in humans appears to fulfil the functions of the rodent mdr1a and mrd1b, as MDR2 codes for another type of P-gp transporter (*mdr2* in rodents), which does not appear to play roles in drug export or multi-drug resistance (Demeule et al., 2002, Begley, 2004). P-gp is expressed on the luminal membrane at the BBB in humans and rodents, expelling products back into the circulation restricting their penetration into the brain (Eyal et al., 2009).

P-gp transports a huge array of substrates, particularly those that are lipophilic, uncharged or weakly basic, (although some acidic compounds can also be transported (Varatharajan and Thomas, 2009) and this large substrate range has made it difficult to design specific inhibitors. Included in these substrates are therapeutic drugs and so P-gp remains a major obstacle for CNS drug delivery. Studies have shown in mice that brain permeation of drugs (that were known substrates of P-gp) increased 100-fold when *mdr1a* was knocked out compared to wild-type (wt) controls, but that the increase had consequences for the toxicity of the drugs (Schinkel and Jonker, 2003).

P-gp has been demonstrated to have two substrate binding sites, which are divided between two almost symmetrical halves (domains) of the protein (see figure 1.5) (Bruggemann et al., 1989). When expressed at the cell membrane the protein folds to bring the two halves in close proximity (dimerisation), with the substrate binding site acting as one unit (Begley,

2004). When transporting, the single unit utilises two ATP molecules for a single transport cycle, one inducing a conformational change in the transporter which expels the substrate, and the other bringing the transporter back to its original shape (Begley, 2004). Despite the importance of P-gp and the large amount of literature directed toward its study, the precise dimerising mechanisms have yet to be elucidated.

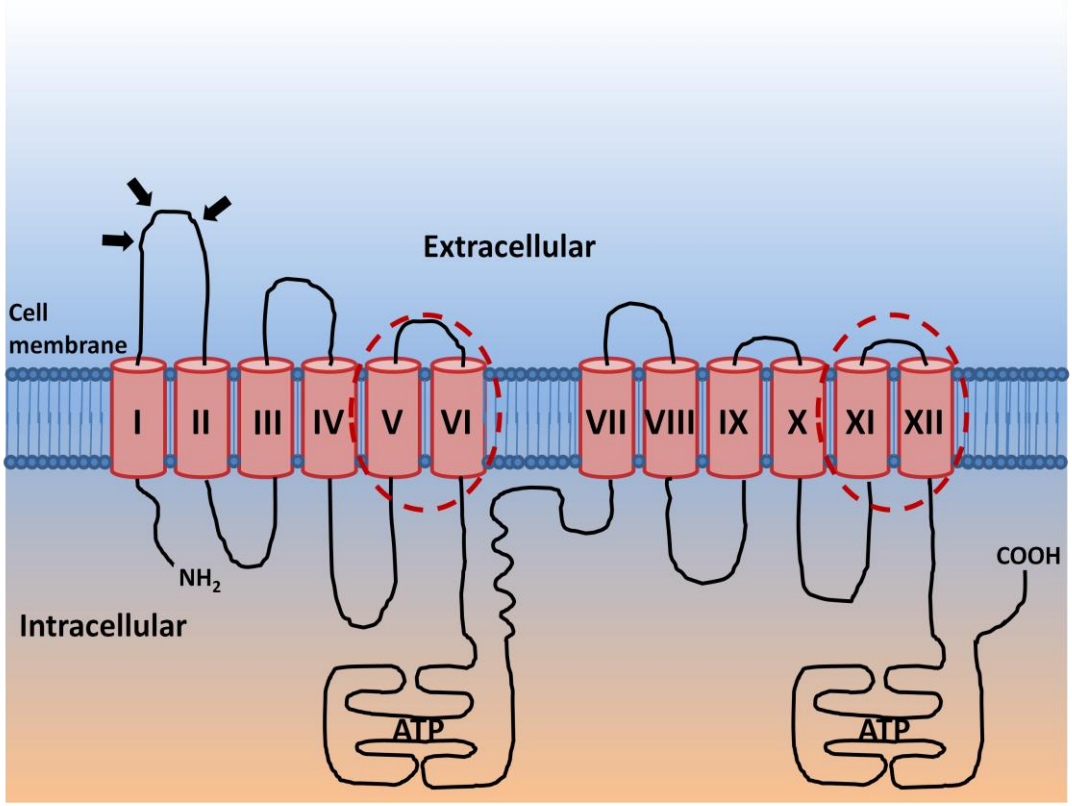

Figure 1.5. The putative structure of P-gp. P-gp has 12 transmembrane regions (I-XII) spanning the cell membrane. The drug-binding regions are associated with transmembrane domains V and VI and XI and XII, and are highlighted here by broken red circles. The black arrows point to glycosylation sites. The two intracellular ATP-binding domains (known as nucleotide-binding domains) are shown and the molecule is known to be divided into two near-symmetrical halves by a linker protein (curving line). Figure adapted from (Begley, 2004).

Another major MDR ABC transporter family are the multidrug resistance-associated proteins (MRPs). There are 9 members to this family, coded for by the genes ABCC1-9 in humans (Bernacki et al., 2008). Of the 9 members, MRP-4, 5, 8 and 9 have a 'short' structure consisting of 12 transmembrane regions between 2 domains, with 2 membrane spanning domains attached to a nucleotide (ATP) binding domain (NBD), similar to P-gp (Chen and Tiwari, 2011). The remaining 5 MRPs (MRP-1 to 5) are known as the 'long' structure MRPs and

have a third domain giving them 17 transmembrane spanning regions (see figure 1.6), although the function of this extra domain remains elusive. Despite the structural similarities between P-gp and MRPs, it is believed that MRPs do not dimerise or associate with other membrane proteins to function as efflux transporters (Begley, 2004).

MRPs predominantly transport organic anions but in addition transport neutral organic compounds and some require the presence of co-factors such as glutathione to mediate transport (Deeley et al., 2006). Many of their substrates overlap with P-gp, making it difficult to distinguish functionally between the two ABC transporter families, although it is known the MRPs have a preference for organic anions and drugs that are conjugated to glutathione, sulphate or glucuronate by enzymatic activity in the CNS (Minn et al., 2002).

Their expression at the BBB has been confirmed in several species, with MRP1, 2, 3, and 5 confirmed in human BMECs, with MRP1 and 2 believed to play major roles in protecting the brain and CVOs from xenobiotics and the associated toxicity (Borst et al., 2000, Begley, 2004, Bernacki et al., 2008).

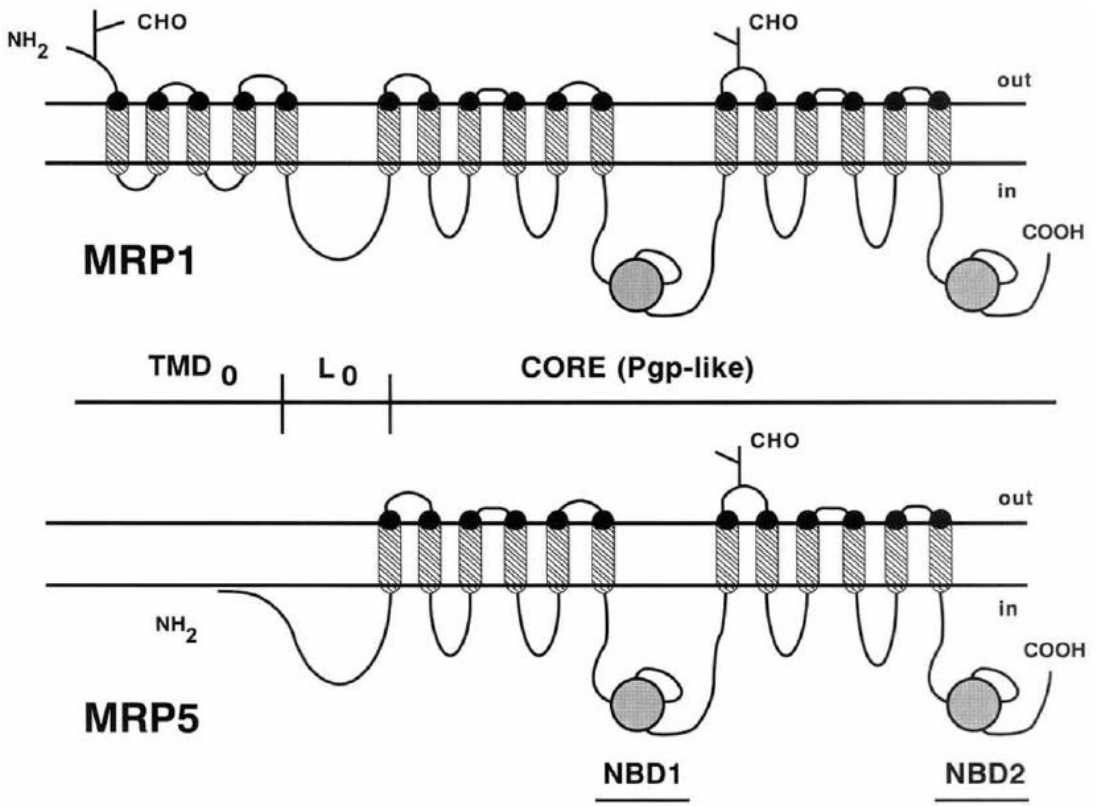

Figure 1.6. Structure of 'long' and 'short' MRPs. 'Long' MRPs (MRP1, 2, 3, 6 and 7) have 17 transmembrane regions grouped into 3 domains. The extra domain (on the top left of MRP1) compared to the P-gp-like **core** is known as transmembrane domain $_0$ (**TMD_0**) and is joined the core by linker protein **L_0**. The 'short' or truncated MRPs (MRP4, 5, 8 and 9) are shorter with only 12 transmembrane regions divided between two domains, in a similar arrangement to P-gp. The purpose of the extra domain on the 'long' MRPs is not clear. **NBD** - nucleotide binding domain. From (Begley, 2004).

Breast cancer resistance protein (BCRP), coded by the ABCG2 gene in humans is the second most prominent MDR ABC transporter expressed at the BBB following P-gp, with a similar substrate specificity (Begley, 2004, Tai et al., 2009b) and luminal expression profile, indicating its importance in efflux of xenobiotics from the brain and BBB (Cooray et al., 2002). As the name suggests, BCRP confers cancer cells drug resistance by expelling chemotherapy drugs including doxorubicin and daunorubicin (Doyle et al., 1998). It has also been demonstrated BCRP expression increases 3-fold at the BBB in mdr1a $^{-/-}$ mice, which demonstrates a P-gp compensatory role for the transporter in rodents (Cisternino et al., 2004).

Unlike P-gp and MRPs, BCRP has only 1 domain consisting of 6 transmembrane regions with a single NBD, and is believed to function as a homodimer (Bernacki et al., 2008) (see figure

1.7). This dimerisation of BCRP proteins represents an attractive target for pharmacological intervention in cancer treatment (Ni et al., 2010).

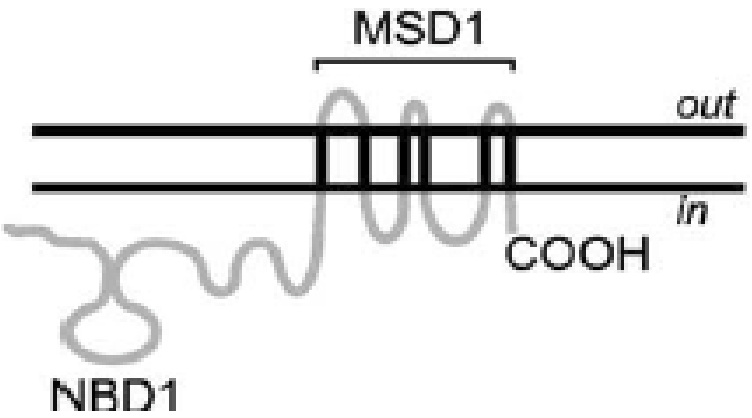

Figure 1.7. Putative structure of BCRP. BCRP consists of a single domain with a NBD and 6 transmembrane regions. It has been demonstrated to function as an efflux transporter in a homodimer. Taken from (Leslie et al., 2005).

ABC transporters are not expressed exclusively at the BBB; many are widely expressed throughout the NVU and nervous system (and many other tissues). The focus of the thesis however is on the BBB, and so for an overview of transporter expression in the NVU see (Neuwelt et al., 2011).

1.8.5. Solute carriers

The vast majority of facilitated diffusion carrier proteins and secondary active transporters expressed by all cells constitute the solute carrier transport group (SLC transporters, see figure 1.3). SLCs can be divided into 46 recognised families with a combined membership of over 380 different proteins in humans, making the SLC group of transporters the second biggest after G protein-coupled receptors (Hoglund et al., 2011).

At the BBB, SLC transporters can be expressed in either a polarised manor – at luminal or abluminal membranes – or at both membranes (Abbott, 2002, Bernacki et al., 2008, Abbott et al., 2010). Their widespread distribution at the BBB along with the fact that their expression is partly regulated by components of the NVU (Abbott et al., 2006) highlights their importance as nutrient suppliers to the brain.

One well studied nutrient transport system at the BBB is the SLC2 family, which consists of 13 transporters – GLUT1-12 and HMIT – which facilitate the transport of glucose and lactate to the brain (Simpson et al., 2007). GLUT1 is the major isoform expressed at the BBB, accounting for up to 90% of BBB glucose transport (Pardridge et al., 1990). GLUT1 has been found at both luminal and abluminal membranes of BMECs, as well as intracellularly (Harik et al., 1990, Farrell and Pardridge, 1991). It has been hypothesised that the intracellular pool of GLUT1 may upregulate GLUT1 membrane expression to replenish depleted supplies to glucose during conditions of increased demand such as during hypoglycaemia (Simpson et al., 1999).

The organic anion transporter (OAT) family and the organic anion-transporting polypeptide (OATP) family are SLC transporters with broad substrate specificities. OATs make up the SLC22 family and transport organic anions against chemical and ion gradients (VanWert et al., 2010). OAT1 and OAT3 are believed to have important substrate transporting roles at the BBB as suggested by murine and porcine models (Sauer et al., 2010, Miyajima et al., 2011).

OATPs are sodium-independent, multi-specific anion exchangers (i.e. they exchange a drug for another ion or molecule), some of which are expressed at both luminal and abluminal membranes (Figure 4). OATP-mediated transport can be bidirectional, depending on local substrate concentration gradients. Among OATP family members, three transporters have been identified at the human BBB. OATP1A2 and OATP2B1 are localized at the luminal membrane of brain endothelial cells and the thyroid hormone transporter, OATP1C1 has also been identified in the human brain endothelium , but its precise localization has yet to be identified (Eyal et al., 2009).

Due to the huge varieties of SLC transporters at the BBB, an abundant wealth of knowledge about their roles in physiology and homeostasis of the brain is well published in the scientific literature. This knowledge has also been exploited pharmacologically. SLCs can be targeted by transport inhibitors, which block their function, but also by drugs that mimic endogenous substrates in order to improve delivery to the brain for the treatment of many diseases and adverse conditions. An example of this is with L-DOPA, the precursor to the neurotransmitter dopamine, used in the treatment of Parkinson's disease. Patients with Parkinson's disease are deficient in dopamine which in its active form is unable to cross the BBB. L-DOPA, however, is transported across the BBB into the brain by system L transporter large neutral amino acid transporter 1 (LAT1) (Kageyama et al., 2000).

For further descriptions of SLC transporters, the reader is directed to the general review by (Hediger et al., 2004). For the purposes of this thesis, I shall concentrate on amino acid transporters, which will be discussed extensively in the following section (1.9).

1.9. Endogenous molecule interactions at the BBB – amino acids

The human brain has evolved complex cognitive capacity and it can be argued that feeding habits are directly linked to the development of civilisation as people's choice of what-to and what-not-to eat are heavily influenced by religion, society and culture (Gomez-Pinilla, 2008). This complexity in brain function attributes to a high metabolic rate and so the brain must be continually supplied with nutrients. One crucial group of nutrients required by the brain (and all other organs) in constant supply are amino acids (AAs), which are central to biochemistry for metabolism and protein synthesis purposes.

There are 22 'standard' amino acids that are incorporated into proteins and polypeptides in the human body, 20 of which are coded for by the universal genetic code. However, 9 of these cannot be created in humans and so are known as 'essential' amino acids that must be taken in the form of food and are transported to tissues and organs throughout the body via the circulatory system along with other AAs synthesised elsewhere in the body (Campbell and Reece, 2002). The BBB contains a huge variety of AA specific transporters that traffic AAs in and out of the brain. Some of these circulating AAs, such as tryptophan and L-DOPA, are precursors for neurotransmitters such as serotonin and the already discussed dopamine (in section 1.8.5) (Pardridge, 1998, Kageyama et al., 2000).

BBB AA transport plays critical roles in the regulation of several pathways of brain AA metabolism. This is because the rate-limiting enzymes involved in the cerebral biosynthesis of serotonin, dopamine and other neurotransmitters are not saturated by normal concentrations of precursor amino acid substrates in brain cells (Pardridge, 1998). Therefore, the availability of AAs within brain cells is proportional to biosynthesis through these rate-limiting steps, and this AA availability is determined by BBB transport (Pardridge, 1977). Brain protein synthesis is also inhibited by supraphysiological concentrations of amino acids and therefore altered amino acid availability in the brain can result in proportionate decreases in cerebral protein synthesis (Pardridge, 1977, Pardridge, 1998). These roles played by AA availability in brain functioning highlight the importance of AA transport mechanisms at the BBB.

A variety of different SLC transport systems exist at either or both the luminal and abluminal membranes of the BBB and transport neutral AAs (NAA), anionic AAs (AAA) and cationic AAs (CAA) in and out of the brain. These AA transporters can be functionally classified as either Na^+-dependent or independent. This thesis will cover the CAA transport systems and

the reader's attention is turned to (Mann et al., 2003) and (Hawkins et al., 2006) for reviews of the other AA transport systems.

1.9.1. Cationic amino acids

Out of the 22 'standard' AAs, 3 are positively charged; Arginine, Lysine and Histidine (see figure 1.8). Of these 3, only Arginine and Lysine carry a positive charge at the physiological pH of 7.4. These amino acids and others produced *in vivo* that carry a positive charge are known as CAAs.

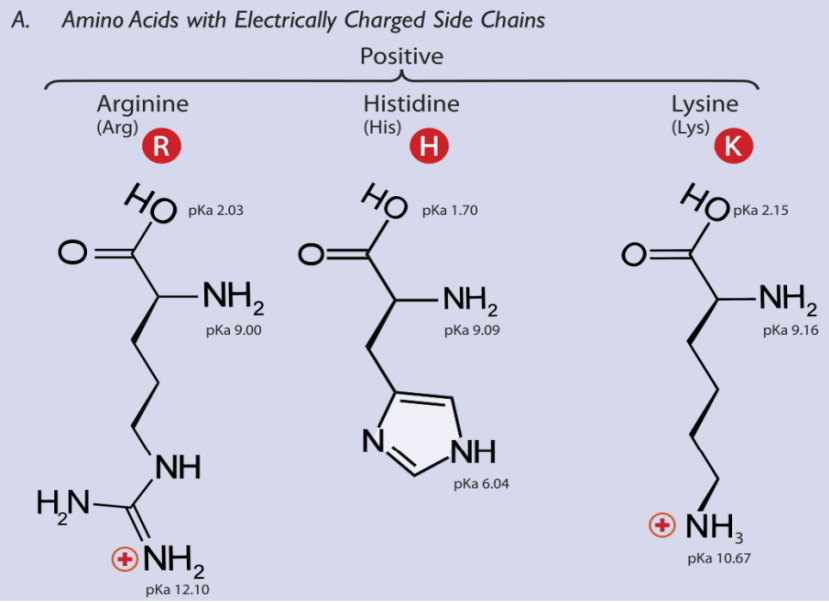

Figure 1.8. The 3 standard cationic amino acids and their structures. Only Lysine and Arginine carry their positive charge at pH 7.4 **(+)** Figure taken from Dan Cojocari, University Health Network, University of Toronto with permission.

1.9.2. CAA transporters

CAAs are transported in and out of cells by two families: the broad-scope amino acid transporter (BAT) family transport and the cationic amino acid transporter (CAT) family. Transport systems $b^{0,+}$, $y^{+}L$ and $B^{0,+}$ are collectively known as the BATs and system y^{+} transporters are known as CATs (see table 1) (Closs et al., 2004). Another transport system which does not belong to either the CAT or BAT families, b^{+}, has also been shown to exhibit

CAA transport although so far this system has only be found in mouse blastocysts and so isn't discussed here (Van Winkle and Campione, 1990).

1.9.3. Broad-scope amino acid transporters

Although they aren't the principle CAA transporters, the BATs are able to transport CAAs in a Na^+-independent manner (except for system $B^{0,+}$ which requires Na^+) but also retain affinity for NAAs (Mann et al., 2003).

System $b^{0,+}$ has two covalently-linked heavy and light chain protein subunits called rBAT and $b^{0,+}$AT which are coded by the genes SLC7A9 and SLC3A1 in humans respectively, and associate to form a heterodimeric transporter which exhibit affinities for CAAs and L-cystine as well as NAA (Wagner et al., 2001, Verrey et al., 2004). $b^{0,+}$AT has been found in the gut with rBAT, which has been found in the mouse brain (Dahlin et al., 2009). Their messenger ribonucleic acid (mRNA) expression has been demonstrated in a human *in vitro* model of the BBB (Carl et al., 2010).

System y^+L has 2 proteins called y^+LAT1 and y^+LAT2 which are coded by SLC7A6 & SLC7A7 in humans, and were first identified in the early 1990s (Deves et al., 1992). Both proteins associate with a ubiquitous transmembrane protein called 4F2hc (also called CD98 coded by human gene SLC3A2) to form heterodimeric structures which exhibit y^+L activity in the ionic-dependent transport of CAAs and NAAs (Torrents et al., 1998, Mann et al., 2003). 4F2hc also forms the light subunit of LAT1 and this combined with the fact that the transporters exhibit greater affinity to NAA compared to system y^+ gives it the name y^+L (Torrents et al., 1998). Distinguishing functionally between systems y^+ and y^+L is somewhat difficult due to their affinities for CAAs and the lack of a specific inhibitor for y^+L. However, it has been demonstrated that flux of L-lysine through system y^+L can be inhibited by L-leucine (NAA) in the presence of Na^+, whereas the same experiment through system y^+ causes no effect (Estevez et al., 1998, Rotmann et al., 2007). Expression patterns between y^+LAT1 and y^+LAT2 differ, with the former found in kidney and lung epithelia, and the latter found in the brain, heart, small intestine and testis (Broer et al., 2000). The mRNA expression of both y^+LAT1 and y^+LAT2 has also been demonstrated in a human *in vitro* model of the BBB (Carl et al., 2010).

System $B^{0,+}$ (not to be confused with system $b^{0,+}$) was discovered in a murine blastocysts *in vitro* following experiments studying alanine transport where it was discovered that L-lysine and 2-amino-2-norbornanecarboxylic acid (BCH) were competitive inhibitors (Van Winkle et

al., 1985). System $B^{0,+}$ comprises one protein member known as $ATB^{0,+}$ which is coded by SLC6A14 in humans, transports a wide variety of CAAs and NAAs in a Na^+-dependent manner (Deves and Boyd, 1998, Sloan et al., 2003) and has been hypothesised to be the principle β-alanine SLC protein (Anderson et al., 2008). It is expressed heavily in the gut and also the hippocampus in the murine and bovine models (Sloan and Mager, 1999). As the 14th member of SLC6, $ATB^{0,+}$ shares homology with the other members, some of which are important neurotransmitter transporters in the brain (Mann et al., 2003, Anderson et al., 2008). Interestingly, $ATB^{0,+}$ has been found at the bovine BBB *in vitro* with polarised expression (Sanchez del Pino et al., 1995, Czeredys et al., 2008). $ATB^{0,+}$ has also been shown to transport the intracellular fatty acid transport compound L-cartinine in another bovine model of the BBB, which is known to accumulate in the brain, although in this assay, transport was found to occur at both luminal and abluminal membranes (Berezowski et al., 2004). Despite these interesting observations, the expression and role of $ATB^{0,+}$ at the human BBB has been poorly studied.

Table 1.1. Amino acid transport systems implicated in cationic amino acid transport.

Transport system	Protein	Human gene & chromosome	Expressed at BBB?	Primary substrates	Inhibitors	Na^+ dependent	Reference
y^+	CAT-1	SLC7A1 Chromosome 13; 13q12-q14	Yes	Lysine, Arginine Ornithine, Histidine NAA (weakly)	L-Homoarginine & N-ethylmaleimide	No for CAA, but yes for NAA.	(Bogle et al., 1995, Nicholson et al., 1998, Closs et al., 2006, Hawkins et al., 2006, O'Kane et al., 2006)
	CAT-2A & CAT-2B	SLC7A2 (A&B) Chromosome 8; 8p22-p21.3	Yes	Lysine, Arginine, Ornithine	Unknown (CAT-2A) L-Homoarginine (for CAT-2B)	Unknown No	(Bogle et al., 1995, Closs et al., 2006, O'Kane et al., 2006)
	CAT-3	SLC7A3 Chromosome X; Xq13.1	Unknown	Lysine, Arginine	Unknown	No	(Huang et al., 2007)
	CAT-4	SLC7A4 Chromosome 22; 22q11.21	Unknown	Unknown	Unknown	Unknown	(Closs et al., 2006, Yeramian et al., 2006)

Transport system		Protein	Human gene & chromosome	Expressed at BBB?	Primary substrates	Inhibitors	Na^+ dependent	Reference
b^+		b_1^+ & b_2^+	Unknown	Unknown (only found in mice blastocysts so far)	Lysine, Arginine, L-Homoarginine, S-2-aminoethyl-L-cysteine (b_2^+ has greater CAA affinity)	L-histidine and D-arginine inhibit system b_1^+ more strongly than L-tryptophan, (reverse for system b_2^+)	No	(Van Winkle and Campione, 1990)
BAT	$b^{0,+}$	$b^{0,+}$AT & rBAT	SLC7A9 Chromosome 19; 19q13.1 & SLC3A1 Chromosome 2; 2p16.3	Unknown	Lysine, Arginine, Leucine. NAA	Harmaline	No	(Van Winkle and Campione, 1990, Deves et al., 1998)
	y^+L	y^+LAT1 & y^+LAT2	SLC7A7 Chromosome 14; 14q11.2 & SLC7A6 Chromosome 16; 16q22.1	Yes	Lysine, Arginine NAA	Unknown	No for CAA, but yes for NAA.	(Deves et al., 1998, Omidi et al., 2003)
	$B^{0,+}$	$ATB^{0,+}$	SLC6A14 Chromosome X; Xq23-q24	Yes	Lysine, Arginine, Alanine, Tryptophan. NAA	BCH, α-methyltrytophan	Yes	(Czeredys et al., 2008, Karunakaran et al., 2008)

AAT – amino acid transport **ADMA** = asymmetric dimethylarginine **BBB** = blood-brain barrier **BAT** – broad-scope AAT family **BCH** = 2-amino-2-norbornane-carboxylic acid **NAA** = neutral amino acids **CAA** = cationic amino acid **CAT** = cationic amino acid transporter **NMMA** = N^G monomethyl-L-arginine **SLC** = solute carrier

1.9.4. Cationic amino acid transporter (CATs)

System y^+ transporters are the only family of transporters that are specific for CAAs (Deves and Boyd, 1998), although they are able to weakly transport NAAs in the presence of Na^+ (White, 1985). It is also the principle transport system for CAAs in endothelial cells (Baydoun et al., 1994, Closs et al., 1997a, Hawkins et al., 2006). This is also no exception at the BBB where they are expressed at both luminal and abluminal membranes of the BMECs of mice (O'Kane et al., 2006, Hawkins et al., 2006). The system was first described in the 1960s *in vitro* (Christensen and Antonioli, 1969, Christensen and Handlogten, 1969, Christensen et al., 1969) but not named until the early 1980s (White et al., 1982, White and Christensen, 1982). System y^+ transports CAAs, particularly the L isomeric forms L-arginine, L-ornithine and l-lysine in a bidirectional manner dependent on substrate concentration in the μM range and membrane potential (Verrey et al., 2004). Another characteristic of system y^+ is stimulation of transport by substrate on the opposite side of the membrane, so called '*trans*-stimulation', the sensitivity of which varies between members of the transport system (Closs et al., 2006). There are 4 members to the family, aptly named CAT-1, CAT-2, CAT-3 and CAT-4, which are coded by the human genes SCL7A1–4 respectively and distinguished functionally by their affinity to protonated histidine (Closs et al., 2006).

CAT-1, with an almost ubiquitous expression (except for the liver), was one of the first amino acid transporters to be identified and cloned in mice (Kim et al., 1991) with its expression level in tissue regulated by a wide variety of stimuli including hormones, nutrients and cell proliferation (Hatzoglou et al., 2004). It is highly sensitive to *trans*-stimulation and in the rat brain, mRNA for CAT-1 is expressed >40 times in the BBB compared to the rest of the brain tissue (Stoll et al., 1993). CAT-1 appears to be the major system y^+ transporter and deletion of mCAT-1 in mice in lethal, with pups dying 1 day after birth. Under targeted mutagenesis, mCAT1 gene mutation also produces pubs that are 25% smaller than normal littermates and decreased red blood cells and haemoglobin levels, suggesting crucial roles for the transporter in haematopoiesis and growth control during mouse development (Perkins et al., 1997). It is believed CAT-3 compensates to some extent for CAT-1 gene deletion to allow the developing mice to make it to birth as its expression increases in CAT-1 knockout cell lines (Nicholson et al., 1998). CAT-1, along with the other CAT proteins, is sensitive to inhibition by L-homoarginine and N-ehylmaleimide (Stoll et al., 1993, Deves and Boyd, 1998). The localisation of CAT-1 puts it in physical contact with endothelial nitric oxide synthase (eNOS) -

an enzyme that catalyses the reaction of L-arginine to L-citrulline and NO in endothelium - at caveolae the plasma membrane, signifying the importance of the transporter in the production of NO (McDonald et al., 1997, Mann et al., 2003, Li et al., 2005).

Human CAT-2 is found as two splice variants known as CAT-2A and CAT-2B which differ from one another by 42 amino acids (Closs et al., 1997a). CAT-2B has higher affinity for CAAs than CAT-2A and exhibits similar substrate specificity to CAT-1 although is less sensitive to *trans*-stimulation (Closs et al., 1997b, Vekony et al., 2001). Conversely, CAT-2A is almost completely insensitive to *trans*-stimulation (Closs et al., 1993). CAT-2A is predominantly expressed in the liver whereas CAT-2B, referred to as the inducible CAT isoform, is often only located in inflammatory cells following cytokine or lipopolysaccharide treatment and is often induced with inducible/immune nitric oxide synthase (iNOS) (Hatzoglou et al., 2004). CAT-3, expressed strongly in the thymus and brain of humans, exhibits strong affinity for CAAs and is somewhat sensitive to *trans*-stimulation, although not as sensitive as CAT-1 (Vekony et al., 2001). CAT-4 is expressed in the brain, testes and placenta of humans, although no CAA transport role has been attributed to it and its physiological significance is unknown (Sperandeo et al., 1998, Wolf et al., 2002).

Human CATs expressed in *Xenopus laevis* oocytes exhibit a Michaelis half-saturation constant (K_m) for L-arginine of 70-250μM for CAT-1, 2-5mM for CAT-2A, 38-380μM for CAT-2B, and 40-450μM for CAT-3, with similar values for L-ornithine and L-lysine (Closs et al., 1993, Kavanaugh et al., 1994, Closs et al., 1997a, Closs et al., 1997b). L-histidine is a poor substrate for all members of system y^+ at physiological pH, but good at pH 5.5 when protonated, except for CAT-3 which does not recognise histidine in any form (Kim et al., 1991). In rat *in situ* brain perfusion models, CATs have been reported to have a K_m of 30-100μM for L-arginine, 70-100μM for L-lysine and 109μM for L-ornithine (Mann et al., 2003). Data from human brain endothelium varies, but falls within the latter concentrations. These transport kinetic data illustrate the differences between the CATs themselves as well as differences between species and models. It has also been shown that CAT activity is voltage dependent and maximum influx rate (V_{max}) is increased with membrane hyperpolarisation induced by vasoactive substances such as bradykinin (Nilius and Droogmans, 2001).

The predicted structure of CATs based on numerous data show 14 transmembrane domains with intracellular N-and C-terminals (figure 1.9 below) (Closs et al., 2006). The third

extracellular domain serves as a binding site for murine leukaemia viruses, a finding which attributed its position to be extracellular (Kim et al., 1991, Albritton et al., 1993). This loop is heavily N-glycosylated and shows great variability between species, although doesn't appear to hold transport functions (Kim and Cunningham, 1993). It has also been established that CATs exhibit few polymorphisms, which suggests slight alterations in protein sequence are not tolerated for proper functioning (Closs et al., 2006).

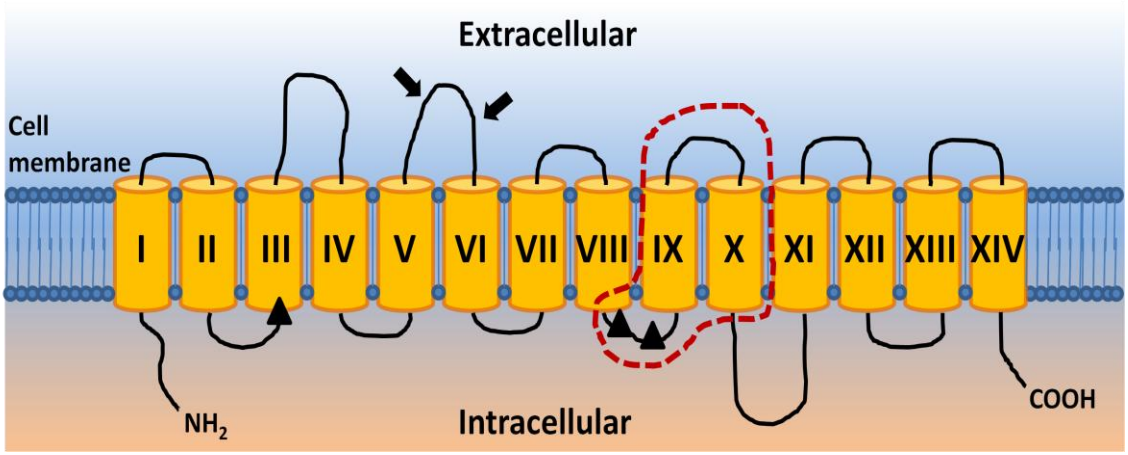

Figure 1.9. The putative structure of CATs 1-3 (4 is unknown). CATs have 14 transmembrane domains (yellow cylinders), intracellular N- and C-termini (NH_2 and COOH) and are glycosylated at positions which vary between species. The region highlighted in red confers differences in transport function between the CATs. Black arrows indicate known glycosylation sites. Black triangles indicate areas crucial for substrate recognition and transport function. Adapted from (Verrey et al., 2004) and (Closs et al., 2006).

1.9.5. L-arginine

The CAA L-arginine is classified as a 'conditionally essential' or 'semi-essential' amino acid on the grounds that it can be synthesised in sufficient quantity in adults, but in developing animals and adults suffering certain disease or trauma it is obtained from the diet to supplement endogenous synthesis (Barbul, 1986). However, as not all tissues in the healthy adult contain the necessary enzymes for the *de novo* synthesis of L-arginine, careful regulation of its supply in relation to its consumption is crucial, and is maintained by a balance between intracellular metabolism and membrane transport (Wiesinger, 2001). Endogenous L-arginine synthesis involves the mitochondria-based enzymes ornithine carbamoyltransferase and carbamoylphosphate synthetase I which are involved in the urea cycle and heavily expressed in liver hepatocytes, but not found in the CNS (Morris, 1992). In addition to the more widely expressed arginosuccinate synthase enzymes which catalyse the recycling of L-citrulline to L-arginine and are important for NO production. Deficiency in this specific process can have severe consequences for patients – which includes progressive hepatic disease and continued intellectual impairment – highlighting the importance of endogenous L-arginine production (Erez et al., 2011).

The role of L-arginine in the body is dependent on the cell-type and the desired end-product. Besides a role in the urea cycle (see (Morris, 2002) for a thorough review), L-arginine participates in creatine, L-ornithine, and L-glutamate synthesis and is the precursor for polyamines, proline and spermidine (see (Grillo and Colombatto, 2004) and the references within).

Arguably, the most important role of L-arginine is that it is the primary substrate for all isoforms of nitric oxide synthase (NOS) enzymes (including endothelial NOS (eNOS), neuronal nitric oxide synthase (nNOS) and inducible nitric oxide synthase (iNOS), which are classified by their tissue and cell distribution and expression) and hence involved in the production of NO, as briefly mentioned in previous sections of this thesis. The enzymes, which share an approximate 50% sequence homology and function as homodimers, catalyse the NADPH and O_2-dependent oxidation of L-arginine to L-citrulline and NO (Vallance and Leiper, 2002) (see figure 1.10 below).

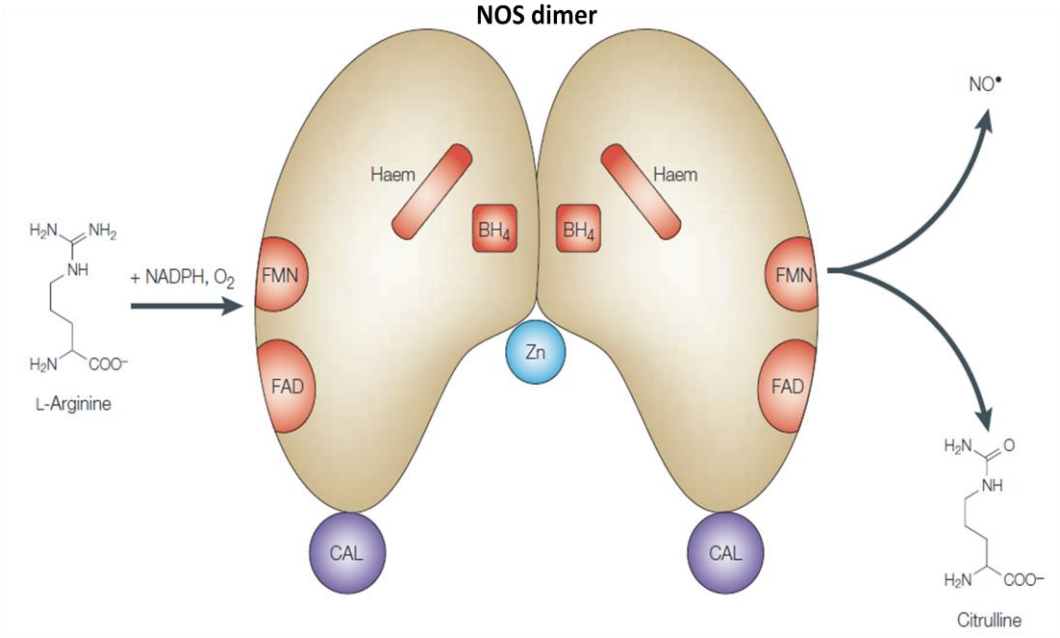

Figure 1.10. L-arginine metabolism by NOS. NOS enzymes form homodimers and bind the cofactors haem, flavin mononucleotide (FMN), flavin adenine dinucleotide (FAD) and tetrahydrobiopterin (BH_4) for enzymatic activity. Each NOS dimer also coordinates a single zinc (Zn) atom. On binding calmodulin (CAL), the active enzymes catalyse the oxidation of L-arginine to L-citrulline and NO using NADPH and O_2 as co-substrates. Adapted from (Vallance and Leiper, 2002).

1.9.6. Nitric oxide – action and targets

The importance of NO in physiology was epitomised when it was named 'molecule of the year' by the journal *Science* in 1992 (Culotta and Koshland, 1992). NO is a gaseous free radical signalling molecule in the respiratory, gastrointestinal, genitourinary, cardiovascular and nervous systems, and disordered NO generation is implicated in a wide range of diseases (Alderton et al., 2001, Vallance and Leiper, 2002). In the respiratory system, NO improves pulmonary vascular integrity, improving arterial oxygenation which is related to its effect on blood-flow distribution in the lungs (Giacoia, 1995). NO plays similar roles in the gut such as regulation of blood supply and helping maintenance of gut epithelial integrity, but it also exhibits protective effects by inhibiting gastric acid secretion (Lanas, 2008, Stanek et al., 2008). In the genitourinary system too, NO is implicated in a wide variety of roles including penile erection, localised renal blood flow and tubular function (Burnett, 1995). In the cardiovascular system, eNOS generates NO to vasodilate the vasculature which maintains it in a relaxed state

to promote blood flow, inhibit platelet and immune cell adhesion, and to inhibit smooth-muscle cell replication (Strijdom et al., 2009). The many effects of NO on the cardiovascular system are reviewed in detail in (Loscalzo and Welch, 1995).

It is believed NO reacts with four main cellular targets: thiols, metals, molecular oxygen and reactive oxygen species (ROS) (such as superoxide (O_2-)) and that NO signalling is dependent on the redox state of the cell. This allows the highly reactive NO can be involved with numerous signalling pathways, and probably explains why NO can have both physiological and pathophysiological influences on the body (Vallance and Leiper, 2002).

NO signalling often occurs via interaction with the soluble lysase enzyme guanylyl cyclase (sGC), stimulating its activity which results in the production of the secondary messenger 3',5'-cyclic guanosine monophosphate (cGMP) from guanosine triphosphate (GTP) (Burnett, 1995) which induces downstream activation of protein kinases and subsequent downstream signalling events resulting in smooth-muscle relaxation and a variety of other physiological processes (Guix et al., 2005). This type of signalling has been shown to occur in rat BBB cells (Janigro et al., 1994). NO signalling can also happen through cyclooxygenase, Akt kinase, and by S-nitrosylation of pathway components, in which it binds to thiol groups of proteins and non-protein molecules to regulate cell signalling components (Guix et al., 2005, Calabrese et al., 2007).

1.9.7. NO, the brain, and the BBB

NO can act on both the peripheral nervous system (PNS) and CNS. In the PNS, NO produced from nNOS is important in the relaxation of vascular and non-vascular smooth muscle and a variety of other locally-acting processes (see (Vallance and Leiper, 2002)). In both the PNS and the CNS, NO is also able to act as a secondary neurotransmitter via cGMP mechanisms, which was first shown in a landmark paper demonstrating that NO was produced as a result of N-methyl-D-aspartate (NMDA) receptor stimulation by glutamate (Garthwaite et al., 1988). This process was subsequently described at several brain regions including the hippocampus and hypothalamus, which showed that via a retrograde mechanism NO is also able to inversely stimulate glutamate release which is crucial in memory function of the brain (Guix et al., 2005). NO has also been implicated in the release of other types of neurotransmitters including serotonin (Lorrain and Hull, 1993) and noradrenalin (Feldman and Weidenfeld, 2004) as well as in neuronal survival and neuronal protection (Calabrese et al., 2007).

In the cerebrovasculature, NO comes from eNOS in BMECs and BECs (Moncada et al., 1991), and nNOS from brain neurons (Bhardwaj et al., 2000) or autonomic nitrergic nerves (Toda and Okamura, 2003) which controls cerebral blood flow, vascular tone, vascular resistance, and vascular growth, which have direct effects on local blood flow at the BBB (Toda et al., 2009). At the BBB, NO appears to have functional and protective roles as well as deleterious effects depending on its source and the state of brain and cerebrovascular health. As well as acting upstream of smooth-muscle cells to induce vasodilation, NO from eNOS which is highly expressed at caveolae of BMECs via palmitoylation with caveolin proteins, appears to be involved in regulating transendothelial permeability during endocytotic and transcytotic events (Thiel and Audus, 2001). This was demonstrated by (Schnitzer et al., 1996) *in situ* and *in vitro* with rat models who showed the hydrolysis of GTP by NO activated cGMP was crucial in the fission of caveolae away from the plasma membrane. NO was shown in an *in vitro* rat co-culture model (astrocytes and BMECs) to scavenge ROS during hypoxia and reoxygenation events, protecting the BBB at a functional and molecular level (Utepbergenov et al., 1998). NO, has also been shown in patch-clamp electrophysiology work, to party regulate BMEC membrane hyperpolarisation *in vitro* by regulating inward ionic currents (Janigro et al., 1994).

As well as its important physiological roles, NO is implicated in several cerebrovascular and brain pathologies. Neurodegenerative diseases such as Parkinson's disease (PD), Alzheimer's disease (AD) and Huntington's disease (HD) and cerebrovascular diseases such as ischemia and stroke, all exhibit a varying degree of oxidative stress, producing free radicals which can form $ONOO^-$ – a powerful oxidant that modifies lipids and proteins by nitration (see (Guix et al., 2005) –- upon reaction with NO. The source of this NO is believed to be iNOS, the inducible form of NOS which is only expressed during a pro-inflammatory response, which is a hallmark of neurodegenerative disease (Thiel and Audus, 2001). In mouse BBB cells *in vitro*, NO has been shown to increase permeability by interactions with TJ proteins (although a mechanism wasn't demonstrated) and inhibit P-gp efflux of a well characterised P-gp substrate rhoadamine 123, which was believed to be a result of an ATP production decrease due to the inhibition of glycolytic enzymes (Yamauchi et al., 2007). NO alongside $ONOO^-$ can function as downstream effectors of tissue plasminogen activator (tPA, a serine protease involved in blood-clot metabolism) mediated excitotoxicity, which results in neuronal cell death and BBB breakdown *in vivo* (Parathath et al., 2006). However, it is important to point out that $ONOO^-$

also has conflicting data regarding its toxicity and has been demonstrated to convey a neuroprotective role against NO-mediated apoptosis (Garcia-Nogales et al., 2003).

The source of NO and the health state of the brain may explain conflicting data pointing to positive and negative roles of NO in brain and cerebrovascular pathologies, and this provides compelling reason to further understand the mechanisms and physiology of NO, to assist therapeutic intervention.

1.9.8. Asymmetric dimethylarginine

The first described competitive NOS inhibitors were L-arginine analogues: N^G-monomethyl-L-arginine (L-NMMA), N^G-nitro-L-arginine (L-NNA) and its methyl ester (L-NAME), and N-iminoethyl-L-ornithine (L-NIO) (Rees et al., 1990). Around the same time, another related L-arginine analogue with perhaps more clinical relevance was discovered (figure 1.11). This molecule, N^G,N^G-dimethylarginine or asymmetric dimethylarginine (ADMA) (isolated in 1987 (Ogawa et al., 1987a)) was first demonstrated to inhibit NOS activity (Vallance et al., 1992b, Vallance et al., 1992a). Since these early data, there have been over 1500 peer-reviewed publications relating to 'asymmetric dimethylarginine' with the number increasing annually (NCBI PubMed searches December 2011).

ADMA potently inhibits all NOS isoforms in a competitive manner by competing with L-arginine for the NOS binding site (Siroen et al., 2006) with reported inhibition constants (K_i) of 0.4µmol/L for nNOS (Kielstein et al., 2007), 0.9µmol/L for eNOS (Anderssohn et al., 2010) and 3.9µmol/L for iNOS (Tsikas et al., 2000).

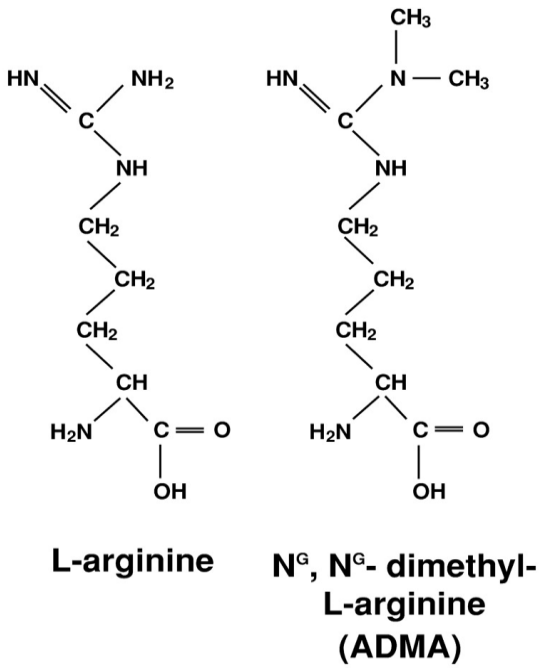

Figure 1.11. The chemical structures of L-arginine and ADMA. Despite their similarity, L-arginine is the primary substrate for all forms of NOS, whereas ADMA is a potent inhibitor for all forms of NOS. Picture adapted from (Boger, 2003).

1.9.9. Production of ADMA

ADMA, along with L-NMMA and the closely related symmetric dimethylarginine (SDMA, which does not inhibit NOS but is a marker of renal failure (Kielstein et al., 2006b) are endogenously produced as a result of proteolysis of methylated arginine residues on proteins by a group of enzymes referred to as protein-arginine methyltransferases (PRMTs) (Leiper and Vallance, 1999, Pope et al., 2009). These methylarginines are continuously produced intracellularly by PRMTs during normal protein turnover, with the primary protein source being nucleolar proteins (Leiper and Vallance, 1999, Zoccali, 2006b). PRMTs methylate the guanidino group of arginine residues on proteins (Rawal et al., 1995), which are then hydrolysed, forming the methylarginines (Zoccali et al., 2007).

There are currently 11 PRMTs in mammals, 9 of which exhibit PRMT activity and are divided into type groups depending on their catalytic capabilities (Krause et al., 2007). Type I PRMTs catalyse the production of ADMA, type II PRMTs, SDMA, and both types catalyse L-NMMA production (Bedford and Richard, 2005). The methylation of protein-arginine residues is a

wide-spread post-translational method of protein modification involved in a wide variety of cell functions which include subcellular protein localisation, protein-protein interactions and signal transduction (see (McBride and Silver, 2001) for a detailed review). With no other synthetic route of production identified, methylarginines only appear in the cytosol as a result of PRMT methylation and protein degradation, meaning their presence is governed by protein turnover, clearance and PRMT activity (Leiper and Nandi, 2011). Although ADMA is produced throughout in the body, the concentrations do vary in tissues, with the cardiovascular system and lungs major sources of ADMA due to their high expression of type I PRMTs (Bulau et al., 2007).

1.9.10. ADMA metabolism and clearance

From the 300µmol of ADMA produced daily in the human body, almost 80% is metabolised intracellularly and the remaining 20% is eliminated from the body by the renal route (Achan et al., 2003, Zoccali, 2006b). This metabolism was first demonstrated to be mediated by a group of intracellular enzymes called NG,NG-dimethylarginine dimethylaminohydrolases (DDAH) in 1987 (Ogawa et al., 1987a, Ogawa et al., 1987b), confirming the theory that a metabolic pathway must exist for ADMA following the observation that the amount of SDMA in urine was 30-fold higher than ADMA in rabbits (McDermott, 1976). DDAH activity has also been demonstrated against L-NMMA, but not SDMA which is almost completely cleared from the body through renal excretion (Richir et al., 2008).

DDAH is expressed as two isoforms (DDAH-1 and DDAH-2), both of which are responsible for ADMA catabolised at varying sites in the body (Leiper et al., 1999) although which isoform is the most responsible is not known (Pope et al., 2009). The isoforms display a 62% AA sequence homology (Tran et al., 2003) and both catalyse the reaction of ADMA to L-citrulline and dimethylamine (Palm et al., 2007). DDAH-1 is widely expressed, especially in the kidney and liver – which are the major sites of ADMA metabolism (Nijveldt et al., 2003, Nijveldt et al., 2004) – but also (to a lesser extent) in the brain, pancreas, and aorta (Palm et al., 2007). It has also been shown to be expressed in the vascular endothelium (Konishi et al., 2007). The high expression of DDAH-1 in the kidney and liver has lead to it being referred to as the 'guardian of circulating ADMA' (Palm et al., 2007). The expression of DDAH-1 is generally thought to be associated with tissues where nNOS expression is high, and the two enzymes have been demonstrated to co-localise (Leiper et al., 1999, Pope et al., 2009). Using purified recombinant

human DDAH-1 it has been demonstrated that DDAH-1 exhibits a K_m of 68.7µM and V_{max} of 356nmol/mg/min for ADMA (Forbes et al., 2008).

The DDAH-2 isoform is expressed predominantly in tissues associated with eNOS and has been shown to be complexed with eNOS in endothelial cells (Palm et al., 2007). DDAH-2 exhibits a 5.1-fold greater expression of mRNA over DDAH-1 (Wang et al., 2007) and overexpression of DDAH-2 and not DDAH-1 has been shown to reverse impaired NO production in endothelial cells (Lu et al., 2007). These observations nominate DDAH-2 as the predominant DDAH isoform in the vascular endothelium. It is highly expressed in the heart and also in immune tissues such as the thymus, lymph nodes and immune cells expressing iNOS (Tran et al., 2000). Recombinant human DDAH-2 has been shown to have a K_m of 16µM and V_{max} of 4.8nmol/mg/min for ADMA, demonstrating a kinetic rate 70 times less than DDAH-1 (Pope et al., 2009). This work is also supported by the observation that decreasing DDAH expression using small interfering ribonucleic acids (siRNA) against DDAH-1 in rats caused a 50% increase in plasma ADMA levels, but no change in plasma levels was observed with DDAH-2 down regulation, (although there was a 40% decrease in endothelium-dependent relaxation by 40%) (Wang et al., 2007). These observations suggest DDAH-1 could be the principle ADMA catabolising enzyme in the body.

It is worth mentioning that a separate ADMA and methylarginine catabolic pathway has been shown involving an enzyme called alanine-glycoxylate aminotransferase (Rodionov et al., 2010). This separate pathway however is believed to metabolise less than 20% of the total 80% of ADMA which is ultimately catabolised, meaning DDAHs play the major ADMA catabolic roles (Leiper and Nandi, 2011). Another important observation to report is that DDAHs can also exert effects independently of the ADMA-NOS pathway. This was recently demonstrated that DDAH2 can upregulate expression of VEGF through Sp1 transcription factor promoter activation *in vitro*, although evidence so far suggests this role is of less importance compared to its ADMA-NOS pathway role (Hasegawa et al., 2006, Leiper and Vallance, 2006).

The importance of DDAH in ADMA metabolism was calculated using estimates of daily protein methylation content and protein turnover in human plasma and urine from (Vallance et al., 1992a), which revealed that if ADMA metabolism did not occur there would be a 5µmol per L increase in plasma ADMA per day (Achan et al., 2003). This value greatly exceeds the K_i values for all forms of NOS and would cause dramatic inhibition of NOS production and

signalling throughout the body. This highlights the importance of the ADMA-DDAH-NOS pathway (summarised in figure 1.12) and how imbalances could lead to adverse conditions.

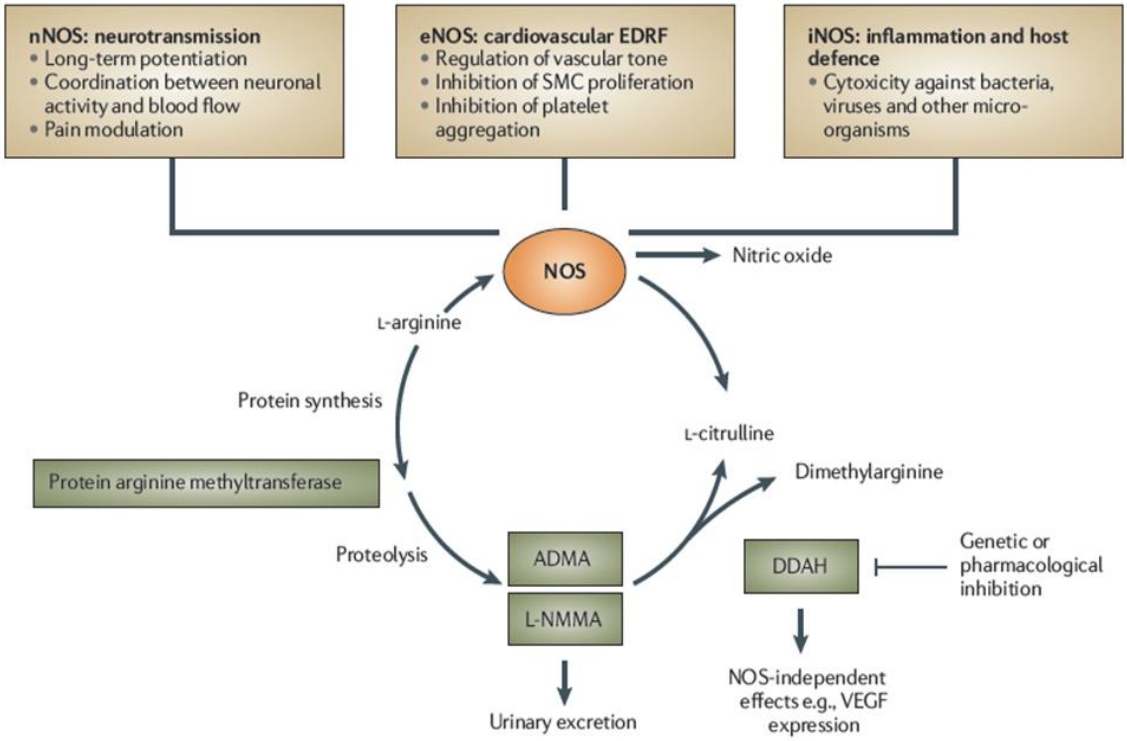

Figure 1.12. The ADMA-DDAH-NOS pathway. Nitric oxide (**NO**) synthesis is catalysed by three isoforms of nitric oxide synthase (**NOS**), neuronal NOS (**nNOS**), endothelial NOS (**eNOS**) and inducible/immune NOS (iNOS), which have varying tissue distributions. L-arginine residues incorporated into proteins can be methylated by protein arginine methyltransferases during normal protein turnover and degradation processes. Proteolysis of these arginine-methylated proteins release methylarginines into the cytosol. Two of these methylarginines, asymmetric dimethylarginine (**ADMA**) and N^G-monomethyl-L-arginine (**L-NMMA**) are potent competitive inhibitors of all forms of NOS. Both ADMA and L-NMMA are removed from the body through catabolism by dimethylarginine dimethylaminohydrolases (**DDAH**), and to a lesser extent, renal excretion. DDAH enzymes can induce physiological effects via NOS-independent pathways such as regulation of vascular endothelial growth factor (**VEGF**). **EDRF**, endothelium-derived relaxing factor; **SMC**, smooth muscle cell. Figure adapted from (Leiper and Nandi, 2011).

1.9.11. ADMA and the 'L-arginine paradox'

As the precursor for NO, L-arginine is crucial for normal NO production in physiology. It has also been widely used as a supplement to alleviate the effects of NO impairment in cardiovascular associated conditions such as hypercholesterolemia (Creager et al., 1992) and coronary artery disease (Yin et al., 2005). L-arginine induces widespread vasodilation in these conditions, improving blood-flow and endothelial dysfunction which is often associated with impaired NO production (Bode-Boger et al., 2007).

On closer inspection, when one observes eNOS enzyme kinetics combined with physiological concentrations of L-arginine, the observations are extremely puzzling. eNOS function should by fully saturated by both normal plasma and intracellular concentrations of L-arginine (Palm et al., 2007) (which are around 60-100μM in human plasma and range from 100-800μM in endothelial cells), as the enzyme has an L-arginine K_m of 2.9μM (Miner et al., 2004, Boger, 2007). Therefore, there should be more than sufficient amounts of L-arginine already present in patients – yet L-arginine increases NO production when supplemented. This curiosity has been named the 'L-arginine paradox' and there are two main theories that could explain the phenomenon.

One theory is that NOS activity is dependent on transport of extracellular L-arginine into the cell of – which has quick access to eNOS due to the close association of CAT-1 and eNOS – and is supported by observations *in vitro* showing eNOS activation in relation to increased L-arginine transport (Ogonowski et al., 2000, Miner et al., 2004). However, *in vivo* data is currently lacking. For this theory to work, it would be required that the intracellular L-arginine concentrations were compartmentalised away from eNOS, which could also explain why intracellular concentrations are significantly higher than extracellular concentrations. This compartmentalisation of L-arginine has been proposed with compelling *in vitro* data demonstrating not only did regeneration of L-arginine from exogenous citrulline did not alter bulk intracellular L-arginine concentrations, but all the enzymes involved in the regeneration were directly associated with eNOS in the plasma membrane sub-compartment, the plasmalemmal caveolae, in bovine aortic endothelial cells (Flam et al., 2001). The compartmentalisation of eNOS may allow cells to regulate the amount of active eNOS in contact with the CAT complex (Sbaa et al., 2005). Intracellular L-arginine levels are also regulated by the enzyme, arginase, which converts L-arginine to L-ornithine and urea and an increase in their activity in certain conditions (including hypoxia) could deplete the intracellular

L-arginine pools away from eNOS. Thus the intracellular arginine concentrations would no longer be saturating the eNOS activity and would make the enzyme sensitive to extracellularly-sourced substrate (Tousoulis et al., 2007).

The second theory involves ADMA. As a potent inhibitor of eNOS, an increasing amount of ADMA (associated with many conditions, see section 1.9.12) would increase the ADMA/L-arginine ratio, stopping the production of NO. L-arginine supplementation would therefore normalise the ratio by displacing ADMA from NOS, returning NO production to normal (Boger, 2004). This process has been observed in patients suffering with hypercholesterolemia, hyperhomocysteinemia and hypertriglyceridemia, adding weight to the theory (Boger et al., 1998, Lundman et al., 2001, Sydow et al., 2003). It is possible that due to the sensitivity of CAT-1 to *trans*-stimulation, and the similarity of L-arginine and ADMA, that L-arginine uptake could be stimulated by an increasing presence of intracellular ADMA, and conversely an increasing extracellular concentration of L-arginine could stimulate the cellular exit of ADMA (Bode-Boger et al., 2007). However, there is currently no published experimental data demonstrating this.

1.9.12. ADMA in health and disease

If ADMA has a deliberate role in normal physiological processes is open to debate. Most believe it does not – that ADMA is merely a by-product of protein methylation – but it has been suggested that ADMA could be a mediator of vascular tone regulation through the inhibition of eNOS, resulting in vasoconstriction (Zoccali, 2006a). It was demonstrated in guinea pigs that a 10μM plasma concentration of ADMA is sufficient to increase blood pressure by 15% (Vallance et al., 1992a), although under normal healthy conditions ADMA plasma concentrations range from 0.5–1μM in humans (with similar concentrations in other mammals) (Lajer et al., 2008, Wang et al., 2008, Wang et al., 2009). Although, these healthy plasma concentrations are just sufficient to inhibit eNOS and nNOS, they are well below the K_m and V_{max} for both isoforms of DDAH (as mentioned in 1.9.11) and so unlikely to cause effects through the NOS pathway. Instead, it is the intracellular concentrations of ADMA which may play more of a role in physiological and pathophysiological processes. It has been demonstrated that the intracellular levels of ADMA from aortic endothelial cells were up to 10 times more that those in plasma (Masuda et al., 1999). Similar intracellular concentrations were observed in freshly isolated rat brain slices (Cardounel and Zweier, 2002). These

concentrations would be more than sufficient to inhibit NO production, especially if DDAH activity was impaired.

DDAHs are extremely sensitive to oxidative stress due to the presence of a sulfhydryl group on a cystine residue in their active sites (Knipp, 2006). The non-protein amino acid homocysteine has been demonstrated to oxidise this group, inhibiting DDAH-1 *in vitro* (Stuhlinger et al., 2001). Oxidative stress can result from many conditions with ADMA itself able to induce superoxide production. During conditions of BH_4 depletion (critical cofactor in NO production, see figure 1.10), ADMA has been shown to uncouple eNOS, which causes NO production to be replaced by the production of superoxides, which inhibit DDAH and in-turn cause an increase in ADMA (Druhan et al., 2008). This cycle is therefore able to perpetuate production of oxidative stress in endothelial cells, leading to endothelial dysfunction, a feature associated with many diseases where ADMA is at extracellular pathophysiological concentrations (Chen et al., 2008). These concentrations vary depending on the model and disease itself, but generally, a plasma concentration of around 2-5μM is reported in human pathologies (Boger, 2003, Boger and Ron, 2005, Bode-Boger et al., 2007, Teerlink et al., 2009). If these levels are high enough to induce or mediate pathophysiology *in vivo* remains uncertain, but they are unlikely to be high enough to cause any problems for DDAH metabolism, under normal healthy conditions. What may be more important regarding ADMAs role in disease are the intracellular levels (as mentioned previously), but these have not been thoroughly researched and remain an enticing line of investigation.

It is also apparent that some conditions can upregulate the expression and activity of PRMTs in the production of ADMA. It was demonstrated 2000 that both native and oxidised low-density lipoprotein (LDL) cholesterol can upregulate activity of PRMTs in primary human endothelial cells, increasing production of ADMA (Boger et al., 2000), although the mechanism itself was not demonstrated. This finding could be very important, particularly in cardiovascular disorders where LDL cholesterols are well known mediators of disease.

The metabolism of ADMA by the DDAHs may be an important regulator of endothelial permeability. It has been demonstrated that ADMA metabolism is able to determine pulmonary endothelial barrier function by modulation of small guanosine triphosphatases (GTPases), which are known regulators of cell adhesion through the organisation of junctional proteins and cell cytoskeleton proteins (Spindler et al., 2010). ADMA has been shown to

differentially regulate known actin dynamic regulators RhoA, Rac1 and Cdc42 *in vitro* (Wojciak-Stothard et al., 2007). The authors of this work later described how ADMA down regulated Rho GTPase Rac1 activity in confluent monolayers of pulmonary endothelial cells and *in vivo* (both models deficient for DDAH-1) which resulted in an increase in paracellular permeability, through a protein kinase G (PKG) and NO pathway, involving vasodilator-stimulated phosphoprotein (VASP) and independent of ROS formation (Wojciak-Stothard et al., 2009). VASP link intercellular junction proteins and integrins with the actin cytoskeleton, under close association with Rac1, and changes in the phosphorylation of VASP by PKG have previously been shown to increase permeability (Benz et al., 2008). The authors stipulated that the increase in permeability induced by VASP could involve interactions with the TJ protein ZO-1, which was previously shown with protein kinase A (Comerford et al., 2002).

Pathophysiological concentrations of ADMA appear sufficient enough to elicit human coronary and endothelial gene expression *in vitro*. ADMA was demonstrated to induce substantial changes in gene expression at doses as low as 2µM, some of which were independent of the NO pathway, even in the presence of >300µM L-arginine. One of the genes affected by ADMA encoded PRMT enzymes, demonstrating ADMA may be able to induce its own production, although no mechanism was demonstrated. In this revealing study, the authors argued that these NOS-independent changes in gene expression could explain why supplementation of L-arginine is sometimes unable to reverse the effects of increased ADMA levels, which has been noted in ADMA-associated kidney failure (Smith et al., 2005).

As plasma ADMA levels are sourced from all over the body, they are good indicators of intracellular levels and therefore markers of dysfunction of the PRMT-ADMA-DDAH-NOS pathway. High levels of plasma ADMA have been the subject of intense study and are associated with a wide variety of diseases, in particular those affecting the cardiovascular, renal and hepatic systems and tissues with high NOS expression (Vallance et al., 1992a, Boger, 2003, Siroen et al., 2006, Anderssohn et al., 2010, Mookerjee et al., 2007). Please see the references in this section for more detail on ADMA in these conditions. For the purposes of this thesis, I will focus on the role of ADMA in brain and cerebrovascular disease.

1.9.13. ADMA and the brain

Rather than a disease 'cause or effect' argument, it is perhaps more appropriate to debate ADMAs 'marker or mediator' role, particularly since several recent works describing increased

ADMA levels in disease and decreased L-arginine/ADMA ratios (see table 1.2) have advanced the latter notions in brain and cerebrovascular disease.

Increased levels of ADMA have been noted in patients with AD. In perhaps the biggest study to date, (Arlt et al., 2008) demonstrated in 80 AD patients, an increase in plasma ADMA and a decrease in cerebrospinal fluid (CSF) levels compared to 80 control patients. These findings were similar in an earlier study using 25 AD patients and 25 controls (Selley, 2003). Both sets of authors argued that these finding could link ADMA to AD disease progression through an increase in NO production and oxidative stress in the cerebrovasculature and brain tissue. However, another study reported no such changes in ADMA concentrations in CSF or plasma (Mulder et al., 2002). These conflicting reports are likely due to the small cohorts used for the studies and as there are only a few groups looking into the associated of ADMA with AD, it requires further study to draw any accurate conclusions from these data.

The majority of ADMA data from brain studies relates to its role in cerebrovascular disease and endothelial dysfunction through inhibition of NO production. A recent MRI study was performed on over 700 Japanese patients, 146 of which were identified as having microangiopathy-related cerebral damage (MARCD), and whom had their ADMA plasma concentrations determined using high performance liquid chromatography. The authors discovered a significant increase in levels of ADMA (0.6 µmol/l from 0.5µmol/l in controls) and decreases in the L-arginine/ADMA ratio, between MARCD patients and controls, all of whom were from a similar ethnic section of society (Notsu et al., 2009). The authors pointed out that their findings supported earlier work showing how ADMA infusion induced a significant reduction in cerebral blood flow, without affecting overall blood-pressure in humans (Kielstein et al., 2006a), suggesting that both lines of evidence support a hypothesis that cerebral vasculature is either more sensitive to ADMA or has differing regulatory systems. This claim was supported by the authors of the original work, in a reviewer commentary titled 'ADMA and the Brain: An unfolding Story' (Kielstein and Kielstein, 2009). Notsu *et al*., continued that the fact that increases of plasma ADMA in most forms of vascular diseases (including cerebrovascular disease) are small in comparison to controls, suggests high sensitivity of the regulatory mechanisms involved, which in the brain is supported by the fact that nNOS is by far the most sensitive NOS to ADMA, a point demonstrated previously *in vitro* (Faraci et al., 1995). It has also been recently demonstrated that over expression of DDAH-1 in mice can reverse

neurovascular dysfunction induced by ADMA, emphasising the importance of functioning DDAH in the cerebrovasculature (Dayoub et al., 2008).

Associations between ADMA and stroke have also been made in numerous studies. Elevated ADMA plasma levels have not only been indicated as an independent marker of acute stroke and transient ischemic attacks (Wanby et al., 2006), but they have also been shown to be directly associated with an increased risk of stroke in elderly patients (Yoo and Lee, 2001). Kielstein et al., argued that this could be down to ADMA-induced arterial stiffness, an independent predictor of stroke related to NO availability (Wilkinson et al., 2002), which they then demonstrated in healthy volunteers by non-invasive pulse wave analysis (Kielstein et al., 2006a). In this way, ADMA was implicated as a mediator in the pathogenesis of cerebrovascular disease. Increased ADMA levels in CSF has also been associated with stroke severity (Brouns et al., 2009).

If DDAH activity was decreased or inhibited during a cerebrovascular disease, it is possible that elevated levels of ADMA could induce an increase in BBB permeability through interactions with small GTPases and junctional proteins, as described in section 1.9.12. This is an interesting hypothesis considering the increase in plasma ADMA seen in AD, stroke and cerebrovascular disease, the conditions of which (such as hypoxia or ROS formation) would be able to inhibit DDAH activity at the BBB and cerebrovascular system. As the largest surface area for molecular exchange in the brain, it is somewhat surprising that the interaction of ADMA with the BBB has not been directly studied, and this is particularly relevant with regards to the association of ADMA with stroke and cerebrovascular disease.

Table 1.2. The L-arginine/ADMA ratio in the plasma of patients with cerebrovascular complications. Adapted from (Bode-Boger et al., 2007).

Condition (n of patients)	L-arginine (μM)	ADMA (μM)	L-arginine/ADMA ratio ± SD	Reference
Healthy controls (average from 657 patients over 14 studies)	80	0.63	158 ± 28	(Bode-Boger et al., 2007)
Non-cardio-embolic infarction (239)	90	0.51	160 ± 60	(Bode-Boger et al., 2007)
Haemorrhagic stroke (22)	77	0.55	140 ± 34	(Bode-Boger et al., 2007)
Transient ischemic attack (31)	70	0.51	140 ± 31	(Bode-Boger et al., 2007)
Preeclampsia (67)	29	0.43	88.9 (range = 41 – 137)	(Maas et al., 2004)
Hypertension (13)	54	0.57	95 ± 22	(Palloshi et al., 2004)
Acute myocardial infarction (37)	99	3.04	34 ± 16	(Bae et al., 2005)
Hemodialysis (10)	66	2.2	32.6 ± 3.7	(Mochizuki et al., 2005)

1.9.14. Membrane transport of ADMA

As an analogue of L-arginine, ADMA is also hydrophilic and therefore expected to poorly cross cell membranes by diffusion alone. L-arginine utilises CAA membrane transport systems for cellular movement as mentioned in section 1.9.5, and therefore it is believed ADMA uses similar mechanisms. The fact that concentrations of ADMA fluctuate in plasma demonstrates that the molecule must be a substrate for cellular exit transport systems, as well as influx systems (which can be both as with system y^+), which allow the induction of the effects of administered and endogenously produced ADMA.

System y^+ is the only CAA transport system which is selective for CAAs and it helps to maintain a dynamic equilibrium between plasma and intracellular concentrations and so remains the most likely ADMA transport system. However, data elucidating ADMA transport is severely lacking, although there are several lines of indirect evidence using *in vitro* systems. Schmidt et al., demonstrated in a mouse glioblastoma cell line that related molecules L-NNA and the L-NMMA intermediate L-NMA could enter cells by system L and system y^+ transporters respectively (Schmidt et al., 1994) and showed this in a mouse glioblastoma cell line (Schmidt et al., 1995). Around the same time, it was demonstrated that ADMA inhibits CAT-1 in human endothelial cells and mouse macrophages, competing with radiolabelled L-NMMA (Bogle et al., 1995). Shortly afterwards, ADMA was shown to compete with L-arginine for entry to *Xenopus laevis* oocytes via human CAT-2B (Closs et al., 1997a), although the ADMA concentrations seen in physiological and pathophysiological conditions are unlikely outcompete physiological concentrations of L-arginine for transport. More recently, $ATB^{0,+}$ was demonstrated to transport ADMA and other methylarginines in a Na^+ dependent manner *in vitro* and when cloned and expressed in *Xenopus laevis* (Hatanaka et al., 2001).

Data describing ADMA transport mechanisms are important with respect to disease research and therapeutic intervention. This is because the transporters involved are also regulating factors in the physiological and pathophysiological effects of ADMA, along with PRMT production and DDAH metabolism. As well as increases or decreases in expression and activity of the ADMA producing and metabolising enzymes, increase and decreases in expression and function of CAA transporters are also regulable through physiological and pathophysiological events. Oxidative stress, tissue damage, cell growth and repair are all factors that can regulate expression and function of CAA transporters, as well as DDAHs and PRMTs (Teerlink et al., 2009). If function of CAA transporters were inhibited, it is likely

intracellular concentrations of ADMA would increase, perpetuating the effects of ADMA on NOS dependent and NOS independent pathways.

1.9.15. Endogenous molecule interactions at the BBB– a human *in vitro* BBB model

The study of ADMA transport at the BBB is unprecedented. However, the transport of CAAs has been well described at the BBB in a variety of mammalian models including primary human BMECs (Oldendorf and Szabo, 1976, Stoll et al., 1993, Sanchez del Pino et al., 1995, Pardridge, 1998, Omidi et al., 2003, Berezowski et al., 2004, Hawkins et al., 2006, O'Kane et al., 2006). Many investigations on the human BBB have used primary human BMECs as an *in vitro* model. However, primary BMECs are notoriously difficult to keep for more than a few passages before undergoing cellular senescence and are phenotypically unstable due to a failure to recreate the precise *in vivo* conditions they require to function and survive (Weksler et al., 2005). There are several immortalised human BMEC lines described in literature, but these have failed to gain widespread recognition as suitable immortalised human BBB cell lines due to their BBB phenotype specificity (Muruganandam et al., 1997, Gu et al., 2003, Kusch-Poddar et al., 2005, Ketabi-Kiyanvash et al., 2007). However, there is one well characterised immortalised human *in vitro* BMEC cell line – the human cerebromicrovascular endothelial cell line (hCMEC/D3) – that retains many BBB specific traits over a large amount of passages.

The hCMEC/D3s were derived from brain tissue obtained following surgical excision of an area from the temporal lobe of an adult female with epilepsy carried out at King's College Hospital, London, in accordance with the guidelines of the Local Ethics Committee and research governance guidelines. It is now a commercially available cell line. The isolated cells were immortalised via lentiviral transduction of the catalytic subunit of human telomerase to prevent telomere shortening, and the oncogene SV40 large-T antigen, which transforms cell lines. The whole procedure is described in detail in the first paper describing the hCMEC/D3 cell line (Weksler et al., 2005) with further characterisation in subsequent publications (Cucullo et al., 2008, Forster et al., 2008, Poller et al., 2008, Mkrtchyan et al., 2009, Tai et al., 2009c, Carl et al., 2010). The hCMEC/D3 cell line is considered to be the most promising immortalized human BBB cell line available today, exhibiting many of the characteristics that are essential for a good predictive BBB in vitro model (Weksler et al., 2005, Poller et al., 2008). These include expression of tight junction proteins and polarized expression of multiple ABC/SLC transporters (Dauchy et al., 2009, Tai et al., 2009c).

The hCMEC/D3 cells are the most suitable and user friendly human in vitro BBB model available to date and as such were chosen for the work in this thesis.

1.9.16. Endogenous molecule interactions at the BBB– aims:

Plasma concentrations of ADMA are increased in several brain and cerebrovascular disorders indicating underlying roles for ADMA regulation in CNS disease pathogenesis. This is made even more interesting considering the high sensitivity of the cerebrovasculature and nNOS to ADMA concentrations combined with the fact that the brain is a major source of ADMA as well as site of DDAH-1 expression. It has also been demonstrated that in the peripheral endothelium, ADMA has been shown to induce endothelial dysfunction, altering endothelial permeability. These situations provide an exciting platform for the research detailed in this thesis, which have been investigated using the hCMEC/D3 human *in vitro* BBB model.

The aims of this thesis are to:

1) investigate the effects of ADMA on the integrity of the human BBB *in vitro*;
2) elucidate the transport mechanisms utilised by ADMA at the human BBB and compare them to those used by L-arginine;
3) investigate whether
    a. intracellular ADMA can *trans*-stimulate the transport of extracellular L-arginine into the hCMEC/D3s;
    b. extracellular L-arginine can *trans*-stimulate the transport of intracellular ADMA into the hCMEC/D3s;
4) explain the role of ADMA in the L-arginine paradox.

1.10. Exogenous molecule interactions at the BBB – Drug transport

As the largest continuous cell surface area in the brain, the BBB represents a gateway, not just for endogenous molecules and nutrients, but also for exogenous therapeutics. With an aging population, there comes an increase in neurological and neurodegenerative disease prevalence. This has resulted in an increased need to deliver therapeutic drugs to the brain and as such the BBB is likely to become an even more important area for future research in both academic institutions and the biopharmaceutical industry. When compared to cardiovascular and cancer acting drugs, CNS acting drugs have an extremely low clinical trial success rate, and this is mostly due to the presence of the BBB (Alavijeh et al., 2005) (figure 1.13).

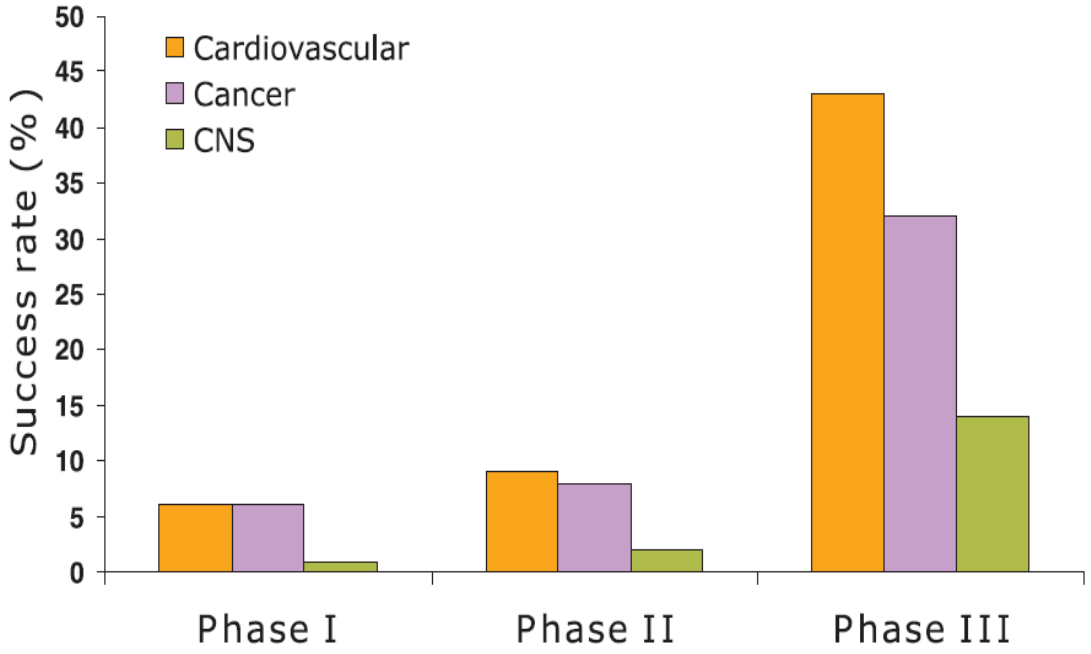

Figure 1.13. Cumulative success rates of drugs through clinical trials to market by therapeutic area. Figure taken from (Alavijeh et al., 2005).

It is estimated that up to 98% of all small molecule drug candidates fail to cross the BBB (Pardridge, 2002) and thus it remains a major challenge not only scientifically, but financially to design drugs for brain delivery. As a result of this low success rate, and despite its importance, it is apparent that <1% of biopharmaceutical companies have an active BBB drug targeting programme, with the number of academic research programmes studying the BBB also low (Pardridge, 2005). These figures are alarming when considering the amount of drugs currently

used to treat CNS conditions. It is therefore likely that a lack of understanding about how these drugs interact with the BBB is hindering their efficacy. This accentuates the need to understand and exploit the basic BBB properties for efficacy to be improved. A current example of this situation can be found in sub-Saharan Africa.

1.10.1. Human African Trypanosomiasis

Human African trypanosomiasis (HAT) is a neglected, zoonotic parasitic disease that affects the rural populations in 36 countries, of sub-Saharan Africa (see (Brun et al., 2010) for details of epidemiology). There are currently about 10,000 reported cases of HAT per annum (WHO, 2010) and that 48,000 people died from the disease in 2008 (WHO, 2009). It is caused by *Trypanosoma brucei gambiense* (*T. b. gambiense*) and *Trypanosoma brucei rhodesiense* (*T. b. rhodesiense*), two species of parasitic flagellate protozoans belonging to the genus *Trypanosoma* that occupy distinct geographical regions (Burri and Brun, 2003) and cause different symptoms (Kuepfer et al., 2011).

The parasites partially develop in and are transmitted by blood-feeding tsetse flies of the genus *Glossina* which feed on a variety of mammals (which themselves act as reservoirs for the parasites), thereby acting as both an intermediate host and a vector for the disease. The life cycle of the parasite is summarised in figure 1.14 below.

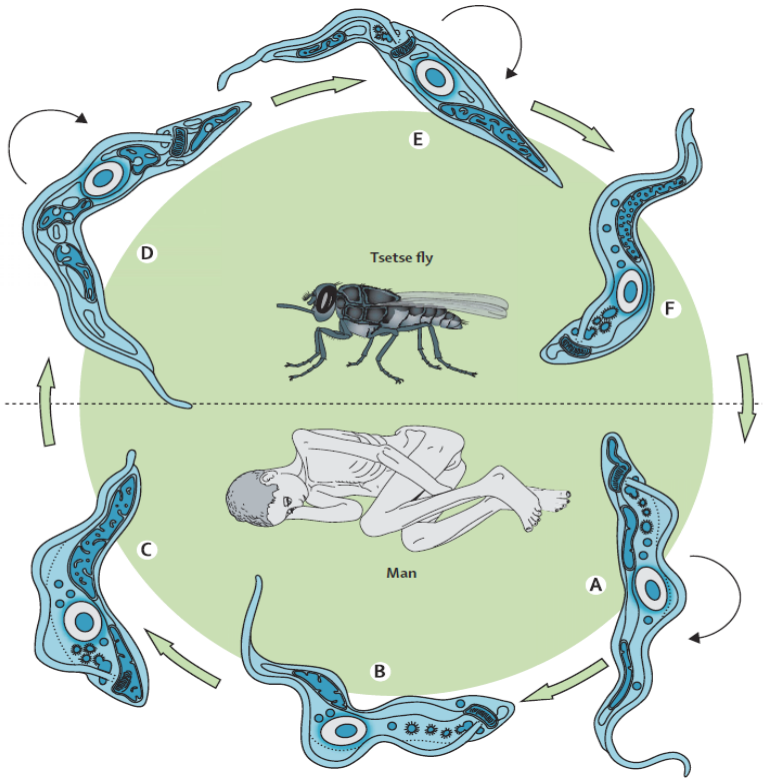

Figure 1.14. The life cycle of African trypanosomes. In man, the bloodstream forms of trypanosomes show a polymorphism with (A) dividing (black arrows) 'slender' forms, (B) 'intermediate' forms, and (C) 'stumpy' forms. In the tsetse fly vector/intermediate host, bloodstream forms of trypanosomes transform to (D) dividing midgut forms, then (E) the migrating epimastigote forms, which develop in the salivary glands to (F) the infective metacyclic forms, which are injected into the blood of the mammalian host during fly feeding. Taken from (Brun et al., 2010).

The clinical features of HAT arise from the two distinct stages of infection and disease progression. The first stage (S1) of HAT is known as the haemolymphatic stage and characterised by the presence of trypanosomes in the blood and lymphatic systems of patients (Priotto et al., 2007). Initially, S1 is asymptomatic, but once the parasite numbers increase patients can suffer from chronic and intermittent fever, pruritus and lymphadenopathy (Brun et al., 2010). To avoid detection and eradication by the host immune system, trypanosomes are able to continuously change their variant glycoprotein coats, allowing them to persist in the blood and lymphatic systems (see (Donelson et al., 1998) for a in depth review of this process).

Depending on the parasite involved, progression to the second stage (S2) of HAT, also known as the meningoencephalitic stage, can occur months (*T. b. rhodesiense*) or years *(T. b. gambiense*) after the initial infection (Odiit et al., 1997, Checchi et al., 2008). S2 of HAT is characterised by trypanosome invasion of the CNS as the parasites cross from the blood to the brain by traversing the BBB and leakier BCSFB. How the parasites do this is an ongoing area of research with some groups reporting trypanosomes are able to cross the BBB by transcytosis without affecting TJ proteins (Mulenga et al., 2001) or by an unidentified mechanism involving the pro-inflammatory cytokine interferon gamma (IFN-γ) (Masocha et al., 2007). Other groups have shown during S2 infections with *T. b. brucei* (the infectious bovine form) in rodents that the BBB is damaged (Philip et al., 1994) and it has been shown that transient increases in BBB permeability allow movement of *T. b. rhodesiense* across the human BBB *in vitro* (Grab and Kennedy, 2008).

The trypanosome invasion of the CNS in S2 gives rise to a variety of debilitating CNS disorders. The hallmark of S2 is insomnia and changes in sleeping cycle which give the disease its nickname 'sleeping sickness'. Other neurological symptoms include tremor, limb paralysis, motor weakness and Parkinson-like movements due to muscular hypertension (see (Kristensson et al., 2010) for a detailed review on CNS conditions arising from HAT). These conditions are not seen in S1 and increase in severity with the duration and progression of S2, until the patient falls into a coma with death following shortly afterwards. The progression of S2 HAT varies depending on the parasite involved. Typically, *T. b. rhodesiense*-induced disease progresses more rapidly (Balasegaram et al., 2009).

For diagnosis of HAT, the card agglutination test for trypanosomiasis (CATT) is typically used, particularly for *T. b. gambiense* infections which tend to be asymptomatic at S1 (Chappuis et al., 2002). CATT is a fast and practical serological diagnostic test that allows many individuals to be rapidly screened with a good percentage of accuracy and sensitivity (Checchi et al., 2008). Enzyme-linked immunosorbent assays are also used along with microscopic examination of lymph node aspirate and/or blood for more accurate confirmation of parasites (Brun et al., 2010). For S2 HAT, a lumbar puncture is required for CSF inspection. According to recommendations by the World Health Organisation (WHO), the presence of trypanosomes or more than 5 white blood cells per µl or CSF, or increased protein content (>370µg/µl) defines S2 (Brun et al., 2010).

HAT is 100% fatal if left untreated, which is of particular significance when considering not only the resource-poor setting of sub-Saharan Africa, but the initial asymptomatic disease manifestation meaning people do not seek medical intervention until the disease proper has manifested. It is lapses in disease surveillance that appear to be the main reasoning behind re-emergence of HAT as it believed to be an eradicable disease by the WHO. This relationship is displayed in figure 1.15 below.

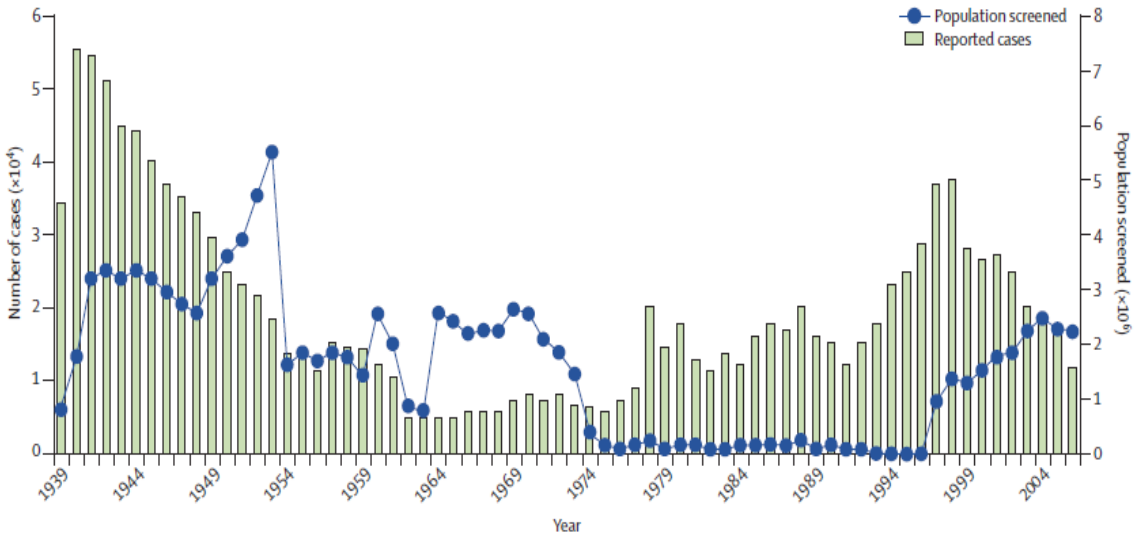

Figure 1.15. Comparison between new cases of *T. b. gambiense* infection and populations placed under surveillance. The number of reported cases (green bars) and populations screened (blue circles) in Africa between 1939 and 2004. Figure taken from (Brun et al., 2010).

1.10.2. Treatment of HAT

A small number of drugs are available for the treatment HAT, depending on the stage of disease. Pentamidine and suramin are used for S1, and melarsoprol, eflornithine and nifurtimox for S2 (see figure 1.16 for their respective chemical structures). All of these drugs are donated to the WHO by the manufacturers (Brun et al., 2010). Information on S1 and S2 acting drugs against *T. b. rhodesiense* or *T. b. gambiense* and summarised in table 1.3. Following the drug descriptions below, information on their transport at the BBB is discussed in section 1.10.9.

1.10.3. Pentamidine

Pentamidine ($C_{19}H_{24}N_4O_2$ MW = 240.42 g/mol) is an aromatic diamine [1,5-bis (4-amidi-phenoxypentane]) and the current drug of choice for S1 HAT caused by *T. b. gambiense*. It was

developed after a related compound, known as synthalin, was shown to have anti-trypanosomal activity (Sands et al., 1985). Injected intramuscularly, pentamidine is water soluble and exhibits a slow anti-trypanosomal action against *T. b. gambiense* (Docampo and Moreno, 2003). By reaching high concentrations in the parasite it is believed that pentamidine inhibits multiple cellular targets in the parasites such as selectively inhibiting the plasma membrane transporter Ca^{2+}-ATPase (Benaim et al., 1993), although the precise mechanisms of the anti-trypanosomal action has yet to be fully elucidated. Pentamidine accumulation within the parasite involves multiple transporters such as the P2 adenosine transporter which demonstrates affinity for adenosine and polyamines. Therefore it is believed that transporters are likely crucial to its mode of action of the drug as well as in its delivery (discussed further in section 1.10.9) (Basselin et al., 1997, Sanderson et al., 2009). Although generally well tolerated by patients, pentamidine can induce adverse reactions including diarrhoea, injection site pain and nausea. Drug resistance against pentamidine has also been identified with the loss of P2 function also involved here (please see (Gehrig and Efferth, 2008) for a recent review of drug resistance amongst trypanosomes).

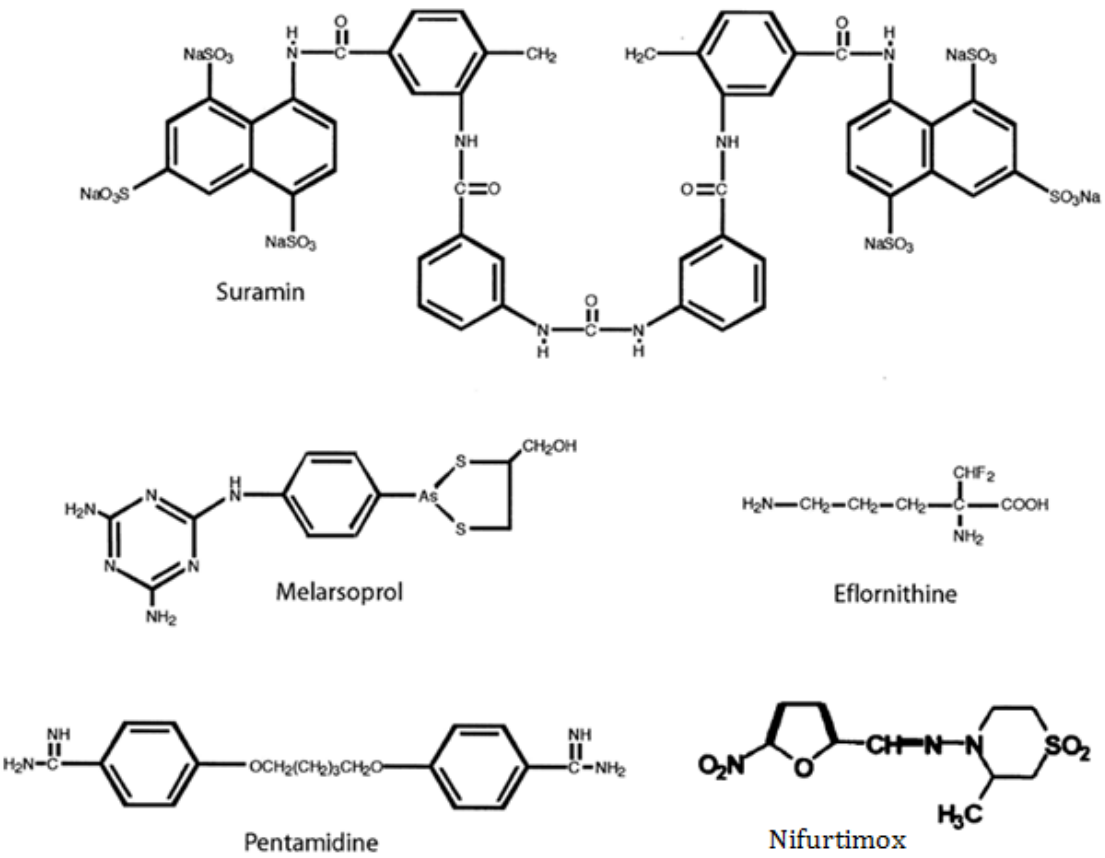

Figure 1.16. Drugs available for treatment of S1 and S2 HAT. Adapted from (Docampo and Moreno, 2003).

1.10.4. Suramin

Suramin ($C_{51}H_{40}N_6O_{23}S_6$ MW = 1297.29 g/mol) is a symmetrical polysulfonated naphthylamine polyanionic compound that is the current first choice S1 treatment drug used in infections by *T. b. rhodesiense*. It is a potent anti-trypanosomal drug which has been in use since 1922 (Docampo and Moreno, 2003). The potency of the drug gives patients severe adverse reactions (which include hypersensitivity reactions and peripheral neuropathy), and due to its extremely short half-life in air (must be solubilised in water) it must be intravenously injected rapidly after preparation over a lengthy treatment regime, which can last up to 30 days (Brun et al., 2010). Suramin is believed to exhibit its anti-trypanosomal effects by binding to and inhibiting the parasite's glycolytic enzymes (Wang, 1995).

1.10.5. Melarsoprol

Melarsoprol ($C_{12}H_{15}AsN_6OS_2$ MW = 398.341 g/mol), first used in 1949, is the most widely used drug is melarsoprol for S2 HAT induced by *T. b. rhodesiense* (Nok, 2003). The drug is poorly soluble in water, ether or alcohol and must be dissolved in propylene glycol before intravenous administration, with the solvent causing pain upon injection (Docampo and Moreno, 2003, Nok, 2003). As an organoarsenic derivative, melarsoprol is highly toxic to patients and adverse reactions to its administration are common. In 5-10% of cases, melarsoprol induces severe encephalopathic syndrome which causes death in 50% of these patients (Kennedy, 2004). This encephalopathic syndrome itself requires careful management through labour intensive means and drug treatment.

Melarsoprol is believed to work by inhibiting glycolytic enzymes as with suramin, but also by lysing the trypanosomes themselves, and it is believed this lysing action is a reason the drug is so toxic to patients (Balasegaram et al., 2005). It is also apparent that in some regions trypanosomes are developing resistance to melarsoprol, in which the trypanosome P2 adenosine transporter is implicated (Barrett et al., 2007).

Melarsoprol is also effective against *T. b. gambiense* but due to the toxicity of the drug in patients, eflornithine is the preferred alternative.

Table 1.3. Standard drugs used for treatment of stage 1 and stage 2 human African trypanosomiasis with adverse reactions. Adapted from (Brun et al., 2010).

Parasite species	Drug	Stage	Route of application	Dosing	Adverse drug reactions
Trypanosoma brucei gambiense	Pentamidine	1	Intramuscular	4mg/kg bodyweight at 24h intervals for 7 days	Hypoglycemia, injection site pain, nausea, diarrhoea, vomiting
	Eflornithine	2	Intravenous Infusion of >30 minutes	100mg/kg bodyweight at 6h intervals for 14 days	Diarrhoea, nausea, vomiting, convulsions; anaemia, leucopenia, and thrombocytopenia
	Melarsoprol	2	Intravenous	2.2mg/kg bodyweight at 24h intervals for 10 days	Encephalopathic syndromes, skin reactions, peripheral motoric or sensorial neuropathies
Trypanosoma brucei rhodesiense	Suramin	1	Intravenous	Test dose of 4-5mg/kg bodyweight at day 1, then five injections of 20mg/kg bodyweight every 7 days; maximum dose per injection 1g	Hypersensitivity reactions (acute, late); albuminuria, cylinduria, haematuria, peripheral neuropathy
	Melarsoprol	2	Intravenous	3 series of 3.6, 3.6, 3.6mg/kg bodyweight, the series spaced by intervals of 7 days; maximum dose per day 180mg	Encephalopathic syndromes, skin reactions, peripheral motoric or sensorial neuropathies

1.10.6. Eflornithine

Eflornithine (DL-alpha-difluoremethylornithine or DFMO, $C_6H_{12}F_2N_2O_2$ MW = 182.2 g/mol), has been nicknamed the 'resurrection drug' after its ability to revive comatose patients suffering from S2 HAT (Jennings et al., 1997). Initially synthesised as an anti-cancer drug, eflornithine has been used as a trypanocide since the 1980s as it inhibits the parasite's ornithine decarboxylase, a key enzyme in the synthesis of polyamines needed for cell proliferation and reduced production of the trypanosome specific redox active metabolite trypanothione (Vincent et al., 2010). Due to the short half-life of the drug, treatment with eflornithine requires an extensive administration process – 4 infusions of 100mg/kg body weight daily for up to 2 weeks is not uncommon (Burri and Brun, 2003). Despite this intensive treatment regime and although several side effects are apparent, eflornithine is generally tolerated well by patients and so is now the recommended treatment choice for *T. b. gambiense*, being active against both S1 and S2 forms of the parasite. Unfortunately, it is ineffective against *T. b. rhodesiense* due to the parasites resilience to the drug through the parasites high ornithine decarboxylase turnover (Iten et al., 1997). The drug is also expensive, and this is again unrealistic in a resource-poor setting. There have also been instances of eflornithine therapeutic failure with relapse rates of 8.1% reported, meaning eflornithine, along with melarsoprol, remain far from an ideal treatments for S2 HAT (Balasegaram et al., 2006).

1.10.7. Nifurtimox

Nifurtimox ($C_{10}H_{13}N_3O_5S$ MW = 287.293 g/mol), currently licensed for treatment of the closely related American trypanosomiasis (Chagas disease) caused by *Trypanosoma cruzi,* was originally only used in HAT for compassionate melarsoprol refractory cases (Pepin et al., 1989) but due to the limitations of melarsoprol and eflornithine, the drug has recently come into the fray for fighting both S1 and S2 HAT. Nifurtimox is a trypanocidal nitrofuran and has several advantages compared to the intensive intravenous administration regimes of the current S2 drugs, which are often accompanied by adverse reactions. These advantages include the facts that nifurtimox is orally active and considerably cheaper than current S2 drugs (Lutje et al., 2010) and that it is also effective against *T. b. gambiense* and *T. b. rhodesiense* (albeit to a lesser extent) (Haberkorn, 1979, Bouteille et al., 2003, Lutje et al., 2010). Despite these advantages, treatment with nifurtimox can also have toxic side-effects which include neurological aggravations such as headaches, confusion and sleep dysfunction as well as

nausea/vomiting and dyspepsia (Priotto et al., 2007). However, nifurtimox is generally better-tolerated than the other S2 HAT drugs, and many of the adverse condition associated are dose and duration dependent (Priotto et al., 2009).

1.10.8. Parasite resistance

Initiatives to counter the emergence of drug-resistant parasite populations, whilst improving efficacy and reducing the toxic side-effects of the anti-HAT drugs when used alone (monotherapy) have resulted in large-scale trials of combination therapy (CT). CT of suramin with the three S2-acting drugs has shown improved cure rates compared to monotherapy in rodent models (Clarkson et al., 1984, Raseroka and Ormerod, 1986, Jennings, 1993). Other results from human trials combination therapy of melarsoprol with nifurtimox (NMCT) and eflornithine (MECT) have demonstrated improved efficacy compared to melarsoprol monotherapy, but toxicity was still a major issue (Mpia and Pepin, 2002, Bouteille et al., 2003, Priotto et al., 2006). One large-scale trail started in 2003 and finishing in 2008 tested nifurtimox and eflornithine combination therapy (NECT) and concluded NECT had an improved toxicity profile and shortened treatment regime compared to eflornithine monotherapy (Priotto et al., 2009). The authors argued that despite a more complicated logistic implementation, NECT represented the best form of treatment for S2 HAT (Priotto et al., 2009). As a result, NECT is now the treatment of choice for S2 HAT caused by *T. b. gambiense* and implemented by the WHO (Simarro et al., 2011).

1.10.9. BBB transport of anti-HAT drugs

Besides slowing trypanosome drug resistance, the precise reasoning why CT improves drug efficacy against S2 HAT is not yet completely understood and led to the hypothesis that perhaps CT improves drug delivery to the brain (Enanga et al., 1998). This is of particular significance for S2 as the parasites are in the host CNS and for the drugs to be effective they must be able to cross the BBB. Despite this significance, interactions between S2 HAT-acting drugs and the BBB has been under-researched until fairly recently. This is even more alarming considering the fact that S2 HAT acting drugs are actively being used in the field.

Much of what was known about the ability of the trypanocidal drugs to cross biological membrane has been deduced from their chemical structures and lipophilicity. Pentamidine for instance, is hydrophilic and poor at crossing biological membranes, yet has been shown to accumulate in trypanosomes at concentrations in excess of 1mM, which suggests there is

facilitated diffusion for the drug (Damper and Patton, 1976a, Damper and Patton, 1976b). It has since been demonstrated that pentamidine requires the action of several polyamine and adenosine transporters in the outer membranes of parasites to enter and exhibit trypanocidal action including the adenosine insensitive high-affinity and low-affinity pentamidine transporters and the adenosine P2 transporter already mentioned (see (de Koning, 2001) for more detail).

As with pentamidine, suramin is poor at crossing intact biological membranes and it is believed the ability of trypanosome transporters to take up the drug from plasma owes to its success as a potent anti-trypanosomal agent. Because of its charged nature, suramin is able to bind to many serum proteins and it was suggested that perhaps it was transported into trypanosomes by binding to LDL and proceeding through RMT system and this was demonstrated in trypanosomes (Pal et al., 2002).

Due to their poor lipophilic properties, pentamidine and suramin are believed not to cross the BBB and as such are used in S1 treatment only, although this was not looked at directly until work by our group using *in situ* brain perfusion mouse models of trypanosomiasis. For suramin, our group investigated the ability of the drug to cross the mouse BBB and the effects of CT on its brain distribution. It was discovered that suramin poorly crossed the BBB and was not affected by the presence of other trypanocidal drugs or by P-gp knockout animals, confirming the suspicion that it is a not a suitable S2-acting drug (Sanderson et al., 2007). Conversely in similar experiments, it was discovered that pentamidine was able to cross the BBB, but a large proportion was retained in the mouse BMECs, meaning the concentration that reached the brain would be insufficient for effective parasite removal (Sanderson et al., 2009). It was also shown that pentamidine was a substrate for MRPs and P-gp as demonstrated using FVB-Mdr1a/1b (+/+) and FVB-Mdr1a/1b (-/-) mice and that CT with nifurtimox, suramin and melarsoprol caused changes in brain distribution of pentamidine (increase, decrease and decrease respectively). These data demonstrated unequivocally that pentamidine (and possibly melarsoprol and nifurtimox) interacted with transport systems at the BBB and CVOs, particularly efflux systems. It is interesting to point out that several ABC transporter genes have been discovered in trypanosomes (Maser and Kaminsky, 1998), although it has not been demonstrated if trypanosomes are able to efflux drugs through these mechanisms. The results regarding suramin are more equivocal however, as trail data has shown improved rodent cure rates with CT involving suramin (see 1.10.8). It is unlikely that suramin interferes with

transport mechanisms at the BBB to improve delivery and so perhaps drug-drug interactions (DDI) reduced the toxicity of the S2-acting drugs which saw cure rate increases.

Studies on melarsoprol distribution have revealed that the presence of its arsenoxide group confers lipid solubility, enabling BBB traversal (Pepin and Milord, 1994, Pepin et al., 1994). Melarsoprol is also transported into trypanosomes by the P2 adenosine transporter as with pentamidine and it is believed mutations in the transporter confer drug resistance to trypanosomes, but the utilisation of BBB transport mechanisms has not been demonstrated (de Koning, 2001). It therefore remains likely that it is the high lipophilicity of the drug allows it to cross the BBB to kill trypanosomes within the brain.

As a S2-acting drug, eflornithine was assumed to cross the BBB and has been shown to accumulate intracellularly to millimolar ranges in bloodstream forms of trypanosomes (Iten et al., 1997). The study by Iten and colleagues showed similar intracellular concentrations were reached at 4°C and 26°C, indicating that passive diffusion was the method as opposed to facilitated diffusion. However, the study only looked at 60 minute time points and not early stage time points, which give better indications of facilitated diffusion via transporters. Intracellular levels of a charged molecule such as eflornithine are unlikely to reach such levels by passive diffusion alone. On the contrary, in an earlier study, it was shown that eflornithine uptake in trypanosomes was indeed temperature dependent, reminiscent of transport activity (Bellofatto et al., 1987). Work by our group showed that eflornithine poorly traversed the murine BBB and perhaps this was an explanation as to why such an intensive treatment regime using this is necessary – to get sufficient quantities of eflornithine into the brain to exhibit trypanocidal effects (Sanderson et al., 2008). The data here also showed no interaction between P-gp and eflornithine, but that CT with suramin improved distribution of eflornithine into the brain, the mechanism of which is unknown, but may be evidence of RMT of LDL-suramin-eflornithine DDI complexes. CT with excess eflornithine, pentamidine, melarsoprol and nifurtimox caused no significant changes in brain distribution of eflornithine, suggesting a passive diffusion method of brain entry. However, perhaps a species difference in transporters could explain why eflornithine delivery to the brain is efficacious in humans but not mice, or that other transport systems are involved in eflornithine BBB transport that were not investigated.

As the name suggests, eflornithine is an analogue of the CAA ornithine and so this proposes that CAA transport systems could be involved in eflornithine transport at the BBB and in trypanosomes. Evidence for involvement of eflornithine in a CAA system was shown when ablation of the amino acid transporting gene *TbAAT6* in *T. brucei brucei* conferred them both viable and resistant to the action of eflornithine (Vincent et al., 2010). More recent evidence from genome-wide RNAi screens revealed a loss-of-amino acid transporter 6 (AAT6) function, representing not only a method of eflornithine entry into parasites, but another method of drug resistance (Baker et al., 2011).

With NECT becoming the treatment of choice for S2 HAT, our group also recently investigated the BBB-crossing abilities of nifurtimox, alone or in CT with other trypanocidal drugs. We showed that nifurtimox was highly lipophilic and able to cross the murine BBB, but was expelled by an unidentified efflux transport process not involving P-gp (Jeganathan et al., 2011). The research demonstrated that CT of nifurtimox with pentamidine increased the brain distribution of nifurtimox, which is interesting because not only was pentamidine previously demonstrated to be a P-gp substrate, but P-gp deficient mice caused no changes in the brain distribution of nifurtimox in the *in situ* brain perfusion model. That nifurtimox caused an increase in pentamidine brain distribution suggests a different transport system is at work as well as P-gp and provides an opportunity for novel investigation.

1.10.10. Exogenous molecule interactions – AIMS:

The fact remains that the difficulty of developing new drugs which are able to cross the BBB means it is unlikely that new S2 anti-HAT drugs will be developed in the near future. It is therefore crucial to understand the interactions of the HAT drugs with the BBB to improve their efficacy and harness all the potential CT has to offer.

By studying L-arginine and ADMA transport at the human BBB *in vitro* by using the hCMEC/D3 cell line, this project also aims to:

1) combine our lab expertise in anti-HAT drug delivery with the knowledge gained from CAA transport to research the possibility the eflornithine is a substrate for CAA systems;
2) follow on from our previous *in situ* research to investigate if CT alters delivery of both eflornithine and nifurtimox to the brain;
3) elucidate the efflux mechanisms utilised by the human BBB to expel nifurtimox compare with mouse data already published by our group.

Chapter 2. General Methods

2.1. The hCMEC/D3 cell line

2.1.1. Source

The hCMEC/D3 cells used in this thesis were provided by Professor Pierre O. Couraud (Institut Cochin, Université Paris Descartes, CNRS, Paris, France), Dr Ignacio Romero (The Open University, Department of Life Sciences, Walton Hall, Milton Keynes, UK), and Professor Babette Weksler (Weill Medical College of Cornell University, New York, New York, USA) under an academic material transfer agreement.

The production of the hCMEC/D3 cells is described in section 1.9.15 and also in the original publication (Weksler et al., 2005).

2.1.2. General culture conditions

The cells were cultured in 25cm^2 (T-25) or 75cm^2 (T-75) flasks (Thermo Scientific Nunc™, Thermo Scientific Nunclon™, Loughborough, UK), pre-coated for 2 hours at 37^{o}C with 0.1mg/ml of rat tail collagen type-I (Gibco, Invitrogen,) made in Hank's balanced salt solution (HBSS, Sigma Aldrich Company Ltd, Poole, UK) before being washed twice with Dulbecco's Phosphate-Buffered Saline with calcium, magnesium, but without phenol red (referred to as DPBS+) to remove suspended collagen.

During the seeding procedure, viable cell numbers were calculated using a haemocytometer with 0.4 % Trypan Blue solution (Sigma Aldrich Company Ltd, Poole, UK) and seeded at a density of 2.5 x 10^4 cells/cm^2, following media aspiration, washing with Dulbecco's Phosphate-Buffered Saline without calcium, magnesium and phenol red (referred to as DPBS-) and trypsinisation with 0.25% Trypsin-EDTA solution (both from Gibco, Invitrogen,). All hCMEC/D3s used in this thesis were between the passages of 25 to 35.

For routine culturing, hCMEC/D3 cells were grown using the Clonetics® EGM®-2MV BulletKit® (Lonza, Wokingham, UK). The kit contains endothelial basal medium (EBM-2) which was supplemented with the enclosed SingleQuots™ of insulin-like growth factor-1, vascular endothelial growth factor, epidermal growth factor, hydrocortisone and basic fibroblast growth factor (bFGF) according to the manufacturer's instructions and as previously described (Poller et al., 2008). Lonza has optimised the composition of this medium and so declined to disclose the concentrations of the supplements. Next, sterile filtered foetal bovine serum (FBS), also contained within the BulletKit®, was added to the media (becoming 2.5% of total

volume), along with penicillin-streptomycin (Gibco, Invitrogen, Paisley, UK) (also at 2.5%) and HEPES (Sigma Aldrich Company Ltd, Poole, UK) to 10mM. The final volume of the complete media was 500mls. Cells were grown in an incubator with a saturated humidity at 37°C in 5% CO_2 and 95% fresh air and grown to 80-90% confluency before seeding (after 3-4 days) with media changed every 2-3 days.

For storing, cells were frozen in 1ml aliquots in 95% FBS 'gold' (PAA the Cell Culture Company, Yeovil, Somerset, UK) with 5% dimethyl sulfoxide (DMSO, Sigma Aldrich Company Ltd, UK) for 24 hours at -80˚C, before being placed in liquid nitrogen. When growing stocks of cells (frozen cells stored in liquid nitrogen), the vials were thawed quickly in a 37°C water bath and the contents added with warm media to a collagen pre-coated flask and media was renewed after 24 hours, allowing time for cells to attach and debris and DMSO to be removed.

2.1.3. Culturing in 96-well plates

For experiments examining the accumulation and toxicity of molecules in the hCMEC/D3 cells, 96-well plates (Thermo Scientific Nunc™, UK) were pre-coated with 0.1mg/ml rat tail collagen type-I, and cells seeded and cultured as in section 2.1.2, except when 96 well plates were used for MTT assays assessing toxicity in permeability medium (see sections 3.2.2 for permeability medium description and section 2.5 for the MTT assay). They were then grown to 100% confluency (reached at 4-5 days) and left for a further 3 days before experimentation (therefore 7-8 days after initial seeding to allow contact inhibition of cells to initiate differentiation into BBB phenotype) with media changed every 2-3 days.

2.2. Accumulation assay

Drug accumulation experiments were performed on confluent monolayers of hCMEC/D3s, grown in the centre 60 wells of sterile 96 well plates (see figure below). The accumulation assays used in this thesis are a modified version of a previous assay developed by our group (Chishty et al., 2004). Medium was removed from wells and replaced with a 37˚C pre-heated 200µl aliquot of accumulation buffer consisting of sterile distilled water (dH_2O), 135mM NaCl, 10mM HEPES, 5.4mM KCL, 1.5mM $CaCl_2$, 1.2mM $MgCl_2$, 1.1mM glucose, all sterile filtered with a 0.2µm filter and purchased from Sigma Aldrich Company Ltd, Poole, UK and adjusted to pH 7.4 with 1M HCL. The stock solutions of these accumulation buffer components are described in appendix section 1.1. The radiolabelled test molecule (labelled with tritium, [^{3}H]), and carbon-14 labelled sucrose ([^{14}C]sucrose, which is a marker of non-specific binding and

extracellular space because it has no transporter at the BBB and crosses only in negligible amounts (Ennis and Betz, 1986), with or without unlabelled transporter inhibitor/substrate (see Table 2.1 below) were then added to the accumulation buffer.

Columns of wells (6 wells per column, 10 columns per plate) were exposed to the accumulation buffer for 1, 2.5, 5, 20 or 30 minutes. This allowed accumulation of the radiolabelled test molecules into the cells to be assessed. The accumulation assays were performed on a temperature-controlled shaker (THERMOstar, BMG Labtech, Offenburg, Germany) at 37˚C and 120 rpm. Once each column of cells had been exposed for the correct length of time to the radiolabelled test molecule containing buffer, the buffer was aspirated and wells were washed 3 times with ice-cold phosphate-buffered saline (PBS) 1x in dH_2O (diluted from a 10x stock solution, pH 7.4, purchased from Gibco, Invitrogen, Paisley, UK) to stop any membrane transport processes and remove radiolabelled study molecules and buffer that had not accumulated in the cells. The cells were then lysed by adding 200µl of 1% Triton x-100 in dH_2O (Gibco, Invitrogen, Paisley, UK) per well for 1 hour at 37°C to liberate any accumulated radiolabelled test molecules and solubilise the cell proteins. 100µl of fluid from each well was then added to a scintillation vial along with 4 ml scintillation fluid (Optiphase Hisafe 2, PerkinElmer, UK) and counted using a Packard Tri-Carb 2900TR liquid scintillation counter to determine the radioactivity of each sample in disintegrations per minute (dpm). The remaining 100µl in each well were used to perform a BCA protein assay, using the wells around the central 60 as standards (see section 2.3). The procedure is outlined in figure 2.1.

Table 2.1. A complete list of all transporter inhibitors and substrates used in this thesis.

Drug	Dissolved in DMSO?	Transporters affected*	Substrate or Inhibitor?	Source	Reference
α-methyl-DL-tryptophan	No	**$ATB^{0,+}$**	Inhibitor	**MP Biomedicals Europe, Cambridge, UK**	(Karunakaran et al., 2008)
BCH	No	**system L, system A, $ATB^{0,+}$**	Inhibitor Inhibitor Inhibitor	**Sigma Aldrich Company Ltd, Poole, UK**	(Zuzack et al., 1985, Yamauchi et al., 2009)
Dexamethasone	Yes	**P-gp** **system A**	Substrate Inhibitor	**MP Biomedicals Europe, Cambridge, UK**	(Nadziejko and Reichberg, 1984, Mason et al., 2008)
Haloperidol	Yes	**P-gp**	Inhibitor	**Sigma Aldrich Company Ltd, Poole, UK**	(Matsson et al., 2009)
Ko143	Yes	**BCRP**	Inhibitor	**Tocris Bioscience, Bristol, UK**	(Matsson et al., 2009)
L-arginine	No	**system y^+**	Substrate	**Sigma Aldrich Company Ltd, Poole, UK**	(O'Kane et al., 2006)
L-homoarginine	No	**system y^+**	Substrate	**Sigma Aldrich Company Ltd, Poole, UK**	(Kakoki et al., 2004)
L-lysine	No	**system y^+**	Substrate	**Sigma Aldrich Company Ltd, Poole, UK**	(O'Kane et al., 2006)
L-ornithine	No	**system y^+**	Substrate	**Sigma Aldrich Company Ltd, Poole, UK**	(Kakoki et al., 2004)

Drug	Dissolved in DMSO?	Transporters affected*	Substrate or Inhibitor?	Source	Reference
L-leucine	No	**system y^+L, system L, $ATB^{0,+}$**	Substrate	**Sigma Aldrich Company Ltd, Poole, UK**	(Rotmann et al., 2007)
Pheophorbide A	Yes	**BCRP**	Substrate	**MP Biomedicals Europe, Cambridge, UK**	(Weiss et al., 2007)
Indomethacin	Yes	**MRP1**	Inhibitor	**Sigma Aldrich Company Ltd, Poole, UK**	(Rosenbaum et al., 2005)
PAH	Yes	**OATs**	Inhibitor	**Acros Organics, Thermo Fisher Scientific, Loughborough, UK**	(Gibbs and Thomas, 2002, Sauer et al., 2010)
Probenecid	Yes	**MRP 1&2, OATs, OATPs**	Inhibitor Inhibitor Inhibitor	**Sigma Aldrich Company Ltd, Poole, UK**	(Gibbs and Thomas, 2002, Potschka et al., 2004, Jorgensen et al., 2007)
TCA	Yes	**OATPs**	Inhibitor	**Acros Organics, Thermo Fisher Scientific, Loughborough, UK**	(Gibbs and Thomas, 2002)

BCH - 2-amino-2-norbornanecarboxylic acid, **PAH** - para-aminohippuric acid, **TCA** – taurocholic acid. *at the concentrations used.

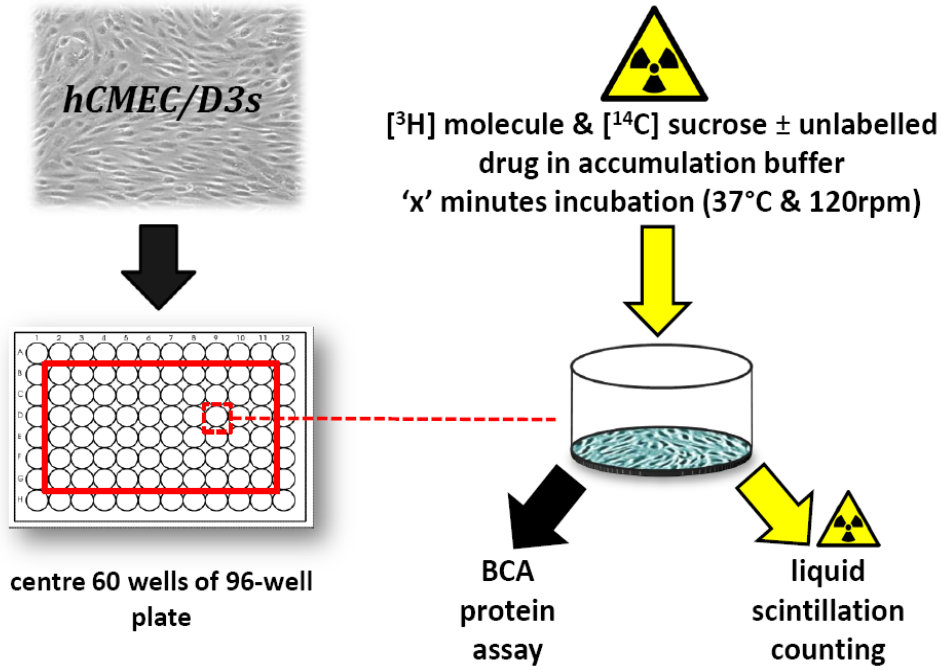

Figure 2.1. Schematic diagram illustrating the standard accumulation assay. Cells (**hCMEC/D3s**) were grown in the centre 60 wells of 96-well plates for 7-8 days before experimentation. The media was removed and replaced with accumulation buffer containing the **[^{3}H]**-labelled molecule of interest, **[^{14}C]sucrose** as a marker of non-specific binding and extracellular space, with or without a transporter inhibitor/substrate (**unlabelled drug** on diagram). The cells were incubated in this buffer for a varying time up to 30 minutes depending on the type experiment (**'x' minutes**) before being lysed with 200µl 1% Triton X-100 and taken for the **BCA protein assay** and **liquid scintillation counting**.

2.3. BCA protein assay

The Pierce® BCA protein assay (purchased from Thermo Scientific, Loughborough, UK) is a detergent-compatible kit using bicinchoninic acid (BCA) to colourimetrically quantify total protein from a sample. It is based on the reduction of Cu^{2+} to Cu^{1+} which in an alkaline environment reacts with BCA to produce a purple complex, whose absorbance can be read at 562nm in a spectrophotometer. The kit reagents, 'A' and 'B' (mixed at a 50:1 ratio) were added to 100µl bovine serum albumin standards (BSA in dH_2O) in empty wells on a 96-well plate, along with wells containing 100µl samples. The plates were then left at 37°C for 30 minutes and then read on a Labsystems Multiscan reader attached to a computer with Ascent

software. The protocol is outlined in detail in the manufacturer's 2011 instruction manual (http://genome.med.yale.edu/images/a/aa/BCA.pdf).

2.4. Expression of results

Total accumulation of the radiolabelled study molecule was calculated as the sum of accumulation and efflux and termed the volume of distribution (V_d). V_d is derived from the ratio of dpm/mg protein to dpm/µl buffer. The V_d values for ^3H molecules were always corrected with the V_d values for background radiation (accumulation buffer alone without radioactive drugs in scintillation fluid) and [^{14}C]sucrose, which was used as a marker of non-specific binding, barrier integrity and extracellular space.

2.5. (3-(4,5-Dimethylthiazol-2-yl)-2,5-diphenyltetrazolium bromide (MTT) cytotoxicity assay

The cytotoxic effects of the molecules used in this study were assessed using an (3-(4,5-Dimethylthiazol-2-yl)-2,5-diphenyltetrazolium bromide, a yellow tetrazole (MTT) assay, a colorimetric assay where MTT is reduced to form a purple formazan in living cells, which can then be dissolved and measured spectrophotometrically (Denizot and Lang, 1986). The assay was performed on confluent monolayers of cells in 96-well plates grown in the medium type used for the particular study under investigation (normal or permeability media).

Cells underwent incubations by the addition of a 200µl aliquot of accumulation buffer containing the radiolabelled and unlabelled test molecules into each well (see section 2.2). At the appropriate time, the buffer was aspirated and replaced with a 100µl aliquot of 1mg/ml MTT (Sigma Aldrich Company Ltd, UK) in Dulbecco's modified Eagle's medium (DMEM) without phenol red (Gibco, Invitrogen, UK). The cells were then placed for 4 hours at 37°C in an incubator, the solution was then removed and replaced with 100µl propan-2-ol (Sigma Aldrich Company Ltd, UK) per well, and the absorbance was measured at a wavelength of 560nm in the Multiscan reader with Ascent software as mentioned in section 2.3. Absorbance values were corrected by protein content (determined using the BCA assay described in section 2.3 on adjacent wells containing cells that were seeded at the same density) and expressed as percentage viability compared to control untreated cells.

2.6. Data analysis

Comparisons were made between control plates of cells and differences at $p < 0.05$ considered significant. Multiple-time accumulation, data were analysed by Two Way Repeated Measures ANOVA tests and Holm-Sidak posthoc tests, MTT assay and permeability assay data were compared against controls using One Way ANOVA and Bonferonni post-hoc tests using Sigma Plot version 11.0 software (SPSS Science Software UK Ltd, Birmingham UK). All data are expressed as mean ± SEM, except MTT data which are expressed as percentage viability.

2.7. SDS-PAGE and Western blotting

The expression of specific cell proteins under investigation were determined using the well known protein analytical techniques of sodium dodecyl sulphate polyacrylamide gel electrophoresis (SDS-PAGE) and western blotting (WB). These procedures allow cell proteins to be denatured and separated by their molecular weight, transferred to a membrane and detected with specific antibody probing (Towbin et al., 1979). The procedure is outlined in brief in figure 2.2 below. The whole protocol was developed with personal communication from Dr. Rachel Brown's WB protocol with permission and optimisation.

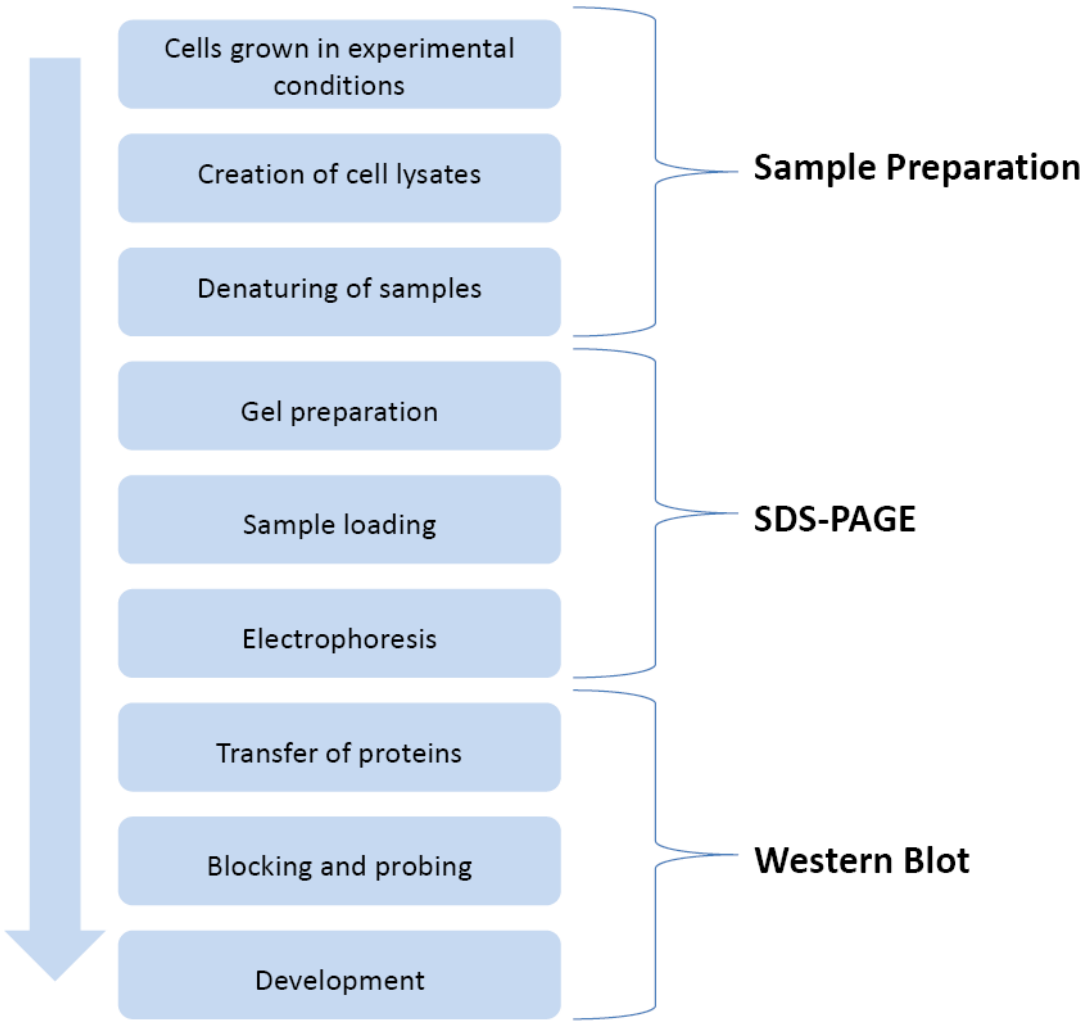

Figure 2.2. A schematic outlining the procedures of the protein analytical techniques of SDS-PAGE and western blotting, based on personal communication with Dr Rachel Brown.

2.7.1. Sample preparation

To validate protein expression during experimental conditions, cells were grown in 6-well plates (Thermo Scientific Nunc™, Thermo Scientific Nunclon™, Loughborough, UK) for the same time period and in the same media used in experiments (see results chapters), before being turned into lysates for SDS-PAGE and WB. Once this stage was reached plates were placed on ice, media was aspirated from cells, and they were washed twice (wash, aspirate) with ice-cold PBS. 200µl of ice-cold TGN lysis buffer consisting of 50mM Tris, 150mM NaCl, 10% glycerol, 50mM glycerophosphate B, 1% Tween-20 and 0.2% NP-40 (all purchased from

Sigma Aldrich Company Ltd, Poole, UK, see Appendix 1.2 for stock solution details) was then added to each well. The wells were then scraped repeatedly with a cold plastic cell scraper (Greiner Bio-One Ltd, Gloucestershire, UK) for several minutes and the cell suspension was transferred to a pre-cooled 1.5 ml tube along with a 1:100 aliquot of Proteoblock™ protease inhibitor cocktail (Fermentas Life Sciences, North Yorkshire, UK) and left on ice for 30 minutes, occasionally vortexed to maintain agitation and allow solubilisation of the proteins. The tubes were then centrifuged at 12,000 rpm for 20 minutes at 4°C using a Thermo Electron Corporation Heraeus Fresco17 bench-top micro-centrifuge. Following centrifugation, the supernatants were then aspirated into fresh pre-cooled 1.5 ml tubes on ice and the pellets discarded. The protein content of the supernatants was quantified using a BCA protein assay (section 2.3) and then stored at -20°C until use. Before SDS-PAGE, cell lysates were thawed at RT and had loading buffer added, before being boiled at 95°C for 5 minutes. The loading buffer was purchased from Fermentas (Fermentas Life Sciences, North Yorkshire, UK) in a 5x concentration and consisted of 0.313 M Tris-HCl (pH 6.8 at 25°C), 10% SDS, 0.05% bromophenol blue and 50% glycerol. 100µl of β-mercaptoethanol (Sigma Aldrich Company Ltd, Poole, UK) was added per 1 ml of the 5x loading buffer to act as a protein disulphide bridge reducing agent. This mix was added with a sample of the thawed cell lysate to become 1x. The buffer not only allows the lysates to be viewed easily for loading into and running through the gel, but denatures the proteins along with the boiling step, allowing smooth migration of the proteins down the gel, with their migration patterns dependant on molecular weight (MW).

2.7.2. SDS-PAGE

Prior to one-dimensional electrophoresis, 1mm polyacrylamide gels were prepared. Polyacrylamide gels form from the polymerisation of acrylamide with the cross-linking agent N, N-methlenebisacrylamide (Bis). The polymerisation is initiated with the addition of ammonium persulfate (APS) and N,N,N',N'-tetramethylenediamine (TEMED). Gels differ by the relative size of their pores which is determined by the total amount of acrylamide and cross-linker present. These differences are denoted as percentages. The lower the percentage, the larger the pores and so the easier it is for larger proteins to move through the gel during electrophoresis. Polyacrylamide gels consist of stacking gels where protein is loaded and separating gels where the proteins are separated by their MW. The % of separating gels varied depending on the protein under investigation. For most WBs a 10% gel was used (see appendix 1.3 for the recipe). But in some circumstances a precast 4-20% gel was used (Biorad Europe, Hemel

Hempstead, UK). The stacking gels used in all SDS-PAGE in this thesis were 4% (please see appendix 1.3 for the recipe). Separating gels were constructed in Biorad Mini-Protean 3 tanks and left to set for about 1 hour before stacking gels were set on top for a further hour, complete with plastic combs that formed the protein loading wells when removed. The gels were then placed in Biorad mini gel apparatus which was filled with running buffer (see appendix 1.3). Prepared samples (see previous section, 2.7.1) were then loaded into the wells along with Page Ruler™ Prestained 10-170 kDa Protein Ladder (Fermentas Life Sciences, North Yorkshire, UK) and electrophoresis took place once the power was switched on to 125V until the blue dye ran to the bottom (anode) of the gel. The gel was then removed, resized and prepared for the transfer stage.

2.7.3. Western blot

Once the gel was removed, it was soaked in transfer buffer (see appendix 1.3) for 20 minutes prior to the semi-dry transfer, using an Invitrogen Novex® Semi-dry blotter. While the gel was equilibrating, other components used to make the transfer sandwich (see figure 2.4), were prepared. Invitrogen filter paper was also pre-soaked in transfer buffer along with methanol-activated 0.45µm Immobilon-P polyvinylidene fluoride (PVDF) membrane (Millipore UK Ltd, Watford, UK). This membrane has a high affinity for amino acids and during the transfer, immobilises proteins to its surface which can then be probed with specific antibodies. Once all components were soaked, the sandwich was prepared carefully with a roller to remove any bubbles and the semi-dry blotter lid (cathode) was placed on top. Transfer commenced for 30-50 minutes at constant 25V.

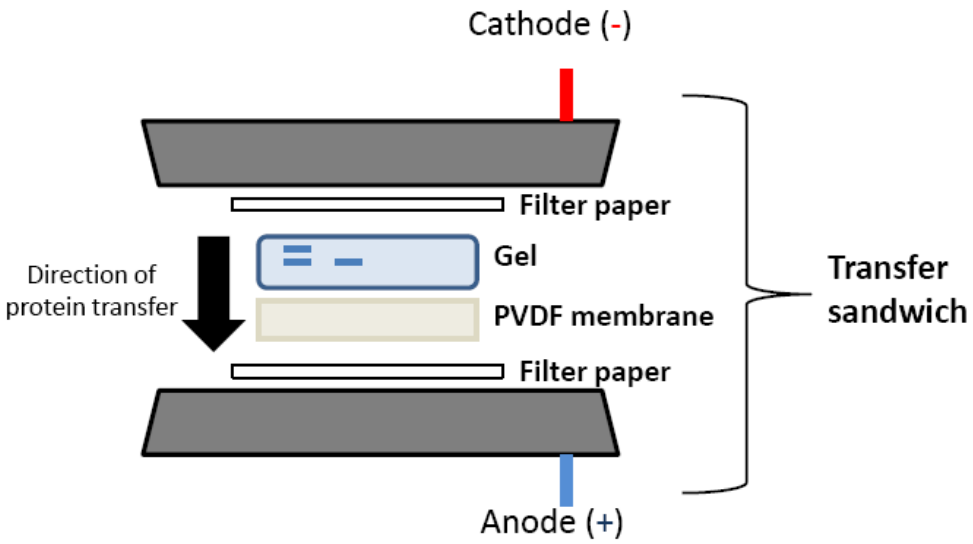

Figure 2.3. The transfer sandwich. A schematic of the semi-dry transfer sandwich set-up used to transfer proteins from polyacrylamide gels used in western blotting.

Following transfer, the PVDF membrane was removed and immediately incubated for 2 hours under constant agitation at RT in blocking buffer consisting of PBS-Tween (PBS-T, see appendix 1.3) with 5% milk powder, (Tesco, UK) to stop non-specific binding of the antibodies to the membrane. After blocking, membranes were washed twice with PBS-T and incubated with the necessary protein specific primary antibody (see Table 2.2) in PBS-T with 0.5% BSA overnight at 4°C under constant agitation. Following the overnight primary incubation, membranes were washed three times (20 minutes each time) in PBS-T, before being incubated with the appropriate horseradish peroxidise (HRP) conjugated secondary antibody (see table 2.2 below) for 1 hour at RT. HRP produces a detectable signal during enhanced chemiluminescence (ECL) which is visualised during the development phase.

Table 2.2. Details of antibodies used for protein expression studies.

Protein	Primary antibody	Secondary antibody WB	Secondary antibody IF
$ATB^{0,+}$	Rabbit anti-human SLC6A14/ $ATB^{0,+}$ polyclonal (MBL, Calteg-MedSystems Ltd, Buckingham, UK). **WB** dilution - 1:1000 in PBS-T with 0.5% BSA. **IF** dilution – 1:500 in PBS.	Goat anti-Rabbit HRP conjugated polyclonal (Abcam, Cambridge, UK). Dilution – 1:5000 in PBS-T with 0.5% BSA.	Goat anti-rabbit Alexa Fluor 488 conjugated (Invitrogen, Paisley, UK). Dilution – 1:200 in PBS.
BCRP	Mouse anti-human ABCG2/BCRP monoclonal [BXP-21] (Abcam, Cambridge, UK). **WB** dilution - 1:1000 in PBS-T with 0.5% BSA.	Rabbit anti-mouse HRP conjugated polyclonal (Abcam, Cambridge, UK). Dilution – 1:2000 in PBS-T with 0.5% BSA.	—
CAT-1	Rabbit anti-human SLC7A1/CAT-1 polyclonal (Abcam, Cambridge, UK). **WB** dilution - 1:250 in PBS-T with 0.5% BSA. **IF** dilution – 1:100 in PBS.	Goat anti-Rabbit HRP conjugated polyclonal (Abcam, Cambridge, UK). Dilution – 1:5000 in PBS-T with 0.5% BSA.	Goat anti-rabbit Alexa Fluor 488 conjugated (Invitrogen, Paisley, UK). Dilution – 1:200 in PBS.
DDAH-1	Goat anti-human DDAH-1 polyclonal (Abcam, Cambridge, UK). **WB** dilution – 0.2µg/ml PBS-T with 0.5% BSA.	Rabbit anti-goat HRP conjugated polyclonal (ProteinTech Europe, Manchester, UK). Dilution – 1:2500 in PBS-T with 0.5% BSA.	—
eNOS	Rabbit anti-human NOS3/eNOS polyclonal (BD Biosciences, VWR, Leicestershire, UK). **WB** dilution – 1:2000 in PBS-T with 0.5% BSA.	Goat anti-Rabbit HRP conjugated polyclonal (Abcam, Cambridge, UK). Dilution – 1:5000 in PBS-T with 0.5% BSA.	—

GAPDH	Mouse anti-human GAPDH monoclonal (ProteinTech Europe, Manchester, UK). **WB** dilution – 1:2000 in PBS-T with 0.5% BSA.	Rabbit anti-mouse HRP conjugated polyclonal (Abcam, Cambridge, UK). Dilution – 1:2000 in PBS-T with 0.5% BSA.	—
P-gp	Mouse anti-human MDR1/P-gp [C219] (Abcam, Cambridge, UK). **WB** dilution – 1:80 in PBS-T with 0.5% BSA.	Rabbit anti-mouse HRP conjugated polyclonal (Abcam, Cambridge, UK). Dilution – 1:2000 in PBS-T with 0.5% BSA.	—
VCAM-1	Mouse anti-human VCAM-1 [CD106] (Millipore UK Ltd, Watford, UK). **IF** dilution – 0.5µg/ml PBS.	—	Goat anti-mouse 546 conjugated polyclonal (Abcam, Cambridge, UK). Dilution – 1:1000 in PBS.
vWF	Rabbit anti-human vWF (Dako, Stockport, UK). **IF** dilution – 1:200 in PBS.	—	Goat anti-rabbit Alexa Fluor 488 conjugated (Invitrogen, Paisley, UK). Dilution – 1:200 in PBS.
ZO-1	Rabbit anti-ZO-1 (Abcam, Cambridge, UK). **IF** dilution – 1µg/ml in PBS.	—	Goat anti-rabbit 546 conjugated polyclonal (Abcam, Cambridge, UK). Dilution – 1:1000 in PBS.

ATB$^{0,+}$ *– amino acid transporter B$^{0,+}$,* ***BCRP*** *– breast cancer resistance protein,* ***CAT-1*** *– cationic amino acid transporter 1,* ***DDAH-1*** *– dimethylarginine dimethylaminohydrolase 1,* ***eNOS*** *– endothelial nitric oxide synthase,* ***GAPDH*** - glyceraldehyde 3-phosphate dehydrogenase, **IF** – immunofluorescence, **PBS** – phosphate buffered saline, **P-gp** – P-glycoprotein, **VCAM-1** – vascular cell adhesion molecule 1, **vWF** – von Willebrand factor, **WB** – western blot, **ZO-1** – zonula occludens 1.

After the secondary incubation, the membrane was washed three times (20 minutes each) in PBS-T before being taken to the dark room where 1:1 Pierce ECL Detection Reagent 1 and 2 were added (Thermo Scientific, Loughborough, UK) and incubated with the membrane for 5 minutes at RT. Membranes were then wrapped in cling film and exposed to Kodak(R) BioMax™

XAR film (Sigma Aldrich Company Ltd, Poole, UK) which in turn was processed in an automatic Fuji table top X-ray developer machine.

2.8. Immunofluorescence (IF)

For protein visualisation studies, IF studies were performed. The protocols used were based on an adapted version of a published immunofluorescence procedure (Miecz et al., 2008) and advice from Mr. Enrico Cristante of Imperial College London (for filter staining).

The hCMEC/D3 cells, grown on sterile rat-tail collagen type 1 coated glass coverslips or 12-well transwell filters, had their medium removed and were washed twice rapidly with HBSS at RT, before being fixed with 4% formaldehyde (Sigma Aldrich Company Ltd) in PBS for 10 minutes at 4°C. The coverslips and filters were then washed three times with PBS and permeablised for 5 minutes with 0.1% Triton X-100 in PBS at room temperature (RT). Next, coverslips and filters were washed three times in PBS and then non-specific binding was blocked by incubating the coverslips in PBS containing 10% goat serum (Sigma Aldrich Company Ltd) and 0.1% Triton X-100 for 30 minutes at RT. Following this, the coverslips and filters were incubated overnight at 4°C with primary antibody under constant agitation (please see table 2.2 above for list of antibodies). Following overnight incubation, coverslips were washed three times with PBS and the fluorescent secondary antibodies were added for 1 hour at RT under constant agitation. The coverslips were then washed in PBS twice, and incubated in PBS containing 0.1µg/ml 4',6-diamidino-2-phenylindole (DAPI) blue nucleus stain (New England Biolabs, Bristol, UK) for 30 minutes under agitation at RT. Coverslips and filters were subsequently washed a final time in PBS, dipped in dH_2O and mounted onto slides with PVA-DABCO® mounting medium (Invitrogen, Paisley, UK). Filters were mounted onto coverslips before being mounted onto slides. The slides were then left to dry at 4°C overnight before microscopy.

2.9. Octanol saline partition coefficient (OSPC)

A partition coefficient is a measure of differential solubility of a compound between two immiscible solvents which are at equilibrium (Leo et al., 1971). As such, it allows a prediction of a molecules distribution in the body. 1µCi/0.037 MBq of the radiolabelled test molecule was added to 3ml of 1 x PBS (pH 7.4, Gibco, Invitrogen, Paisley, UK) at room temperature (RT) and vortexed thoroughly. Then, equal volumes (0.75 ml) of the radioactive PBS and octanol (1-octanol, purchased from Sigma Aldrich Company Ltd, Poole, UK) were added together in a 1.5

ml tube and shaken vigorously before being centrifuged at 4000 rpm for 5 minutes in a Thermo Electron Corporation Heraeus Fresco17 bench-top micro-centrifuge. The upper phase (octanol) and lower saline phase (aqueous) were then separated carefully and 3 times 100µl samples from each phase per tube were added to scintillation vials containing 3.5 ml scintillation fluid and the radioactivity was determined using the Packard Tri-Carb 2900TR liquid scintillation counter as described in section 2.2. The partition coefficient was calculated as the ratio of labelled substance in the octanol phase to concentration in the PBS/aqueous phase (Williams et al., 1996). All OSPC measurements were performed in triplicate.

2.10. Software used for thesis

The thesis was written using Microsoft Word 2007 edition from Microsoft Office, with diagrams made in Microsoft PowerPoint. Referencing was done using EndNote X3 software under licence from King's College London. For confocal imaging, Zen 2009 software was used before photos were annotated in PowerPoint. Western blots were scanned and also annotated in PowerPoint. Data were collected and processed in Microsoft Excel and annotated in GraphPad Prism 5 before display here.

Chapter 3. Endogenous molecule interactions – Part I – Effects of ADMA on the integrity of the BBB.

3.1. Chapter 3 – Introduction and aims

Associations between ADMA and endothelial dysfunction have been made in a variety of pathological conditions including chronic heart failure, renal failure, and a variety of diabetic complications such as renin-angiotensin system (RAS)-mediated diabetic retinopathy (Boger et al., 1998, Leiper et al., 2007, Chen et al., 2009, Chen et al., 2011). ADMA and DDAH have also recently been implicated as regulators of pulmonary endothelial barrier function through the modulation of small GTPases. This has been demonstrated in both *in vitro* and *in vivo* with mouse models (Wojciak-Stothard et al., 2007, Wojciak-Stothard et al., 2009).

One of the hallmarks of endothelial dysfunction is an increase in leakiness via the paracellular route. Whereas the abovementioned studies investigated the effects of ADMA on endothelium away from the cerebral vasculature, no group has yet studied ADMA and the BBB. This is of particular importance because not only is BBB integrity paramount for maintaining homeostasis within the cerebral microenvironment, but concentrations of ADMA are increased in brain and cerebrovascular disorders such as ischemic stroke – where ADMA has also been implicated in endothelial dysfunction (Scherbakov et al., 2012).

Therefore, with the association between ADMA and brain pathologies growing, we decided to investigate the effects of ADMA on the integrity of the human BBB *in vitro* using the hCMEC/D3 cell line in a paracellular permeability model. Other *in vitro* studies have only investigated ADMA in on-cerebral endothelial dysfunction at high concentrations (100µM), so we decided to look at a range covering the physiological and pathophysiological concentrations of ADMA. We hypothesised that ADMA would lead to increased BBB permeability, especially at higher concentrations in line with previous non-BBB studies, but didn't rule out the possibility that lower concentrations may also induce permeability changes.

3.2. Methods

A major issue with BBB research (as with most other fields) is that the wide variety of models in use can make it difficult to relate and compare data, particularly between species. For example, much of the CAA transport work has utilised single cloned transporters expressed in *Xenopus laevis* oocytes and this is unlikely to give an accurate indication of the situation in mammalian systems where multiple transporters are present. To shed light on the situation at the human BBB and to keep our findings consistent throughout this thesis, we used the commercially available hCMEC/D3 immortalised *in vitro* BBB model in all of our investigations.

3.2.1. Cell culture

Please see chapter 2, sections 2.1.1 and 2.1.2 for details of hCMEC/D3 source and culture conditions.

3.2.2. Culturing on Transwell filter inserts

For experiments examining the transendothelial permeability of molecules across the hCMEC/D3 cell line, cells were seeded onto Transwell filter inserts (filters) on 12-well plates (Corning® Transwell® polyester membrane inserts, pore size 0.4µm, membrane diameter 1.12 cm^2, Sigma Aldrich Company Ltd, Poole, UK) at a density of 120,000 cells per filter (determined using a haemocytometer as described in section 2.1.2). Filters were pre-coated for 2 hours with 0.15mg/ml rat tail collagen type-I in HBSS, before being washed once with DPBS+ at 37˚C and then incubated in permeability media before seeding (0.5 ml in donor well/filter insert and 1.5 ml in receiver wells, see figure 3.1 below).

The permeability media is a reduced growth factor media which has been optimised by Professor Pierre O. Couraud's group (Institut Cochin, Université Paris Descartes, CNRS, Paris, France) and follows an established protocol allowing the cells to differentiate and form restrictive tight junctions, restricting paracellular permeability (Poller et al., 2008, Zougbede et al., 2011). Permeability media consisted of EBM-2 endothelial basal medium from the Clonetics® EGM®-2MV BulletKit® with 5% FBS 'gold' (PAA the Cell Culture Company, UK), 1% penicillin-streptomycin (Gibco, Invitrogen, UK), 1.4µM hydrocortisone, 5µg/ml ascorbic acid, 10mM HEPES and 1ng/ml bFGF, all purchased from Sigma Aldrich Company Ltd, UK. The cells were also grown in an incubator with a saturated humidity at 37°C in 5% CO_2 and 95% fresh air. Media was changed every 2-3 days and cells used for experiments were between 8-10 days post-seeding.

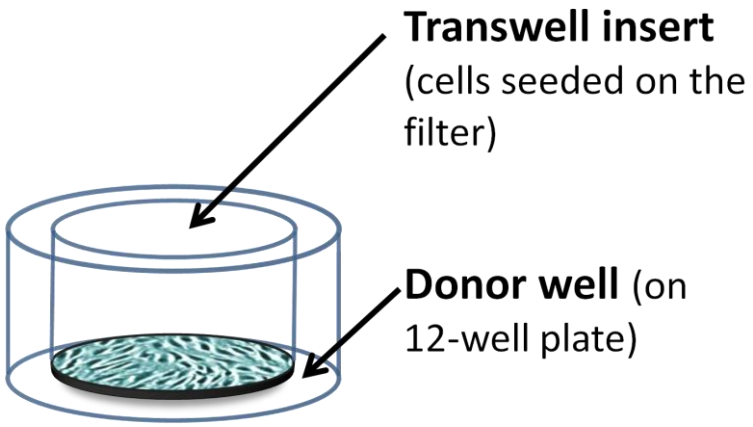

Figure 3.1. The donor and receiver well arrangement on 12-well plates, used for permeability studies. Inserts contained 0.5ml media and donor wells contained 1.5ml media.

3.2.3. Transendothelial electrical resistance (TEER)

When studying transendothelial permeability of molecules across a BBB cell monolayer, it is important to check the paracellular tightness of any *in vitro* model. This is to ensure the effects you are seeing are down to transendothelial membrane permeation, rather than leakiness through the paracellular (TJ) pathway. TEER gives such a measurement of BBB integrity, functional tight junctions and overall cell monolayer paracellular restrictiveness by measuring ionic permeability. The method gives a real time reading in a discreet fashion, monitoring BBB 'physical barrier' development in a model intended for the measurement of molecule permeability (such as drugs). Electrical resistance is derived from Ohm's law where V=IR (V for voltage, I for current, R for resistance). As current pulses are passed across the cell monolayer, the presence of effective tight junctions will impede the paracellular permeation of ion which carry the current, and therefore reduce the resulting voltage drop, registering as recording of resistance.

TEER was measured with an STX-100C chopstick electrode pair connected to an EVOM meter (World Precision Instruments, WPI, Inc., Sarasota, FL, USA). Before measurement, the STX-100C chopstick electrode was first immersed in ethanol (70% v/v) for 20 minutes to sterilise it in a sterile hood. The electrode pair was then immersed in the same medium the cells were growing in (D5546) for 5 minutes to wash off the ethanol and equilibrate to the same conditions as the cells. The 12-well plate cover was removed and replaced with a custom-made (Mr. B. Taylor, King's College London) 12-well plate jig (first sterilised with 70% ethanol before use) for holding the electrode in place over the filters. The jig kept constant the

depth of the electrode pair in the inserts and the wells and produced a stable and reliable reading on the EVOM meter with minimal handling.

To obtain the TEER of a cell monolayer, the resistance (Ω) of a collagen-coated blank filter insert (without cells but kept in the same media conditions and time-frame as cells) was subtracted from the resistance measured across the insert with cell monolayer. The resulting value was multiplied by the surface area of the filter insert (1.12 cm^2) to express results as Ωcm^2.

This protocol and equipment were developed by Dr. Siti Yusof and Professor Joan Abbott and used with permission for the work described in this thesis.

3.2.4. Expression of endothelial markers vWF, VCAM-1 and ZO-1

As the hCMEC/D3 model was new to our group, it was necessary to inaugurate the cell line by looking for endothelial markers before moving on to investigations. The vascular endothelial markers vWF (Hirano et al., 2000) and inducible VCAM-1 (Li et al., 1993, Schram et al., 2003, Weksler et al., 2005) and the TJ protein ZO-1 (Wolburg and Lippoldt, 2002), were therefore visualised to confirm an endothelial phenotype and establish the hCMEC/D3 cell line in our group. The protocol is detailed in chapter 2, section 2.8.

Briefly, following preparation and fixing, cells grown on rat tail collagen type-1 coated sterile glass the coverslips were incubated overnight at 4°C with primary antibody (either anti-vWF at 1:200 in PBS, or anti-VCAM-1 at 0.5µg/ml PBS) and for cells grown on 12-well transwell filters incubated with anti-ZO-1 at 1µg/ml in PBS under constant agitation (please see table 2.2 in chapter 2 for sources of antibodies). Following overnight incubation, coverslips and filters were washed with PBS three times and incubated with the fluorescent secondary antibodies. For vWF, goat anti-rabbit Alexa Fluor 488 conjugated secondary antibody was diluted at 1:200 in PBS. For VCAM-1, goat anti-mouse 546 conjugated polyclonal was diluted at 1:1000 in PBS, and for ZO-1, goat anti-rabbit 546 conjugated polyclonal was diluted at 1:1000 in PBS (see table 2.2 for source details of secondary antibodies).

Following mounting and drying, the slides were then left to dry at 4°C overnight before being viewed at 63x with oil emersion using a Zeiss LSM710 confocal microscope and image analysis software Zen 2009 (Zeiss, Germany).

As VCAM-1 expression is inducible by pro-inflammatory cytokines, it was required that cells were stimulated overnight with 5ng/ml human recombinant human tumour necrosis factor alpha (TNF-α, Gibco, Invitrogen, UK) before fixing and staining. Staining without TNF-α stimulation was also performed to investigate baseline expression.

3.2.5. Permeability assay

To investigate the effect of ADMA on the integrity of the hCMEC/D3s, the paracellular permeability was investigated using permeability assays on confluent monolayers of hCMEC/D3s grown on 12-well plate transwell filter inserts, as described in section 3.2.2. The assay was kindly demonstrated to me by Mr. Miguel Alejandro Lopez-Ramirez of the Open University, UK.

At 8-10 days post seeding, the TEER of the monolayers on the filters was measured as described in section 3.2.3, at least 4 hours before the assay. Filters with TEERs less than the standard hCMEC/D3 TEER value of 30 ohm.cm^2 were not used for the permeability assays. For the permeability assays, permeability media was replaced 24 hours before the assay in both the insert (0.5ml) and donor wells (1.5ml) with fresh media containing one of the following concentrations: 0.5µM ADMA, 3µM ADMA, 10µM ADMA, 100µM ADMA or 500µM ADMA. In a separate series of experiments, media was added to the cells for 24 hours containing either L-NIO (a non-selective inhibitor of NOS isoforms, manufactured by Cayman Chemicals and purchased from Cambridge Bioscience Ltd, Cambridge, UK) at a concentration of 5µM (which is within the 3.9µM K_i range of eNOS (Rees et al., 1990), or 5ng/ml recombinant human TNF- α with 5ng/ml recombinant human IFN-γ (Gibco, Invitrogen, UK).

On the day of the experiment, this media was removed from the transwell filter insert and the donor well, and 1.5ml pre-warmed (to 37°C) DMEM (without phenol red) + 2% FBS Gold was added to the wells of fresh 12-well plates. 40kDa fluorescein isothiocyanate labelled dextran (FITC-Dex) was diluted to 2mg/ml in a separate vial of DMEM + 2% FBS assay media and used as a BBB paracellular marker for the assay (Hoffmann et al., 2011) by adding 0.5ml of it to the transwell filter insert only (see figure 3.2).

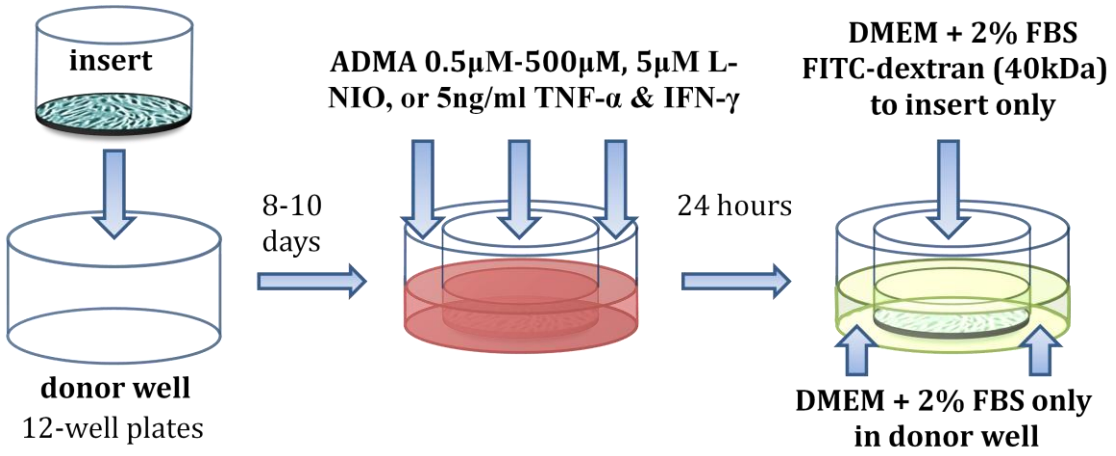

Figure 3.2. Schematic of transwell permeability assay using FITC labelled dextran (40 kDa). hCMEC/D3 cells, seeded onto transwell filter inserts on 12-well plates were grown for 8-10 days, before the permeability media in both the insert and donor wells was replaced with fresh permeability media containing either 0.5µM ADMA, 3µM ADMA, 10µM ADMA, 100µM ADMA or 500µM ADMA. 5µM L-NIO or 5ng/ml TNF-α & 5ng/ml IFN-γ were used also added to the media and incubated for 24 hours in a separate series of experiments. 24 hours later, the media was removed from the insert and donor well and DMEM + 2% FBS was added to well in a fresh 12-well plate. The inserts were then added to the DMEM + 2% FBS wells and DMEM + 2% FBS with 2mg/ml 40kDa FITC-Dex was added to the insert only. The inserts were then moved to a fresh well every 10 minutes for 60 minutes, before the fluorescence of the wells were measured with a fluorescent plate reader. See text for further description.

The filter was then moved into a new donor well on flat bottom 12-well plates (containing DMEM + 2% FBS) at 10-minute intervals for 60 minutes. The assay was performed in a sterile flow-cabinet and incubated in a cell culture incubator between filter insert moves. The fluorescence in each well of 12-well plate was then measured in a FlexStation® 3 Bench top Multi-Mode Microplate fluorescent plate reader at an excitation wavelength of 485nm and emission wavelength of 530nm, using SoftMax® Pro Microplate Data Acquisition & Analysis software.

As a precautionary measure, the impact of media change on the TEER of the monolayers was also measured in a separate series of experiments. Cells on filters had their TEER measured before media change (at resting after 8 days post-seeding) and 1 hour after media change with either normal permeability media (as described in 3.2.4) or permeability assay media (DMEM + 2% FBS).

Permeability of FITC-Dex over the treatments is given as permeability coefficients which take into account the relation between the permeability of the monolayer and the permeability of empty filter pre-coated with rat-tail collagen type-1 (without cells). These calculations are based on work by (Dehouck et al., 1992) and (Cecchelli et al., 1999), and have been used in subsequent hCMEC/D3 publications (Weksler et al., 2005, Poller et al., 2008, Tai et al., 2009c). The clearance of each filter relates to clearance of empty filter wells. The equations are expressed below (equation 3.1 and equation 3.2).

The cleared volume (in µl/ml) represents the volume of FITC-Dex solution passing through the cell monolayer at a particular time. It was calculated as:

$$\frac{AUa - AUb}{Fi}$$

Equation 3.1

where *AUa* is the total fluorescence (arbitrary units) in the donor compartment, *AUb* is the background fluorescence, and *Fi* is the fluorescence of the initial solution (Au/ml). The volume cleared was plotted against time, and the slope curves were used to calculate permeability coefficients (P_e in cm/min) of the hCMEC/D3 monolayers as:

$$\frac{1}{PS} = \frac{1}{PSef} - \frac{1}{PSf} \text{ and } Pe = \frac{PS}{S}$$

Equation 3.2

where *PSef* is the gradient of the curve for cells grown on filters, and *PSf* is the gradient of the curve for filter alone (both ml/min). *PS* is the permeability surface area of the cell monolayer (ml/min) and *S* is the surface area of the filter. The higher the P_e value, the more permeable a monolayer is to FITC-Dex (Tai et al., 2009c).

3.2.6. Cytotoxicity assay

The potential of the treatments used in this accumulation study to cause cytotoxicity to the hCMEC/D3 cells was assessed using an MTT assay, the protocol of which is described in section 2.5. The effect of these compounds was compared to untreated control hCMEC/D3 cells.

3.2.7. eNOS and DDAH-1 expression

To investigate the expression of eNOS and DDAH-1 in the hCMEC/D3s, SDS-PAGE and WBs were performed (as described in methods section 2.7) on whole cell lysates, prepared in TGN lysis buffer as described in 2.7.1. Lysates were prepared from cells grown for 8 days in permeability medium. 30µg of each lysate was loaded per well. For eNOS and DDAH-1 expression, human umbilical vein endothelial cell (HUVEC) whole cell lysate in RIPA buffer (purchased from Santa Cruz Biotechnology, Inc, California, US) was used as positive controls (Murakami et al., 2006, Zhang et al., 2011).

Goat anti-human DDAH-1 primary antibody was used at a dilution of 0.2µg/ml PBS-T with 0.5% BSA as described in table 2.2. Rabbit anti-human NOSIII/eNOS primary antibody was used at a dilution of 1:2000 in PBS-T and 0.5% BSA also as described in table 2.2. Rabbit anti-goat HRP conjugated secondary antibody was used at a dilution of 1:2500 in PBS-T with 0.5% BSA for chemiluminescence detection for DDAH-1 and goat anti-rabbit HRP conjugated secondary antibody was used at a dilution of 1:5000 in PBS-T with 0.5% BSA for chemiluminescence detection for eNOS. GAPDH was probed as a loading control using mouse anti-human primary antibody at 1:2000 in PBS-T with 0.5% BSA, and rabbit anti-mouse HRP conjugated secondary at 1:2000 in PBS-T with 0.5% BSA was used for chemiluminescence (see table 2.2).

3.3. Results

3.3.1. Expression of endothelial phenotype

The hCMEC/D3 cell line (displaying an endothelial phenotype in figure 3.3) was examined for evidence of vascular endothelial cell markers vWF (figure 3.4 a), inducible VCAM-1 before (figure 3.4 b) and after (figure 3.4 c) TNF-α stimulation, and the TJ protein ZO-1 (figure 3.5). Phase contrast microscopy of the hCMEC/D3 cells showed a typical 'cobble-stone to spindle-shaped morphology' (Malek and Izumo, 1996). The IF results indicate normal expression of the markers comparable to other publications (see (Norgall et al., 2007) for example of vWF expression,(Thompson and Debinski, 1999) for example of human endothelial VCAM-1 expression and (Weksler et al., 2005) for hCMEC/D3 ZO-1 expression.

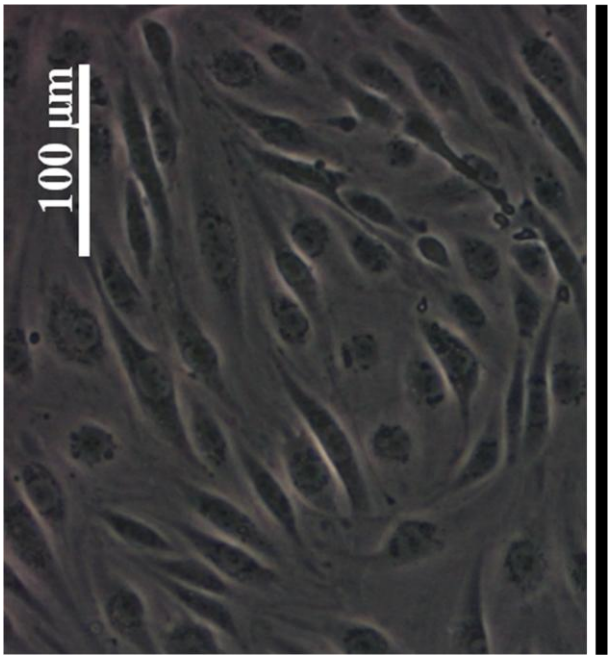

Figure 3.3. Phase contrast microscopy of hCMEC/D3 cells approaching confluency. Cells in live culture viewed 20X with phase contrast microscopy and showed a typical endothelial phenotype.

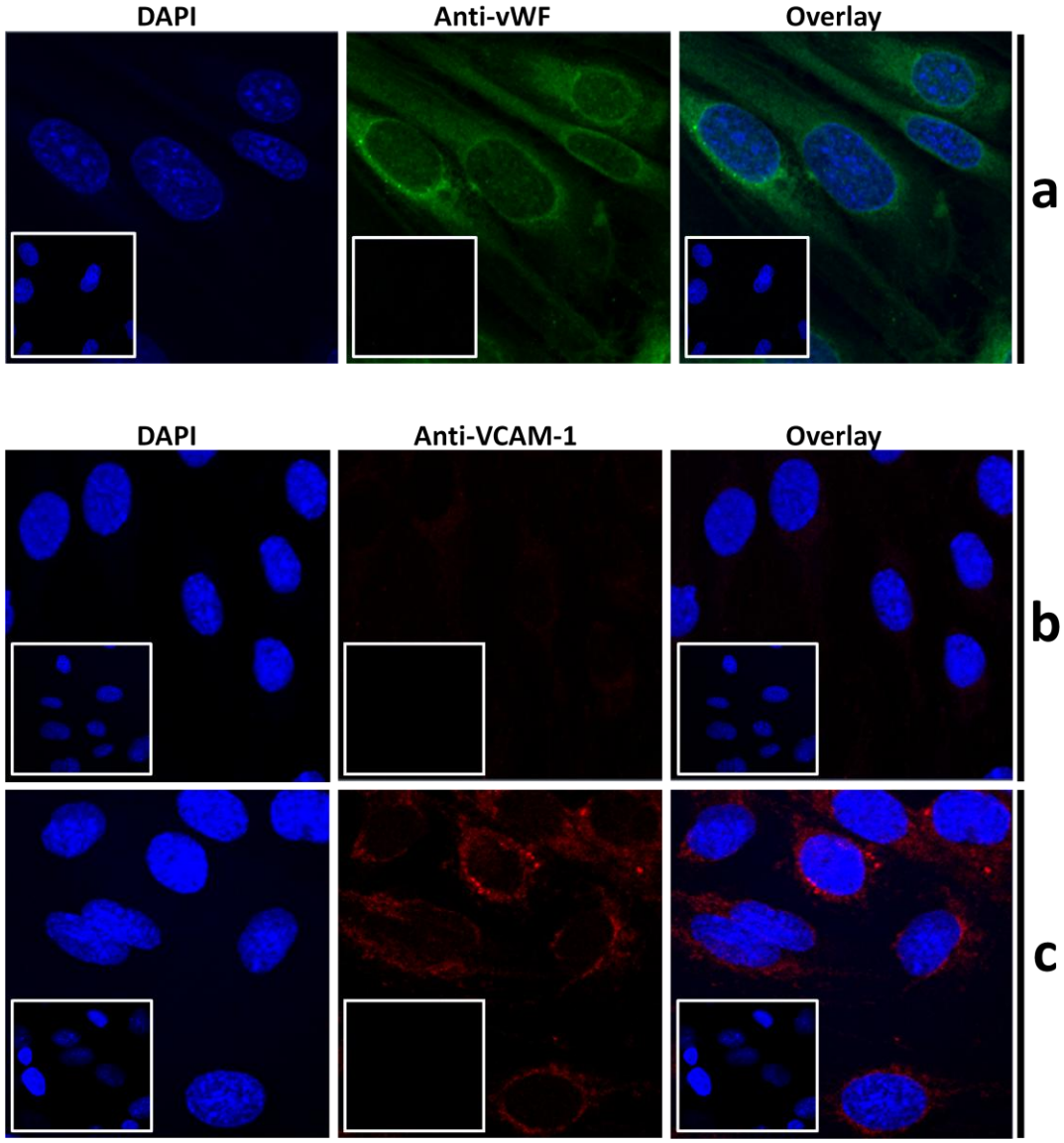

Figure 3.4. Immunofluorescence and confocal microscopy of vascular endothelial markers in hCMEC/D3 cells. **a|** hCMEC/D3 cells were grown on rat tail collagen type-1-coated coverslips fixed with 4% formaldehyde and stained for vWF with primary and secondary antibody as described in section 3.2.4. Cell nuclei were counterstained with 1µg/ml DAPI. For negative staining, cells were stained with secondary antibody only along with DAPI (inserts). **b|** hCMEC/D3 cells were grown on rat tail collagen type-1-coated coverslips, fixed, and stained for VCAM-1 without TNF-α stimulus with primary and secondary antibody as described in section 3.2.4. Data illustrate negligible expression. Cell nuclei were counterstained with 1µg/ml DAPI. For negative staining, cells were stained with secondary antibody only along with DAPI (inserts). **c|** hCMEC/D3 cells were stained for VCAM-1 following overnight incubation with 5ng/ml TNF-α stimulation (as above and in section 3.2.4), demonstrating increased expression. Cell nuclei were counterstained with 1µg/ml DAPI. For negative staining, cells were stained with secondary antibody only along with DAPI (inserts). Cells viewed at 63x with oil emersion using a Zeiss LSM710 confocal microscope. IF was carried out 3 times in duplicate (n=3). Results displayed are representative of the 6 coverslips used per stain.

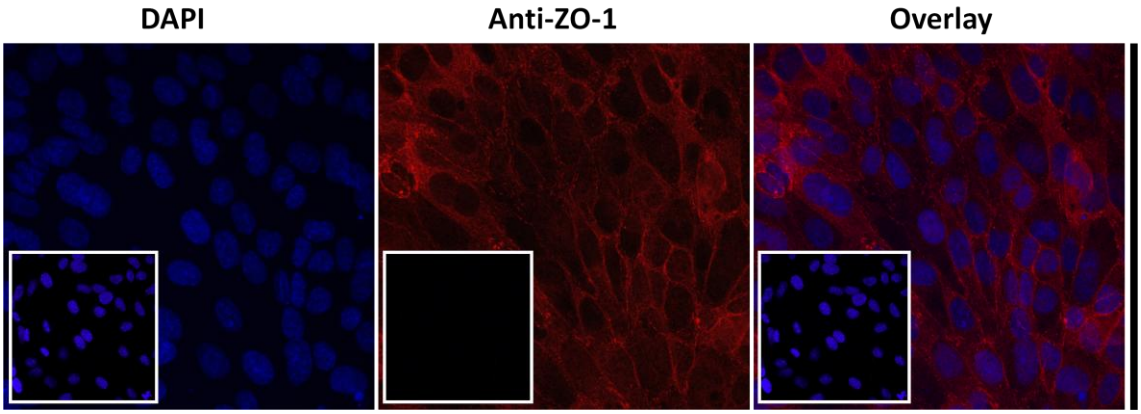

Figure 3.5. Immunofluorescence and confocal microscopy of integral TJ protein, ZO-1 in hCMEC/D3 cells grown on transwell filters. hCMEC/D3 cells were grown on rat tail collagen type-1-coated transwell filters for 7 days, fixed with 4% formaldehyde and stained for ZO-1 with primary and secondary antibody as described in section 3.2.4. Cell nuclei were counterstained with 1µg/ml DAPI. For negative staining, cells were stained with secondary antibody only along with DAPI (inserts). Cells viewed at 63x with oil emersion using a Zeiss LSM710 confocal microscope. Picture representative of IF that was carried out 3 times in duplicate (n=3).

3.3.2. Treatment effects on TEER of hCMEC/D3 monolayers

Before performing the permeability assay, the effects of the permeability assay media (DMEM + 2% FBS) on the TEER of the cell monolayers in comparison to normal permeability media (EGM2-MV) was investigated over 1 hour incubations following media change. There were no statistically significant differences in TEER values between any of the treatments as measured using a One-way ANOVA with Bonferroni's Multiple Comparison post hoc test. Data are displayed in figure 3.6.

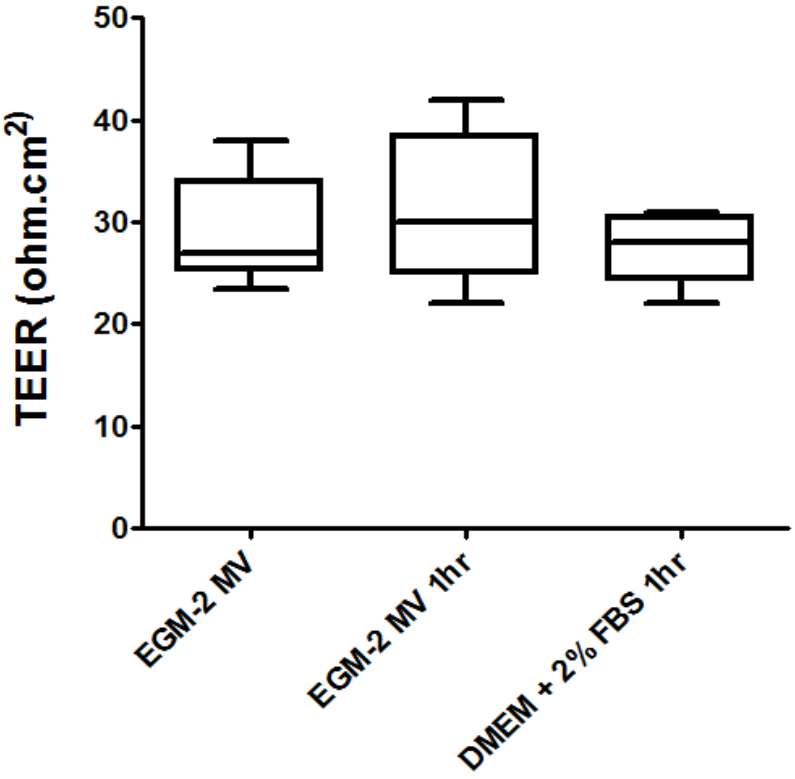

Figure 3.6. Effects of permeability assay media on TEER of hCMEC/D3 monolayers grown on transwell filters. As a precautionary measure, the impact of the media change on the TEER of the hCMEC/D3 cells was investigated and compared to cells grown for 8 days in normal permeability media (before media change). TEER values following replenishment with normal permeability media and assay media following 1 hour incubations were investigated and compared. Each whiskers plot represents 6 filters. Data were analysed with One-way ANOVA and Bonferroni's post hoc test.

3.3.3. Effects of ADMA on hCMEC/D3 permeability

To investigate the impact of ADMA on the integrity of the hCMEC/D3s, cells grown on transwell filters for 8-10 days were incubated with a range of ADMA concentrations for 24 hours before permeability assays with FITC-Dex. The concentrations of ADMA used reflected the physiological (0.5µM), pathophysiological (3µM) human plasma ranges, as well as 10µM and 100µM (values used in previous *in vitro* studies). 500µM was used as an extreme reference point. The data are displayed in figure 3.7 below.

There were no significant differences between the 0.5µM, 3µM and 10µM ADMA treatments between each other or control cells (untreated) on the permeability of the hCMEC/D3 cells to FITC-Dex. However, the incubation of the cells with 100µM ADMA saw a significant increase in the permeability to FITC-Dex when compared to controls (52% increase, $p<0.05$) and 10µM ADMA (53% increase, $p<0.05$).

The incubation of 500µM ADMA caused a significant increase in permeability when compared to all other ADMA treatments and controls ($p<0.01$ in all instances); 84% increase vs. controls; 67% increase vs. 0.5µM ADMA; 73% increase when compared to 3µM; and an 85% increase compared to 10µM ADMA. There were no significant differences in permeability coefficients between 100µM and 500µM ADMA treatments.

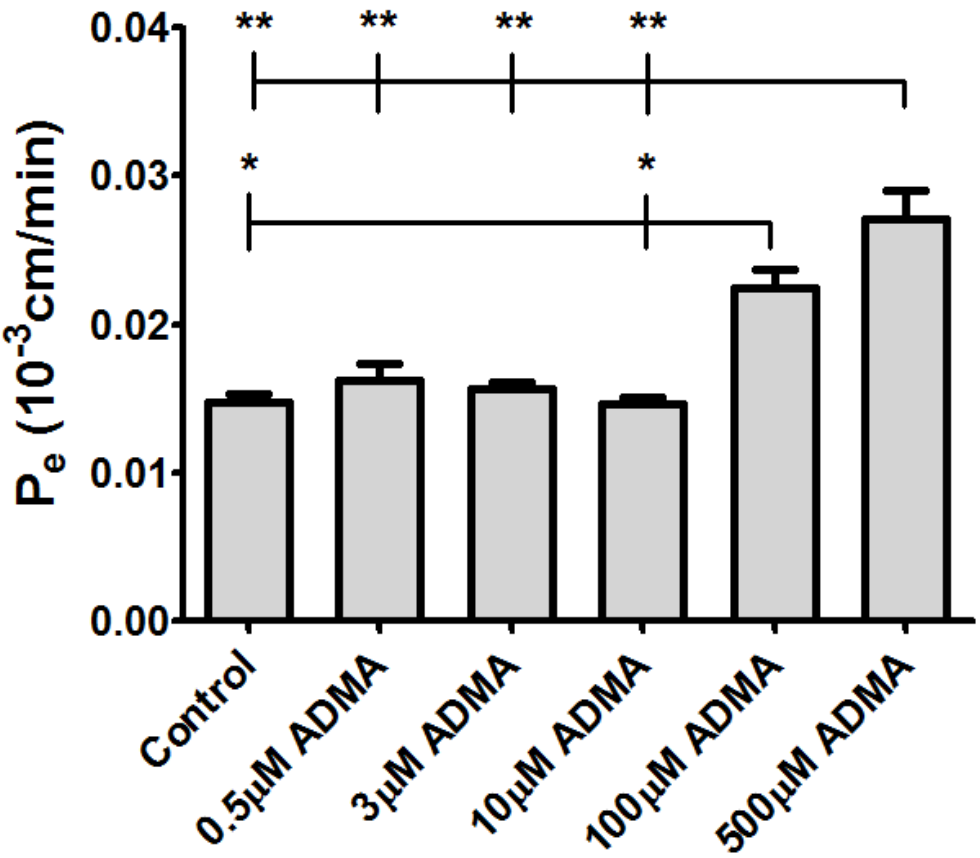

Figure 3.7. Impact of ADMA on hCMEC/D3 permeability to 40kDa FITC-Dex. Confluent monolayers of hCMEC/D3 cells, grown on rat tail collagen type-1 coated transwell filter inserts for 8-10 days, were incubated for 24 hours with a range of ADMA concentrations and then their permeability to 40kDa FITC-Dex investigated from insert-to-donor well direction, and compared to control (untreated) cells. Data represent means ± SEM from 12-15 transwell filter inserts per treatment. Data analysed with One-way ANOVA and Bonferroni's post hoc test. ADMA – asymmetric dimethylarginine.

3.3.4. Effects of L-NIO, TNF-α and IFN-γ on hCMEC/D3 permeability

The potent eNOS inhibitor L-NIO and the pro-inflammatory cytokines TNF-α and IFN-γ were incubated with the hCMEC/D3s grown on transwell filter inserts, to investigate their effects on permeability to 40kDa FITC-Dex. The data are displayed below in figure 3.8.

When compared to controls, 5µM L-NIO caused no significant changes in permeability. When incubated with 5ng/ml TNF-α and 5ng/ml IFN-γ, hCMEC/D3 cells had significantly increased permeability to FITC-Dex when compared to controls (*p<0.001*) and L-NIO (*p<0.001*). The percentage increases were 200% compared control and 204% compared to L-NIO.

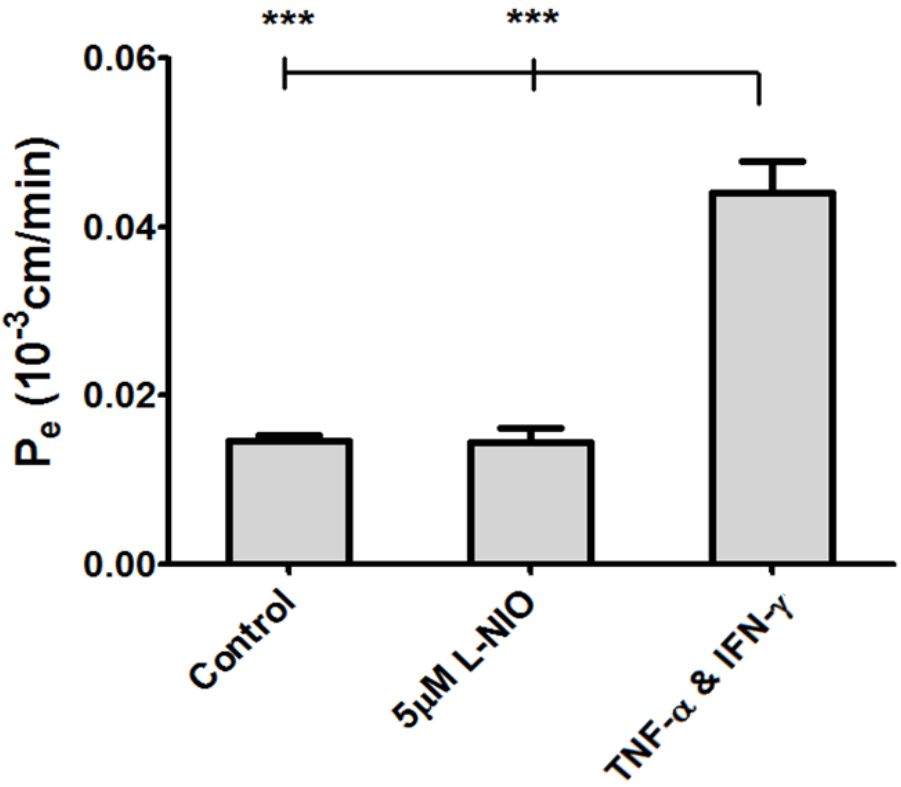

Figure 3.8. Impact of L-NIO, TNF-α and IFN-γ on hCMEC/D3 permeability to FITC-Dex. Confluent monolayers of hCMEC/D3 cells, grown on rat tail collagen type-1 coated transwell filter inserts for 8-10 days, were incubated for 24 hours with either 5µM L-NIO or 5ng/ml TNF-α & 5ng/ml IFN-γ and then their permeability to 40kDa FITC-Dex investigated from insert-to-donor well direction, and compared to control (untreated) cells. Data represent means ± SEM from 12 transwell filter inserts per treatment. Data analysed with One-way ANOVA and Bonferroni's post hoc test. IFN-γ – interferon gamma, L-NIO – N-iminoethyl-L-ornithine, TNF-α – tumour necrosis factor alpha.

3.3.5. Cytotoxicity of treatments on hCMEC/D3 cells

The cytotoxic potential of all compounds used in this study over the 24 hour time-frame was assessed in the hCMEC/D3 cells using an MTT assay, comparing treated cells to untreated control cells.

There were significant decreases in cell viability between 100µM ADMA (*p<0.05*), 500µM (*p<0.01*), 5ng/ml TNF-α and 5ng/ml IFN-γ (*p<0.01*) when compared to control untreated cells (figure 3.9 below).

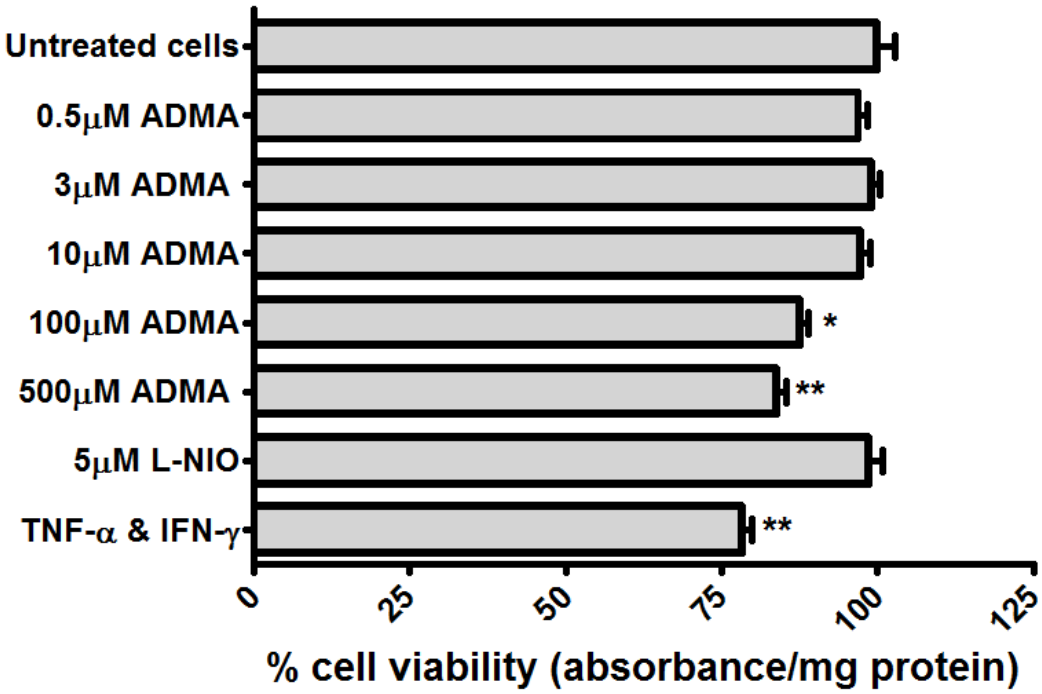

Figure 3.9. Cytotoxicity of permeability treatments on hCMEC/D3s. The treatments used in this chapter were assessed for any cytotoxic potential using an MTT assay with confluent monolayers of hCMEC/D3 cells in 96 well plates, grown in permeability medium as described in section 2.5. The results are expressed as percentage viability ± S.E.M and compared to control untreated cells, which were incubated in permeability medium alone. TNF-α and IFN-γ were used together at 5ng/ml each. n=3 (plates), 6 replicates per n (6 wells). ADMA – asymmetric dimethylarginine, IFN-γ – interferon gamma, L-NIO – N-iminoethyl-L-ornithine, TNF-α – tumour necrosis factor alpha.

3.3.6. hCMEC/D3 expression of eNOS and DDAH-1

To look for expression of the ADMA interacting enzymes eNOS and DDAH-1, SDS-PAGE and WBs were performed on hCMEC/D3 whole cell lysate, with HUVEC whole cell lysate used as positive controls. GAPDH was used as a loading control.

Blots at the expected sizes (140kDa for eNOS and 37kDa for DDAH-1) were visible in both the hCMEC/D3s and HUVEC positive controls. The blots are displayed below in figure 3.10.

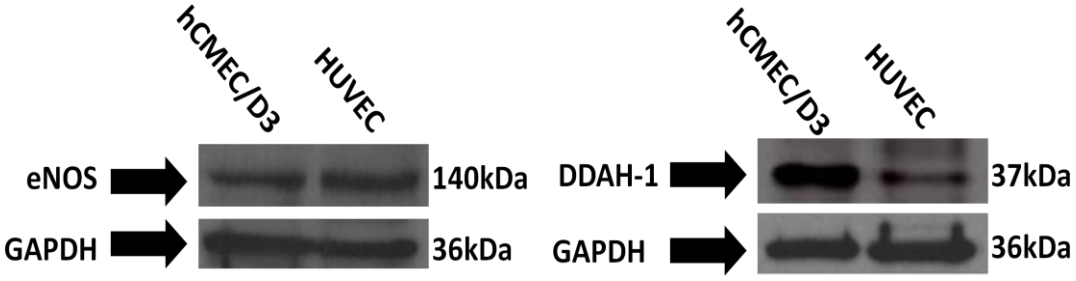

Figure 3.10. The expression of eNOS and DDAH-1 in hCMEC/D3 cells. hCMEC/D3 cells were grown for 8 days in permeability media before being turned to lysate with TGN lysis buffer as described in section 3.2.7 and probed for eNOS and DDAH-1 expression, as well as GAPDH as a positive control. HUVEC cell lysate was used as positive controls.

3.4. Discussion

The idea that ADMA plays roles in endothelial dysfunction and disease pathogenesis is gaining momentum due the accumulating *in vitro* and *in vivo* data from a variety of studies on different body regions. In the context of the brain and cerebrovasculature, ADMA has been implicated as not only a marker, but also a mediator of cerebral perfusion and cognitive impairment in microangiopathy-related cerebral damage (Kielstein and Kielstein, 2009, Notsu et al., 2009). In acute stroke, increased levels of ADMA have been observed in transient ischemic attacks and cardioembolic infarctions (Wanby et al., 2006, Scherbakov et al., 2012) and ADMA levels in CSF are believed to be correlated with stroke severity in humans (Brouns et al., 2009). ADMA has also been implicated in humans as a mediator of cerebral vascular tone, by increasing arterial stiffness and decreasing cerebral blood flow independent of blood-pressure (Kielstein et al., 2006a). In relation to the BBB however, the action of ADMA on vascular tone occurs upstream of brain capillaries which are devoid of smooth muscle cells (Pardridge, 1999). Despite this, pericytes of the NVU act as contractile cells and it has been recently shown that ischemia induces sustained contraction of pericytes in microvessels of the mouse brain, impeding capillary microcirculation (Yemisci et al., 2009). Nitric oxide has also been shown to relax cultured bovine retinal pericytes (Haefliger et al., 1994). If ADMA has any direct or indirect effects on pericytes and the BBB has not been studied and is likely to have wider implications on the cerebrovasculature and indeed peripheral vasculature, particularly at the level of the endothelium. We therefore decided to investigate its effects on the human BBB by using the hCMEC/D3 *in vitro* BBB model.

Before we started these studies, we sought to establish the hCMEC/D3 in our group with expression studies of vascular endothelial markers, demonstrating the presence of vWF, inducible VCAM-1 and the TJ protein, ZO-1. The expression of inducible VCAM-1 and ZO-1 matches the findings described using fluorescence-activated cell sorting and IF studies in the original hCMEC/D3 paper (Weksler et al., 2005). vWF expression has also been previously confirmed in the hCMEC/D3s (Fasler-Kan et al., 2010). These data, combined with the fact that the cells were grown under well-established conditions and sourced from the creators, satisfied us that the model was a suitable for our investigations.

To investigate the effects of ADMA on the BBB, we used a permeability assay where the hCMEC/D3 cells were grown to confluence on filters in permeability medium and were

incubated for 24 hours with a range of ADMA concentrations. The P_e values obtained in this study are similar to those previously published with 40-70kDa FITC-Dextrans for the hCMEC/D3s, although in the lower range (Weksler et al., 2005, Forster et al., 2008). At the concentrations of 100µM and 500µM we observed significant increases in permeability to 40KDa FITC-Dex when compared to untreated controls. The permeability increase seen with 500µM ADMA was also significantly higher than all other treatments, bar the 100µM ADMA treatment. These data are consistent with previous *in vitro* studies investigating ADMA and endothelial dysfunction. In one such study, Chen et al., used bovine retinal capillary endothelial cells in a permeability model with transwell filters, and similarly incubated the cells with 100µM ADMA for 24 hours. They illustrated a similar result to the one obtained here that ADMA significantly increased permeability to their paracellular marker (horseradish peroxidise which is 44kDa) (Chen et al., 2011). They also demonstrated that ADMA downregulated the expression of the TJ protein occludin in their cells, following 24 hour incubation with 100µM ADMA. In another study by Wojciak-Stothard et al., porcine pulmonary artery endothelial cells were used in a transwell permeability model and also incubated with 100µM ADMA for 24 hours. The authors noted a significant increase in permeability compared to control cells (Wojciak-Stothard et al., 2009). In a more recent study, these findings were echoed when ADMA was shown to increase the permeability of HUVECs on transwell filter inserts to 40kDa FITC-Dex and FITC-apelin-13 (MW 2053) in a dose-dependent (25-200µM ADMA) and time-dependent (4, 8, 16 and 24 hour) manner (Wang et al., 2011a).

Chen et al., showed cell proliferation was markedly decreased by ADMA in a dose-dependent manner, but did not link these effects as a possible explanation behind their increase in permeability. In our study, 24 hour incubations with 100µM and 500µM decreased cell viability, which are likely to explain the permeability increases. The mechanism of toxicity in our model however, was not investigated here and varies between studies. Interestingly, Chen *et al*., authors used antioxidants to reverse the ADMA-induced permeability affects, suggesting that it was the formation of ROS induced by ADMA that caused the permeability increase by inducing endothelial dysfunction (Chen et al., 2011). Wang et al., also attributed ADMA-induced ROS formation to increases in endothelial permeability by inhibiting the NADPH oxidase pathway – the major source of ROS in endothelium (Wang et al., 2011a). Wojciak-Stothard *et al*., conversely, did not find any evidence of ADMA-induced cytotoxicity (to 100µM ADMA) or that ROS formation had changed in their porcine pulmonary artery

endothelial cells, following ADMA incubation, but instead showed ADMA-induced cytoskeletal and adherens junction remodelling via modulation of the small GTPase Rac1 (Wojciak-Stothard et al., 2009). Small GTPases are widely implicated in the control of microvascular permeability; with Rac1 a major GTPase required for barrier stabilisation and maintenance (Spindler et al., 2010). These conflicting observations could suggest that the impact of ADMA on ROS formation could be cell/tissue specific and dependent on sensitivity to oxidative stress. The brain and the cerebrovasculature for example are extremely sensitive to oxidative stress, due in part to the increased expression of NADPH-oxidase in BECs compared to peripheral endothelial cells (Uttara et al., 2009, Tripathy et al., 2010). One way in which ADMA is believed to induce ROS formation is by eNOS uncoupling. In an uncoupled state, electron flow from the reductase domain to the oxygenase domain of the enzyme are diverted to molecular oxygen rather than to L-arginine, resulting in the production of superoxides instead of NO (Sydow and Munzel, 2003). With this in mind, we looked for and confirmed the expression of eNOS in our cells. The addition of the eNOS inhibitor L-NIO in our permeability experiments however, did not induce any significant differences in permeability, although the action of the inhibitor has not been demonstrated to induce ROS formation. Therefore, it remains possible that in our model ADMA could induce ROS formation via eNOS uncoupling – in a dose-dependent fashion – resulting in decreases in cell viability. Yemisci et al., showed microvessels are major site of superoxide and peroxynitrite production following ischemia (Yemisci et al., 2009).

Another possibility is that under such conditions of oxidative stress, DDAH activity could be inhibited as a growing body of data suggest that DDAH enzymes are highly susceptible to oxidative and nitrosative stress, which decreases their ADMA-metabolising abilities (Sydow and Munzel, 2003, Sydow et al., 2003, Palm et al., 2007). For example, in one study, both human dermal microvascular endothelial cells and rat vascular smooth muscle cells incubated in high glucose (25.5mmol/L) showed significantly decreased DDAH activity compared to controls, due to the increased oxidative stress induced by the hyperglyemia (Lin et al., 2002). These effects were reversed by co-incubation with antioxidants. In another study using rat kidney homogenates, it was demonstrated that the superoxide donor 2,3-dimethoxy-1,4-naphthoquinone was able to significantly reduce the activity of DDAH in a dose-dependent manner (Tain and Baylis, 2007). In conditions such as hypoxia and stoke, oxidative stress is increased in the cerebrovasculature, promoting conditions associated with diminished DDAH function (see (Sandoval and Witt, 2008) and (Chrissobolis et al., 2011) for extensive reviews).

We looked for the presence of DDAH-1 in our model, confirming its expression. The ADMA concentrations that impacted here and in previous studies are usually in the 100µM range – well above the clinically relevant plasma concentrations of ~3µM, although the intracellular concentrations of ADMA, especially in different disease states, have not been fully characterised and are likely to be relevant in future studies. Intriguingly, smaller concentrations of extracellular ADMA (1-10µM) have been shown to induce increases in ROS formation in mouse 3T3-L1 adipocytes (Yang et al., 2009) and cause vasoconstriction of cerebral vessels in rabbits (Faraci et al., 1995). If DDAH-1 were knocked-down or inhibited, then the action of ADMA on the BBB may be more pronounced and this would be a very interesting direction of study that could further implicate more relevant ADMA concentrations in a variety of cerebrovascular and brain pathologies where oxidative stress is an issue. Loss of DDAH-1 function in mice has been demonstrated to result in increased ADMA levels and endothelial dysfunction (Leiper et al., 2007). In relation to this, it has been demonstrated *in vivo* and *in vitro* with mice aorta and cerebral arterioles over-expressing DDAH-1 are protected against ADMA-induced endothelial dysfunction using 100µM ADMA (Dayoub et al., 2008).

ADMA may also contribute to endothelial dysfunction via a mechanism independent of eNOS competitive inhibition. In a recent paper investigating the role of ADMA in chronic kidney disease, Kajimoto et al., demonstrated that ADMA concentrations representative of plasma levels in mice chronic kidney disease models (3-4µM) were able to reduce eNOS phosphorylation in HUVECs (Kajimoto et al., 2012). This feature was also suggested when Smith et al., argued that their data demonstrating that 2µM ADMA was shown to induce significant changes in expression of a variety of genes using gene chips in human coronary artery endothelial cells when incubated for 24 hours in the presence of >300µM L-arginine was also independent of eNOS competitive inhibition (Smith et al., 2005). The finding of Smith et al., is also extremely interesting because it demonstrates that ADMA is able to exert effects even in the presence of saturating L-arginine concentrations, and that extracellular concentrations of ADMA are able to modulate aspects of endothelial function. This is of particular interest because one of the major issues with our assay (indeed any assay involving ADMA and L-arginine) was the large amounts of CAAs present in the commercially purchased media. These high concentrations are likely to have effects on NOS activity and the metabolism of ADMA because not only would CAA transport systems would be saturated, but NOS would also be saturated, working at maximal rates even in the presence of ADMA that may normally

be inhibitory (Teerlink et al., 2009). It has also been demonstrated that in ranges of 50-400μM, L-arginine can dose dependently inhibit the degradation of ADMA by inhibiting the action of DDAH (Wang et al., 2006).

By carefully controlling the cell media components to represent those of physiological significance, one may further reduce the restrictiveness of the already leaky hCMEC/D3 barrier, highlighting a major issue with the hCMEC/D3 BBB model. Efforts have been made to reduce the paracellular permeability in this model, but thus far all methods have fallen short of achieving a model representative of the *in vivo* situation.

TNF-α and IFN-γ have been show to increase BMEC permeability through disruption of cell-cell junctional complexes (Minagar and Alexander, 2003) via activation of the transcription factor NFκB (Sandoval and Witt, 2008) and tyrosine-phosphorylation of adherens junction proteins via GTPases (Dejana et al., 2008). Their effect on hCMEC/D3 permeability has also been recently demonstrated (Fletcher et al., 2011) with a similar increase in permeability to FITC-Dex noted (albeit using 70kDa FITC-Dex). Combination of TNF-α and IFN-γ can also lead to cytotoxicity in endothelial cells, as demonstrated with murine vascular endothelial cells (Yamaoka et al., 2002). It appears likely that in our permeability model a combination of these effects was apparent in that the hCMEC/D3 junctional complexes were altered and that apoptosis of the cells also increased the permeability affect.

3.5. Conclusions

The data here show that ADMA is able to increase paracellular permeability in human BBB cells. Our BBB model has its limitations regarding leakiness, but it does express eNOS and DDAH-1, which make it a good human *in vitro* BBB model to use to study the effects of ADMA and NO inhibition. Although it was high ADMA concentrations that induced these permeability increases, that does not rule out the role of more clinically relevant concentrations, especially considering the sensitivity DDAH enzymes to oxidative stress which can be induced from several sources during various disease states. In the cerebrovasculature, BMECs are extremely sensitive to oxidative stress due in part to their high expression of NADPH-oxidase, and this makes them vulnerable to increased concentrations of ROS from other sources. ADMA has been demonstrated to induce ROS formation by uncoupling NOS so that it no longer produces NO, resulting in endothelial dysfunction. This could have serious implications in brain and cerebrovasculature pathologies, as well as on the integrity of the BBB itself, and this remains an exciting area of study not yet undertaken.

Chapter 4. Endogenous molecule interactions – Part II – The L-arginine and ADMA transport mechanisms at the human BBB.

4.1. Chapter 4 – Introduction and aims

As closely related molecules, L-arginine and ADMA are believed to share similar CAA SLC transport mechanisms and limited data indirectly show this (see section 1.9.15). However, it is important to note that although data *directly* looking at ADMA membrane transport is lacking. Furthermore, at the site of the BBB, the transport of ADMA has yet to be investigated either directly or indirectly despite the emerging role of the molecule in brain and cerebrovascular pathologies. Contrary to this, the transport mechanisms for L-arginine at the bovine BBB have been described and it is well established that the principle L-arginine BBB transporters are CAT-1, CAT-2B and CAT-3, which are all members of system y^+ (O'Kane et al., 2006). Interestingly, other data have embroiled the system y^+L transporters y^+LAT1 and y^+LAT2 (Carl et al., 2010) in human *in vitro* models and the system $B^{0,+}$ transporter $ATB^{0,+}$ (Berezowski et al., 2004, Czeredys et al., 2008) in bovine *in vitro* models, in CAA transport at the BBB (see section 1.5.1).

Thus we hypothesised that ADMA would have a similar transport profile to L-arginine in human brain endothelial cells and so compared the transport of the two molecules in a drug accumulation model using the established hCMEC/D3 BBB model.

Furthermore, their transport and subsequent accumulation was investigated with well-described CAA transporter inhibitors and substrates over short time-frames to record instances of cellular influx and longer time-frames to elucidate cellular efflux events. We hypothesised that the main transporter involved would be members of system y^+, especially CAT-1 which is ubiquitously expressed throughout the body – heavily so at the rodent BBB (Stoll et al., 1993), but didn't rule out the potential influence of other transporters, particularly $ATB^{0,+}$ and y^+LAT1 and y^+LAT2. As a result of the functional studies we also investigated the presence of CAT-1 and $ATB^{0,+}$ in the hCMEC/D3s, as the expression of CAT-1 has yet to be demonstrated in the cell line.

4.2. Methods

A description of the generation of the hCMEC/D3 cells can be found in the general methods chapter section 1.9.15.

4.2.1. Cell culture

Please see section 2.1.2 in chapter 2 for details of hCMEC/D3 culture conditions.

4.2.2. Radioactivity studies – Materials

Tritium labelled L-arginine was purchased from American Radiolabelled Chemicals, Inc., MO, US and had a specific activity of 43 Ci/mmol. [^{14}C]sucrose was purchased from Moravek Biochemicals and had a specific activity of 4980 mCi/mmol. [^{3}H]ADMA was custom radiolabelled by GE Healthcare, Amersham, UK and had a specific activity of 8 Ci/mmol. Unlabelled ADMA was purchased from Sigma Aldrich Company Ltd.

4.2.3. L-arginine and ADMA Octanol-saline partition coefficient

To gain an indication of the lipophilicity of the study molecules [^{14}C]sucrose, [^{3}H]ADMA and [^{3}H]L-arginine, an OSPC was performed using 0.037 MBq (1 µCi) of each molecules in 1 ml of saline as described in the detailed protocol in section 2.9. These analyses were performed with fellow laboratory members Mr. Murat Dogruel and Mr. Mehmet Fidanboylu.

4.2.4. L-arginine and ADMA accumulation

To investigate the accumulation of [^{3}H]L-arginine and [^{3}H]ADMA (using [^{14}C]sucrose as a correction value for non-specific binding and extracellular space) in the hCMEC/D3 cells, the protocol described in section 2.2 was used.

4.2.5. Arginine

[^{3}H]L-arginine (0.0111 MBq or 300 nCi, 7nM) and [^{14}C]sucrose (0.0148 MBq or 400 nCi, 972nM) was added to every 1ml of accumulation buffer. The concentrations used were the lowest possible that still allowed accurate detection and discrimination of [^{3}H] and [^{14}C] radioactivity. Studies were performed in the absence and presence of varying CAA transport substrates and inhibitors (see table 2.1 in chapter 2 for source information and references). For self-inhibition experiments which provides evidence of influx mechanisms, 100µM unlabelled L-arginine – a similar concentration to that present in human plasma – was added to the accumulation buffer along with the [^{3}H]L-arginine and [^{14}C]sucrose.

The system y^+ competitive substrate L-homoarginine (20mM) and the broad scale system A, system L and system $B^{0,+}$ inhibitor 2-aminobicyclo-(2,2,1)-heptane-2-carboxylic acid (BCH) (4mM) were also used in separate groups of experiments for evidence of functional transporter activity. Leucine (100µM) was used to investigate the role of BAT transporters (y^+L, $b^{0,+}$ and $ATB^{0,+}$) on the transport of L-arginine, as unlike system y^+ which has a poor affinity for leucine, BAT transporters readily transport leucine in the presence of Na^+ ions.

As well as these molecules, in a separate series of accumulation experiments, the effects of a range of ADMA concentrations on [^{3}H]L-arginine accumulation were also assessed. Thus the normal plasma concentration of 0.5µM, the 3µM concentration associated with pathological conditions, and a supraphysiological concentration of 500µM (as an extreme reference point) were added separately to the accumulation buffer alongside [^{3}H]L-arginine and [^{14}C]sucrose.

4.2.6. ADMA

[^{3}H]ADMA was used at a concentration of 38nM (0.0111 MBq or 300 nCi in 1ml accumulation buffer) [^{14}C]sucrose (used at the same concentration as with [^{3}H]L-arginine; 972nM). This ensured that the radioactivity could be detected appropriately. Evidence for influx transport activity was assessed by self-inhibition studies using 0.5µM, 3µM and 500µM unlabelled ADMA alongside [^{3}H]ADMA and [^{14}C]sucrose in the accumulation buffer. The influence of 100µM unlabelled L-arginine, 100µM leucine, 20mM L-homoarginine and 4mM BCH were also separately investigated. The results guided us to further uncover the influence of $ATB^{0,+}$ and so the specific inhibitor of this transporter (α-methlytryptophan at 500µM) was used at the published concentration (Karunakaran et al., 2008). We also performed a [^{3}H]ADMA and [^{14}C]sucrose accumulation study in buffer absent of Na^+ and Cl^- ions based on a published recipe by (Tamai et al., 1995) and detailed in appendix 4, to stop the action of the Na^+ and Cl^- dependent $ATB^{0,+}$ to investigate the role of this transporter in [^{3}H]ADMA accumulation.

4.2.7. MTT cytotoxicity assay

The potential of the all the compounds used in this accumulation study to cause cytotoxicity to the hCMEC/D3 cells was assessed using an MTT assay following the protocol described in section 2.5. The effect of these compounds on hCMEC/D3 viability was compared to untreated control hCMEC/D3 cells. Triton x-100 was used as a positive control.

4.2.8. Expression of CAT1 and $ATB^{0,+}$

The expression of both CAT-1 and $ATB^{0,+}$ in the hCMEC/D3 cells and MCF-7 cells (positive control) were ascertained by SDS-PAGE, WB, and IF with confocal microscopy.

For SDS-PAGE and WB, the protocol in chapter 2, section 2.7 was used and hCMEC/D3 cell lysate was prepared in TGN lysis buffer as described in section 2.7.1. 30µg was loaded in each well. Rabbit anti-human CAT-1 primary antibody was used at a dilution of 1:250 in PBS-T and 0.5% BSA as described in table 2.2. Rabbit anti-human $ATB^{0,+}$ primary antibody was used at a dilution of 1:1000 in PBS-T and 0.5% BSA also as described in table 2.2. Goat anti-rabbit HRP conjugated secondary antibody was used at a dilution of 1:5000 for chemiluminescence detection for CAT-1 and $ATB^{0,+}$ WB. Whole wild-type MCF7 cell lysate, prepared in TGN lysis buffer as described in 2.7.1 acted as positive controls for these transporters – see (Karunakaran et al., 2011) for $ATB^{0,+}$ and (Abdelmagid et al., 2011) for CAT-1 – and was a kind gift from Mr. Evangelos Pazarentzos (Imperial College London).

Obtaining a clear blot of $ATB^{0,+}$ was initially difficult because it is heavily N-glycosylated in mammalian systems (Broer, 2008). To deglycosylate the cell lysate, N-linked-glycopeptide-(N-acetyl-beta-D-glucosaminyl)-L-asparagine amidohydrolase (PNGase F, from New England Biolabs) was used according to the manufacturer's protocol and described in appendix 5. The PNGase F kit was kindly lent to us by Mr. Evangelos Pazarentzos.

IF with confocal microscopy was performed on hCMEC/D3s grown on rat tail collagen type 1 coated sterile glass coverslips was performed as described in section 2.8 for CAT-1 and $ATB^{0,+}$. Goat anti-rabbit Alexa Fluor 488 conjugated secondary diluted at 1:200 in PBS was used for both proteins. More details of these antibodies can be found in table 2.2 of chapter 2.

4.3. Results

4.3.1. Octanol-saline partition coefficient of [^{3}H]L-arginine and [^{3}H]ADMA

As outlined in section 2.9, an OSPC was performed on all radiolabelled compounds to assess their lipophilicity which would give an indication of their potential to cross cell membranes by passive diffusion and accumulate in the cells. The mean octanol-saline partition values for [^{3}H]L-arginine (MW 174.2 g/mol^{-1}) and [^{3}H]ADMA (MW 202.25 g/mol^{-1}) were 0.0015 ± 0.0002 and 0.0023 ± 0.0001 respectively (n=3) which was statistically significant (*p<0.01*). Our group also performed OSPC analysis on [^{14}C]sucrose (n=3) obtaining a mean value of 0.0004 ± 0.00001, which was statistically significant when compared to [^{3}H]L-arginine and [^{3}H]ADMA (both *p<0.001*).

4.3.2. [^{3}H]L-arginine and [^{3}H]ADMA control accumulation comparison

Before transport mechanisms were assessed, the control values of [^{14}C]sucrose and protein corrected [^{3}H]L-arginine and [^{3}H]ADMA accumulation assays were compared directly. The accumulation of [^{3}H]ADMA increased in a time-dependent manner from a V_d of 13.58 ± 0.66 at 1 minute, to a V_d of 61.24 ± 2.92 at 30 minutes. In a similar manner, the accumulation of [^{3}H]L-arginine increased in a time-dependent manner from a V_d of 33.75 ± 1.70 at 1 minute, to a V_d of 106.79 ± 1.73 at 30 minutes At all time points, [^{3}H]L-arginine V_d values were significantly higher than those from [^{3}H]ADMA (*p<0.001* at all time points). See table 4.1 below.

Table 4.1. [^{14}C]sucrose and protein corrected [^{3}H]ADMA and [^{3}H]L-arginine accumulation in the hCMEC/D3s.

Mean V_d ± S.E.M

Time (minutes)	[^{3}H]ADMA	[^{3}H]L-arginine	*p*
1	13.575 ± 0.658	33.575 ± 1.703	*<0.001*
2.5	25.363 ± 0.857	57.997 ± 5.422	*<0.001*
5	41.317 ± 4.230	79.840 ± 2.423	*<0.001*
20	58.757 ± 2.435	100.301 ± 2.007	*<0.001*
30	61.236 ± 2.915	106.794 ± 1.732	*<0.001*

ADMA – asymmetric dimethylarginine

4.3.3. [^{14}C]sucrose comparison from [^{3}H]L-arginine and [^{3}H]ADMA control accumulation

The control values of protein corrected [^{14}C]sucrose from [^{3}H]L-arginine and [^{3}H]ADMA accumulation assays were also compared directly. There were no significant differences between the treatments. See table 4.2 below.

Table 4.2. Protein corrected [^{14}C]sucrose results from [^{3}H]ADMA and [^{3}H]L-arginine accumulation in the hCMEC/D3s.

	Mean V_d ± S.E.M		
Time (minutes)	**[^{14}C]sucrose (ADMA)**	**[^{14}C]sucrose (L-arginine)**	***p***
1	1.362 ± 0.305	1.659 ± 0.428	*n.s*
2.5	1.407 ± 0.219	1.816 ± 0.662	*n.s*
5	2.402 ± 0.320	2.613 ± 0.516	*n.s*
20	3.401 ± 0.240	3.623 ± 0.497	*n.s*
30	3.489 ± 0.419	3.931 ± 0.682	*n.s*

ADMA – asymmetric dimethylarginine, *n.s* – not significant

4.3.4. Accumulation of [^{3}H]L-arginine and [^{14}C]sucrose – Role of CAA transporters

To assess the roles of CAA transporters on the transport and accumulation of [^{3}H]L-arginine in the hCMEC/D3s, 100µM unlabelled L-arginine, 20mM L-homoarginine, 100µM leucine, and 4mM BCH were added individually to the accumulation buffer alongside [^{3}H]L-arginine and [^{14}C]sucrose, and compared to appropriate controls. The data are displayed in figure 4.1.

4.3.5. [^{14}C]sucrose in [^{3}H]L-arginine studies

No significant differences between [^{14}C]sucrose accumulation was observed with any of the treatments involving 100µM unlabelled L-arginine, 20mM L-homoarginine, 100µM leucine or 4mM BCH when compared to the controls cells which received no CAA interacting drugs (displayed as insert in figure 4.1). There were also no significant differences in [^{14}C]sucrose accumulation when unlabelled ADMA treatments were used in the cross-competition studies (displayed as the insert in figure 4.2).

4.3.6. [^{3}H]L-arginine accumulation

The addition of 100µM unlabelled L-arginine caused a marked decrease in the accumulation of [^{3}H]L-arginine ($p<0.001$), with an average percentage decrease between the time points of 73% (figure 4.1). Accumulation almost completely inhibited (an approximate decrease of 98% was seen across all time points) with the addition of 20mM L-homoarginine ($p<0.001$). The

addition of 4mM BCH and 100µM leucine to the accumulation buffer caused no significant changes in [^{3}H]L-arginine accumulation.

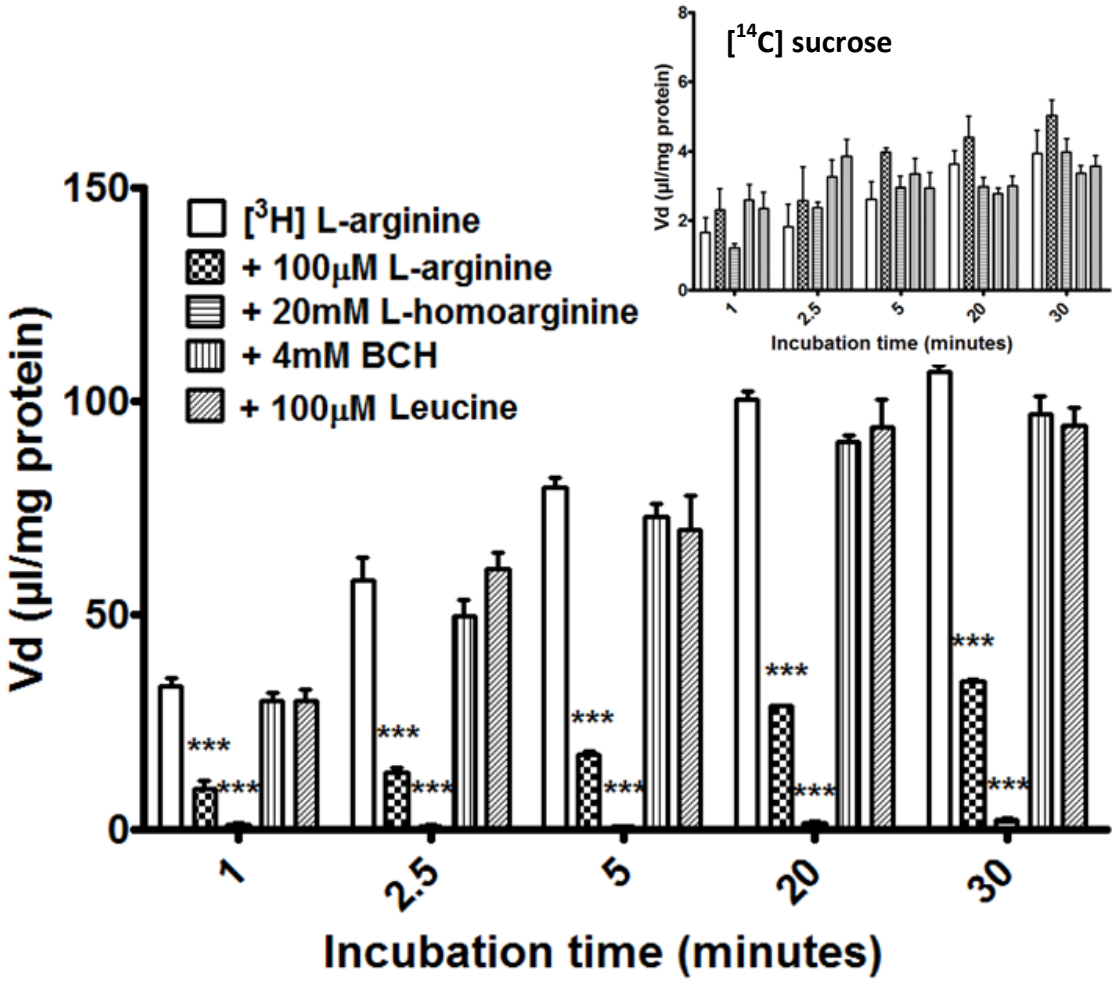

Figure 4.1. The roles of CAA transporters on accumulation of [^{3}H]L-arginine and [^{14}C]sucrose in hCMEC/D3 cells. To understand the roles CAA transporters played in the transport and subsequent accumulation of [^{3}H]L-arginine, self-inhibition and the addition of known CAA transporter interacting drugs was performed in an accumulation model using confluent hCMEC/D3s. [^{14}C]sucrose was used as a marker of non-specific binding, barrier integrity and extracellular space for accumulation experiments (insert). ****p<0.001*. [^{3}H]L-arginine data are corrected for [^{14}C]sucrose and protein content (with [^{14}C]sucrose corrected for protein only) and expressed as means ± S.E.M, n=6 (plates) with 6 replicates (wells) per n. BCH – 2 -aminobicyclo-(2,2,1)-heptane-2-carboxylic acid.

To investigate the possible competitive effect of ADMA on the influx and accumulation of [^{3}H]L-arginine, 0.5µM, 3µM, and 500µM unlabelled ADMA were added individually to the accumulation buffer. When 0.5µM and 3µM ADMA was added, there were no significant differences in accumulation when compared to [^{3}H]L-arginine controls. However, an average

decrease in [^{3}H]L-arginine accumulation of 83% across the time points was revealed with the addition of 500µM ADMA ($p<0.001$) when compared to controls (figure 4.2).

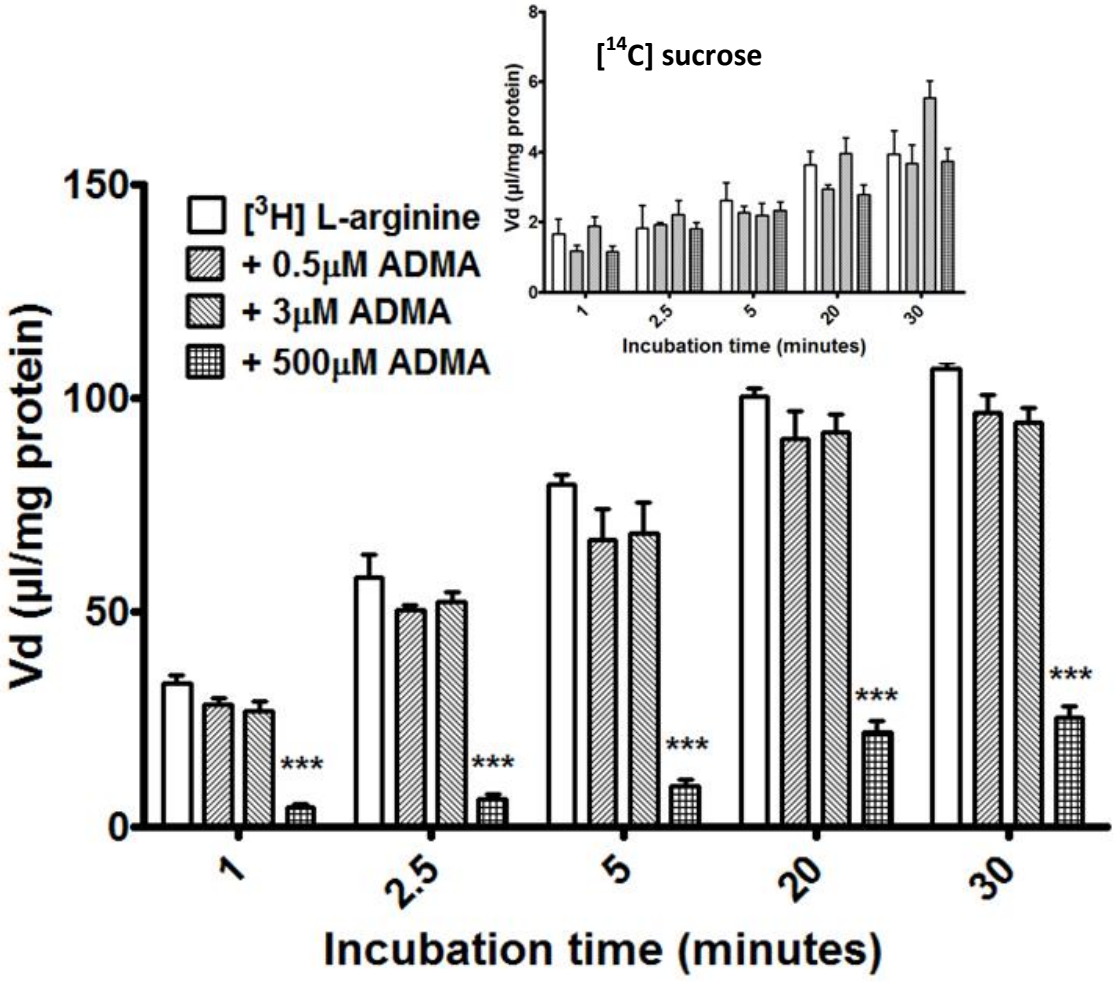

Figure 4.2. The competitive effects of unlabelled ADMA on accumulation of [^{3}H]L-arginine and [^{14}C]sucrose in hCMEC/D3 cells. 0.5µM, 3µM and 500µM ADMA were added individually to accumulation buffer to observe and competitive effects on [^{3}H]L-arginine accumulation in confluent monolayers of hCMEC/D3 cells. ****p<0.001*. The addition of 0.5µM, 3µM and 500µM ADMA caused no significant changes in [^{14}C]sucrose accumulation over the 30 minute time period in the cells (insert). All [^{3}H]L-arginine data are corrected for [^{14}C]sucrose and protein content (with [^{14}C]sucrose corrected for protein only) and expressed as means ± S.E.M, n=5-6 (plates) with 6 replicates (wells) per n. ADMA – asymmetric dimethylarginine.

4.3.7. Accumulation of [^{3}H]ADMA and [^{14}C]sucrose – Role of CAA transporters

To elucidate the transport mechanisms utilised by ADMA in the hCMEC/D3s, a series of accumulation experiments similar to those used for [^{3}H]L-arginine were designed to assess the

effects of self-inhibition, competitive inhibition and CAA transporters on the transport and resulting accumulation of [^{3}H]ADMA and [^{14}C]sucrose.

4.3.8. [^{14}C]sucrose in [^{3}H]ADMA studies

There were no significant changes in the accumulation of [^{14}C]sucrose with the self-inhibition studies involving ADMA concentrations of 0.5µM, 3µM or 500µM unlabelled ADMA, or 100µM L-arginine, in the presence of [^{3}H]ADMA (figure 4.3 insert). No differences were observed in [^{14}C]sucrose accumulation with the addition of AA transporter affecting drugs 20mM L-homoarginine, 4mM BCH, 500µM α-methyltryptophan, 100µM leucine or when Na^{+} and Cl^{-} free buffer was used, as demonstrated in the figure 4.4 insert.

4.3.9. [^{3}H]ADMA

To investigate self- and cross-competition on [^{3}H]ADMA transport interaction and accumulation, 0.5µM, 3µM and 500µM unlabelled ADMA as well as 100µM L-arginine were added individually to the accumulation buffer with [^{3}H]ADMA and [^{14}C]sucrose. 0.5µM ADMA caused no significant changes to accumulation, but 3µM caused significant decreases at 20 minutes and 30 minutes (both $p<0.05$). A decrease in [^{3}H]ADMA accumulation of 87% was observed across all time points on the addition of 500µM ADMA ($p<0.001$). 100µM L-arginine also caused a decrease (average decrease of 36% across time points), but statistical significance was only apparent after 5 minutes 20 minutes and 30 minutes ($p<0.05$) (figure 4.3).

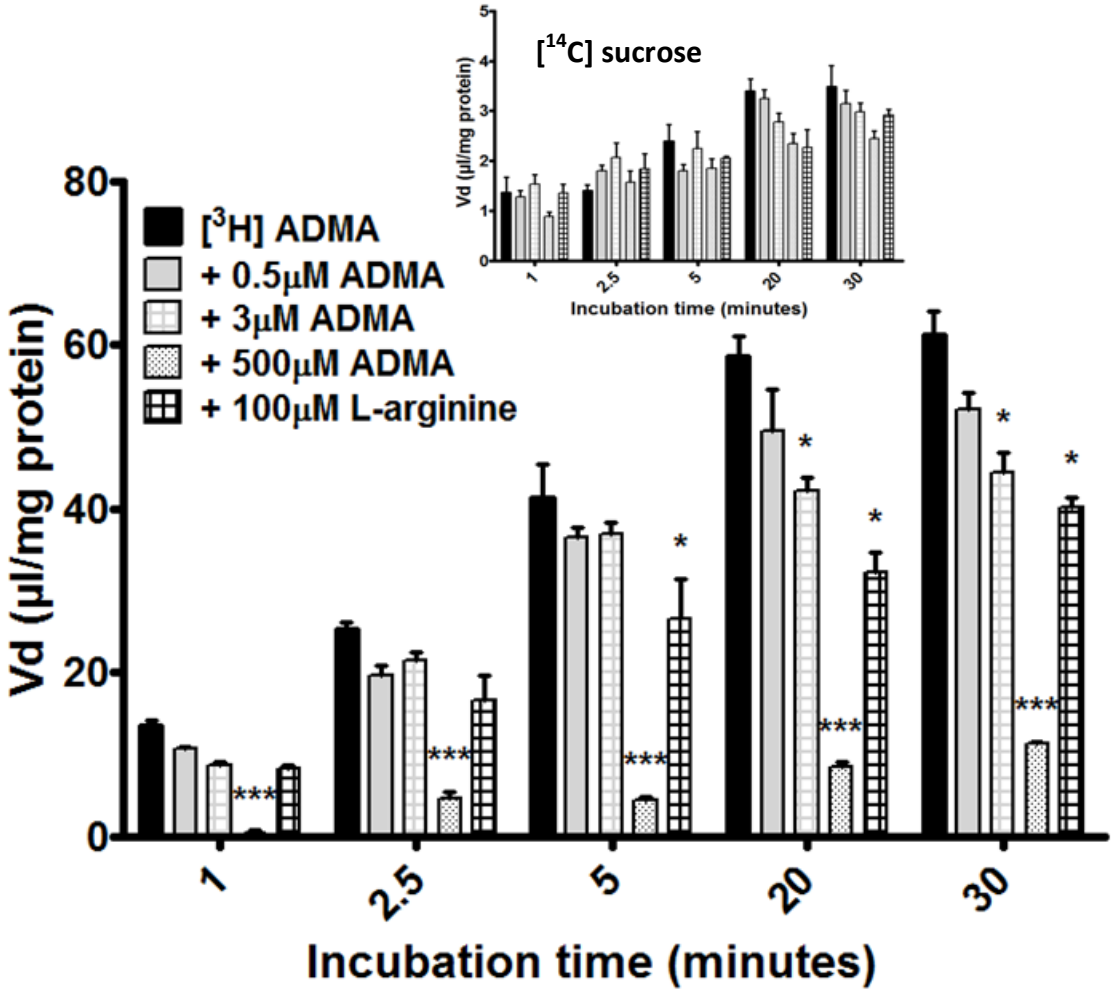

Figure 4.3. The effect of self and competitive inhibition on the transport and accumulation of [^{3}H]ADMA and [^{14}C]sucrose in hCMEC/D3 cells. To investigate self and competitive inhibition on [^{3}H]ADMA transport and accumulation, 0.5µM, 3µM and 500µM unlabelled ADMA and 100µM L-arginine were added individually to the accumulation buffer. *$p<0.05$, ***$p<0.001$. The addition of 0.5µM, 3µM and 500µM unlabelled ADMA and 100µM L-arginine individually to the accumulation buffer caused no significant changes in the accumulation of [^{14}C]sucrose (insert). All [^{3}H]ADMA data are corrected for protein content and [^{14}C]sucrose (with [^{14}C]sucrose corrected for protein only) and expressed as means ± S.E.M, n=5 (plates) with 6 replicates (wells) per n. ADMA – asymmetric dimethylarginine.

The influence of CAA transporters on [^{3}H]ADMA and [^{14}C]sucrose was initially deduced using 20mM L-homoarginine and 4mM BCH. The addition of 20mM L-homoarginine caused a large decrease in accumulation of [^{3}H]ADMA at all time points, which gained higher significance as the incubation time increased – at 1 minute *p<0.05*, 2.5 minutes to 30 minutes *p<0.01*. The percentage decreases in Vd induced by L-homoarginine were 47% for 1 minute, 64% for 2.5 minutes, 75% for 5 minutes, 8%1 for 20 minutes and 76% for 30 minutes. The data are displayed in figure 4.4. The addition of 100µM leucine saw significant decreases in [^{3}H]ADMA accumulation from 5 minutes (21% decrease), to 20 minutes (40% decrease) and 30 minutes (38% decrease) (all *p<0.05*). Conversely, 4mM BCH induced a significant, 32% increase in accumulation at 5 minutes (*p<0.05*), and at 20 (36%) and 30 minutes (78%), both *p<0.01*.

The $ATB^{0,+}$ inhibitor α-methyltryptophan was also added (500µM) to the normal accumulation buffer alongside [^{3}H]ADMA and [^{14}C]sucrose, and also resulted in significant increases in accumulation at all time points from 5 minutes; 39% increase at 5 minutes (*p<0.05*), 81% at 20 minutes (*p<0.01*), and 88% 30 minutes (*p<0.01*). To investigate this observation further, Na^{+} and Cl^{-} free accumulation buffer was used with [^{3}H]ADMA and [^{14}C]sucrose and caused a significant increase in [^{3}H]ADMA accumulation at all time points from 5 minutes, increasing in significance with incubation time (46% increase at 5 minutes *p<0.05*, 68% increase at 20 minutes *p<0.01* and 160% increase at 30 minutes *p<0.001*). These data are also displayed in figure 4.4.

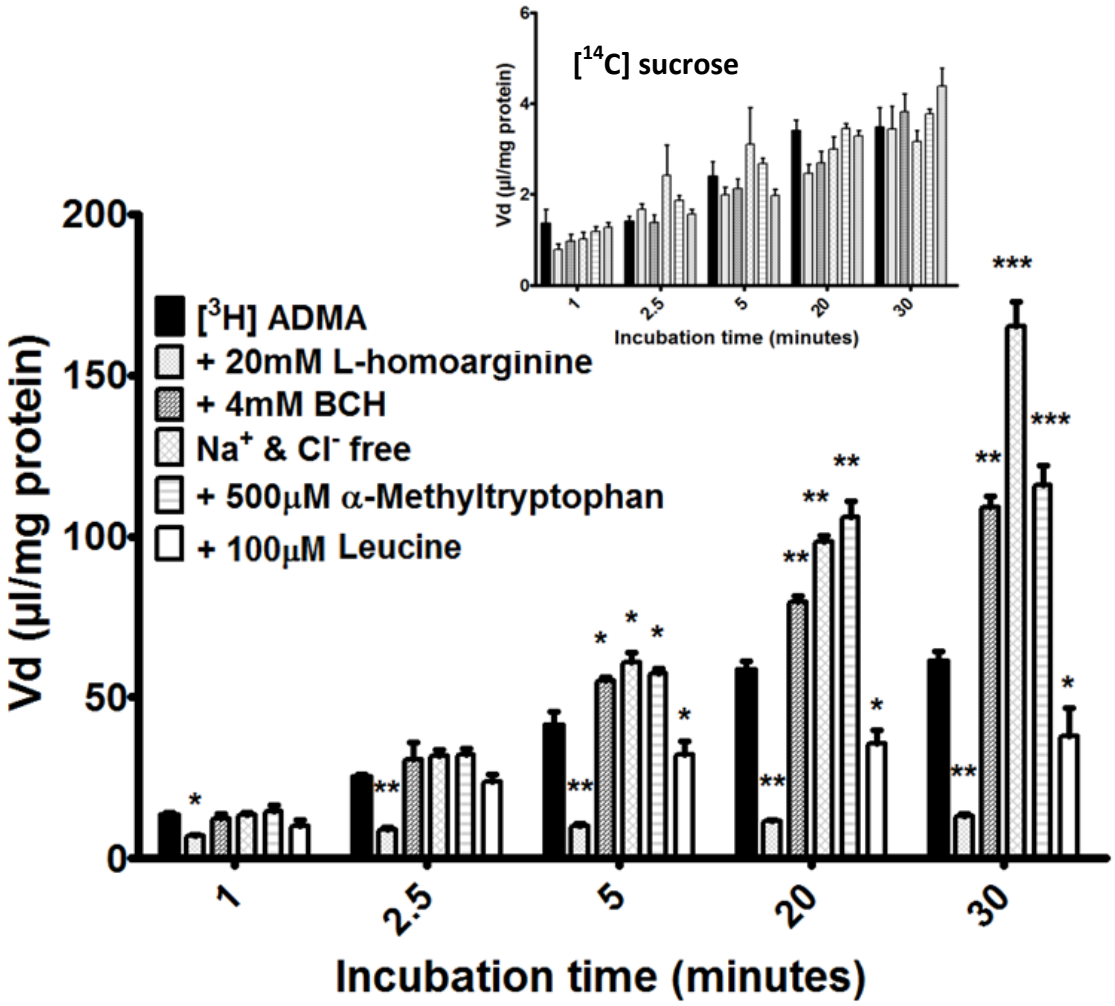

Figure 4.4. Roles of CAA transport systems on the accumulation of [^{3}H]ADMA and [^{14}C]sucrose in hCMEC/D3 cells. To understand the roles CAA transporters played in the transport and subsequent accumulation of [^{3}H]ADMA, the addition of known CAA transporter interacting drugs was performed in an accumulation model using confluent hCMEC/D3s. *$p<0.05$, **$p<0.01$ and ***$p<0.001$. The addition of 20mM L-homoarginine, 4mM BCH, 100µM leucine and 500µM α-methyltryptophan, as well as removal of Na^{+} and Cl^{-} from the accumulation buffer caused no significant changes in [^{14}C]sucrose accumulation over the 30 minute time period (insert). All [^{3}H]ADMA data are corrected for [^{14}C]sucrose and protein content (with [^{14}C]sucrose corrected for protein only) and expressed as means ± S.E.M, n=4-6 (plates) with 6 replicates (wells) per n. ADMA – asymmetric dimethylarginine, BCH – 2 -aminobicyclo-(2,2,1)-heptane-2-carboxylic acid.

4.3.10. Cytotoxicity of compounds used in accumulation study

The cytotoxic potential of all compounds used in this study over the 30 minute time-frame was assessed in the hCMEC/D3 cells using an MTT assay, comparing treated cells to untreated control cells. There were no significant differences in cell viability between the treatments except when using the positive control 1% Triton x-100 ($p<0.01$, figure 4.5 below).

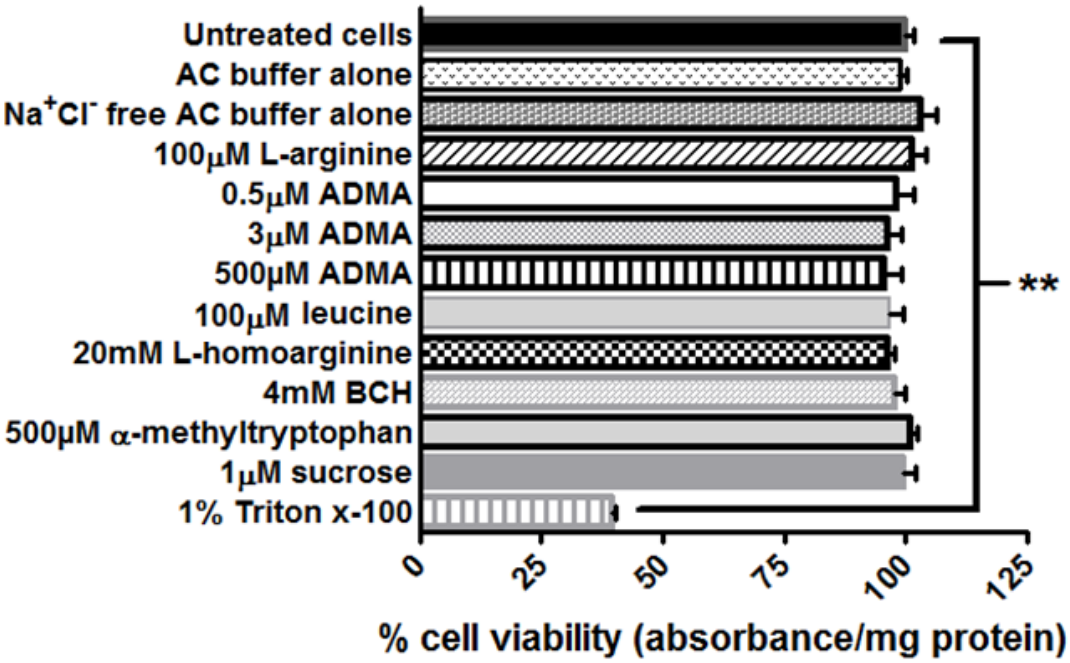

Figure 4.5. The cytotoxic effects of study compounds on confluent monolayers of hCMEC/D3 cells. The study compounds were assessed for any cytotoxic potential using an MTT assay during 30 minute incubation with confluent monolayers of hCMEC/D3 cells in 96 well plates, as described in section 2.5. The results are expressed as percentage viability ± S.E.M and compared to control untreated cells, which were incubated for 30 minutes in culture medium. n=4 (plates), 6 replicates per n (6 wells). AC = accumulation, ADMA – asymmetric dimethylarginine, BCH – 2 -aminobicyclo-(2,2,1)-heptane-2-carboxylic acid.

4.3.11. Expression of CAA transporter CAT-1 in hCMEC/D3 cells

Rabbit anti-human CAT-1 primary antibody was used with goat anti-rabbit HRP conjugated secondary antibody for WB detection of CAT-1 in the TGN lysed hCMEC/D3s and wt MCF7 whole cell lysates. The blot revealed a positive expression of CAT-1 of the expected size of 60-70kDa according to the antibody manufacturer (figure 4.6 a).

CAT-1 expression was also observed with IF and subsequent confocal microscopy in the hCMEC/D3s (figure 4.6 b) using rabbit anti-human CAT-1 primary antibody and goat anti-rabbit Alexa Fluor 488 conjugated secondary antibody by the protocol described in section 4.2.8. It showed typical membrane/cytoskeletal-like patterning (Closs et al., 2004).

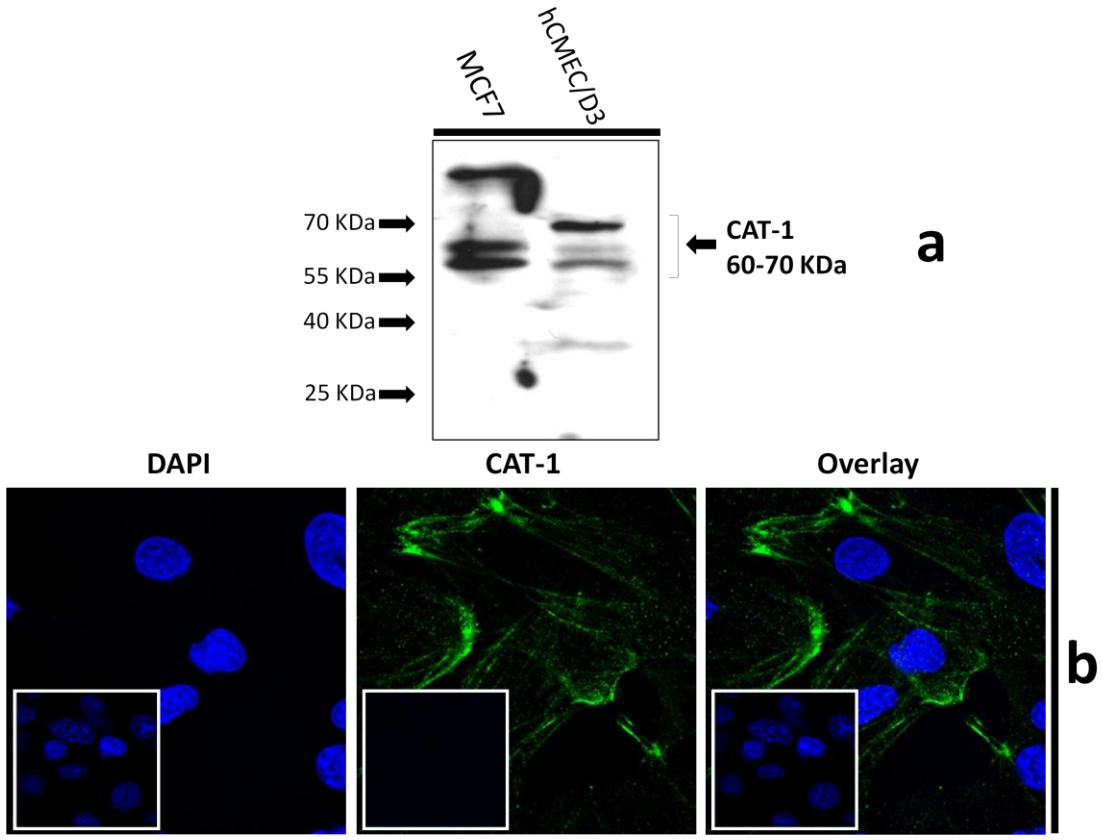

Figure 4.6. Expression of CAT-1 in hCMEC/D3s. a| SDS-PAGE and WB analysis revealed CAT-1 expression in hCMEC/D3 (passage 28) and wt MCF7 whole cell lysate lysed in TGN lysis buffer, as described in section 2.7. **b|** CAT-1 expression was also demonstrated by IF performed with hCMEC/D3 cells (passage 28) grown on rat tail collagen type-1-coated coverslips, fixed with 4% formaldehyde and stained for with primary and secondary antibody as described in section 4.2.8. Cell nuclei were counterstained with 1µg/ml DAPI. For negative staining, cells were stained with secondary antibody only along with DAPI (inserts).

4.3.12. Expression of CAA and NAA transporter $ATB^{0,+}$ in hCMEC/D3 cells

Rabbit anti-human $ATB^{0,+}$ primary antibody was used with goat anti-rabbit HRP conjugated secondary antibody for WB detection of CAT-1 in the TGN lysed hCMEC/D3s and wt MCF7 whole cell lysates, before and after deglycosylation. PNGase F was used to deglycosylate the lysates. Following deglycosylation, the blot at an expected size of 55-70kDa was visible, confirming expression of the protein (figure 4.7 a). During the time of writing this thesis, a publication has also since confirmed functional expression of this transport protein (Kooijmans et al., 2012).

The expression and localisation of $ATB^{0,+}$ was also visualised by using the rabbit anti-human $ATB^{0,+}$ primary antibody and goat anti-rabbit Alexa Fluor 488 conjugated secondary antibody with confocal microscopy (figure 4.7 b). It showed both membrane and cytoskeletal patterning, which is typical for this transporter (Czeredys et al., 2008).

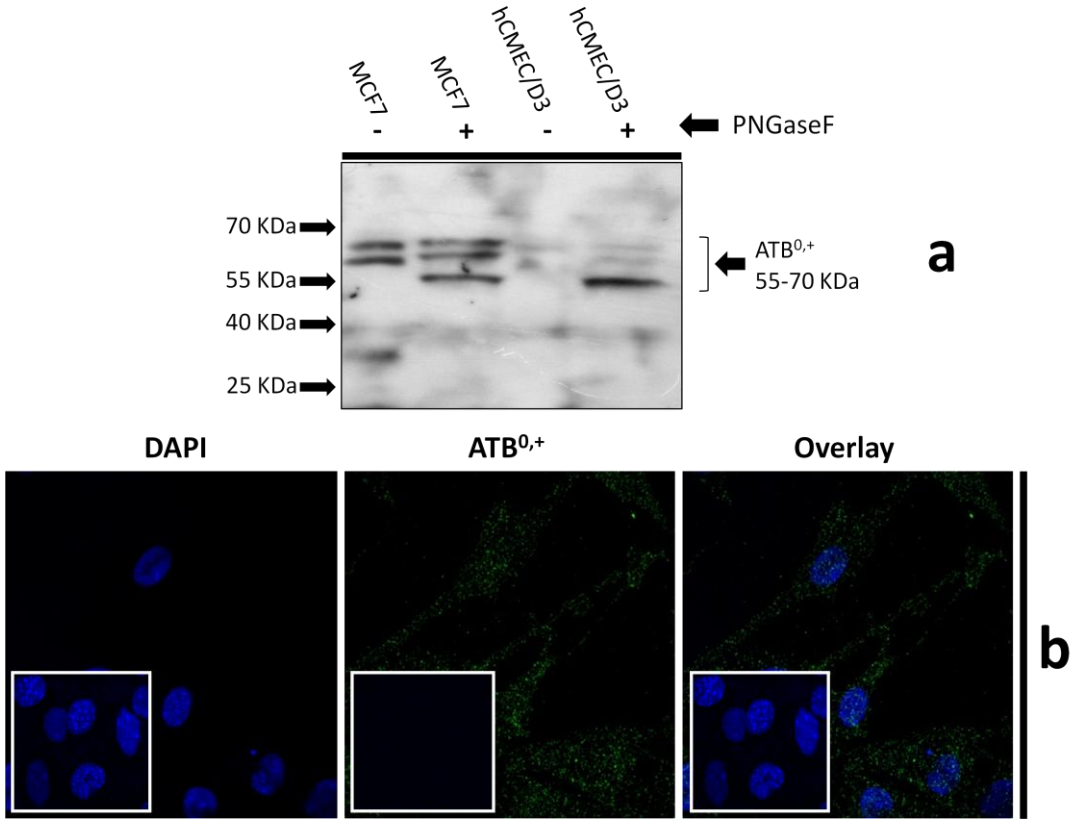

Figure 4.7. Expression of $ATB^{0,+}$ in hCMEC/D3s. a| Following deglycosylation with PNGase F, SDS-PAGE and WB analysis revealed $ATB^{0,+}$ expression in hCMEC/D3 (passage 30) and wt MCF7 whole cell lysate lysed in TGN lysis buffer, as described in section 2.7. **b|** $ATB^{0,+}$ expression was also demonstrated by IF performed with hCMEC/D3 cells (passage 30) grown on rat tail collagen type-1-coated coverslips, fixed with 4% formaldehyde and stained for with primary and secondary antibody as described in section 4.2.8. Cell nuclei were counterstained with 1µg/ml DAPI. For negative staining, cells were stained with secondary antibody only along with DAPI (inserts).

4.4. Chapter 4 – Discussion

Numerous studies have indicated the presence of an increased ADMA concentration in the plasma of patients with cerebrovascular disease and brain pathologies compared to normal plasma concentrations in healthy patients (see table 1.2 in the introduction chapter). These differences in concentrations, although small, could have large implications in the cause and progression of disease due to the large number of effects ADMA can have on endothelium and NO production. Therefore, we decided to investigate the transport mechanisms of ADMA at the BBB using a human BBB *in vitro* model, the immortalised hCMEC/D3s.

L-arginine and ADMA are very similar in structure and composition and so we decided to base the ADMA investigation on the results of those generated from L-arginine studies, hypothesising that both molecules would have a very similar transport profile. Before looking at the transport and accumulation of both molecules, we aimed to deduce the OSPC values for the molecules under investigation, giving us an indication of their lipophilicity and membrane penetration without the influence of transporters. The data indicated that both [^{3}H]L-arginine and [^{3}H]ADMA had high hydrophilicity and low lipophilicity, with [^{3}H]L-arginine having statistically lower lipophilicity than [^{3}H]ADMA. Both molecules had higher lipophilicity than that of [^{14}C]sucrose, which is a common paracellular permeability and non-specific binding marker in BBB studies. This means without the interaction of transporters, the accumulation of [^{3}H]L-arginine and [^{3}H]ADMA in the cells should be low, but in a range similar or higher than [^{14}C]sucrose. Therefore, our findings that both [^{3}H]L-arginine and [^{3}H]ADMA readily accumulated in the cells at values much greater than [^{14}C]sucrose provides compelling evidence for transporter interaction.

When directly compared, we saw that both molecules accumulated in a time-dependent manner – which is typical of transport interaction – but that the control [^{3}H]L-arginine accumulated at significantly higher amounts when compared to control [^{3}H]ADMA. Differences between the [^{14}C]sucrose values of both control treatments failed to obtain statistical significance when directly compared. These initial findings suggested that perhaps the transport systems at work favoured L-arginine over ADMA.

The accumulation of [^{3}H]L-arginine was decreased significantly with the addition of the normal adult L-arginine plasma concentration of 100µM (Moller et al., 1979, Moller et al., 1983) indicating transport competition for influx mechanisms. Further experiments with

20mM L-homoarginine revealed that the influx mechanisms utilised was a member of system y+, with an almost complete halt of accumulation immediately (98% decrease) and for the rest of the 30 minute time period observed with the addition of 20mM L-homoarginine. It is well established that L-homoarginine competitively inhibits system y^+ (White, 1985) and the concentration used here was based on that of a previous *in vitro* BBB study using bovine BMECs (O'Kane et al., 2006). The impact of L-homoarginine here also dismisses the L-arginine transport roles of other CAA influx mechanisms such as system y^+L transporters and $ATB^{0,+}$ at the human BBB (O'Kane et al., 2006). The addition of BCH, a broad acting inhibitor of NAA transporters including $ATB^{0,+}$ (Van Winkle et al., 1985) and the NAA leucine also supported the finding that system y^+ appears to be the primary transport system used by L-arginine in these cells.

These data were not unexpected, as it has been well established that system y^+ is the principle CAA transport system in mammals. Which CAT isoform is responsible remains at large, but as CAT-1 is well characterised at the BBB, it remains likely that this protein is involved. The expression of CAT-1 was confirmed in the hCMEC/D3s through WB and IF analysis showing typical cytoskeletal/caveoli localisation where it is believed CAT-1 activity is modulated (Closs et al., 2004) (as previously demonstrated in pulmonary artery endothelial cells (McDonald et al., 1997, Zharikov et al., 2001).

Unlabelled ADMA appeared to reduce accumulation of [^{3}H]L-arginine, but failed to attain significance with 0.5µM and 3µM additions, but a large and significant decrease was observed following the addition of 500µM ADMA. This provides useful information in two ways. In one respect, this finding provides evidence that both molecules can interact with the same transport mechanisms for entry to the cells. The other respect regards transport competition and that although a marked decrease in accumulation was observed, the concentration of 500µM ADMA is supraphysiological and never likely to be reached in the body. Due to the low concentration of [^{3}H]L-arginine used (7nM) it is therefore unlikely that the relevant physiological and pathophysiological concentrations of 0.5µM and 3µM would compete in the body for cellular entry via system y^+, especially considering the average plasma concentration of L-arginine is in the region of 100µM in normal healthy individuals. A similar observation has been previously published using human dermal microvascular endothelial cells where 2.5µM and 10µM ADMA did not significantly reduce L-arginine accumulation (Xiao et al., 2001).

When investigating the accumulation of [^{3}H]ADMA, self-inhibition was not evident with the additions of 0.5µM and 3µM, until 20 minutes when 3µM significantly decreased accumulation. 500µM ADMA saw a significant decrease at all time points (an average of 87% across the times points). These self-inhibition data collectively suggest the evidence of influx mechanisms, along with the decreases noted when 100µM L-arginine was added at the 5, 20 and 30 minute incubation time points. The fact that the 38nM [^{3}H]ADMA used was more than 10 times less than the lowest concentration of addition unlabelled ADMA and not greatly affected by the ADMA additions until later time points, suggests either that the transporter being used has affinity for ADMA and required a very high concentration to slow influx action.

The results from the addition of 100µM L-arginine show a slight decrease in accumulation (at the three last time points) despite being at a concentration more than 2000 times greater than [^{3}H]ADMA, which, along with the decrease caused by 20mM L-homoarginine – which was not as dramatic as that seen with [^{3}H]L-arginine – suggest the idea that multiple influx transporters are at work is certainly plausible. Indeed, our data illustrated decreases in accumulation of [^{3}H]ADMA were apparent with the addition of the NAA leucine to the accumulation buffer at the approximate human physiological plasma concentration (Psychogios et al., 2011). This finding demonstrates that influx transport systems separate from system y^+ could also be transporting ADMA as system y+ is insensitive to leucine (Rotmann et al., 2007). The most likely candidates are y^+L and $b^{0,+}$ proteins, which have affinities for both CAA and NAAs in the presence of Na^+ ions dependent manner (O'Kane et al., 2006, Rotmann et al., 2007), although the proteins were not looked for here, both have been recently demonstrated at mRNA level in the hCMEC/D3s recently (Carl et al., 2010).

Carl *et al*., are the only group other than us to have data that suggests the existence of several AA transporters in the hCMEC/D3 cells (Carl et al., 2010) which could be candidates for ADMA influx transporters. Their report describes SLC7A5-A9 and A11 mRNA expression, with SLC7A5, A6 and A11 having the highest mRNA levels respectively. In their paper, the authors described these genes as coding for system y^+ CAA transporters, although these descriptions appear to be incorrect. According to the NCBI Gene database, in humans SLC7A5 codes for a large NAA transporter, SLC7A6 and SLC7A7 code for system y^+L transporters y^+LAT1 and y^+LAT2, SLC7A8 codes for a system L NAA transporter, SLC7A9 codes for the heavy chain of the system $b^{0,+}$ transporter, and SLC7A11 codes for the cystine and glutamate anionic AA transporter xCT. Interestingly, the paper also describes a large mRNA expression of SLC3A2,

the gene that codes for the ubiquitous transmembrane protein 4F2hc, involved in the formation of heterodimeric structures which exhibit y^+L and xCT activity (Broer, 2008). There is also expression of SLC3A1 which codes for the light chain of the system $b^{0,+}$ transporter. These data combined with our findings suggest that both system y^+L and $b^{0,+}$ could have functional proteins in the hCMEC/D3s which may possibly be utilised by ADMA (and L-arginine to a lesser extent), but also highlight the confusing nomenclature used to name AA transporters. It is likely that some confusion resulted from the naming of SLC transporters between different species. In several instances, names of human genes are similar in mice, but code for totally different transporters. For example, SLC7A11 codes for an anionic AA transporter in humans, but according to the NCBI Gene database in mice Slc7a11 codes for a system y^+ transporter. It is also possible that the array descriptions could be incorrect and that the authors had in fact gone with the manufacturer's descriptions rather than their own. It is important to note, the PCR array used by Carl et al., (RT^2 Pathway-Focused Profiler Array, PAHS-70A from SA Biosciences) did not include transcripts for CAT-1 (SLC7A1) or $ATB^{0,+}$ (SLC6A14) (nor did they look for CAT-2A, CAT-2B – both coded for by SLC7A2 – CAT-3 (SLC7A3) or CAT-4 (SLC7A4), and so the mRNA for these proteins was not investigated. We are subsequently the first to report the expression of CAT-1 in the hCMEC/D3 cells, with a recent paper reporting the protein expression of ATB in the hCMEC/D3s (Kooijmans et al., 2012).

Perhaps a more surprising result was the evidence for an ADMA cellular exit transport system. The addition of 4mM BCH saw significant increases in [^{3}H]ADMA at all time from 5 minutes. BCH is a broad ranging inhibitor of NAA systems including system L, system A and system $B^{0,+}$ (Mann et al., 1989, Yamauchi et al., 2009) and as only system $B^{0,+}$ is able to transport CAA, we decided to investigate this observation further by removing Na^+ and Cl^- ions from the accumulation buffer. The $B^{0,+}$ transporter, $ATB^{0,+}$ unlike CATs, is a dependent on Na^+ and Cl^- ions to exhibit CAA transport and when removing these ions from the buffer we observed a larger increase in [^{3}H]ADMA accumulation from 5 minutes, with comparable values to BCH. CATs on the other hand would not be affected by such a change and would continue to transport [^{3}H]ADMA into the cell. We also obtained a specific inhibitor of $ATB^{0,+}$, α-methyltryptophan, using it at 500μM – twice the half maximal inhibitory concentration (IC_{50}) (Karunakaran et al., 2008), which produced very similar effects to those demonstrated by BCH and Na^+ and Cl^- free accumulation buffer.

To our knowledge, we are the first group to show this protein act as an AA exiting system or antiport transporter. $ATB^{0,+}$ is normally shown as an influx cotransporter (symporter) where it utilises the Na^+ and Cl^- gradient to influx its substrates (Broer, 2008), which results in inwards currents that are measurable by voltage-clamp techniques (Hatanaka et al., 2004). In a recent study using the hCMEC/D3s, $ATB^{0,+}$ was shown to be a saturable influx transporter for cationic anti-influenza compounds, rather than an efflux system (Kooijmans et al., 2012). CAA efflux from cells is normally carried out by bidirectional transporters such as CATs (Torrents et al., 1998); exchangers such as $rBAT/b^{0,+}$ (Broer, 2008); or transporters that are susceptible to *trans*-stimulation such as CAT-1 (Hatzoglou et al., 2004). However, unlike $ATB^{0,+}$, none of these transporters are dependent on the Na^+ and Cl^- gradient for CAA transport.

The data here could suggest that $ATB^{0,+}$ was exchanging freshly added extracellular Na^+ and Cl^- ions in the accumulation buffer for intracellular ADMA, which could explain why there was no significant increase in accumulation (when the ATB inhibitors and Na^+ and Cl^- free buffer was used) until 5 minutes when perhaps the intracellular ADMA concentration had exceeded that of the extracellular concentration. This would only be plausible if the protein was an antiporter, which to our knowledge has not been demonstrated. A study looking into expression of $ATB^{0,+}$ in a polarised model of the bovine BBB noted that the transporter appeared to be expressed predominantly at the apical membrane, but also at basolateral membranes (Czeredys et al., 2008). If $ATB^{0,+}$ is involved in substrate transport across the BBB in a unidirectional manner and expressed at both membranes in the hCMEC/D3s, then blocking the action of the transporter would also likely see an increase. Although the IF and WB expression of $ATB^{0,+}$ were investigated, the polarisation of the transporter was not. The IF expression appears to show even distribution of the protein throughout the cell, not just the plasma membrane, which was also demonstrated in a recent study investigating the transporter as a means of drug targeting to cancer cells (Karunakaran et al., 2011). Interestingly, it has also been demonstrated that $ATB^{0,+}$ is able to transport ADMA as well as a variety of methylarginines and inhibitors of NOS at high affinity in a study using cloned mouse $ATB^{0,+}$(Hatanaka et al., 2001). Although these $ATB^{0,+}$ data are somewhat equivocal, it seems more likely that the transporter is a unidirectional symporter expressed on both membranes for transport across the BBB. Further work using voltage-clamp techniques to show current direction and transporter over-expression would be required to fully deduce the role of $ATB^{0,+}$ in ADMA transport, as well as studying the situation *in vivo*.

4.5. Conclusions

The results of this study demonstrate that both L-arginine and ADMA predominantly appear to use system y^+ influx mechanisms to enter the hCMEC/D3 BBB cells, as predicted due to their close similarity and chemical composition. This transporter could be CAT-1, and the expression of this transporter was confirmed in our human BBB model. Other influx systems such as systems y^{+L} and $b^{0,+}$ appear to have lesser roles for L-arginine transport, but may have more important roles for ADMA influx. Based on these data, we can assume that physiological and pathophysiological extracellular concentrations of ADMA would be unlikely to compete with L-arginine for entry to the BBB due to the high substrate affinity of the transporters and that ADMA may use transport mechanisms separate from those used by L-arginine. We also observed evidence that ADMA is a substrate of an AA exiting mechanism, most likely the $B^{0,+}$ transporter, $ATB^{0,+}$, which was also expressed in the model, although the precise activity and role of this transporter would require some further investigation before more accurate conclusions can be made.

Chapter 5. Endogenous molecule interactions – Part III – The trans-stimulation of ADMA and L-arginine

5.1. Chapter 5 – Introduction and aims

Many studies have demonstrated that both acute and chronic administration of L-arginine can improve endothelial function in patients suffering from conditions associated with NO dysregulation, but the precise mechanisms behind this improvement remain undisclosed and somewhat puzzling (Bode-Boger et al., 2007). This is because intracellular levels of L-arginine are in the millimolar range and eNOS has a half saturation constant (K_m) in the μM range. Therefore, even before L-arginine supplementation, the enzyme should be fully saturated. In attempts to explain this 'L-arginine paradox', the role of ADMA has been considered.

It is apparent that in conditions involving impaired NO production where by L-arginine supplementation is beneficial, the concentration of extracellular ADMA is increased – thus the L-arginine/ADMA ratio is decreased (see table 1.2) – and it has been hypothesised that the extra L-arginine is able to restore this ratio allowing affected endothelium to produce physiological amounts of NO (Boger, 2004). This may be possible because the major L-arginine transporter CAT-1 is physically associated with eNOS, but would imply that eNOS activity is regulated by extracellular concentrations of L-arginine and ADMA. However, our lab (chapter 4) and others (Xiao et al., 2001) have demonstrated that extracellular pathophysiological concentrations of ADMA are unlikely to outcompete the physiological concentrations of extracellular L-arginine for CAA transport. Another possibility, therefore, is the relationship between intracellular and extracellular concentrations of ADMA and L-arginine. However, it has been demonstrated on numerous occasions that when pathophysiological plasma concentrations of ADMA are detected, NO production is inhibited in a variety of conditions, particularly those with cardiovascular and renal failure (Daniewska-Michalska et al., 1993, Anderstam et al., 1997). These data could point to the high K_m values of CAA transporters or the combined actions of different uptake transport systems, as well as intracellular levels of ADMA, which have been reported to be 8-fold above the 1μM K_i of eNOS and nNOS, and 10- to 20- fold higher than plasma concentrations (Teerlink et al., 2009). This in turn may suggest that both intracellular and pathophysiological plasma concentrations of ADMA are sufficient enough to inhibit NOS in the presence of physiological concentrations of L-arginine, and that supplementation of L-arginine could undo NOS inhibition by ADMA by restoring the L-arginine/ADMA ratio. This could explain the 'L-arginine paradox', but experimental data demonstrating this is somewhat lacking.

The mechanism of this ADMA displacement by L-arginine has been hypothesised to be a result of a process called *trans*-stimulation, where the activity of a transporter is stimulated by substrate on the opposite side of the membrane (Teerlink et al., 2009). Of all the CAA transport systems, system y^+ is by far the most sensitive to *trans*-stimulation, particularly CAT-1 (Hatzoglou et al., 2004), but system y^+L (Mann et al., 2003) and system $b^{0,+}$ (Nguyen et al., 2007) also demonstrate a degree of sensitivity. There has been no evidence of $ATB^{0,+}$ *trans*-stimulation.

The hypothesis behind ADMA displacement is that the increased plasma concentrations of L-arginine would cause the cellular export of ADMA in exchange for L-arginine transport into the cell and that as intracellular levels of ADMA increase, more L-arginine would be transported into the cells.

With an opportunity to test this *trans*-stimulation theory, we decided to investigate the role of ADMA in the *trans*-stimulation of CAA transport, observing cellular exit of radiolabelled ADMA and cellular uptake of radiolabelled L-arginine in an adapted accumulation model using the hCMEC/D3 cells.

5.2. Methods

The reader is directed to the general methods chapter (chapter 2) for detailed descriptions of the generation of the hCMEC/D3 cells.

5.2.1. Cell culture

Please see section 2.1.2 in chapter 2 for details of cell culture reagents and conditions.

5.2.2. Radioactivity studies – Materials

The radiolabelled molecules [^{3}H]ADMA, [^{3}H]L-arginine and [^{14}C]sucrose are described in section the previous chapter 4.2.2.

5.2.3. *Trans*-stimulation assays

To investigate *trans*-stimulation in the hCMEC/D3 cells using ADMA and L-arginine, a series of *trans*-stimulation assays were designed to investigate either the influence of supplemental extracellular amounts of L-arginine (200µM L-arginine) on the cellular exit of preloaded [^{3}H]ADMA with or without unlabelled ADMA, or the effect of increasing concentrations of intracellular ADMA on the influx of extracellular [^{3}H]L-arginine to the hCMEC/D3 cells.

The concentrations of ADMA preloaded with or without [^{3}H]ADMA and ([^{14}C]sucrose) were the physiological plasma concentration of 0.5µM; the pathophysiological plasma concentration of 3µM; and the supraphysiological concentration of 500 µM. Only one radiolabelled test substrate was investigated at a time (i.e. cellular exit investigated for [^{3}H]ADMA and cellular influx investigated for [^{3}H]L-arginine), but [^{14}C]sucrose was included with the radiolabelled molecules as a control as outlined in section 4.2 for the accumulation experiments.

The amount of L-arginine used in supplementation is treatment specific, but a plasma concentration of 200µM is achieved during the treatment of some cardiovascular conditions and was used here (Clarkson et al., 1996, Adams et al., 1997).

The experiments were performed in the centre 60 wells of 96 well plates and were based on the accumulation assays outlined in section 2.2 but included a 20 minute preloading step to preload the cells with 200µl 37°C accumulation buffer containing either:

1) preloading buffer alone (controls) or;
2) [^{3}H]ADMA (40nM) (and [^{14}C]sucrose) or;
3) 0.5µM, 3µM or 500µM unlabelled ADMA with [^{3}H]ADMA (38nM) (and [^{14}C]sucrose) or;

4) 0.5µM, 3µM or 500µM unlabelled ADMA alone (for [^{3}H]L-arginine and [^{14}C]sucrose influx experiments)

This preloading stage is referred to the 'preload' step throughout the thesis.

Following this 20 minute preload step, the buffer was removed and an accumulation assay was performed under the same conditions as those outlined in chapter 2, sections 2.2 and 4.2. The concentrations of radiolabelled molecules used for the *trans*-stimulation assay in this chapter were the same as those used in the previous chapter for the accumulation assay: [^{3}H]L-arginine (0.0111 MBq or 300 nCi, 7nM); [^{3}H]ADMA 38nM (0.0111 MBq or 300 nCi); and [^{14}C]sucrose (0.0148 MBq or 400 nCi, 972nM), all per 1ml accumulation buffer.

The subsequent accumulation assay following the preload step had three treatments:

1) 200µl of fresh 37°C accumulation buffer alone (controls);
2) 200µl of buffer containing 200µM unlabelled L-arginine alone (for [^{3}H]ADMA experiments);
3) or 200µl of buffer containing 200µM unlabelled L-arginine and [^{3}H]L-arginine (7nM).

This accumulation assay had the same time points (1, 2.5, 5, 20 and 30 minute incubations) used in chapter 3 and halted with ice cold PBS and the radioactivity subsequently measured as described in section 2.2.

5.2.4. Cytotoxicity assay

Any cytotoxic effects of the *trans*-stimulation assay treatments on the hCMEC/D3 cells were determined using an MTT assay as outlined in section 2.5, except cells underwent both the 20 minute preload and 30 minute incubation times (50 minutes in total under the same treatments used in the *trans*-stimulation assay described above).

5.3. Results

5.3.1. Influence of unlabelled extracellular L-arginine on the *trans*-stimulation of preloaded [^{3}H]ADMA

To understand the influence of extracellular L-arginine on the *trans*-stimulation of preloaded intracellular ADMA, confluent monolayers of hCMEC/D3s were preloaded with [^{3}H]ADMA with or without 0.5 µM, 3µM or 500µM unlabelled ADMA (and [^{14}C]sucrose) in accumulation buffer for 20 minutes before being replaced for 30 minutes with accumulation buffer containing an L-arginine supplementation concentration of 200µM. The results are displayed in figures 5.1 to 5.4 below.

5.3.2. [^{14}C]sucrose in preloaded [^{3}H]ADMA *trans*-stimulation studies

The differences in [^{14}C]sucrose accumulation between all the[^{3}H]ADMA preload treatments ([^{3}H]ADMA and [^{14}C]sucrose preload with 0.5 µM, or 3µM, or 500µM unlabelled ADMA) failed to obtain statistical significance when compared to controls in these groups ([^{3}H]ADMA and [^{14}C]sucrose preload alone without excess unlabelled ADMA) (see insert graphs in figures 5.1-5.4).

5.3.3. [^{3}H]ADMA *trans*-stimulation studies

When the cells were preloaded with [^{3}H]ADMA and [^{14}C]sucrose alone, the addition of unlabelled L-arginine in the subsequent accumulation assay saw a significant decrease in the accumulation of [^{3}H]ADMA at all times points when compared to the addition of accumulation buffer alone (figure 5.1). The percentage decrease in accumulation was 34% at 1 minute, 47% at 2.5 minutes, 47% at 5 minutes, 114% at 20 minutes and 136% at 30 minutes ($p<0.01$ at all time points).

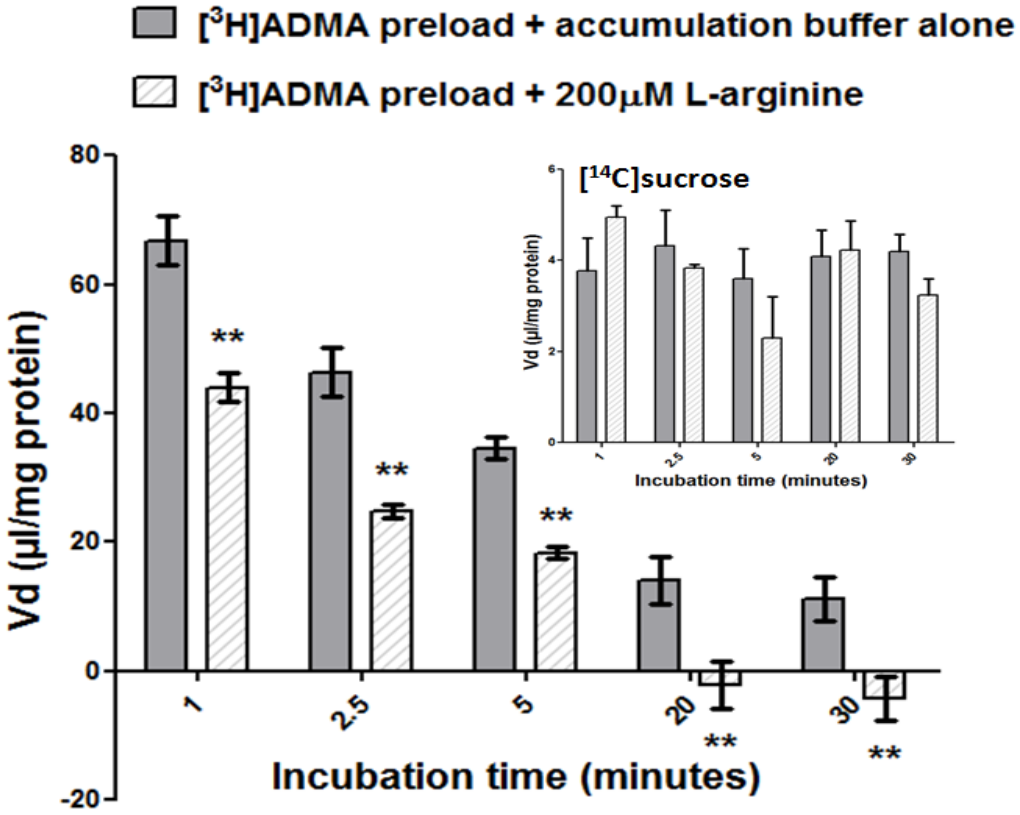

Figure 5.1. The *trans*-stimulation effect of extracellular L-arginine on preloaded [^{3}H]ADMA and [^{14}C]sucrose. To investigate if intracellular ADMA could be *trans*-stimulated by extracellular L-arginine, confluent monolayers of hCMEC/D3 cells were preloaded with [^{3}H]ADMA and [^{14}C]sucrose (as a marker of non-specific binding, barrier integrity and extracellular space, see insert) in accumulation buffer for 20 minutes, before the preload buffer was replaced with accumulation buffer alone or accumulation buffer containing 200μM unlabelled L-arginine for 30 minutes. ***p<0.01*. [^{3}H]ADMA data are corrected for [^{14}C]sucrose and protein content (with [^{14}C]sucrose corrected for protein only) and expressed as means ± S.E.M, n=5 (plates) with 6 replicates (wells) per n. ADMA – asymmetric dimethylarginine.

A similar effect was also noted with the addition of unlabelled L-arginine following the incubation of [^{3}H]ADMA with the ADMA physiological concentration of 0.5μM unlabelled ADMA (figure 5.2). The difference at all time points obtained the same significance ($p<0.01$), except for 20 minutes ($p<0.05$) with the percentage decrease averaging at 53%.

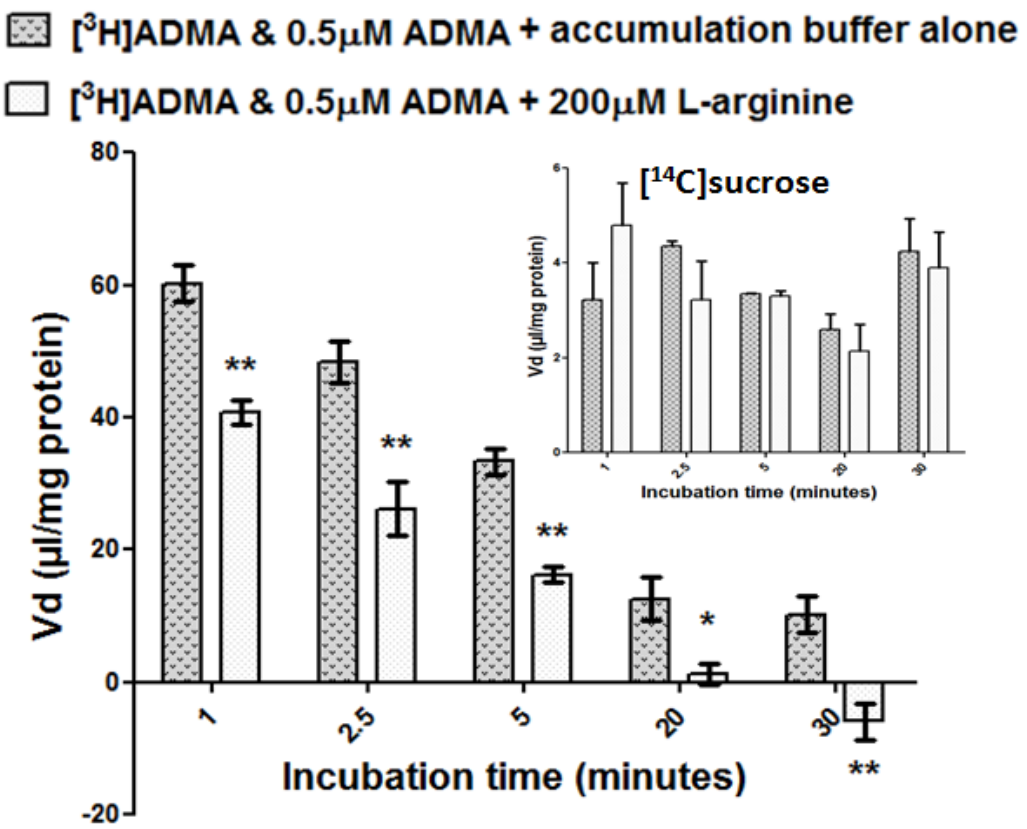

Figure 5.2. The *trans*-stimulation effect of extracellular L-arginine on preloaded [^{3}H]ADMA with 0.5μM ADMA and [^{14}C]sucrose. hCMEC/D3 cells were preloaded with [^{3}H]ADMA along with 0.5μM unlabelled ADMA and [^{14}C]sucrose (as a marker of non-specific binding, barrier integrity and extracellular space, see insert) in preload buffer for 20 minutes, before the being replaced with accumulation buffer alone or accumulation buffer containing 200μM unlabelled L-arginine for 30 minutes. *$p<0.05$, **$p<0.01$. [^{3}H]ADMA data are corrected for [^{14}C]sucrose and protein content (with [^{14}C]sucrose corrected for protein only) and expressed as means ± S.E.M, n=4 (plates) with 6 replicates (wells) per n. ADMA – asymmetric dimethylarginine.

When cells were preloaded with [^{3}H]ADMA and the pathophysiological plasma concentration of 3μM ADMA (figure 5.3), the addition of accumulation buffer with 200μM unlabelled L-arginine saw a large significant decrease in accumulation at all time points when compared to the control treatment of accumulation buffer alone ($p<0.001$). As with the previous experiments, the percentage change between the treatments decreased over time from 33% at 1 minute, to 150% at 30 minutes.

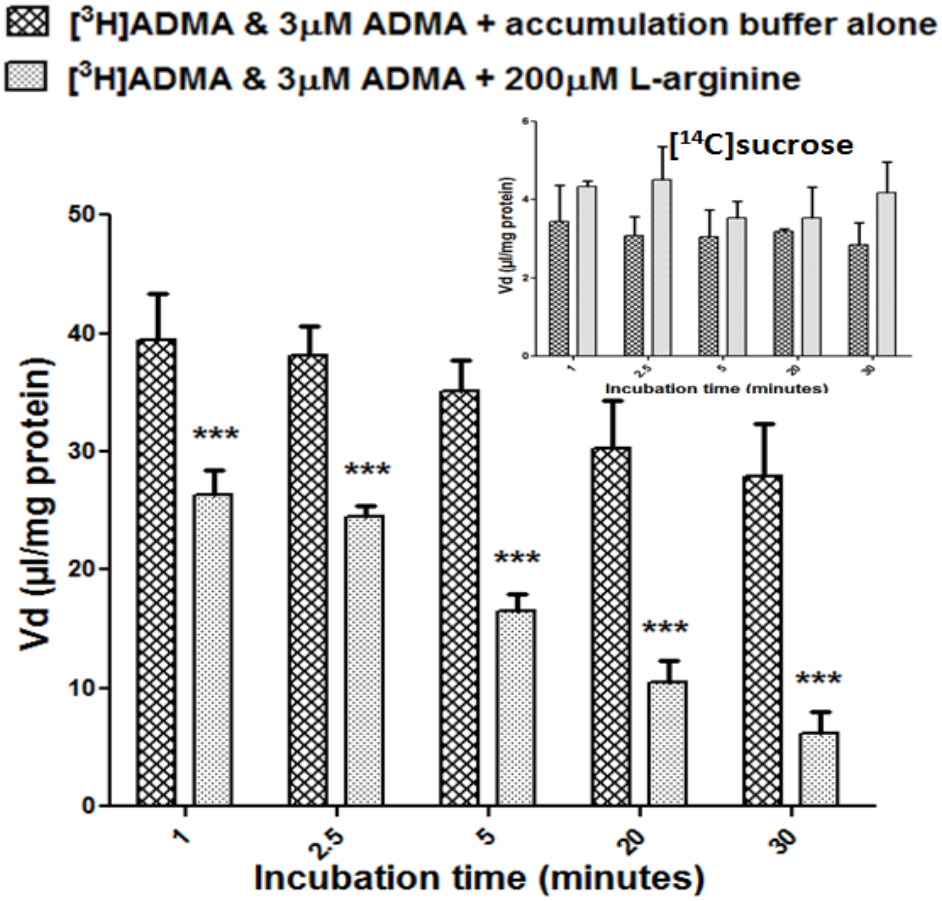

Figure 5.3. The *trans*-stimulation effect of extracellular L-arginine on preloaded [^{3}H]ADMA with 3μM ADMA and [^{14}C]sucrose. To investigate the *trans*-stimulation of intracellular ADMA by extracellular L-arginine, confluent monolayers of hCMEC/D3 cells were preloaded with [^{3}H]ADMA and 3μM ADMA along with [^{14}C]sucrose (as a marker of non-specific binding, barrier integrity and extracellular space, see insert figure) in preloading buffer for 20 minutes, before being replaced with accumulation buffer alone or accumulation buffer containing 200μM unlabelled L-arginine for 30 minutes. ****p<0.001*. [^{3}H]ADMA data are corrected for [^{14}C]sucrose and protein content (with [^{14}C]sucrose corrected for protein only) and expressed as means ± S.E.M, n=5 (plates) with 6 replicates (wells) per n. ADMA – asymmetric dimethylarginine.

The preloading of hCMEC/D3 cells with [^{3}H]ADMA and the supraphysiological concentration of 500μM ADMA also saw significant decreases in [^{3}H]ADMA accumulation following addition of 200μM unlabelled L-arginine compared to accumulation buffer controls (figure 5.4). With the exception of 1 minute, all time points saw significant decreases (*p<0.05*). The percentage decreases were 130% for 2.5 minutes, 280% for 5 minutes, 100% for 20 minutes and 233% for 30 minutes.

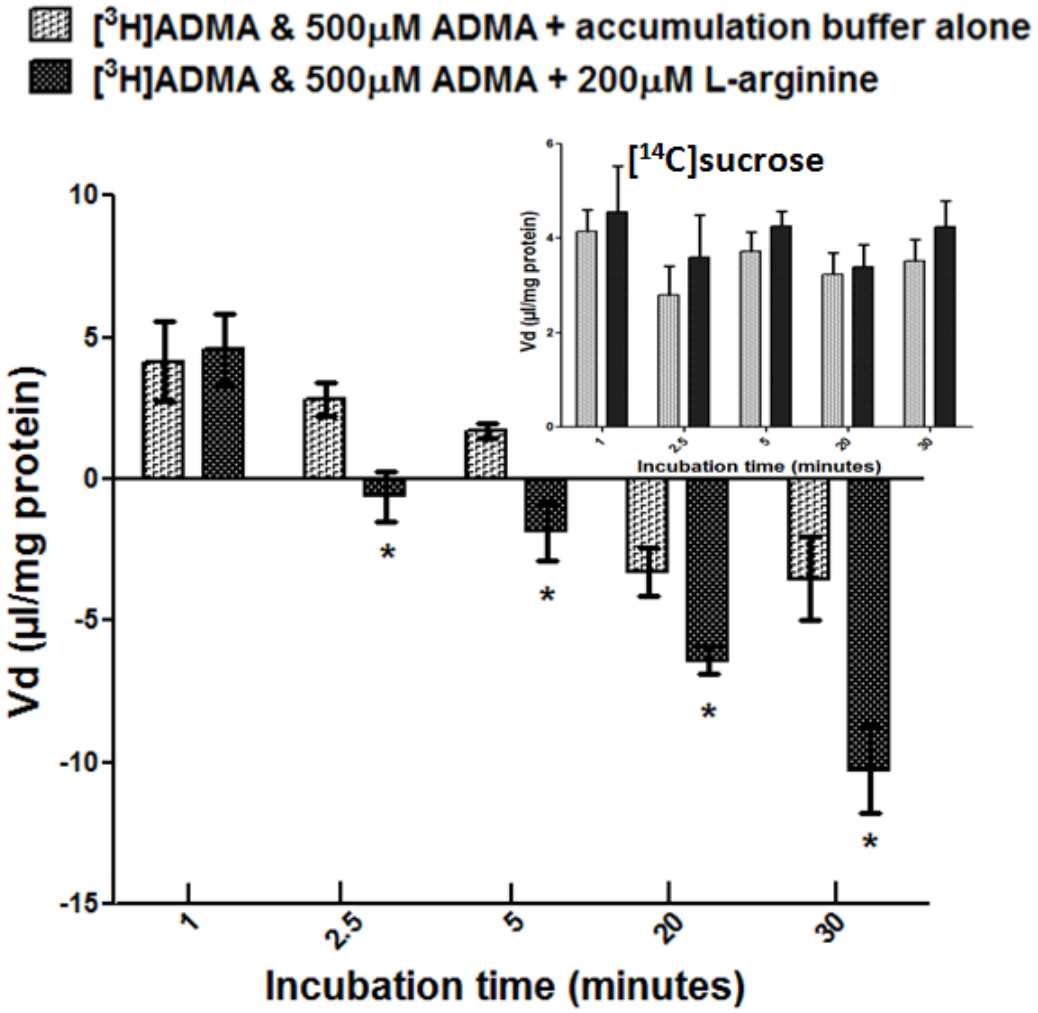

Figure 5.4. The *trans*-stimulation effect of extracellular L-arginine on preloaded [^{3}H]ADMA with 500μM ADMA and [^{14}C]sucrose. 200μM extracellular L-arginine was added with fresh accumulation buffer to assess the impact of L-arginine on the *trans*-stimulation of preloaded [^{3}H]ADMA and 500μM ADMA along with [^{14}C]sucrose (as a marker of non-specific binding, barrier integrity and extracellular space, see insert), compared to the addition of accumulation buffer alone. *$p<0.05$. [^{3}H]ADMA data are corrected for [^{14}C]sucrose and protein content (with [^{14}C]sucrose corrected for protein only) and expressed as means ± S.E.M, n=5 (plates) with 6 replicates (wells) per n. ADMA – asymmetric dimethylarginine.

5.3.4. Influence of pre-loaded unlabelled ADMA on the *trans*-stimulation of extracellular [^{3}H]L-arginine

To investigate if intracellular ADMA could *trans*-stimulate extracellular [^{3}H]L-arginine with the 200µM supplementation concentration, confluent monolayers of hCMEC/D3 cells were preloaded with preload buffer alone or preload buffer containing 0.5µM, 3µM or 500µM unlabelled ADMA for 20 minutes, before the buffer was removed and replaced with accumulation buffer containing either [^{3}H]L-arginine and [^{14}C]sucrose alone or [^{3}H]L-arginine and [^{14}C]sucrose with 200µM unlabeled L-arginine. The data are exhibited in figure 5.5.

5.3.5. [^{14}C]sucrose in [^{3}H]L-arginine *trans*-stimulation studies

No significant differences in [^{14}C]sucrose accumulation were detected between any of the ADMA preloads in the extracellular [^{3}H]L-arginine experiments when compared to the control group (preload buffer alone) (see insert in figure 5.5).

5.3.6. [^{3}H]L-arginine *trans*-stimulation studies

A preload of 0.5µM ADMA saw significant increases in [^{3}H]L-arginine when compared to preloading with preload buffer alone at all time points except 30 minutes (all $p<0.01$ until $p<0.05$ at 20 minutes, figure 5.5). The percentage increases seen at each time point were 553% at 1 minute, 275% at 2.5 minutes, 175% at 5 minutes, and 54% at 20 minutes, which show there was a decrease in the percentage change as incubation time in the accumulation assay increased.

In a similar fashion, the preloading of 3µM ADMA also induced significant increases in the subsequent [^{3}H]L-arginine accumulation when compared to preloading with preload buffer alone at all time points except 30 minutes (all $p<0.01$ until $p<0.05$ at 20 minutes). The percentage increases seen at each time point were 655% at 1 minute, 312% at 2.5 minutes, 233% at 5 minutes, and 41% at 20 minutes, which also demonstrate was a decrease in the percentage change as accumulation assay incubation time increased. When compared directly, there were no significant differences in the [^{3}H]L-arginine accumulation between the 0.5µM and 3µM ADMA preloading treatments at any time point.

Preloading with 500µM ADMA saw a large and significant increase in [^{3}H]L-arginine accumulation compared to both preloading with preload buffer alone and the 5µM and 3µM ADMA preload treatments ($p<0.001$ in all cases). Large percentage increases in [^{3}H]L-arginine accumulation were noted between 500µM ADMA and the control (preload buffer alone)

incubation; with a 1736% increase noted at 1 minute; a similar 1387% increase at 2.5 minutes, 908% at 5 minutes, 595% at 20 minutes, and 564% at 30 minutes.

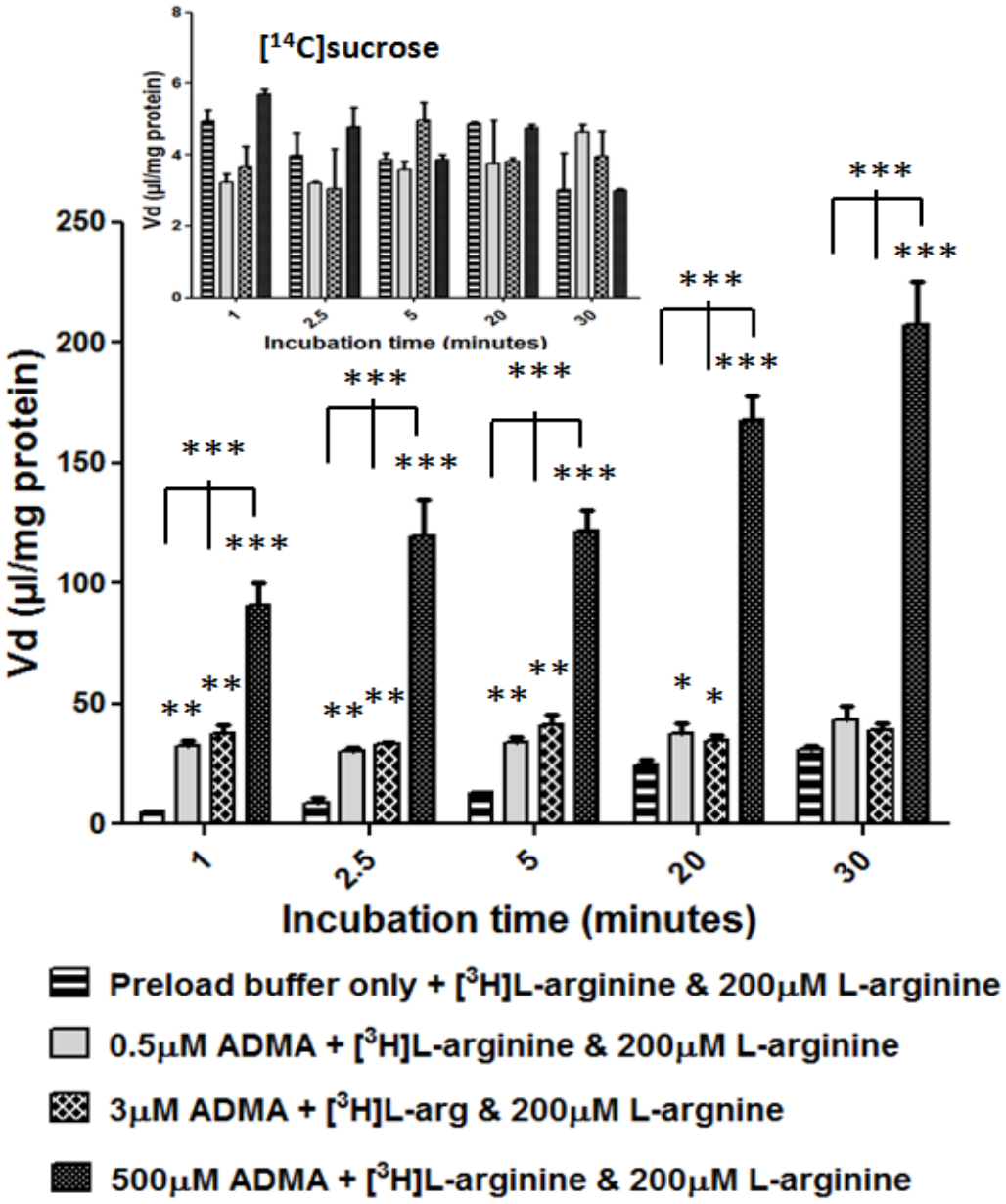

Figure 5.5. The *trans*-stimulation effect of intracellular ADMA on extracellular [^{3}H]L-arginine with 200µM unlabelled L-arginine and [^{14}C]sucrose. hCMEC/D3 cells were preloaded with preload buffer containing 0.5µM, 3µM and 500µM unlabelled ADMA to assess the *trans*-stimulation effect on extracellular [^{3}H]L-arginine with 200µM unlabelled L-arginine and [^{14}C]sucrose (a marker of non-specific binding, barrier integrity and extracellular space, see insert). Data were compared to cells preloaded with preload buffer only. **p<0.05, **p<0.01, ***p<0.001* . [^{3}H]L-arginine data are corrected for [^{14}C]sucrose and protein content (with [^{14}C]sucrose corrected for protein only) and expressed as means ± S.E.M, n=6 (plates) with 6 replicates (wells) per n. ADMA – asymmetric dimethylarginine.

5.3.7. Cytotoxicity of *trans*-stimulation treatments

The cytotoxic potential of all compounds used in this study over the complete 50 minute time-frame (20 minute preload and the subsequent 30 minute accumulation assay) was assessed in the hCMEC/D3 cells using an MTT assay, comparing treated cells to untreated control cells. There were no significant differences in cell viability between the treatments (figure 5.6 below).

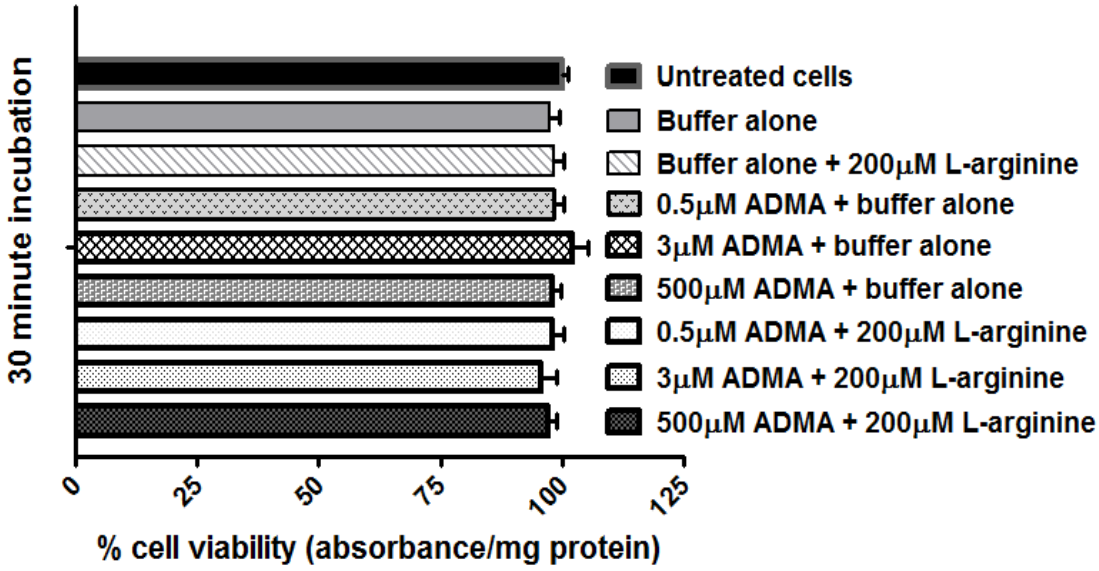

Figure 5.6. The cytotoxic effects of study treatments on confluent monolayers of hCMEC/D3 cells. The study treatments were assessed for any cytotoxic potential using an MTT assay during initial 20 minute preloads followed by 30 minute incubations with confluent monolayers of hCMEC/D3 cells in 96 well plates, as described in section 2.5. Buffer alone refers to 20 minute preloading and 30 minute incubation with accumulation buffer alone. The remaining bar descriptions refer to a 20 minute preload with a varying unlabelled ADMA concentrations before 30 minute incubation with either buffer alone or 200μM unlabelled L-arginine. The data were compared to untreated cells and the results are expressed as percentage viability ± S.E.M and compared to control untreated cells, which were incubated for 30min in culture medium. n=3 (plates), 6 replicates per n (6 wells). Buffer alone treatment = 20 minute preload in preload buffer alone + 30 minute incubation with accumulation buffer alone, ADMA – asymmetric dimethylarginine, BCH – 2 -aminobicyclo-(2,2,1)-heptane-2-carboxylic acid.

5.4. Chapter 5 – Discussion

As more conditions associated with increased ADMA plasma concentrations are recognised, the role of the L-arginine/ADMA ratio is likely to become more clinically relevant. This ratio is of particular importance considering the effects of L-arginine supplementation on attenuating endothelial dysfunction and NO impairment in the conditions where ADMA may be acting pathophysiologically – despite the fact that physiological plasma concentrations of L-arginine are well above the K_m for all form of NOS (Tsikas et al., 2000). It has been hypothesised by numerous authors that ADMA can explain this 'L-arginine paradox', and that the mechanism could be uptake transport competition or the *trans*-stimulation of intracellular ADMA transport by extracellular L-arginine. However, this has not been directly investigated until this present study. Because we had demonstrated that physiological and pathophysiological extracellular ADMA did not induce significant decreases in L-arginine transport into the cell, we decided to investigate the latter of these hypotheses by using the hCMEC/D3 cells in an adapted model of accumulation where an ADMA preloading step was included.

The findings of this study show that preloaded [^{3}H]ADMA was readily exported from the cells once the preload buffer was replaced with accumulation buffer – without the presence of extracellular L-arginine – and this was likely to be due to the movement of the molecule along its concentration gradient from a high (intracellular) concentration to a low (extracellular) concentration. We also demonstrated that at almost all time points, and regardless of the preloaded unlabelled ADMA concentration, the addition of extracellular L-arginine in the subsequent accumulation assay induced a significant decrease in the [^{3}H]ADMA accumulation values in the hCMEC/D3s compared to the controls. These decreases in accumulation indicate that the transport of preloaded intracellular [^{3}H]ADMA was *trans*-stimulated to exit the cells by the addition of extracellular L-arginine.

The transport of extracellular L-arginine was also investigated by using [^{3}H]L-arginine, showing that the presence of preloaded unlabelled intracellular ADMA significantly increased the uptake of [^{3}H]L-arginine in the following accumulation assay when compared to preload only controls, and also that increasing preload concentrations of intracellular ADMA from 3µM to 500µM proportionally increased [^{3}H]L-arginine uptake. Collectively, these data provide evidence for *trans*-stimulation via the action of bidirectional CAA transport systems in the hCMEC/D3 cells.

In the context of the 'L-arginine paradox', our data add weight to the theory that intracellular ADMA is exported via the *trans*-stimulation of CAA transport systems by extracellular L-arginine, but there are issues with the model and theory. It is all well to preload cells with ADMA in the absence of competitive CAAs, but when ADMA is in the presence of L-arginine we have already shown in the previous chapter that ADMA outcompeting L-arginine for uptake is an unlikely event. As eNOS is complexed with CAT-1, that hCMEC/D3s express CAT-1, and as both L-arginine and ADMA appear to be predominately using system y^+, it is likely that this transporter is the one implicated in our *trans*-stimulation data. Therefore, if L-arginine is preferentially transported by CAT-1 compared to ADMA, it remains puzzling how in a more physiological setting, *in vitro* or *in vivo*, extracellular ADMA could accumulate in the endothelium and sufficiently inhibit eNOS. However, as CAT-1 has large affinities for its CAA substrates, it is possible that both L-arginine and ADMA could both accumulate in the cell at concentrations sufficient for their action on eNOS. Indeed, a previous study by Cardounel et al., using bovine aortic endothelial cells, demonstrated that in the presence of 100µM extracellular L-arginine, 5µM extracellular ADMA was able to accumulate in the cells and exert a significant 12% inhibition of NO production (Cardounel et al., 2007). If the pathophysiological concentration of 3µM ADMA is sufficient enough to infer eNOS uncoupling inducing subsequent superoxide production has not been demonstrated. An extracellular ADMA concentration of 100µM however, is enough to elicit such an effect (Sud et al., 2008). Interestingly, Cardounel et al., also noted that 100µM L-arginine only reduced ADMA uptake by 65%, suggesting that either there were different transporters in use, or that the transport proteins involved favoured ADMA to L-arginine. The authors went on to demonstrated that in the absence of L-arginine, extracellular ADMA concentrations of 0.5µM and 10µM significantly increased intracellular ADMA to 4.4µM and 68.4µM respectively, and that with L-arginine present, an extracellular concentration of 10µM gave rise to intracellular concentrations of 23.5µM (Cardounel et al., 2007). This suggests that it is extracellular concentrations of L-arginine and ADMA that regulate NO production.

Intriguingly, in a recent study, Shin et al., used L-arginine ethyl esters that are not transported by CAT-1, but readily accumulate in cells (by passive diffusion) to show that L-arginine accumulation in human A549 endothelial cells via passive diffusion did not alter NO production, in contrast to L-arginine accumulation via CAT-1 (Shin et al., 2011). Their data also suggest that it is indeed extracellular concentrations and not intracellular concentrations of L-

arginine entering the cells via CAT-1 that regulate NO production, and that intracellular pools of L-arginine were separate from the eNOS/CAT-1 complex. The data of Shin et al., suggests that some intracellular pools of L-arginine are not accessible to eNOS. This notion is also supported by the finding of two intracellular pools of L-arginine in human EA.hy926 endothelial cells, one of which is accessible to eNOS, and one which is not (Closs et al., 2000). Another study by the same laboratory using human umbilical vein endothelial cells demonstrated two sub-compartments of the eNOS accessible pool; one that consisted of citrulline to L-arginine recycling that could be depleted by extracellular NAAs; and one that was nourished by protein breakdown that could not be depleted by extracellular CAAs or NAAs. The authors argued that this second sub-compartment represented an area in the cell where ADMA could accumulate and have direct function on eNOS under pathophysiological conditions (Simon et al., 2003). If compartmentalised intracellular ADMA produced by PRMTs has access to eNOS has yet to be demonstrated and little is generally known about intracellular ADMA levels in disease. Intriguingly, Cardounel et al., elegantly demonstrated a 3.6-fold increase of intracellular ADMA in a rat carotid model of experimentally-induced balloon injury – 28 days post injury – which was able to significantly impair endothelium-dependent vascular relaxation and be alleviated by exogenous L-arginine supplementation. Their results demonstrated for the first time that intracellular ADMA is elevated under pathological conditions and could reach levels sufficient to inhibit NOS function (Cardounel et al., 2007). A more recent study also exhibited data to suggest that plasma ADMA poorly reflects intracellular concentrations of ADMA in rabbit models of critical illness (Davids et al., 2011).

Work is required to look at the eNOS accessible intracellular pools for the presence of ADMA, especially during pathophysiological conditions where plasma ADMA is increased to see if there is also an increase intracellularly. It is also crucial to deduce if eNOS inhibition by ADMA is a result of extracellular concentrations, intracellular concentrations or a combination of the two. This is because we have demonstrated that extracellular ADMA can be accumulated and *trans*-stimulated from human BMECs, which could support the theory that pathophysiological concentrations of intracellular ADMA involved in pathogenesis could be removed by L-arginine supplementation, but if it turns out that it is the intracellular pools of ADMA which are not accessible to the extracellular fluid that are responsible for eNOS inhibition, then this would discount the role of *trans*-stimulation in the 'L-arginine paradox'.

It is also debatable if the 'L-arginine paradox' is a paradox at all. Shin et al., also argued that their finding that the L-arginine K_m of cellular (not purified) eNOS is 36.2 ± 9.8μM, would suggest that the 'L-arginine paradox' is not even a paradox because this K_m is within the range of normal plasma concentrations of L-arginine, which when increased with supplementation to around 200μM would increase NO production (Shin et al., 2011).

Modelling the 'L-arginine paradox' *in vitro* to investigate the roles of ADMA is difficult because it would require careful control of cellular access to amino acids as well as measurements of the different intracellular pools and extracellular concentrations of amino acids at all stage of the study. Regarding our experimental design, it may have been more beneficial physiologically to perform the accumulation of ADMA in the presence of physiological concentrations of extracellular L-arginine and other CAAs, before L-arginine supplementation to see if this would've induced *trans*-stimulation. Although these steps would be easier to perform *in vitro* than *in vivo,* there are still issues involving the saturation of cell culture media with AAs. DMEM for example contains 300-400μM L-arginine alone, but no L-ornithine which has a physiological concentration around 55-65μM (Psychogios et al., 2011).

Although our *trans*-stimulation and accumulation experiments were performed in buffer with a controlled composition (i.e. no CAAs), the culture media used to grow the hCMEC/D3s was likely to contain high concentrations of CAAs (the manufacturers declined to reveal the media composition). We also did not measure intracellular and extracellular concentrations of ADMA and L-arginine throughout the culturing or experimental stages.

5.5. Conclusions

We have demonstrated that extracellular L-arginine can significantly induce the export of preloaded intracellular ADMA at a variety of concentrations via *trans*-stimulation of CAA transporters, most likely the system y^+ protein CAT-1, and that preloaded intracellular ADMA can significantly increase the uptake of extracellular L-arginine in a concentration dependent manner. These data could provide evidence for the involvement of ADMA in the 'L-arginine paradox', that supplementation of L-arginine could *trans*-stimulate the efflux of intracellular ADMA during conditions of eNOS inhibition by the methylarginine, returning the L-arginine ratio and NO production to normal. However, this would imply extracellular concentrations of ADMA are responsible for inhibiting eNOS, yet the pathophysiological plasma concentrations are unlikely to compete with other CAAs for cellular transport. Even if these pathophysiological concentrations did enter the cells, it does not explain how ADMA would exhibit an inhibitory effect on eNOS in the presence of saturating L-arginine concentrations. It therefore seems more plausible that the higher intracellular concentrations of ADMA, which are likely to have access to eNOS could be exhibiting the effects, especially considering the evidence of an eNOS accessible intracellular sub-compartment that accumulates L-arginine and other methylarginines from protein breakdown events. During disease and pathophysiological conditions, it is possible that DDAH could become dysfunctional, accumulating more ADMA in this sub-compartment, which could be sufficient enough to inhibit or uncouple eNOS in the presence of physiological concentrations of L-arginine. Supplementation could then possibly revert this, explaining the 'L-arginine paradox'. However, the roles of the L-arginine metabolising enzyme arginase and other eNOS inhibiting methylarginines such as L-NMMA should also be considered before the mystery of the paradox can be solved.

Chapter 6. Exogenous molecule interactions – Part I – Eflornithine interactions at the human BBB.

6.1. Chapter 6 – Introduction and aims

The drug eflornithine is an analogue of the CAA ornithine and used in treatment of S2 HAT. In trypanosomes it targets the enzyme ornithine decarboxylase which causes severe impairment of polyamine synthesis and results in retarded cell growth (Vincent et al., 2010). The trypanosome species *T. b. gambiense* is highly sensitive to the action of eflornithine because of its slow replenishment of ornithine decarboxylase (Phillips et al., 1987), which gives eflornithine potent anti-trypanosomal action. *T. b. rhodesiense* however, have a much higher turnover of ornithine decarboxylase which makes them resistant to eflornithine (Iten et al., 1997). As well as this failing, eflornithine is also relatively expensive in the resource-poor setting of sub-Saharan Africa, as well as requiring intensive administration, and instances of therapeutic short fallings have been reported (Lutje et al., 2010).

In an attempt to increase the action of eflornithine as well as counter the emerging resistant populations of trypanosomes, CT of anti-HAT drugs has become a successful strategy, particularly with nifurtimox-eflornithine combination therapy (NECT). How CT improves the treatment of S2 HAT compared to monotherapy is not clear, but has been suggested to be a result of improved drug delivery to the brain. For drugs to enter the brain to target the trypanosomes that cause S2-HAT they must cross the BBB, and so work by our group has investigated this in murine models. The results from our *in vivo* investigations revealed that eflornithine poorly entered the mouse brain, possibly explaining why intensive treatment regimes are required to ensure efficacy (Sanderson et al., 2008). The work also illustrated that combination of eflornithine with suramin improved the delivery of eflornithine to the mouse brain, possibly by drug-drug interactions (DDIs) between suramin and [^{3}H]eflornithine which induced eflornithine endocytosis via suramin endocytosis (Sanderson et al., 2007, Sanderson et al., 2008).

As well as investigations into CT, the mechanism of eflornithine entry to trypanosomes has also produced interesting data supporting a hypothesis that eflornithine is able to utilise AA transport systems due to its similarity with ornithine. Studies have shown that eflornithine uptake is temperature dependent (Bellofatto et al., 1987) and saturable (Phillips et al., 1987) – hallmarks of transporter activity. It is also apparent that the zwitterionic, charged amino acid properties of eflornithine would also make the drug unfavourable for passive diffusion

(Vincent et al., 2010). Vincent et al., also been recently demonstrated that loss of a trypanosome AA transporter gene conferred eflornithine resistance to *T. brucei brucei*.

These data combined with our knowledge of anti-HAT drugs and CAA transporters at the BBB make it pertinent to investigate eflornithine transport in the hCMEC/D3s. We therefore decided to investigate if eflornithine utilises CAA transport systems and if CT with other HAT drugs can improve eflornithine delivery by using the hCMEC/D3s in a drug accumulation model.

6.2. Methods

A description of the generation of the hCMEC/D3 cells can be found in the general methods chapter (chapter 2) section 2.1.

6.2.1. Cell culture

Please see section 2.1.1 in chapter 2 for details of hCMEC/D3 culture conditions.

6.2.2. Radioactivity studies – Materials

Tritium labelled eflornithine hydrochloride was custom radiolabelled (500 mCi/mmol, radiochemical purity 97.6%) by Moravek, CA, USA. It was used in the accumulation experiments alongside varying CAA transport substrates and inhibitors (see table 2.1 in chapter 2 for source information and references) and the anti-HAT drugs nifurtimox, melarsoprol (both kind gifts from Professor Croft; London School of Hygiene and Tropical Medicine, London, UK), eflornithine, pentamidine and suramin (all from Sigma, UK).

6.2.3. Eflornithine accumulation

To investigate the accumulation of [^{3}H] eflornithine (and [^{14}C]sucrose as a correction value for non-specific binding and extracellular space) in the hCMEC/D3 cells, the protocol described in section 2.2 was used over a 30-minute time period.

For self-inhibition experiments which provide evidence of influx mechanisms, 250µM unlabelled eflornithine, or 55µM ornithine was added to the accumulation buffer along with [^{3}H]eflornithine (0.0111 MBq or 300 nCi, 720nM) and [^{14}C]sucrose (0.0148 MBq, 400 nCi, 972nM). For cross competition experiments, 100µM of L-lysine, 100µM L-arginine, 100µM ADMA or 100µM leucine were added. The y^{+} competitive substrate L-homoarginine (20mM) and the broad scale system A, system L and system $B^{0,+}$ inhibitor 2-aminobicyclo-(2,2,1)-heptane-2-carboxylic acid (BCH) (4mM) were also used separately for initial evidence of transporter activity. We also performed a [^{3}H]eflornithine and [^{14}C]sucrose accumulation study in the previously described buffer absent of Na^{+} and Cl^{-} ions, to stop the action of the Na^{+} and Cl^{-} dependent $ATB^{0,+}$ and investigate the role of the transporter in [^{3}H]eflornithine accumulation. Part of these CAA investigative experiments were performed by BSc project student Ms. Gayathri Sekhar, under supervision.

As well as these molecules, in a separate series of accumulation experiments, the effects of anti-HAT CT on [^{3}H]eflornithine accumulation were also assessed. The clinically relevant doses

from our previous studies (Sanderson et al., 2007, Sanderson et al., 2008, Sanderson et al., 2009, Jeganathan et al., 2011) of 6µM nifurtimox, 10µM pentamidine, 150µM suramin or 30µM melarsoprol were used in the accumulation buffer alongside [^{3}H]eflornithine and [^{14}C]sucrose. Apart from suramin which is water soluble, the remaining anti-HAT drugs were pre-dissolved in dimethyl sulfoxide (DMSO) and added to the accumulation buffer so that the final DMSO concentration was 0.05%. For the CT study involving DMSO, a DMSO [^{3}H]eflornithine and [^{14}C]sucrose control accumulation assay was performed.

6.2.4. MTT cytotoxicity assay

The potential of the compounds used in this accumulation study to cause cytotoxicity was assessed using an MTT assay, the protocol of which is described in section 2.5. The effect of these compounds was compared to untreated control hCMEC/D3 cells.

6.3. Results

6.3.1. Influence of CAA transporters and substrates on the accumulation of [^{3}H]eflornithine and [^{14}C]sucrose

The roles of self-inhibition, CAA substrates and inhibitors on the accumulation of [^{3}H]eflornithine and [^{14}C]sucrose was assessed in the hCMEC/D3s and displayed below in figures 6.1 to 6.3.

6.3.2. [^{14}C]sucrose in CAA studies

The transport and subsequent accumulation of [^{14}C]sucrose was used as an internal control for the accumulation experiments. There were no significant differences between any of the treatments investigated when compared to controls. Data are displayed as inserts in figures 6.1 to 6.3.

6.3.3. [^{3}H]eflornithine in CAA studies – Self-inhibition

To look for evidence of transporter interaction, self-inhibition experiments were initially performed with [^{3}H]eflornithine by using 250µM unlabelled eflornithine and the closely related CAA ornithine at 55µM. Intriguingly, the addition of 250µM eflornithine caused no significant changes in the accumulation of [^{3}H]eflornithine, but the addition of 500µM eflornithine induced significant decreases at all time points, with an average decrease of 38% ($p<0.01$). 55µM ornithine induced significant decreases of 36% and 37% at 20 and 30 minute time periods respectively when compared to controls ($p<0.05$ in both instances). The data are presented in figure 6.1 below.

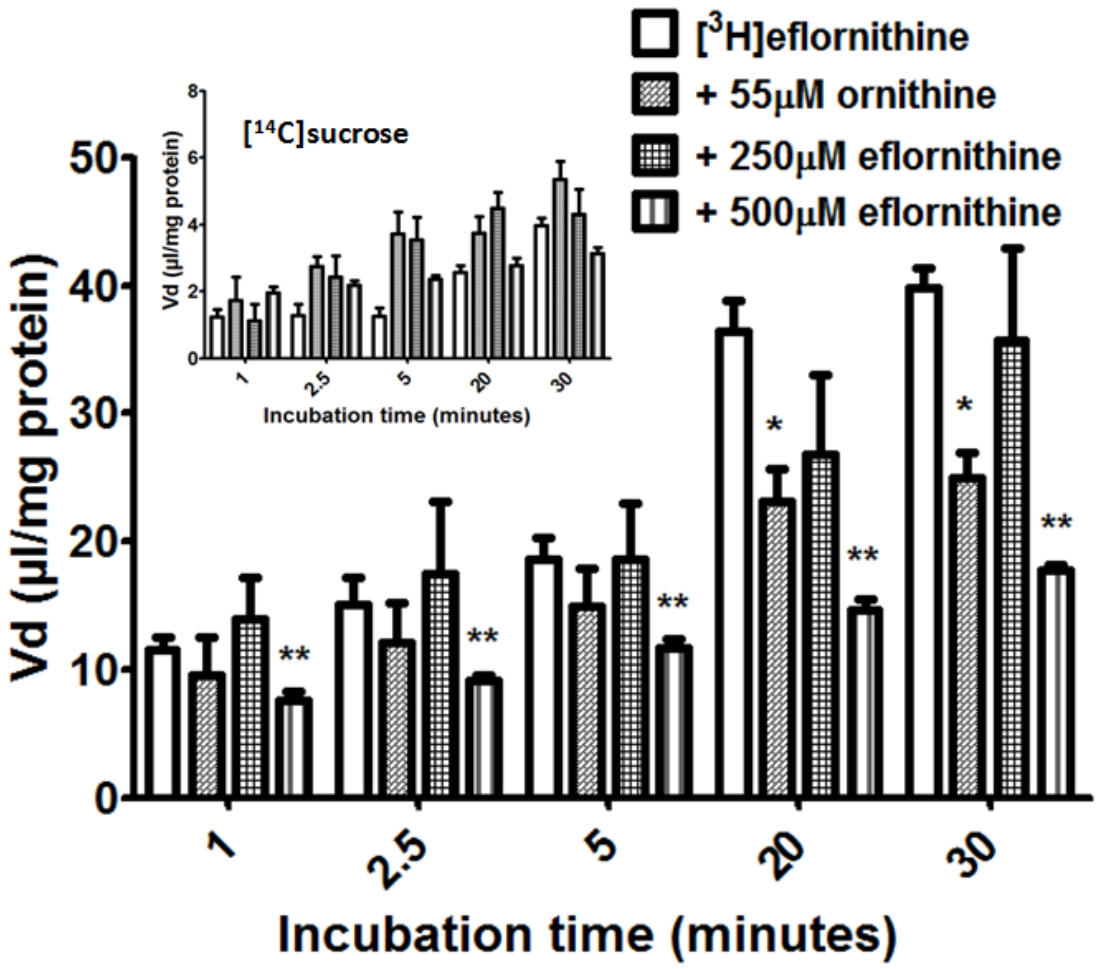

Figure 6.1. The influence of unlabelled eflornithine and ornithine on the accumulation of [^{3}H]eflornithine and [^{14}C]sucrose in hCMEC/D3 cells. Confluent monolayers of hCMEC/D3 cells grown in 96-well plates were incubated in accumulation buffer containing [^{3}H]eflornithine and [^{14}C]sucrose either alone, with 55µM ornithine, 250µM or 500µM eflornithine. [^{14}C]sucrose was used as a marker of non-specific binding, barrier integrity and extracellular space for accumulation experiments (displayed in the insert). *$p<0.05$, **$p<0.01$. All [^{3}H]eflornithine data are corrected for [^{14}C]sucrose and protein content (with [^{14}C]sucrose corrected for protein only) and expressed as means ± S.E.M, n=3-5 (plates) with 6 replicates (wells) per n.

6.3.4. [^{3}H]eflornithine in CAA studies – Cross competition

To look for evidence of transporter interaction, cross-competition experiments were performed with [^{3}H]eflornithine by using the CAAs 100µM L-lysine, 100µM L-arginine and 100µM ADMA and the NAA 100µM leucine. At all time points, the addition of ADMA caused significant decreases in the accumulation of [^{3}H]eflornithine, which increased in significance over time ($p<0.05$ from 1 minute to 5 minutes, and $p<0.01$ at 20 minutes and 30 minutes). In percentages these ADMA-induced decreases were 64% at 1 minute, 71% at 2.5 minutes, 69%

at 5 minutes, 78% at 20 minutes and 79% at 30 minutes. Similar significant decreases were noted with L-lysine from 5 minutes (35%, *p<0.05*) to 20 and 30 minutes (68% and 69%, *p<0.01*). It was not until 20 and 30 minutes when both L-arginine and leucine induced decreases in [^{3}H]eflornithine accumulation (all *p<0.05*). Data are outlined in figure 6.2 below.

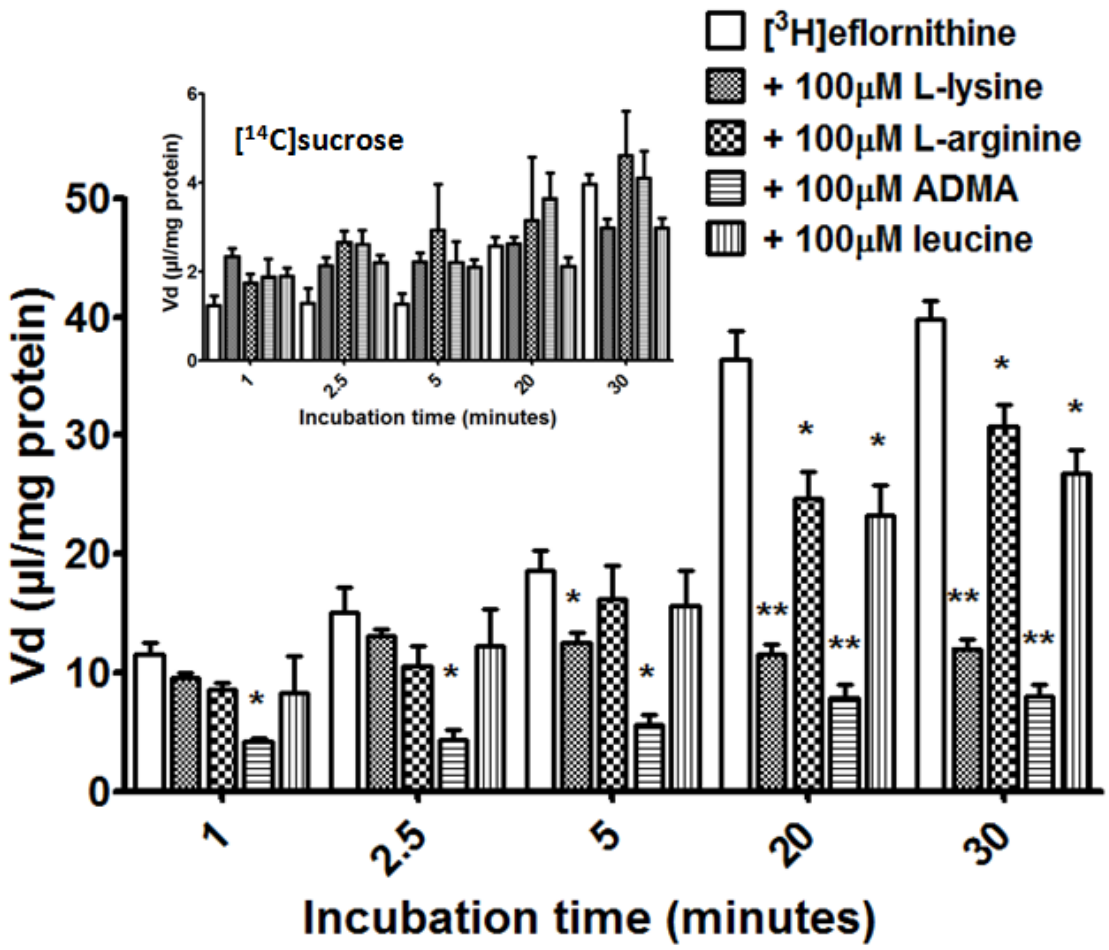

Figure 6.2. The influence of cross-competition on the accumulation of [^{3}H]eflornithine and [^{14}C]sucrose in hCMEC/D3 cells. Confluent monolayers of hCMEC/D3 cells grown in 96-well plates were incubated in accumulation buffer containing [^{3}H]eflornithine and [^{14}C]sucrose either alone, with 100µM of each of the CAAs L-lysine, L-arginine and ADMA or 100µM of the NAA, leucine. [^{14}C]sucrose was used as a marker of non-specific binding, barrier integrity and extracellular space for accumulation experiments (displayed in the insert). **p<0.05, **p<0.01.* [^{3}H]eflornithine data are corrected for [^{14}C]sucrose and protein content (with [^{14}C]sucrose corrected for protein only) and expressed as means ± S.E.M, n=3-4 (plates) with 6 replicates (wells) per n.

6.3.5. [^{3}H]eflornithine in CAA studies – transporter inhibition

By adding the y^+ interacting drug L-homoarginine (20mM), the broad scale system A, system L and system $B^{0,+}$ inhibitor BCH (4mM) and removing Na^+ and Cl^- ions from the accumulation buffer, the role of AA transport systems in [^{3}H]eflornithine uptake were investigated. At all time points, L-homoarginine caused a significant decrease (*p<0.001*) in the uptake and accumulation of [^{3}H]eflornithine, which averaged at 80%. The data are illustrated in figure 6.3 below.

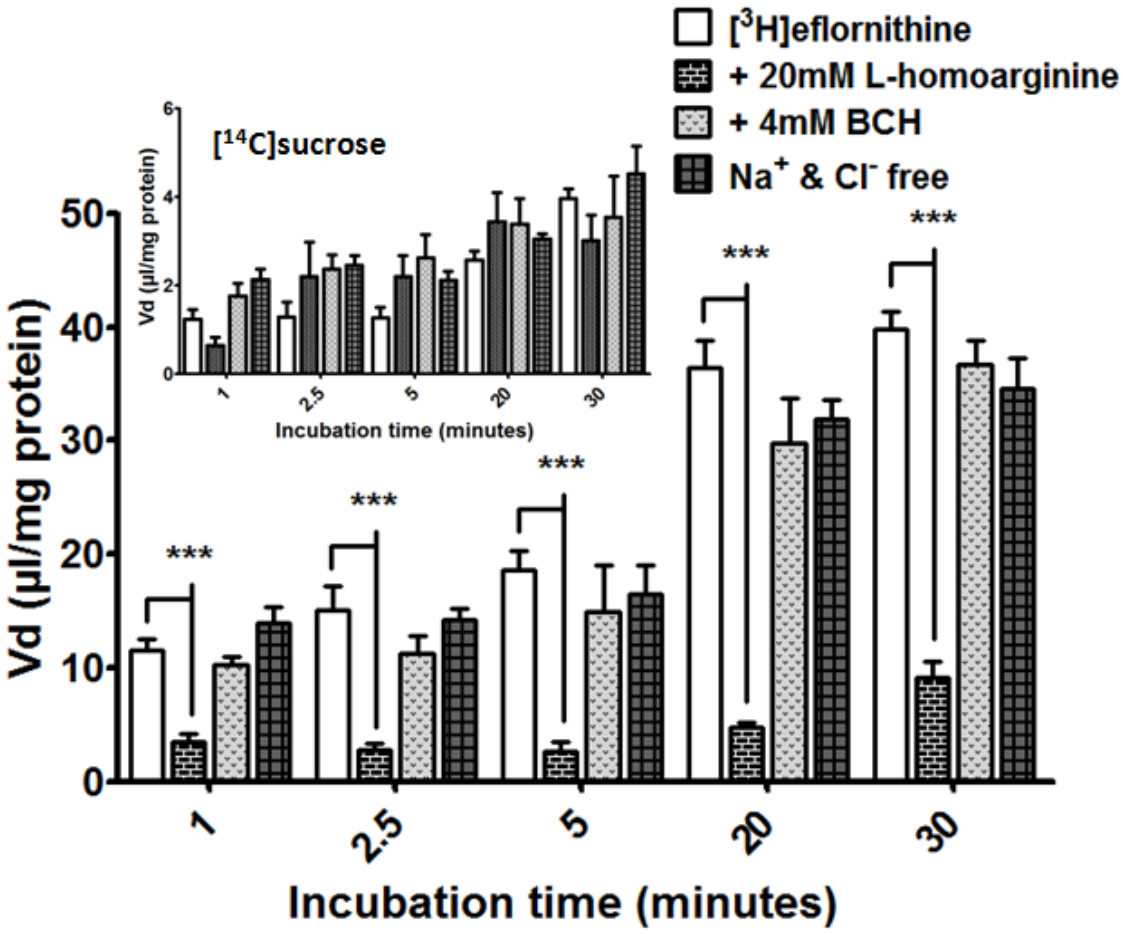

Figure 6.3. The influences of AA transport inhibition on the accumulation of [^{3}H]eflornithine and [^{14}C]sucrose in hCMEC/D3 cells. Confluent monolayers of hCMEC/D3 cells grown in 96-well plates were incubated in accumulation buffer containing [^{3}H]eflornithine and [^{14}C]sucrose either alone, with 20mM of the system y^+ inhibitor L-homoarginine, 4mM of the system A, system L and system $B^{0,+}$ inhibitor BCH or in Na^+ and Cl^- free accumulation buffer. [^{14}C]sucrose was used as a marker of non-specific binding, barrier integrity and extracellular space for accumulation experiments (displayed in the insert). ***$p<0.001$. [^{3}H]eflornithine data are corrected for [^{14}C]sucrose and protein content (with [^{14}C]sucrose corrected for protein only) and expressed as means ± S.E.M, n=3 (plates) with 6 replicates per n.

6.3.6. Influence of anti-HAT drugs on the accumulation of [^{3}H]eflornithine and [^{14}C]sucrose

The roles of CT of anti-HAT drugs on the accumulation of [^{3}H]eflornithine and [^{14}C]sucrose was assessed in the hCMEC/D3s and displayed below in figures 6.4 and 6.5.

6.3.7. [^{14}C]sucrose in CT studies

The transport and subsequent accumulation of [^{14}C]sucrose was used as an internal control for the CT accumulation experiments. There were no significant differences between any of the treatments investigated compared to control studies. Data are displayed in the inserts of figures 6.4 and 6.5.

6.3.8. Influence of CT on the accumulation of [^{3}H]eflornithine

By adding the clinically relevant doses of the anti-HAT drugs pentamidine (10µM), melarsoprol (30µM) and nifurtimox (6µM) in the presence of DMSO (final volume 0.05%), we were able to assess the influence of CT on the uptake and accumulation of [^{3}H]eflornithine (figure 6.4). Out of all the treatments, only the addition of pentamidine caused significant changes in [^{3}H]eflornithine accumulation. Apart from 1 minute where there was no change in accumulation when unlabelled pentamidine was present, a significant decrease was seen at all other time points ($p<0.01$) with an average decrease of 62.75%.

.

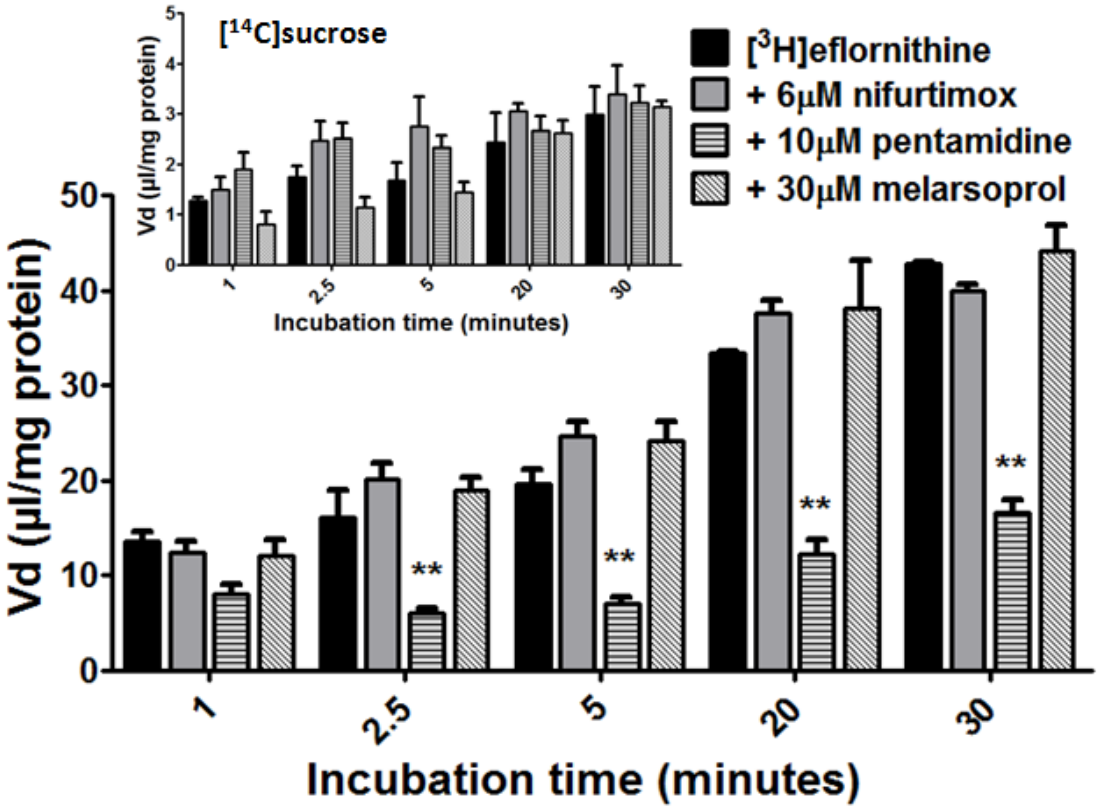

Figure 6.4. The influence of anti-HAT drug CT on the uptake and accumulation of [^{3}H]eflornithine and [^{14}C]sucrose in hCMEC/D3 cells in the presence of DMSO. Confluent monolayers of hCMEC/D3 cells grown in 96-well plates were incubated in accumulation buffer containing [^{3}H]eflornithine and [^{14}C]sucrose either alone, with the anti-HAT drugs pentamidine (10µM), melarsoprol (30µM) and nifurtimox (6µM). [^{14}C]sucrose was used as a marker of non-specific binding, barrier integrity and extracellular space for accumulation experiments (displayed in the insert). ***p<0.01.* [^{3}H]eflornithine data are corrected for [^{14}C]sucrose and protein content (with [^{14}C]sucrose corrected for protein only) and expressed as means ± S.E.M, n=3 (plates) with 6 replicates per n. All treatments here were performed in the presence of 0.05% DMSO.

Suramin (150µM) is water soluble and so was added to the accumulation buffer without DMSO and compared to control [^{3}H]eflornithine, also without the presence of DMSO. There were no significant differences in [^{3}H]eflornithine accumulation between the treatments (figure 6.5). There were also no significant [^{3}H]eflornithine or [^{14}C]sucrose control between experiments in the absence and presence of DMSO.

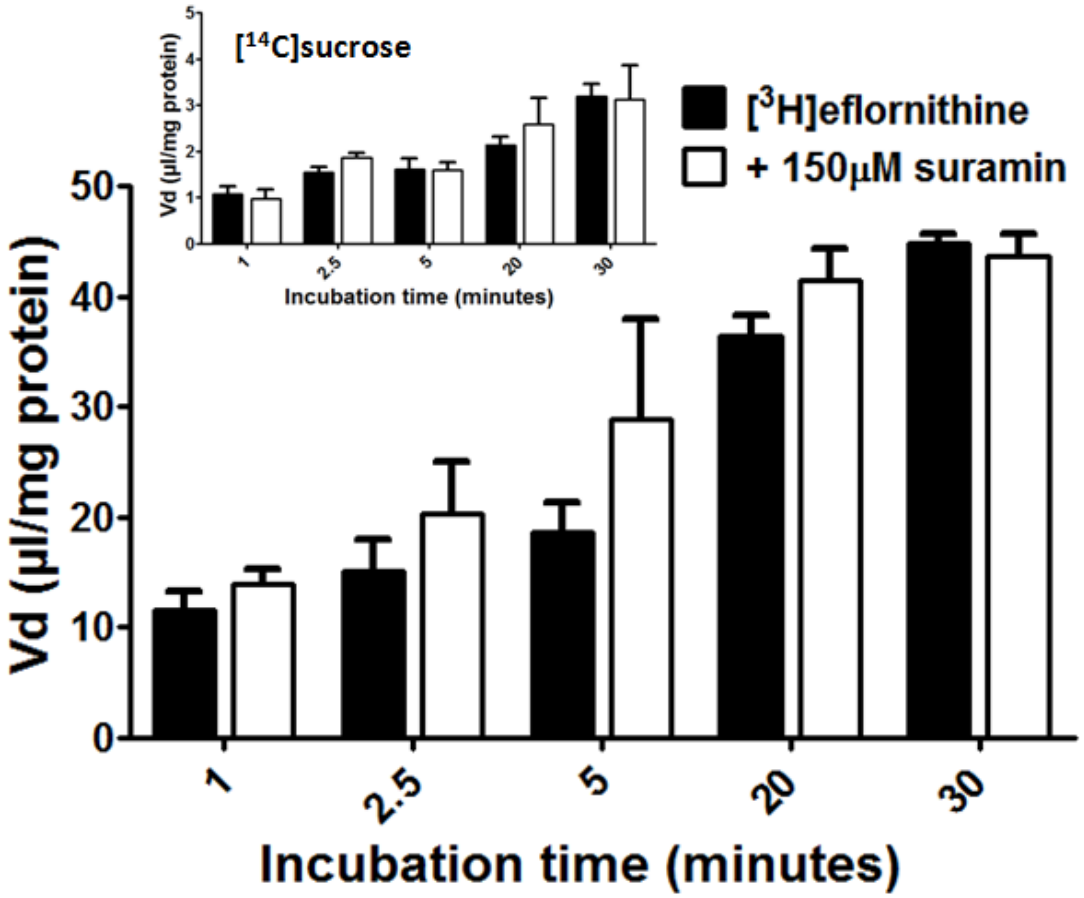

Figure 6.5. The influence of the anti-HAT drug suramin on the uptake and accumulation of [^{3}H]eflornithine and [^{14}C]sucrose in hCMEC/D3 cells in the absence of DMSO. Confluent monolayers of hCMEC/D3 cells grown in 96-well plates were incubated in accumulation buffer containing [^{3}H]eflornithine and [^{14}C]sucrose either alone, with the anti-HAT drug suramin (150µM). [^{14}C]sucrose was used as a marker of non-specific binding, barrier integrity and extracellular space for accumulation experiments (displayed in the insert). [^{3}H]eflornithine data are corrected for [^{14}C]sucrose and protein content (with [^{14}C]sucrose corrected for protein only) and expressed as means ± S.E.M, n=4 (plates) with 6 replicates per n.

6.3.9. Cytotoxicity assay

The cytotoxic potential of compounds used in this study (not studied in previous chapters) over the 30 minute time-frame was assessed in the hCMEC/D3 cells using an MTT assay, comparing treated cells to untreated control cells. There were no significant differences in cell viability between the treatments (figure 6.6 below).

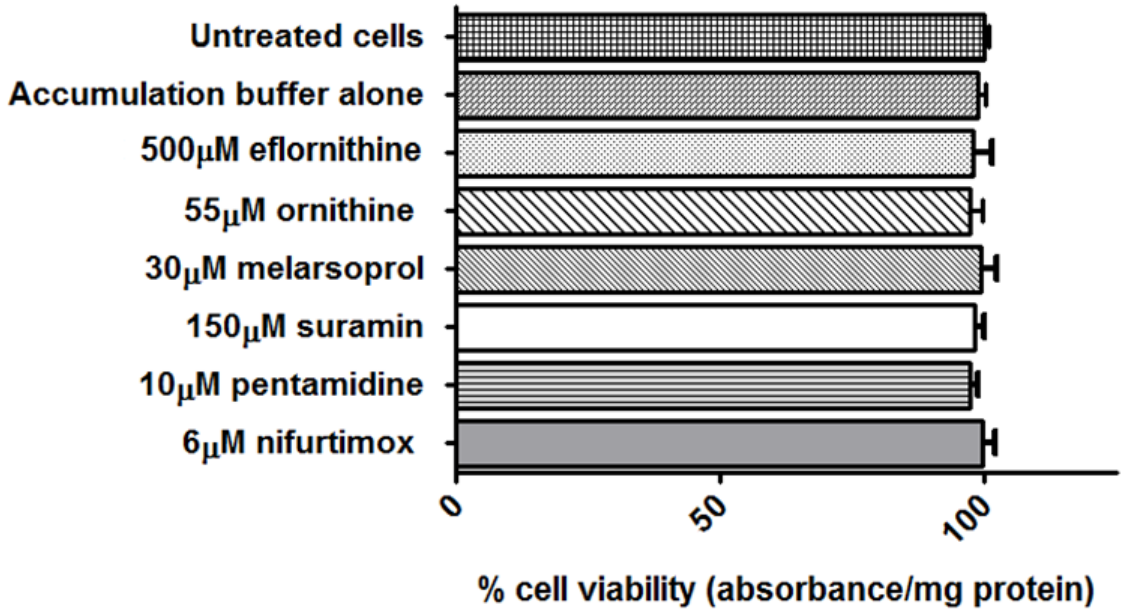

Figure 6.6. The cytotoxic effects of study compounds on confluent monolayers of hCMEC/D3 cells. The study compounds were assessed for any cytotoxic potential using an MTT assay during 30 minute incubation with confluent monolayers of hCMEC/D3 cells in 96 well plates, as described in section 2.5. The results are expressed as percentage viability ± S.E.M and compared to control untreated cells, which were incubated for 30 minutes in culture medium. n=3 (plates), 6 replicates per n (6 wells).

6.4. Discussion

The prospect of survival for patients suffering HAT is poor if diagnosis is not made during S1 of the disease. This is because during S2, the parasites enter the brain and are effectively protected from the action of trypanocidal drugs by the BBB. To kill the parasites in the brain, sufficient concentrations of the drugs must be able to cross to be efficacious. It therefore remains perplexing why little is known about the interactions between the S2 acting drugs and the BBB, and as such this area has been a major field of research by our group over the past 5-7 years with *in vivo* models of HAT. In this study, we decided to investigate the interactions of one S2-acting drug – eflornithine – with the newly established hCMEC/D3 BBB *in vitro* model in terms of uncovering evidence of CAA transport interaction and CT impact on drug uptake.

Eflornithine, as the name suggests, is a closely related molecule to the CAA ornithine (see figure 6.7 below) which is a product of L-arginine metabolism by arginase in the urea cycle (Kawano et al., 2006).

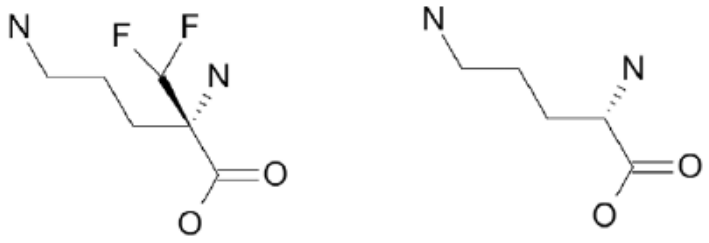

Figure 6.7. Eflornithine (left) is a derivative of ornithine (right) and so proposed to be a CAA transport substrate. Figure taken from (Vincent et al., 2010).

Because ornithine is transported by CAA transport systems such as CAT-1 (Kaneko et al., 2007), it is somewhat logical to assume that eflornithine may also use CAA transport mechanisms. To investigate this in the hCMEC/D3s we used our drug accumulation assay with a variety of CAA and AA transport substrates and inhibitors to assess any impact on the uptake and subsequent accumulation of tritiated eflornithine. Our data show that eflornithine was able to readily accumulate in the hCMEC/D3 cells despite having low lipophilicity as demonstrated by its previously published OSPC value of 0.00487 ± 0.00010 (Sanderson et al., 2008), possibly suggesting evidence of an influx transport system. Furthermore, we showed that co-incubation of [^{3}H]eflornithine with unlabelled ornithine induced a significant decrease

in [^{3}H]eflornithine accumulation at 20 and 30 minute time points which provide evidence of competitive transport interactions. These competitive findings were echoed with the addition of CAAs L-lysine, L-arginine, ADMA and the NAA leucine showing significant decreases in eflornithine accumulation. These data suggest that eflornithine may be using a variety of CAA transport systems, including those not specific for CAAs such as system y^+L and $b^{0,+}$ which are known to transport leucine as well as CAAs (Mann et al., 2003) and are expressed at mRNA level in the hCMEC/D3s (Carl et al., 2010) as discussed in chapter 4. The transporter $ATB^{0,+}$ was not implicated here due to the lack of significant differences between control [^{3}H]eflornithine accumulation and accumulations with either BCH or Na^+ and Cl^- free accumulation buffer. We were also able to narrow the chief transport system to y^+ when we used L-homoarginine showing a highly significant decrease in [^{3}H]eflornithine accumulation during co-incubation.

However, these data are in contrast to those previously demonstrated by our group using *in situ* brain perfusion models, where no evidence of influx transport system for [^{3}H]eflornithine (radiolabelled alone and radiolabelled with 250µM unlabelled eflornithine) interaction was found. Despite this contradiction between studies, our finding that co-incubation of tritiated eflornithine with 250µM unlabelled eflornithine caused no change in accumulation was similar to that of our previous *in vivo* work (Sanderson et al., 2008). Interestingly, a significant decrease in accumulation was only noted when 500µM eflornithine was used – an experiment not previously performed *in situ*. This finding may be explained by a very high affinity of the CAA systems for eflornithine. Another possibility could also be supported by the results obtained from leucine and ADMA co-incubation that eflornithine may be using a variety of transport systems to gain entry to the cells. These are likely to include CAT transporters as well as system y^+L and $b^{0,+}$ transporters, but could include a different transporter all together. siRNA studies investigating eflornithine resistance in *T. brucei brucei* found that a specific amino acid transporter called TbAAT6 was responsible for transporting eflornithine into the trypanosome (Vincent et al., 2010). Although no physiological function has been attributed to the transporter, the authors point out that other AAT family members have had arginine transport and polyamine transport function attributed to them in other trypanosome species and *Leishmania spp.* parasites. This makes it possible that other AA transport systems at the human BBB could be implicated in eflornithine transport. Further studies inhibiting/down regulating the action of or over-expressing specific transport systems is likely to better organise the findings described in our study.

We also took the opportunity to investigate CT on eflornithine uptake and accumulation in the hCMEC/D3s. The only result to gain statistical significance was the addition of 10µM pentamidine (in the presence of DMSO) to the accumulation buffer, which induced a decrease in the accumulation of [^{3}H]eflornithine at all time points from 2.5 minutes. This is of particular interest because not only is it in contrast to the *in vivo* data previously published by our group, but it could link in with the TbAAT6 finding published by Vincent et al, where polyamine transport may be implicated due to the polyamine transport functions of some AAT family members. It is well established that pentamidine is transported into parasites including *Leishmania spp* and trypanosomes by polyamine and nucleoside transporters such as the adenosine-sensitive pentamidine transporter P2, and so the decrease in accumulation of eflornithine could be attributed to influx competition for a pentamidine-sensitive transporter. This would support the idea that there may be influx systems for eflornithine separate from CAA transporters. As far as candidates go at the BBB, polyamine transport has not been extensively investigated, although data from the 1980s in rats suggests that polyamine transport at the BBB is highly limited, although not completely absent (Shin et al., 1985). *In vitro* data from the human endothelial cell line HUVEC suggested presence of two polyamine carriers, but their expression at the BBB or in the hCMEC/D3s is not known.

Pentamidine was previously directly studied by our group in the *in situ* brain perfusion mouse model and showing that it readily accumulates in the endothelial pellet but poorly enters the brain due to it being a substrate for the efflux transporter P-gp (Sanderson et al., 2009). Although it was not directly investigated here, our finding that pentamidine decreases eflornithine accumulation suggests eflornithine is not a substrate for P-gp as this would have resulted in an increase following pentamidine co-incubation. This is in line with our previous *in situ* data (Sanderson et al., 2008).

In contrast to our previous eflornithine data, suramin did not change the accumulation of [^{3}H]eflornithine in the hCMEC/D3s. Although it is of course difficult to directly compare *in situ* brain distribution data with *in vitro* accumulation data – especially so between different species – it was previously demonstrated that suramin improved the delivery of eflornithine to all brain regions, especially to the mouse brain capillary endothelium (Sanderson et al., 2008). We speculated that due to our earlier finding that suramin directly interacted with plasma membranes of CVOs, that perhaps DDIs between eflornithine and suramin lead to increases in accumulation and brain uptake of eflornithine through endocytotic events (Sanderson et al.,

2007, Sanderson et al., 2008). This finding was not evident in our hCMEC/D3 model of BBB drug accumulation.

We also did not demonstrate any differences between control eflornithine accumulation and eflornithine accumulation following incubation with 250µM unlabelled eflornithine, melarsoprol or nifurtimox. These findings were previously demonstrated in our earlier anti-HAT drug BBB interactions (Sanderson et al., 2008). This may have implications for the reasoning behind the increased efficacy of NECT compared to monotherapy strategies – that NECT does not improve drug uptake at the BBB, but counters eflornithine/nifurtimox resistance at the level of the parasite.

6.5. Conclusions

In summary, we have presented data that provides evidence for the first time in a BBB model that eflornithine is able to utilise AA transport systems to accumulate in the hCMEC/D3s, most likely to be CAA transporters such as system y^+ proteins, but polyamine/nucleoside transporters could also be implicated due to our finding with pentamidine. In the field, the fact remains eflornithine requires intensive treatment regimes in humans to gain sufficient efficacy, which suggests the lack of a specific transport system for the drug at the BBB. The success of eflornithine combination therapy with nifurtimox is likely a riposte to eflornithine resistance at the level of the parasite rather than improvements in drug delivery to the brain, although as previous *in vivo* evidence illustrates interaction of anti-HAT drugs with multiple-transporters, improved drug delivery cannot be ruled out – especially given the limitations of an *in vitro* accumulation model in comparison to human trial data.

Chapter 7. Exogenous molecule interactions – Part II – Nifurtimox interactions at the human BBB.

7.1. Chapter 7 – Introduction and aims

Our research group previously investigated the ability of pentamidine, suramin, eflornithine and nifurtimox to cross the murine BBB using an *in situ* brain/choroid plexus perfusion technique in anaesthetised mice (Sanderson et al., 2007, Sanderson et al., 2008, Sanderson et al., 2009, Jeganathan et al., 2011). Our most recent *in situ* study focused on nifurtimox, an anti-parasitic nitrofuran that was originally used to treat Chagas disease; a closely related condition to HAT caused by the trypanosome *Trypanosoma cruzi* (Haberkorn and Gonnert, 1972, Gonnert and Bock, 1972), but has since been used in compassionate treatment for HAT when other methods have failed (Moens et al., 1984, Van Nieuwenhove, 1992). It is now used against S2 in combination with eflornithine (NECT) (Checchi et al., 2007).

Nifurtimox, compared to eflornithine is cheap, orally active and effective against *T. b. gambiense* and, to a lesser extent, *T. b. rhodesiense* (Haberkorn, 1979, Bouteille et al., 2003, Lutje et al., 2010). Importantly, our group have previously demonstrated that nifurtimox is able to cross the murine BBB *in situ*, but undergoes a BBB efflux removal process from the brain via an unidentified process, in which P-gp is not involved (as demonstrated with P-gp knockout mice (Jeganathan et al., 2011). The identify of this efflux mechanism is of particular interest with the fact that NECT is now becoming the first course of treatment against HAT S2 (Yun et al., 2010), having been shown to both improve efficacy and reduce harmful side effects associated with the other anti-HAT drugs (Priotto et al., 2007, Priotto et al., 2009). The precise mechanisms behind the success of NECT have yet to be fully elucidated; but it is possible CT could improve drug delivery to the brain. We have recently shown that nifurtimox delivery to the mouse brain is improved with the addition of the S1 acting drug pentamidine (Jeganathan et al., 2011), which we previously identified as being a substrate for cellular transport mechanisms at the BBB, including P-gp (Sanderson et al., 2009). These findings highlight the need to both elucidate the transport mechanisms utilised by nifurtimox and the effect of CT on the delivery of other anti-HAT drugs at the BBB.

In order to translate the research to the human situation from our earlier work which focused on *in vivo* murine models of the BBB, this present study uses the hCMEC/D3 cell line. The following study is the first to investigate nifurtimox transport interactions in a human model of the BBB, and has recently been published and inserted at the back of the thesis after the appendices (Watson et al., 2012).

7.2. Methods

A description of the generation of the hCMEC/D3 cells can be found in the general methods chapter (chapter 2) section 2.1.

7.2.1. Cell culture

Please see section 2.1.1 in chapter 2 for details of hCMEC/D3 culture conditions.

7.2.2. Radioactivity studies - Materials

Nifurtimox (MW 287.30) was custom labelled with tritium (^{3}H 3,4 furam ring) specific activity: 2 Ci/mmol) by Moravek Biochemicals (California, USA). [^{14}C]sucrose (4980 mCi/mmol) was purchased from Moravek Biochemicals. Unlabelled suramin, eflornithine and pentamidine were purchased from Sigma, UK. Unlabelled nifurtimox and melarsoprol were a kind gift from Professor S. Croft (London School of Hygiene and Tropical Medicine, UK). Probenecid, indomethacin and dimethyl sulfoxide (DMSO) were purchased from Sigma, UK. Dexamethasone and Pheophorbide A (PhA) were purchased from Acros Organics, (Fisher Scientific, Loughborough, UK). Para-aminohippuric acid (PAH) and taurocholic acid (TCA) were purchased from MP Biochemicals, UK. Ko143 and haloperidol were purchased from Tocris Bioscience (Bristol, UK) and Sigma, UK, respectively

7.2.3. Drug accumulation assays:

Drug accumulation experiments were performed on confluent monolayers of hCMEC/D3s, grown in the centre 60 wells of 96 well plates as described in methods section 2.2. Medium was removed from wells and replaced with a 200µl aliquot of [^{3}H]nifurtimox (0.0111 MBq or 300 nCi, 120nM per 1ml accumulation buffer) and [^{14}C]sucrose (0.0148 MBq, 400 nCi, 972nM per 1ml accumulation buffer) in accumulation buffer. We first aimed to investigate the role of CT on [^{3}H]nifurtimox accumulation, before deducing the efflux processes and any transporter interactions involved.

7.2.4. Combination therapy

In a series of experiments to assess the impact of CT on [^{3}H]nifurtimox cellular accumulation, the clinically relevant concentrations of nifurtimox (6µM), pentamidine (10µM), melarsoprol (30µM), suramin (150µM) or eflornithine (250µM) were added to accumulation buffer. Unlabelled suramin, eflornithine and pentamidine isethionate sodium salt were purchased from Sigma Chemical Company (Dorset, UK). DMSO was used to dissolve nifurtimox, pentamidine and melarsoprol to give a final concentration of 0.05% DMSO. Control

experiments here also contained 0.05% DMSO. For unlabelled eflornithine and suramin and the appropriate controls, no DMSO was used as the molecules are water soluble. There were no significant differences between accumulation of [^{3}H]nifurtimox with or without 0.05% DMSO at any time point (data comparison not shown).

7.2.5. Self- inhibition assays:

To study the transport mechanisms being utilised by nifurtimox, a range of unlabelled nifurtimox concentrations in the presence of 0.05% DMSO (6µM, 12µM, 60µM and 150µM) were also used alongside [^{3}H]nifurtimox and [^{14}C]sucrose in the accumulation buffer to assess the effect on [^{3}H]nifurtimox efflux from the cells.

7.2.6. Transporter inhibition assays

To study the transport mechanisms being utilised by nifurtimox, a series of established transporter interacting (substrates and inhibitors) drugs were used alongside [^{3}H]nifurtimox and [^{14}C]sucrose in the accumulation buffer. The impact of these drugs on [^{3}H]nifurtimox and [^{14}C]sucrose accumulation in the cells was assessed at 1, 2.5, 5, 20 and 30 minutes. Haloperidol (40µM), ko143 (1µM), indomethacin (10µM) pheophorbide A (PhA) (1µM), taurocholic acid (TCA) (200µM), para-aminohippuric acid (PAH) (500µM), dexamethasone (200µM) or probenecid (350µM) were added to accumulation buffer in the presence of 0.05% dimethyl sulfoxide (DMSO) in individual experiments to inhibit different transport systems (see methods table 2.1).

To further assess the impact of the ATP dependant ABC-transporters on the accumulation of [^{3}H]nifurtimox, cells were depleted of ATP by incubating them for 1 hour in glucose-free DMEM containing 10mM 2-deoxy-D-glucose (2-DG, Sigma), and cellular ATP was determined using the Promega Enliten® ATP Assay System kit (Promega, Southampton, UK). Cells were grown in rat tail collagen type-1 coated 24 well plates (Thermo Scientific Nunclon™, Loughborough, UK) for 7 days before their medium was removed, washed twice with 1 ml of warm glucose free DMEM (Gibco, Invitrogen) and incubated for 1 hour in 1 ml glucose-free DMEM containing 10mM 2-DG which is a well documented inhibitor of glycolysis and results in a decrease in intracellular ATP *in vitro* (Wang et al., 2011b). After this incubation step, the 2-DG solution was removed and cells were incubated in 100µl of 2% trichloroacetic acid (TCA, Sigma, UK) in glucose-free DMEM, also containing 0.002% xylenol blue dye (a pH colour indicator, Sigma, UK) at RT for 10 minutes following the manufacturer's direction. TCA both

depletes cellular ATP and inhibits enzymes that degrade ATP (Whiteman et al., 2002). As TCA also inhibits the downstream assay, it was neutralised with Tris-acetate (pH 7.75) to bring the total TCA percentage to 0.1% following the manufacturer's direction. Samples were then taken and added with the reconstituted luciferase/luciferin reagent mix from the kit in a sterile white 96-well plate (Nunc) and the ATP luminescence determined in a Biotek Synergy HT luminometer using KC4 software and compared to control cells not treated with 2-DG. For accumulation, cells were treated with 10mM 2-DG before incubation with [^{3}H]nifurtimox as described in the accumulation assay. We would like to thank Dr. Matthew Arno of the KCL Genomics centre for his help with this assay.

7.2.7. Cytotoxicity assay

The potential of the compounds used in this accumulation study (not investigated in previous chapters) to cause cytotoxicity to the hCMEC/D3 cells was assessed using an MTT assay following the protocol described in section 2.5. The effect of these compounds on hCMEC/D3 viability was compared to untreated control hCMEC/D3 cells.

7.2.8. Expression of P-gp and BCRP

For SDS-PAGE and WB, the protocol in chapter 2, section 2.7 was used and hCMEC/D3 cell lysate was prepared in TGN lysis buffer as described in section 2.7.1. The expression of P-gp and BCRP by the hCMEC/D3 and HepG2 cell lines were analysed using Abcam primary mouse anti-P-gp/MDR1 [C219] (ab3364) and mouse anti-BCRP/ABCG2 [BXP-21] (ab3380) monoclonal antibodies at 1:80 and 1:1000 dilutions in PBS-Tween (PBS-T, PBS with 0.05% Tween 20) with 0.5% BSA, (Sigma) respectively. Mouse anti- GAPDH monoclonal antibody [6C5] (ab8245), was used as a loading control, 1:1000 in PBS-T with 0.5% BSA. Details of these antibodies can be found in table 2.2. HepG2 cells were a kind gift from Mr. Enrico Cristante (Imperial College London, UK) and used as positive controls (Vander Borght et al., 2008, Wojtal et al., 2006). For P-gp, a precast 4-20% gradient gel was used (Bio-Rad Europe, 456-1093S). For BCRP, a 10% SDS-PAGE acrylamide/bisacrylamide gel was used with the recipe in appendix section 3.

7.3. Results

7.3.1. Combination therapy and [^{3}H]nifurtimox and [^{14}C]sucrose accumulation

With CTs becoming the treatments of choice for HAT, the effect of their addition to the accumulation buffer was observed on [^{3}H]nifurtimox and [^{14}C]sucrose accumulation.

7.3.2. [^{14}C]sucrose in CT studies

[^{14}C]sucrose was used as an internal control for the accumulation experiments. There were no significant differences between any of the treatments investigated. Data are displayed as inserts in figures 7.1 to 7.2.

7.3.3. Effects of combination therapy on [^{3}H]nifurtimox accumulation

The accumulation of [^{3}H]nifurtimox in the hCMEC/D3s was not significantly affected by unlabelled melarsoprol (30µM), whereas unlabelled pentamidine (10µM) caused an increase at 2.5 minutes ($p<0.01$) and this was maintained onwards to 30 minutes ($p<0.001$), with an average increase of 111% over the time points in comparison to the appropriate [^{3}H]nifurtimox controls (figure 7.1).

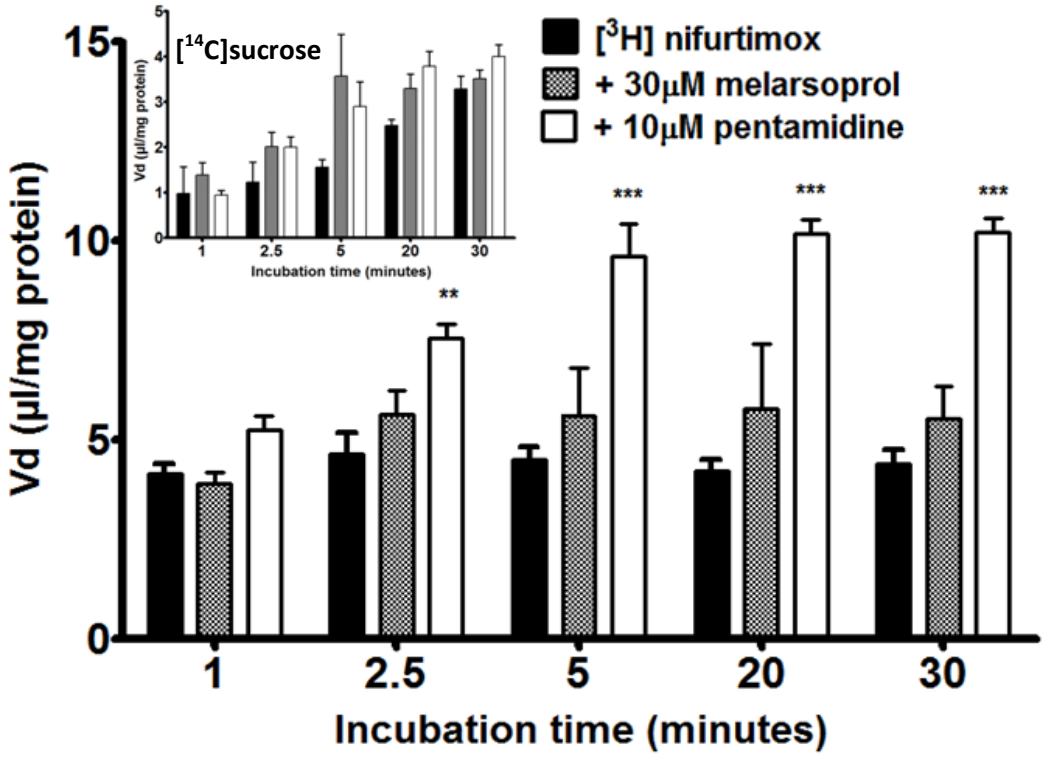

Figure 7.1. Combination of [^{3}H]nifurtimox and [^{14}C]sucrose with melarsoprol and pentamidine. The anti-HAT drugs melarsoprol (30µM) and pentamidine (10µM) were added with [^{3}H]nifurtimox and [^{14}C]sucrose in the accumulation buffer (in the presence of 0.05% DMSO) to assess their impact on accumulation. Unlabelled melarsoprol caused no significant change, but pentamidine induced a significant increase in accumulation of [^{3}H]nifurtimox, from 2.5 minutes onwards (**p<0.01, ***p<0.001). There were no significant treatment-induced differences in [^{14}C]sucrose accumulation when compared to control values (insert). [^{3}H]nifurtimox data are corrected for [^{14}C]sucrose and protein content (with [^{14}C]sucrose corrected for protein only). All data expressed as means ± S.E.M, n= 6 (plates) per graph, with 6 replicates (wells) per plate.

There was no effect of eflornithine (250µM) and suramin (150µM) on the accumulation of [^{3}H]nifurtimox (all without the presence of DMSO as the molecules are water soluble, figure 7.2).

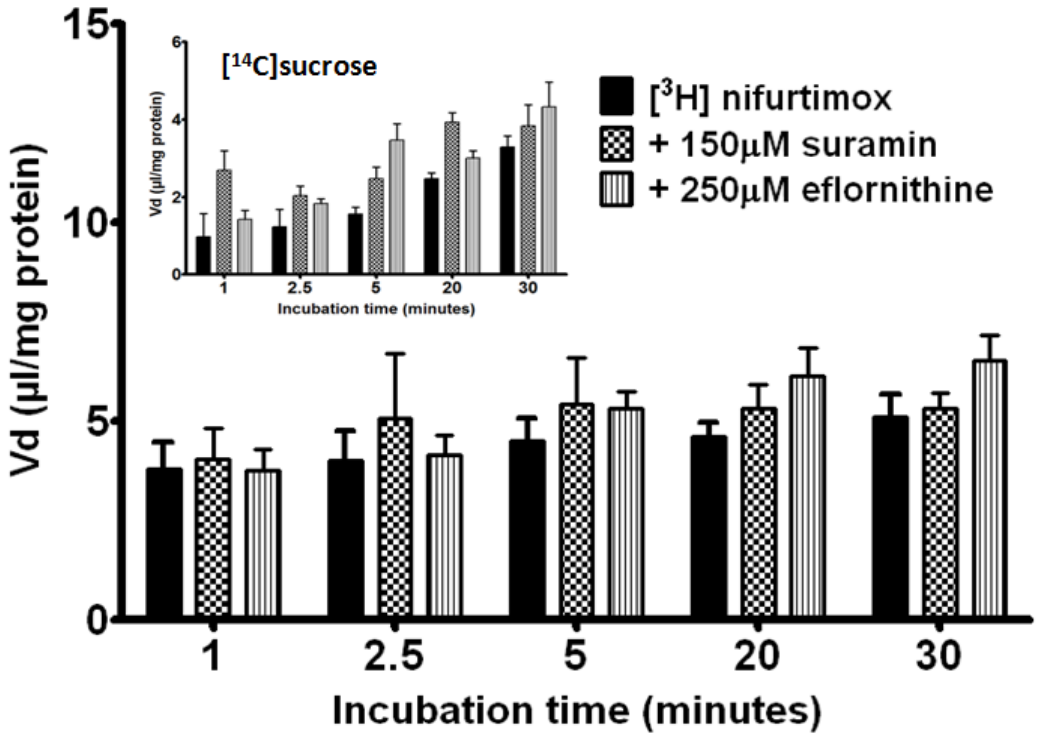

Figure 7.2. Combination of [^{3}H]nifurtimox and [^{14}C]sucrose with suramin and eflornithine. The anti-HAT drugs suramin (30µM) and eflornithine (10µM) were added with [^{3}H]nifurtimox and [^{14}C]sucrose in the accumulation buffer (without DMSO) to assess their impact on accumulation. Both unlabelled melarsoprol and eflornithine caused no significant change in the accumulation of [^{3}H]nifurtimox. There were no significant treatment-induced differences in [^{14}C]sucrose accumulation when compared to control values (insert). [^{3}H]nifurtimox data are corrected for [^{14}C]sucrose and protein content (with [^{14}C]sucrose corrected for protein only). All data expressed as means ± S.E.M, n= 6 (plates) per graph, with 6 replicates (wells) per plate.

7.3.4. Influence of self-inhibition on [^{3}H]nifurtimox accumulation

As nifurtimox has been previously demonstrated to be a substrate of an efflux transport system in our mouse models and no influx system has been demonstrated, we incubated a range of concentrations of unlabelled nifurtimox in accumulation buffer alongside [^{3}H]nifurtimox and [^{14}C]sucrose to see if any efflux system could be detected in the hCMEC/D3s. Accumulation of [^{3}H]nifurtimox was not significantly affected by the addition of unlabelled nifurtimox at a clinically relevant dose of 6µM or an increased dose of 12µM (figure 7.3). The addition of 60µM and 150µM unlabelled nifurtimox however, caused significant increases in [^{3}H]nifurtimox accumulation at all time points ($p<0.001$ for both treatments at all time points) compared to DMSO [^{3}H]nifurtimox controls. 60µM induced an average increase of 310% across all time points, and 150µM induced a larger 400% increase across the time points.

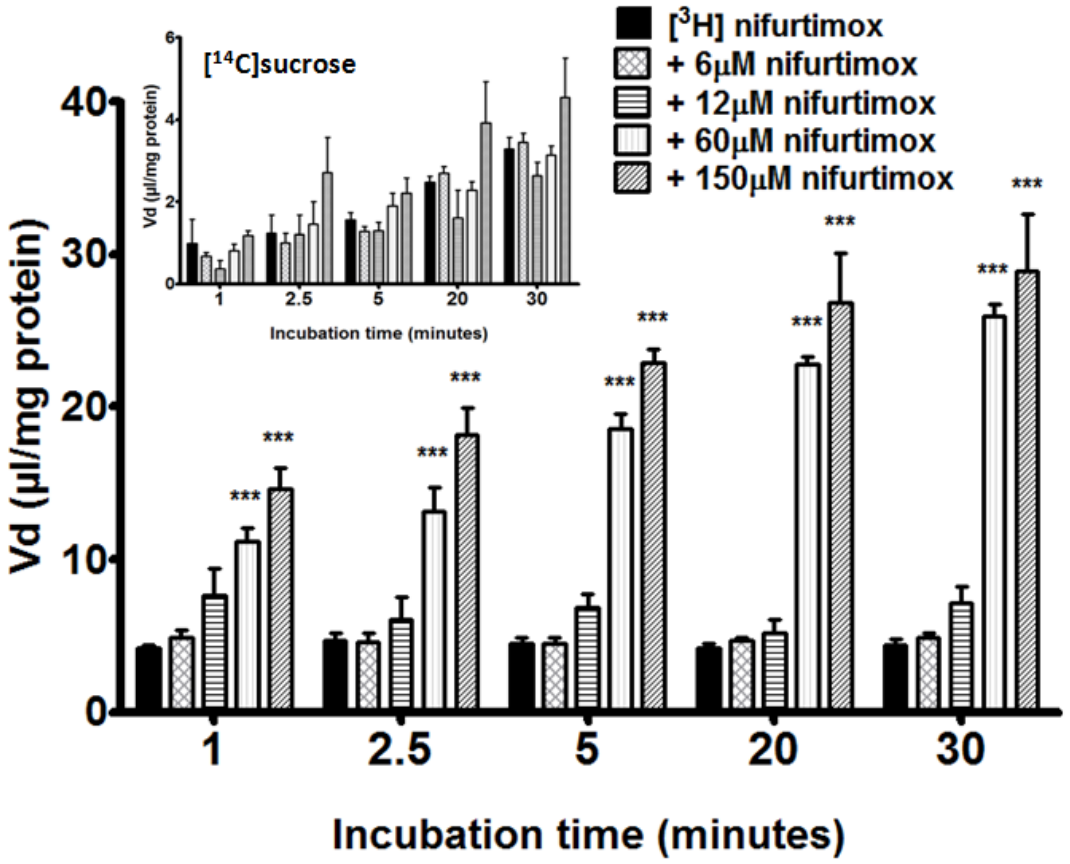

Figure 7.3. Influence of self-inhibition on [^{3}H]nifurtimox and [^{14}C]sucrose accumulation. Unlabelled nifurtimox was added to accumulation buffer in the ranges of 6μM - 150μM in 0.05% DMSO to view the impact of self-inhibition on the accumulation of [^{3}H]nifurtimox in confluent monolayers of hCMEC/D3 cells. At concentrations of 6μM and 12μM, unlabelled nifurtimox caused no change in accumulation of [^{3}H]nifurtimox, but at concentrations of 60μM and 150μM, a highly significant increase in [^{3}H]nifurtimox accumulation compared to controls was observed at all time points (***$p<0.001$). [^{3}H]nifurtimox data are corrected for [^{14}C]sucrose and protein content (with [^{14}C]sucrose corrected for protein only). All data expressed as mean ± S.E.M, n=4-6 (plates), with 6 replicates (wells) per plate.

7.3.5. Roles of P-gp and BCRP in [^{3}H]nifurtimox accumulation

The influences of P-gp and BCRP in the transport of [^{3}H]nifurtimox, were tested using four drugs that have previously been shown to decrease the functions of these transport proteins (table 2.1). There were no significant differences in [^{14}C]sucrose accumulation between any treatments (see figure 7.4 and 7.5 inserts). For P-gp assessment we used haloperidol (40μM)

and dexamethasone (200µM) and for BCRP, ko143 (1µM) and pheophorbide A (PhA) (1µM). The results showed that the P-gp acting drugs, haloperidol and dexamethasone, had no affect on [^{3}H]nifurtimox accumulation (figure 7.4), whereas significant increases in [^{3}H]nifurtimox accumulation were observed with the addition of the BCRP acting drugs, ko143 and PhA (both *p<0.001* against controls) (figure 7.5).

To further assess roles played by ABC transporters in [^{3}H]nifurtimox accumulation, cellular ATP was depleted using 10mM 2-deoxy-D-glucose (as described in the methods). This depletion step resulted in a 76% depletion of intracellular ATP compared to untreated controls (luminescence data not shown). ATP-depletion effectively increased the accumulation of [^{3}H]nifurtimox in the cells compared to controls at all time points (*p<0.01* at 1 minute and *p<0.001* for the remaining time points). When comparing the effect of ATP depletion to that of inhibiting P-gp transport (figure 7.4), there was a significant difference with ATP depletion causing an increased [^{3}H]nifurtimox accumulation when compared with P-gp inhibition by both drugs (*p<0.01* at all time points for both P-gp treatments). In contrast, comparing the effect of ATP depletion to that of BCRP inhibition (figure 7.5) showed that these two treatments caused similar changes to [^{3}H]nifurtimox accumulation after 1, 2.5, 5 and 20 minutes, although it was noted that after 30 minutes ATP depletion caused a significantly greater increase (by 17-20%) in [^{3}H]nifurtimox accumulation (*p<0.05*).

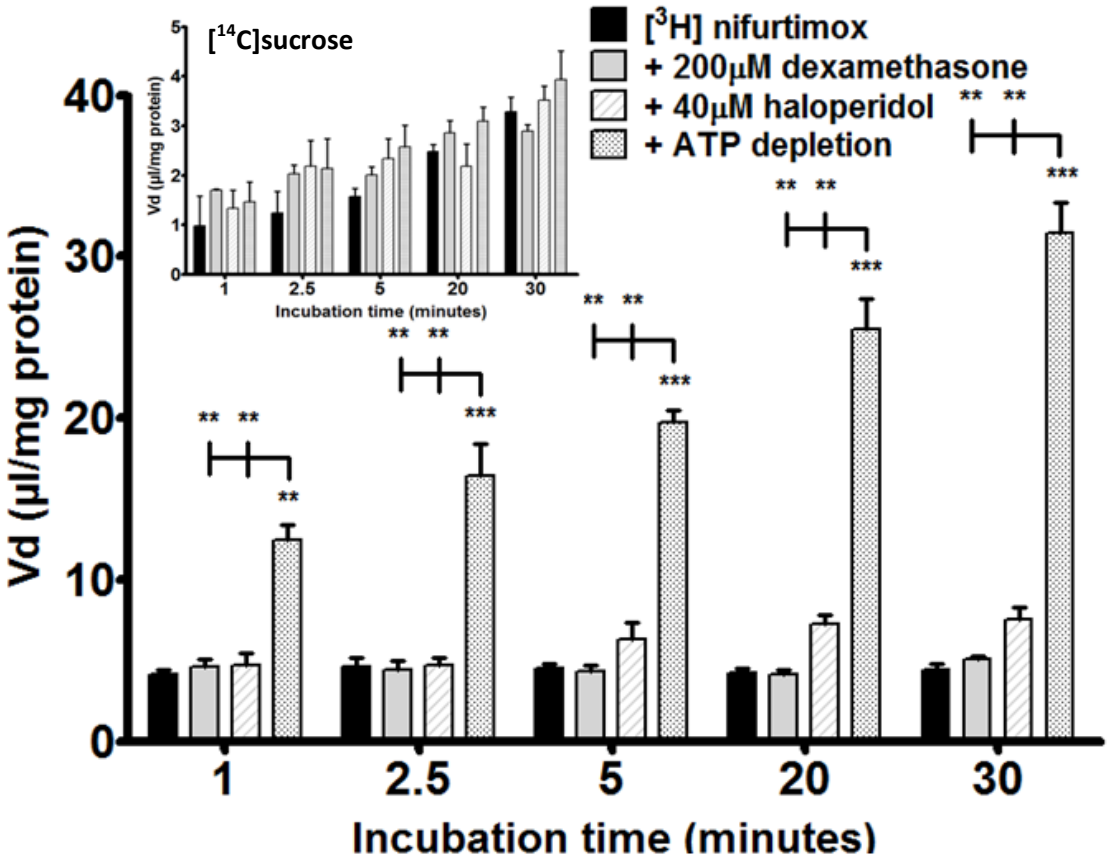

Figure 7.4. The effects of P-gp on [^{3}H]nifurtimox and [^{14}C]sucrose accumulation. To assess the roles played by the ABC transporter, P-gp, in the accumulation of [^{3}H]nifurtimox and [^{14}C]sucrose, the accumulation of [^{3}H]nifurtimox in confluent monolayers of hCMEC/D3 cells in 96 well plates was observed with or without the known P-gp interacting drugs dexamethasone and haloperidol in the presence of 0.05% DMSO. The P-gp substrate and inhibitor (dexamethasone and haloperidol respectively) caused no significant alteration in the accumulation of [^{3}H]nifurtimox. ATP depletion caused a significant increase at all time points compared to both control data and P-gp inhibition (**$p<0.01$ and ***$p<0.001$ vs. control, **$p<0.01$ vs. dexamethasone and haloperidol). [^{3}H]nifurtimox data are corrected for [^{14}C]sucrose and protein content (with [^{14}C]sucrose corrected for protein only). All data expressed as mean ± S.E.M, n=4-6 (plates), with 6 replicates (wells) per plate. ATP – adenosine triphosphate.

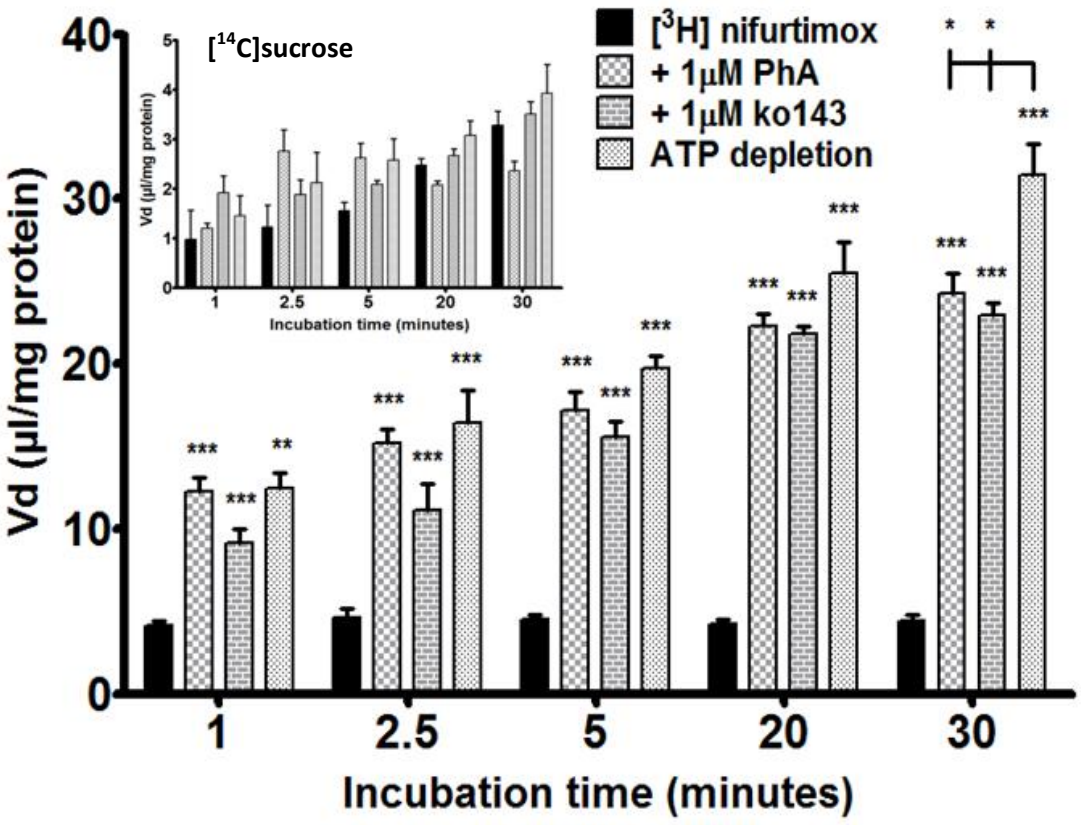

Figure 7.5. The effects of BCRP on [^{3}H]nifurtimox and [^{14}C]sucrose accumulation. To assess the roles played by the ABC transporter, BCRP, in the accumulation of [^{3}H]nifurtimox and [^{14}C]sucrose, the accumulation of [^{3}H]nifurtimox in confluent monolayers of hCMEC/D3 cells in 96 well plates was observed with or without known BCRP interacting drugs PhA and ko143 in the presence of 0.05% DMSO. The BCRP substrate and inhibitor (PhA and ko143 respectively) caused significant increase in the accumulation of [^{3}H]nifurtimox at all time points when compared to controls. ATP depletion caused a significant increase at all time points compared to both control data and P-gp inhibition (**$p<0.01$* and ***$p<0.001$* vs. control, **$p<0.05$* vs. PhA and ko143). [^{3}H]nifurtimox data are corrected for [^{14}C]sucrose and protein content (with [^{14}C]sucrose corrected for protein only). All data expressed as mean ± S.E.M, n=4-6 (plates), with 6 replicates (wells) per plate. PhA – pheophorbide A.

7.3.6. Roles of MRP, OATPs and OATs in [^{3}H]nifurtimox accumulation

Probenecid (350µM) was used to assess contributions to [^{3}H]nifurtimox and [^{14}C]sucrose accumulation from proteins separate to P-gp and BCRP; namely multi-drug resistance associated proteins (MRP) 1 and 2, organic anion-transporting polypeptides (OATPs) and organic anion transporters (OATs). There were no changes in [^{14}C]sucrose accumulation between the treatments (insert of figure 7.6) Figure 7.6 illustrates the significant time dependent effect of probenecid on [^{3}H]nifurtimox accumulation from 2.5 minutes and 5

minutes (*p<0.01*) to 20 and 30 minutes (*p<0.001*) which induced an average increase in accumulation of 114% across all time points. This effect was not matched by the presence of the MRP-1 inhibitor Indomethacin (10µM), where no significant change to [^{3}H]nifurtimox was observed at any time point. Taurocholic acid (TCA, 200µM) and para-aminohippuric acid (PAH, 500µM) were then used to assess function of OATPs and OATs respectively. The addition of TCA caused significant changes in [^{3}H]nifurtimox accumulation from 2.5 minutes (*p<0.01*) and onwards when all three time-points showed significant increases (*p<0.001* figure 7.6), albeit less than those observed with the BCRP inhibitors. PAH caused no significant differences in accumulation of [^{3}H]nifurtimox at any time point.

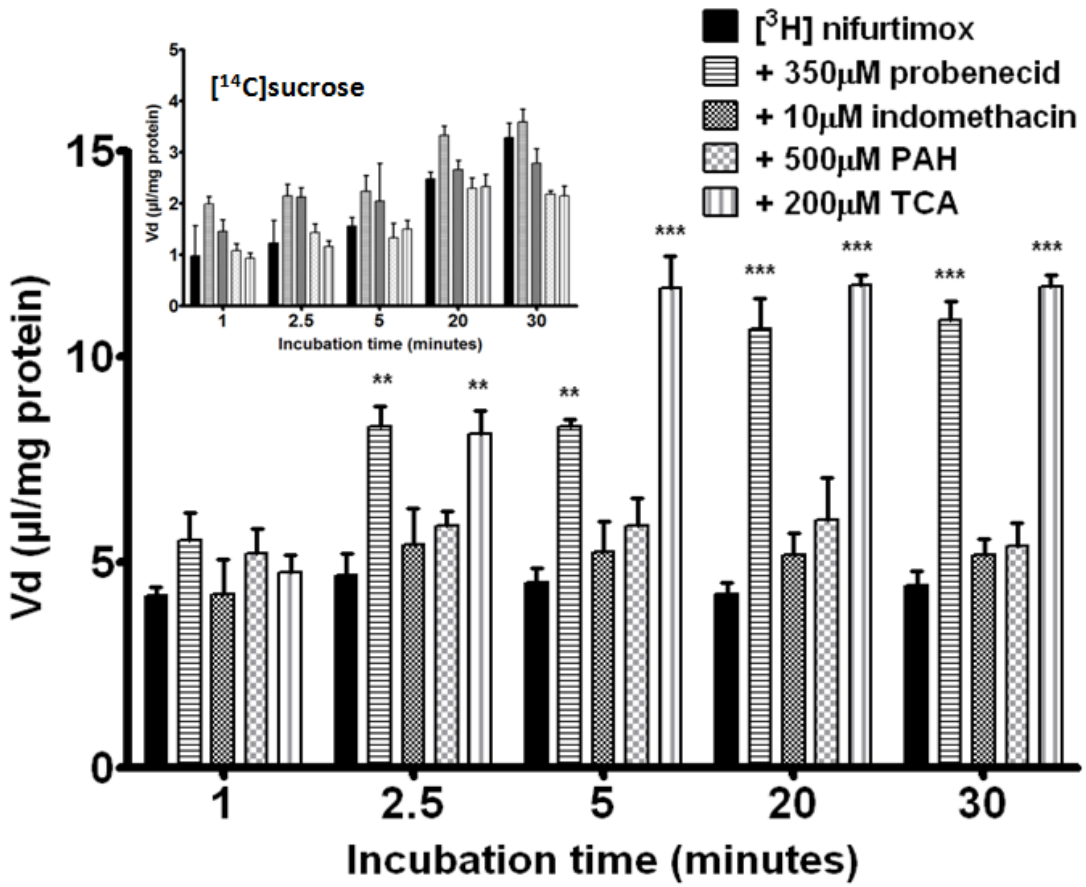

Figure 7.6. The effects of OATs, OATPs and MRPs on [^{3}H]nifurtimox accumulation. To assess the roles played by members of the transport families OATs, OATPs and MRPs in the transport of nifurtimox, the accumulation of [^{3}H]nifurtimox in confluent monolayers of hCMEC/D3 cells in 96 well plates was observed, with or without known transporter interacting drugs, in the presence of 0.05% DMSO. The OAT interacting drug, PAH and the MRP1 interacting drug, indomethacin, caused no significant changes in the accumulation of [^{3}H]nifurtimox. From 2.5 minutes onwards, both probenecid (OATs, OATPs and MRPs) and TCA (OATPs) caused significant increases in the accumulation (**$p<0.01$, ***$p<0.001$). [^{3}H]nifurtimox data are corrected for [^{14}C]sucrose and protein content (with [^{14}C]sucrose corrected for protein only). All data expressed as means ± S.E.M, n= 4-6 (plates), with 6 replicates (wells) per plate. PAH - para-aminohippuric acid, TCA - taurocholic acid.

7.3.7. Cytotoxicity of compounds used

The potential of the compounds used in this study to cause cytotoxicity was assessed using an MTT assay and the effect compared to untreated control hCMEC/D3 cells (figure 7.7). There were no significant differences on cell viability after 30 minutes exposure to the drugs.

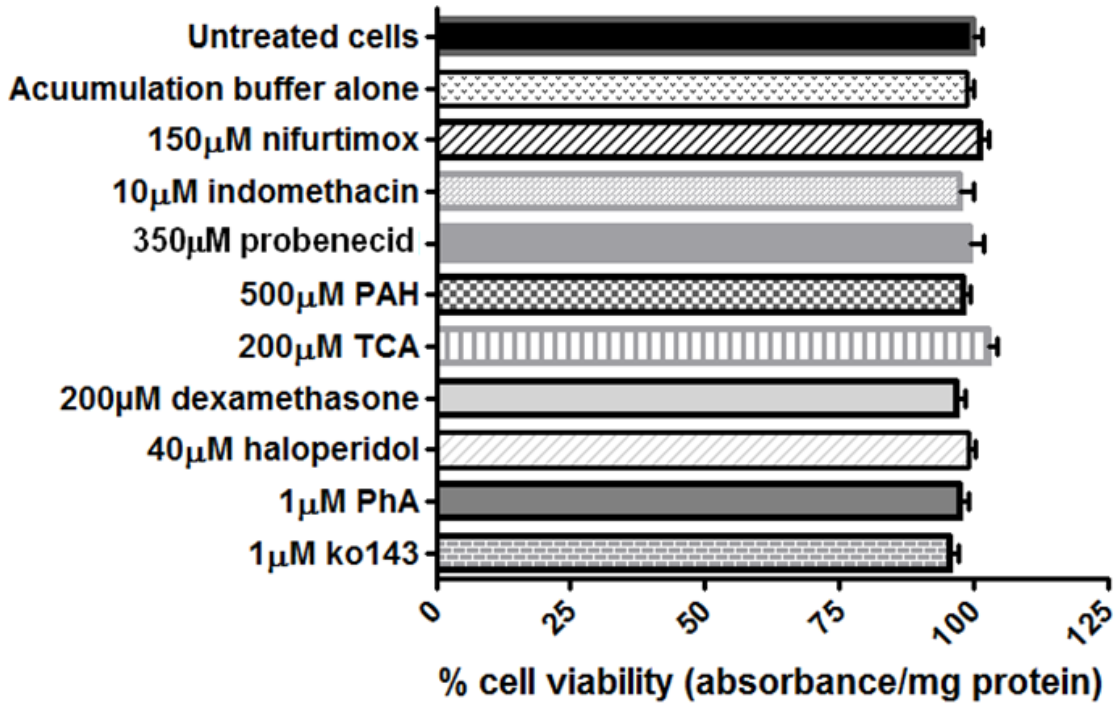

Figure 7.7. Cytotoxic effects of compounds used in the study. The test compounds were assessed for any cytotoxic effects using an MTT assay during 30 minute incubations with confluent monolayers of hCMEC/D3 cells in 96 well plates, as described in section 4.7 of experimental procedures. The results are expressed as percentage viability ± S.E.M and compared to control untreated cells, which were incubated for 30 minutes in normal medium. None of the compounds induced a significant change in cell viability. All data means ± S.E.M, n= 4-6 with n=3 (plates), 4 replicates per n (4 wells).

7.3.8. BCRP and P-gp protein expression in hCMEC/D3s

Mouse anti-human BCRP/ABCG2 and mouse anti-human P-gp/MDR1 monoclonal antibodies were used to detect protein expression of BCRP and P-gp in the hCMEC/D3s using SDS-PAGE and western blotting. Bands detected at the expected molecular weights of 170kDa for P-gp and 70kDa for BCRP confirmed their expression using SDS-PAGE and Western blot analysis (figures 7.8 a and 7.8 b respectively). HepG2 cell lysates were used as positive controls (Wojtal et al., 2006, Vander Borght et al., 2008).

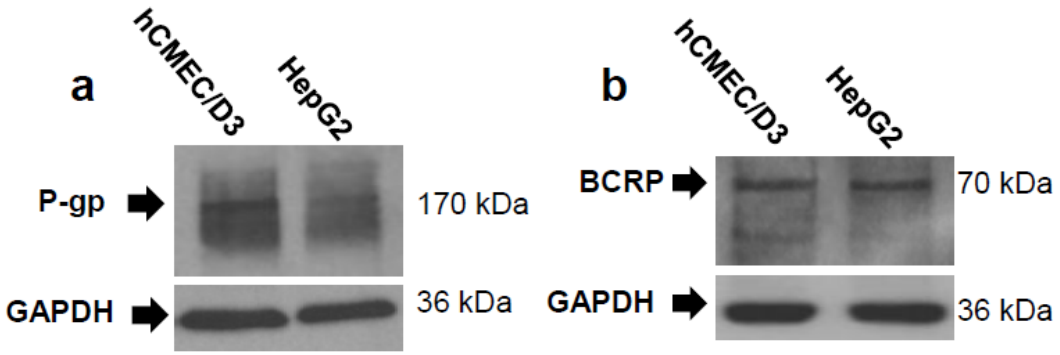

Figure 7.8. Expression of P-gp and BCRP in the hCMEC/D3 cells. Confluent monolayers of hCMEC/D3s and flasks of HepG2 cells were lysed in TGN buffer and the expression of P-gp (*a*) and BCRP (*b*) were analysed using western blotting, as described in section 7.2.8 of the methods section. GAPDH was stained as a loading control.

7.4. Discussion

Human African trypanosomiasis has a large impact, both socially and economically, on affected sub-Saharan communities. A combination of constant surveillance and careful implementation of preventative measures is required by the authorities if the disease is to be successfully combated. Collapses of disease surveillance and changes in political agenda have allowed HAT's prevalence to increase and this is one of the reasons the disease has not been eradicated despite drops in the numbers of reported cases. Another reason is due to the unsatisfactory treatment of the disease which in turn is down to the facts that the anti-HAT drugs available are expensive, can be extremely difficult to successfully administer, have limited efficacy and can cause severe adverse reactions. These features combined with a lack of understanding about anti-HAT drugs and their BBB interaction highlights the need for more research into the treatment of this disease.

The aim of this study was to investigate whether BBB transport proteins were being utilised by the emerging drug of choice for treating HAT, nifurtimox, and also investigated the effects, if any, of anti-HAT CT on its delivery. Our group has previously shown that nifurtimox is a substrate for an efflux protein at the murine BBB, which is unlikely to be P-gp, as shown by the use of P-gp deficient animals (Jeganathan et al., 2011). P-gp is expressed at the luminal membrane of the human BBB and removes a wide variety of substrates from the endothelial cell cytoplasm (Abbott et al., 2006). The lack of interaction between nifurtimox and P-gp was also evident in the hCMEC/D3s through the use of the P-gp substrate dexamethasone and the specific P-gp inhibitor (at 40μM) haloperidol, which did not cause any significant differences in [^{3}H]nifurtimox accumulation over the 30 minute incubation period. However, a promising potential efflux transporter for nifurtimox was suggested in our earlier animal study (Jeganathan et al., 2011). Further investigation in the hCMEC/D3s revealed this efflux transporter to be BCRP through the use of the BCRP substrate PhA and the BCRP specific inhibitor (when used in the range of 0.1-1μM (Matsson et al., 2009) k0143 , identified through the large increases in accumulation which can be attributed to the efflux process being affected. BCRP, like P-gp, is expressed luminally at the BBB and both these proteins are members of the ABC transporter superfamily which play key physiological roles in protecting tissues from toxic xenobiotics and other potentially harmful endogenous metabolites. ABC transporters require energy to function. This energy comes in the form of ATP and so we decided to manipulate this aspect by depleting cellular ATP by inhibiting glycolysis using the

established glycolysis inhibitor 2-DG (Whiteman et al., 2002, Wang et al., 2011b). This ATP-depletion resulted in [^{3}H]nifurtimox accumulation values comparable to those achieved using the BCRP interacting drugs, but not those generated from the P-gp investigations. At the 30 minute stage, accumulation of [^{3}H]nifurtimox was 83% of the accumulation seen following ATP depletion. These similar increases in accumulation by ATP-depletion further support the evidence that BCRP appears to play a crucial role, whereas P-gp plays little or no role in nifurtimox transport. The protein expression of these efflux transporters were confirmed in our model by Western blot, which is consistent with the findings of several other recently published studies using the hCMEC/D3s (Weksler et al., 2005, Poller et al., 2008, Tai et al., 2009a). These data suggest that not only is BCRP functional in the hCMEC/D3s but perhaps inhibiting BCRP could improve the delivery and efficacy of nifurtimox. Indeed, that nifurtimox could be a substrate for BCRP has been previously suggested (Garcia-Bournissen et al., 2010, Jeganathan et al., 2011). In a study investigating nifurtimox transfer in breast milk, Garcia-Bournissen *et al,* suggested that as the antibiotic nitrofurantoin is structurally related to nifurtimox and is a substrate for BCRP (Merino et al., 2005), perhaps nifurtimox may also be a substrate (Garcia-Bournissen et al., 2010). The findings of our study provide direct evidence of this hypothesis for the first time in a human *in vitro* BBB model.

To investigate the roles of other transport systems in nifurtimox transport, a variety of other drugs were used to affect transport activity of MRPs, OATs and/or OATPs. MRPs, other members of the ABC transporter superfamily that also mediate brain-to-blood efflux, play important roles *in vivo* to protect the brain from xenobiotics. OATs and OATPs are membrane transport proteins that play large roles in the transport of endogenous molecules across cell membranes. MRP1 expression has previously been shown in the hCMEC/D3s at mRNA (Carl et al., 2010) and protein levels (Weksler et al., 2005). The expression of MRPs 2,3,4 and 5, OATP1, OATPD and OATP2A1 have been shown at mRNA level only in the hCMEC/D3s (Poller et al., 2008, Carl et al., 2010), and they are also expressed in the human brain (Gibbs and Thomas, 2002). However, neither protein nor mRNA expression has not been demonstrated for members of the OAT superfamily in the hCMEC/D3 cell line. The data here comply with this knowledge somewhat, suggesting that nifurtimox appears to be a substrate of functional OATP and MRP systems from the increases in [^{3}H]nifurtimox from 2.5 minutes onwards, but OAT appear not to be involved. This was demonstrated by use of the broad spectrum MRP, OAT and OATP inhibitor, probenecid; the MRP1 inhibitor, indomethacin; the OATP competitive

inhibitor, TCA and the OAT competitive inhibitor, PAH. OATPs have been suggested as being bidirectional drug transporters (Nozawa et al., 2005) and the increases in accumulation with the addition of TCA could provide some evidence for their role in nifurtimox transport. However, although indomethacin is commonly used as a MRP1 inhibitor, it has been shown to be a substrate of OATPs and OATs, albeit at different concentration ranges than used here (Parepally et al., 2006). The increases in [^{3}H]nifurtimox accumulation were also lower than that seen with the BCRP specific drugs, suggesting lesser roles for OATPs and MRPs in comparison. It is also important to point out that some groups have found that probenecid is a BCRP substrate *in vitro,* and this is also a possible explanation for the increase in [^{3}H]nifurtimox accumulation using this drug (Merino et al., 2006). However, other groups have found no such evidence of BCRP/probenecid interaction (Pan et al., 2007). It has also been reported that neither TCA (Suzuki et al., 2003) nor indomethacin (Elahian et al., 2010) interact with BCRP. The concentrations of drugs used in this study were carefully chosen to follow those used in previous *in situ* studies by our group, to be in line with the clinically relevant doses used in the field (with the anti-HAT drugs) and to be in line with those reported in publications such as Matsson *et al* (Matsson et al., 2009). These data and findings by other groups highlight that drugs affecting transport activity must be used at specific concentrations to affect specific transport proteins. The broadness of some transporter interacting drugs also illustrates the need for use of more specific inhibitors, at specific concentrations which will yield clearer results.

With combination therapy now the most promising method of clinical S2 HAT treatment, we also investigated whether other unlabelled anti-HAT drugs could modulate the accumulation of [^{3}H]nifurtimox in human brain endothelium. In line with previous work by our group, an increase in [^{3}H]nifurtimox accumulation was seen with the addition of 10µM pentamidine. Pentamidine, a S1 HAT acting drug, has been previously shown by our group to be a substrate for P-gp and is also transported by other transport proteins including MRP. This present study with P-gp inhibitors suggests that perhaps this drug also interacts with other membrane transporters. BCRP and members of the MRPs or OATPs could be candidates as indicated by their interactions with PhA, k0143, probenecid and PAH. However, no other drugs from the CT experiments, including eflornithine, caused any significant changes in [^{3}H]nifurtimox accumulation in the cells, which contradicts our previous findings that eflornithine, suramin and melarsoprol caused decreases in the brain distribution of

[^{3}H]nifurtimox *in situ* (Jeganathan et al., 2011). One must of course be careful when comparing *in situ* brain distribution and *in vitro* accumulation data. When observing the *in situ* BBB endothelial cell pellet analysis for [^{3}H]pentamidine previously published by our group, it was evident that the drug accumulated in the cells (Sanderson et al., 2009). [^{3}H]nifurtimox accumulated to a lesser degree *in situ,* although the differences in accumulation with CT were similar to those reported here with an increase observed with the addition of unlabelled pentamidine and little or no difference with the other drugs (Jeganathan et al., 2011). The reasoning behind the improved cure rates of patients using NECT compared to eflornithine alone, based on our results, is unlikely to be due to the interactions of the drugs with membrane transporters. It has been stipulated that the arrestment of parasite defences caused by eflornithine allows the efficacy of nifurtimox to be improved and perhaps this is the main reason behind NECT success (Priotto et al., 2009).

The mechanism by which nifurtimox enters into the cells remains unknown. It is likely that the highly lipophilic properties of nifurtimox (with octanol-saline partition coefficient of 5.46(Jeganathan et al., 2011) allows it to cross cell membranes by passive diffusion and previous work has shown that it not only appears to use a transcellular route of entry, but enters the mouse brain at sufficient amounts to be effective in killing trypanosomes (Jeganathan et al., 2011). However, the role played, if any, by blood-to-brain transporters remains elusive. Any effects the drugs had on the expression of transporters have also not been assessed here. It has been shown previously that some drugs can upregulate functional expression of drug transporters such as P-gp, and this is well documented with dexamethasone (Narang et al., 2008), but the 30 minute time frames of the experiments in this report were unlikely to be sufficient at inducing any significant increase in expression or activity. That some of the drugs used here, although carefully chosen to be within published concentration ranges, had over-lapping affinity for different transport systems only highlights in some cases the difficulty in drawing accurate conclusions to which of the transport systems were being utilised.

7.5. Conclusions

Studying nifurtimox interactions with the BBB is crucial to improving treatment of second stage HAT, especially now that NECT is fast becoming the treatment of choice. Considering the current usage of NECT, it is somewhat surprising that very little is known about the mechanisms being used by these drugs to gain entry to the brain. We report here that nifurtimox appears to be a substrate of BCRP and possibly members of the transport families OATP and MRP in an *in vitro* model of the BBB. We also demonstrate that, with regards to the combination therapy approach to treating HAT, the combination of eflornithine and nifurtimox does not appear to hamper or improve entry of nifurtimox into the BBB and the reasoning behind its success in the field is unlikely due to transporter interactions at the BBB. In addition, our data suggests that pentamidine could actually improve the delivery of nifurtimox, which is in line with previous work by our group in an animal model.

Chapter 8. General Discussion

8.1. Chapter 8 – General discussion

The purpose of this thesis was to gain first insights into the interactions of clinically relevant endogenous and exogenous molecules with the human BBB using the well established immortalised hCMEC/D3 *in vitro* model of the human BBB. The investigations were designed according to prior knowledge in the subject areas – both our own and that of the scientific literature – and allowed us to explore highly novel areas with relation to the human BBB. The information gained from the endogenous studies on ADMA and L-arginine allowed us to design experiments for the exogenous molecule investigations with the anti-HAT drug and CAA analogue eflornithine. Nifurtimox was also investigated due to its link with eflornithine and because of the particular interest of our laboratory in trypanosomiasis chemotherapy.

8.2. Endogenous molecules – L-arginine and ADMA

ADMA is very much a 'hot-topic' of investigation in vascular biology research due to its potency as an inhibitor of NO production and implications in ROS production (Teerlink et al., 2009). It is therefore of acute interest to researchers investigating highly specialised vasculature, the integrity of which is paramount to maintaining precise function. This is no more palpable than at the BBB, and because the role of ADMA in brain and cerebrovascular pathologies is becoming more and more questioned (Kielstein and Kielstein, 2009), we decided this was a perfect opportunity to gain a first insight into interactions between the human BBB and the molecule.

8.2.1. Chapter 3 – ADMA on the paracellular integrity of the BBB

Chapter 3 investigated the impact of ADMA on the permeability of the confluent hCMEC/D3 monolayer grown on transwell filter inserts with the hypothesis in line with previous *in vitro* investigations using peripheral endothelium that supraphysiological concentrations of ADMA would induce permeability increases – although the affects of lower more clinically relevant concentrations on the barrier were not ruled out. Our findings confirmed our initial hypothesis in line with previous studies (Wojciak-Stothard et al., 2007, Wojciak-Stothard et al., 2009, Chen et al., 2011, Wang et al., 2011a), although we linked this increase in permeability to a loss in cell viability which could be induced by the production of ROS through the uncoupling of eNOS (Sydow et al., 2003) – the protein of which was expressed in the hCMEC/D3s alongside the ADMA metabolising enzyme DDAH-1. However, due to time constraints neither ROS production nor the role of small GTPases in cytoskeletal or junctional restructuring (that has

been linked to ADMA in previous studies (Wojciak-Stothard et al., 2009, Chen et al., 2011) were investigated.

Thus, this first insight into ADMA and the human BBB demonstrated that the barrier is indeed sensitive to the molecule (albeit at high concentrations), but results in further questions requiring further investigation. Firstly, the study was designed to assess 24 hour exposure of ADMA. In the body it is possible that in certain conditions, chronic exposure of the vasculature to ADMA is likely to occur. Under such chronic conditions it is possible that smaller, more clinically relevant concentrations of ADMA would elicit effects on endothelium, and this may go some way to explaining the difference between intracellular and extracellular concentrations of ADMA. It would be interesting to investigate a variety of incubation times to assess this. This would be somewhat difficult to physiologically model however as not only would it require careful intracellular and extracellular measuring, it would also likely require constant replenishment of extracellular ADMA as the molecule has a short plasma half-life of 23.5 ± 6.8 minutes in humans (although likely more *in vitro* due to the lack of a complete physiology system (Kielstein et al., 2004) and the activity of PRMTs and DDAH-1 would need to be assessed. This leads to the second point, that the expression and activity of DDAH-2 was not investigated. This is likely to have implications at the BBB because DDAH-2 is predominantly expressed in endothelial cells compared to DDAH-1 which is expressed more extensively throughout the body (Palm et al., 2007). eNOS expression was confirmed, but its functional activity was also not investigated. If functional, then this could add weight to the ADMA-induced eNOS uncoupling theory, especially if the presence of ROS formation was demonstrated by incubation of the hCMEC/Ds with ADMA.

Perhaps an interesting investigation to follow on from chapter 3 would be to look at the effects of ADMA on pericytes which are the contractile cells situated at the BBB that regulate local capillary blood flow (Yemisci et al., 2009). Data demonstrated with pericytes and BMECs is likely to have greater implications physiologically than just with a cell monolayer model and may implicate NO, to which mouse brain pericytes are sensitive *in vitro* (Kovac et al., 2011).

8.2.2. Chapter 4 – Transport interactions of ADMA at the BBB

Chapter 4 explored the transport processes utilised by ADMA in relation to those used by L-arginine, due to the similarity of their chemical structures. This first look at interactions between ADMA and CAA transporters is novel with respect to the human BBB and has wider

implications due to the ubiquitous expression of CAA transporters throughout the body. Very little investigation has been performed on ADMA transport, especially in human endothelial cell systems due to the assumption that it uses system y^+ transporters as with L-arginine (Teerlink et al., 2009). We demonstrated that [^{3}H]ADMA uses a variety of CAA transport systems that included system y^+ alongside L-arginine – with CAT-1 expression confirmed in the cell line – but also leucine sensitive systems which could be members of the BAT transport family such as system y^+L transporters and system $b^{0,+}$ transporters, which have been described at mRNA level in the hCMEC/D3s (Carl et al., 2010). It appeared that the transport systems present on the hCMEC/D3s favoured [^{3}H]L-arginine over [^{3}H]ADMA (based on V_d values alone) although, to get an accurate indication of this, kinetic studies determining K_m and V_{max} would need to be performed.

One of the most intriguing findings of chapter 4 was the strong indication that [^{3}H]ADMA was being effluxed from the cells by a Na^+ and Cl^--sensitive transport system, that appeared to be the system $B^{0,+}$ transporter $ATB^{0,+}$; the protein expression of which was confirmed. These data were extremely perplexing as $ATB^{0,+}$ should co-transport ions and substrate in the same direction (symporter) (Sloan and Mager, 1999, Hatanaka et al., 2004), so when Na^+ free buffer was used and [^{3}H]ADMA accumulation increased this was suggestive of an antiport system. It would require electrophysiology techniques such as voltage-clamp to look at the direction of ion currents as well as polarisation studies to look for the location of the transporter – if located on both luminal and abluminal membranes as a system of movement from the blood-to-brain direction only, these increases in accumulation when blocking the action of $ATB^{0,+}$ may also be explainable as ADMA uses a variety of transporters for entry, but possibly only $ATB^{0,+}$ for exit. Another possibility is that the 'specific' inhibitor for $ATB^{0,+}$, α-methlytryptophan (Karunakaran et al., 2008), is not actually specific and could be affecting a variety of different cellular exit transport systems.

It is also important to point out that we did not look at the mRNA levels of transport proteins in this thesis (as mentioned in chapter 7), so we cannot rule out the possibility of increased expression or increased membrane translocation of CAA transporters at the membrane upon changing media for accumulation buffer or with the introduction of transporter interacting drugs. Increased membrane translocation of GLUT4 from transporter stores in intracellular vesicles has been demonstrated in adipocytes following stimulation with

insulin (Karlsson et al., 2002) and a similar increase in endothelial membrane translocation has been demonstrated for CAT-1 following stimulation with high-density lipoprotein from healthy subjects *in vitro* (Besler et al., 2010). If this phenomenon was occurring in our model in response to an extracellular stimulus, this is interesting to investigate, but it seems unlikely given the short time frames of the accumulation assays.

8.2.3. Chapter 5 – The *trans*-stimulation of ADMA and the 'L-arginine paradox'

The premise behind chapter 5 was to assess if intracellular ADMA could be *trans*-stimulated by extracellular L-arginine and therefore help to explain the phenomenon known as the 'L-arginine paradox'. In this paradox, L-arginine supplementation improves NO impairment and endothelial dysfunction despite the fact that NOS should already be fully saturated by basal concentrations of extracellular L-arginine. Data from chapter 5 provided some evidence of the role of ADMA in the paradox, by revealing that pre-loaded intracellular [^{3}H]ADMA could indeed be *trans*-stimulated by extracellular L-arginine, with the reverse also being demonstrated when intracellular ADMA actually increased the accumulation of extracellular [^{3}H]L-arginine compared to cells that were not preloaded with ADMA. Although this provides evidence for ADMA in the 'L-arginine paradox' the experiments were not performed in a physiologically relevant system where a variety of factors are likely to have an impact on cellular influx and efflux of CAAs and the catabolism of ADMA and L-arginine – the latter important with regards to intracellular pools.

Although plasma concentrations of ADMA have been linked to disease, little is known about intracellular concentrations in physiological states let alone in disease. This is not only important with regards to the 'L-arginine paradox', but will also have implications with ADMA and NO physiology as a whole, especially regarding subcellular pools of ADMA and L-arginine. Data identifying and understanding these pools is limited due to the complexity of their function and cellular location as well as the recent occurrence of the investigations. If L-arginine and ADMA from these intracellular pools have preferential access to the intracellular enzymes that regulate their levels and if extracellular L-arginine and ADMA have access to these pools is the next logical course of investigation to properly clear up the role of ADMA and the 'L-arginine paradox'.

8.3. Exogenous molecules – eflornithine and nifurtimox

Human African trypanosomiasis is classified as a neglected tropical disease because it is confined to specific areas of sub-Saharan Africa and has been poorly managed at the local government level. It is only in the last decade that concerted efforts spearheaded by the WHO and determined health programmes have attempted to counteract this disease. The neglected status of the disease extends to its research which has only recently revealed new drug candidates. These reasons make it important to study what is currently available to treat the disease not only to help the people suffering from the disease, but to help and guide research for better drugs. Our research group is one of the few researching the drug delivery aspect and so we decided to build on our expertise by using a human *in vitro* model of the BBB to isolate specific transport systems.

8.3.1. Chapter 6 – eflornithine interactions with the BBB and other anti-HAT drugs

In chapter 6 we sought to investigate evidence of interactions between eflornithine and the human BBB in terms of CAA transport. This is because eflornithine is a closely related analogue of the CAA ornithine and so it was hypothesised that the molecule could use CAA systems to enter the BBB. We revealed that [^{3}H]eflornithine competed with several CAA substrates for entry to the cell, which was most likely to be a member of the system y^+ transport family as implicated by use of the potent system y^+ inhibitor, L-homoarginine. These data were in contrast to our previous *in situ* brain perfusion work using mouse models, where it was demonstrated that eflornithine had a limited ability to cross the BBB and did not use a transport system (Sanderson et al., 2008). However, it is important to point out that eflornithine appears more likely to cross the human BBB than the mouse BBB according to our data, and this could explain why the drug is efficacious in humans. But an important fact here is that a large concentration of the drug is required over a long time-period to be efficacious in humans, which points to the fact that the drug is poor at crossing the BBB.

The second line of investigation in this chapter concerned the impact of combination therapy on the delivery of eflornithine as improvements of treatments with anti-HAT drugs have been widely reported (Priotto et al., 2006, Priotto et al., 2009). We hypothesised that combination of the drugs would actually improve drug delivery to the brain through transporter interaction or DDIs between the drugs. Linking the first line of investigation with the second in this chapter, our data from the pentamidine co-incubation with [^{3}H]eflornithine implicated polyamine transporters may be able to transport eflornithine across the BBB as

they do in the parasites themselves, but their expression has not been investigated at the human BBB *in vitro* or *in vivo* in any model, and this would be an interesting course of investigation to take in the future with regards to CAA transport of eflornithine.

We found conflicting data when we co-incubated [^{3}H]eflornithine with suramin compared to our previous *in situ* work which showed an improved delivery of eflornithine to all mouse brain regions, which was hypothesised to be due to DDIs between the two drugs that increased the brain uptake of eflornithine through endocytotic events (Sanderson et al., 2008). The other data from the CT studies with the clinically relevant concentrations of nifurtimox, eflornithine and melarsoprol were in alignment with our previous work, where no changes were seen. These data taken together suggest that the success of NECT is due to countering drug resistance in the trypanosomes themselves, rather than an improvement in brain delivery. This has not been investigated directly however, and is also an interesting line of investigation for future research.

The latest review regarding S2 HAT treatment at the time of writing this thesis describes how NECT has brought about a 12% decrease in melarsoprol usage, is cheaper than eflornithine monotherapy and has improved on the adverse affects of monotherapy on patients (Simarro et al., 2012). The review also highlights that NECT is still too expensive for many local authorities and far from an ideal therapy – due to logistical implications and a less than ideal toxicity risks – and calls for more research into better drugs for the disease.

The Drugs for Neglected Diseases initiative (DNDi) has accelerated efforts to eradicate this disease through collaborations between health agencies such as the WHO, pharmaceutical giants such as GlaxoSmithKline and academia and aims to bring a HAT-specific portfolio by 2014, with several exciting new drugs in the pipeline (see: dndi.org/).

8.3.2. Chapter 7 – nifurtimox interactions with the human BBB

Chapter 7 investigated the impact of CT on the delivery of nifurtimox and the roles of efflux transport systems as with eflornithine in chapter 6 due to their association through NECT. For this area of investigation, our data failed to comply with our *in situ* work as no changes in [^{3}H]nifurtimox accumulation were noted with any combination of anti-HAT drug except with the addition of pentamidine where we noted an increase in [^{3}H]nifurtimox accumulation. In our previous *in situ* studies, significant decreases in [^{3}H]nifurtimox brain distribution were noted with all anti-HAT drugs except pentamidine which caused an increase in [^{3}H]nifurtimox

brain distribution (Jeganathan et al., 2011). The finding with pentamidine suggests this drug interacts with an efflux system for nifurtimox, not involving P-gp and therefore future studies investigating this are necessary to understand the culprit – possibly a MRP member or BCRP. The reasoning behind the difference between the other findings of our study in comparison to our earlier work could be due to model and/or species differences. It is important to point out that comparing data between species and models must be taken with caution due to a variety of missing factors in the *in vitro* system that are likely to have direct impact on drug accumulation – such as a lack of flow for instance. It remains unlikely that nifurtimox uses an influx transport systems as self-inhibition would likely have induced a decrease in [^{3}H]nifurtimox accumulation had there been any, and no evidence has been uncovered to suggest otherwise. It may be possible that *in situ* these drug combinations induced DDIs and indeed melarsoprol and nifurtimox have been suggested to have synergism (Bisser et al., 2007), possibly affecting the diffusion of nifurtimox across the BBB, although this is speculation. Detailed studies isolating the precise method of nifurtimox entry would be required to provide more compelling answers.

The second focus of chapter 7 was designed to follow on from previous *in situ* data generated by our group where evidence was uncovered for a nifurtimox efflux system separate from P-gp (Jeganathan et al., 2011). In our previous paper, the role of increasing nifurtimox concentrations was not assessed, and so this was an important aspect of our *in vitro* investigations. The findings that increasing concentrations of unlabelled nifurtimox induced increases in [^{3}H]nifurtimox accumulation, complied with our other data implicating BCRP – through use of BCRP interacting drugs and ATP depletion. However, the data produced from board-scale inhibitors acting on MRP and OATP transport systems also caused significant increases in nifurtimox accumulation, albeit to a lesser extent than the BCRP interacting drugs, and therefore we could not rule out the role of OATP or MRP members in the transport of nifurtimox. These data highlight the specificity problems of transporter inhibitors and the need to be precise when instigating their use in drug transport assays. Our experimental design was carefully planned based on the work of published data (discussed below). It is likely that there was a certain amount of nonspecific interaction between some of the drugs we used, particularly so in our *in vitro* model that was devoid of flow and so the transporter interacting drugs had a greater length of access than they would *in vivo*.

8.4. Model limitations

Throughout this thesis, the immortalised hCMEC/D3 cell line has been the *in vitro* BBB model under investigation. The ease of use and the thorough characterisation of the cell line make it an attractive model for researchers looking at the human BBB. But as with any *in vitro* model, there were several limitations.

The first limitation throughout this study regarded transporter inhibitors during the accumulation assays as touched on above. The lack of specific inhibitors hinders accurate explanation of results and researchers must be careful when designing experiments using them. It is likely that siRNA knockdown experiments of candidate transporters are likely to provide greater evidence of the transporters involved and help to clear up these issues. A siRNA approach is specific, whereas many transporter inhibitors and substrates are non-specific – a limitation for the transporter experiments in the accumulation studies in this thesis. Although efforts were made to use established inhibitors at the correct concentrations, there is still a possibility of non-specific interactions. The inhibitors used in chapter 7 for the ABC-transporters where used at highly specific concentrations according to the very thorough publication by Matsson et al., who demonstrated overlap for many of the inhibitors used today in drug transporter experiments (Matsson et al., 2009).

Regarding the cells themselves, a variety of limitations were apparent. The hCMEC/D3 cells were grown alone in monoculture, not in co-culture with pericytes and/or astrocytes throughout this thesis. It is well established that these two cell types are crucial for proper BBB phenotype formation such as TJ formation and polarisation (Abbott et al., 2006, Abbott et al., 2010, Armulik et al., 2010). Without proper junctional formation, proper polarisation cannot occur, and this leads to doubts of the orientation of transporters. This is a likely reason why the hCMEC/D3 monolayer remains leaky to hydrophilic molecules via the paracellular route and explains the low TEER values of the hCMEC/D3s in chapter 3 when they were grown on transwell filter inserts. Attempts to improve the paracellular tightness of the hCMEC/D3s by co-culture with astrocytes and/or pericytes have shown higher electrical resistance that monocultures (Hsuchou et al., 2010, Hatherell et al., 2011), but the highest TEER values reached were 65 ohm.cm^2, which is well below other *in vitro* models such as bovine co-culture models (bovine BMECs and astrocytes) (Weksler et al., 2005) and porcine co-culture models (porcine BMECs and astrocytes) (Smith et al., 2007). The *in vivo* BBB which is well over 1000

ohm.cm^2 (Abbott, 2002). There are also other ways to improve *in vitro* TEER values in BBB *in vitro* models such as culturing BMECs in astrocyte conditioned media and growing cells in models with shear stress (see (Wilhelm et al., 2011) for a recent detailed review of these). hCMEC/D3s co-cultured with astrocytes have been grown in shear-stress conditions and showed an *in vivo* TEER of 1000 ohm.cm^2 , which dropped to 70 when the same cells were grown on transwell filter inserts in static situations suggesting the shear-stress has greater impact on TEER than astrocytes and pericytes (Cucullo et al., 2008). The reasons for this improved TEER due to shear stress are not clear, but it is known that shear stress induces a variety of metabolic changes in cells, particularly with regards to aerobic metabolism via the improved access to oxygen in the flow model when compared to the static transwell filter inserts (Cucullo et al., 2008). This dynamic flow model remains the most accurate *in vitro* BBB system available for researchers, but the logistical and economical constraints of some labs as well as limited expertise of this model mean many researchers rely on the transwell filter system to generate their data. It is very important to point out however that TEER values are not always reflective of molecular/large drug permeability. It has previously been shown that a TEER above 120-130 ohm.cm^2 does not reduce permeability to 4kDa FITC-Dex (Gaillard and de Boer, 2000, Wilhelm et al., 2011), but as many drugs are below this size, they are still likely to be susceptible to the leaky hCMEC/D3 paracellular route.

With regard to the CAA studies, the glycocalyx was not taken into consideration during this study. The glycocalyx is the layer of extracellular polymeric material on cells and bacterium that has a variety of functions such a protective qualities to acids and immune molecules (Erlandsen et al., 2004). It has been shown to form on cultured endothelial cells (Ebong et al., 2011) and it is known to attract cationic molecules – indeed these are used as dyes to stain it for photographic purposes (Erlandsen et al., 2004). Therefore, if the cationic radiolabelled ADMA and L-arginine were entering the cell or just sticking to it remains unknown. If the hCMEC/D3s have a glycocalyx has not been demonstrated, but it seems plausible as other vascular endothelium have been shown *in vitro* to express it (Ebong et al., 2011). It is important that we used [^{14}C]sucrose as a correction factor for non-specific binding however, as it carries no charge, we cannot rule out the possibility we were measuring extracellular values along with intracellular ones.

8.5. Closing comments

The basic science approach of this thesis was designed to uncover the first evidence of novel interactions between clinically relevant endogenous (ADMA) and exogenous molecules (eflornithine and nifurtimox) and the human blood-brain barrier. In that respect we have provided much novel data that could direct future research in these areas. However, for future work in this field it is important that research funding into this area does not stop. This is a particularly pertinent issue as the population ages and an increase in neurodegenerative diseases are increasingly common. There is still no 'perfect' human BBB *in vitro* model, but optimisation of the hCMEC/D3s with shear-stress and co-culture systems remain the best method of research available before better models can be generated. The advance of medical imaging techniques such as MRI is also allowing researchers to gain non-invasive insight into the workings of the BBB *in vivo* and it seems likely that techniques such as these will only help to improve the understanding of the BBB and its role in disease.

References

ABBOTT, N. J. 2002. Astrocyte-endothelial interactions and blood-brain barrier permeability. *J Anat,* 200**,** 629-38.

ABBOTT, N. J., PATABENDIGE, A. A., DOLMAN, D. E., YUSOF, S. R. & BEGLEY, D. J. 2010. Structure and function of the blood-brain barrier. *Neurobiol Dis,* 37**,** 13-25.

ABBOTT, N. J., RONNBACK, L. & HANSSON, E. 2006. Astrocyte-endothelial interactions at the blood-brain barrier. *Nat Rev Neurosci,* 7**,** 41-53.

ABDELMAGID, S. A., RICKARD, J. A., MCDONALD, W. J., THOMAS, L. N. & TOO, C. K. 2011. CAT-1-mediated arginine uptake and regulation of nitric oxide synthases for the survival of human breast cancer cell lines. *J Cell Biochem,* 112**,** 1084-92.

ACHAN, V., BROADHEAD, M., MALAKI, M., WHITLEY, G., LEIPER, J., MACALLISTER, R. & VALLANCE, P. 2003. Asymmetric dimethylarginine causes hypertension and cardiac dysfunction in humans and is actively metabolized by dimethylarginine dimethylaminohydrolase. *Arterioscler Thromb Vasc Biol,* 23**,** 1455-9.

ADAMS, M. R., MCCREDIE, R., JESSUP, W., ROBINSON, J., SULLIVAN, D. & CELERMAJER, D. S. 1997. Oral L-arginine improves endothelium-dependent dilatation and reduces monocyte adhesion to endothelial cells in young men with coronary artery disease. *Atherosclerosis,* 129**,** 261-9.

ALAVIJEH, M. S., CHISHTY, M., QAISER, M. Z. & PALMER, A. M. 2005. Drug metabolism and pharmacokinetics, the blood-brain barrier, and central nervous system drug discovery. *NeuroRx,* 2**,** 554-71.

ALBERTS, B., BRAY, D., LEWIS, J., RAFF, M., ROBERTS, K. & WATSON., J. D. 1994. *Molecular Biology Of The Cell*, 3rd edition. Chapter 11**,** 508-525.

ALBRITTON, L. M., KIM, J. W., TSENG, L. & CUNNINGHAM, J. M. 1993. Envelope-binding domain in the cationic amino acid transporter determines the host range of ecotropic murine retroviruses. *J Virol,* 67**,** 2091-6.

ALDERTON, W. K., COOPER, C. E. & KNOWLES, R. G. 2001. Nitric oxide synthases: structure, function and inhibition. *Biochem J,* 357**,** 593-615.

ANDERSON, C. M., GANAPATHY, V. & THWAITES, D. T. 2008. Human solute carrier SLC6A14 is the beta-alanine carrier. *J Physiol,* 586**,** 4061-7.

ANDERSSOHN, M., SCHWEDHELM, E., LUNEBURG, N., VASAN, R. S. & BOGER, R. H. 2010. Asymmetric dimethylarginine as a mediator of vascular dysfunction and a marker of cardiovascular disease and mortality: an intriguing interaction with diabetes mellitus. *Diab Vasc Dis Res,* 7**,** 105-18.

ANDERSTAM, B., KATZARSKI, K. & BERGSTROM, J. 1997. Serum levels of NG, NG-dimethyl-L-arginine, a potential endogenous nitric oxide inhibitor in dialysis patients. *J Am Soc Nephrol,* 8**,** 1437-42.

ARLT, S., SCHULZE, F., EICHENLAUB, M., MAAS, R., LEHMBECK, J. T., SCHWEDHELM, E., JAHN, H. & BOGER, R. H. 2008. Asymmetrical dimethylarginine is increased in plasma and decreased in cerebrospinal fluid of patients with Alzheimer's disease. *Dement Geriatr Cogn Disord,* 26**,** 58-64.

ARMULIK, A., GENOVE, G. & BETSHOLTZ, C. 2011. Pericytes: developmental, physiological, and pathological perspectives, problems, and promises. *Dev Cell,* 21**,** 193-215.

ARMULIK, A., GENOVE, G., MAE, M., NISANCIOGLU, M. H., WALLGARD, E., NIAUDET, C., HE, L., NORLIN, J., LINDBLOM, P., STRITTMATTER, K., JOHANSSON, B. R. & BETSHOLTZ, C. 2010. Pericytes regulate the blood-brain barrier. *Nature,* 468**,** 557-61.

ATTWELL, D., BUCHAN, A. M., CHARPAK, S., LAURITZEN, M., MACVICAR, B. A. & NEWMAN, E. A. 2010. Glial and neuronal control of brain blood flow. *Nature,* 468**,** 232-43.

BAE, S. W., STUHLINGER, M. C., YOO, H. S., YU, K. H., PARK, H. K., CHOI, B. Y., LEE, Y. S., PACHINGER, O., CHOI, Y. H., LEE, S. H. & PARK, J. E. 2005. Plasma asymmetric dimethylarginine concentrations in newly diagnosed patients with acute myocardial infarction or unstable angina pectoris during two weeks of medical treatment. *Am J Cardiol,* 95**,** 729-33.

BAKER, N., ALSFORD, S. & HORN, D. 2011. Genome-wide RNAi screens in African trypanosomes identify the nifurtimox activator NTR and the eflornithine transporter AAT6. *Mol Biochem Parasitol,* 176**,** 55-7.

BALABANOV, R. & DORE-DUFFY, P. 1998. Role of the CNS microvascular pericyte in the blood-brain barrier. *J Neurosci Res,* 53**,** 637-44.

BALASEGARAM, M., HARRIS, S., CHECCHI, F., GHORASHIAN, S., HAMEL, C. & KARUNAKARA, U. 2005. Melarsoprol versus eflornithine for treating late-stage Gambian trypanosomiasis in the Republic of the Congo. *Bulletin of the World Health Organization,* 84**,** 765-840

BALASEGARAM, M., HARRIS, S., CHECCHI, F., GHORASHIAN, S., HAMEL, C. & KARUNAKARA, U. 2006. Melarsoprol versus eflornithine for treating late-stage Gambian trypanosomiasis in the Republic of the Congo. *Bull World Health Organ,* 84**,** 783-91.

BALASEGARAM, M., YOUNG, H., CHAPPUIS, F., PRIOTTO, G., RAGUENAUD, M. E. & CHECCHI, F. 2009. Effectiveness of melarsoprol and eflornithine as first-line regimens for gambiense sleeping sickness in nine Medecins Sans Frontieres programmes. *Trans R Soc Trop Med Hyg,* 103**,** 280-90.

BANKS, W. A. 2008. Developing drugs that can cross the blood-brain barrier: applications to Alzheimer's disease. *BMC Neurosci,* 9 Suppl 3**,** S2.

BARBUL, A. 1986. Arginine: biochemistry, physiology, and therapeutic implications. *JPEN J Parenter Enteral Nutr,* 10**,** 227-38.

BARRETT, M. P., BOYKIN, D. W., BRUN, R. & TIDWELL, R. R. 2007. Human African trypanosomiasis: pharmacological re-engagement with a neglected disease. *Br J Pharmacol,* 152**,** 1155-71.

BASSELIN, M., BADET-DENISOT, M. A., LAWRENCE, F. & ROBERT-GERO, M. 1997. Effects of pentamidine on polyamine level and biosynthesis in wild-type, pentamidine-treated, and pentamidine-resistant Leishmania. *Exp Parasitol,* 85**,** 274-82.

BAYDOUN, A. R., BOGLE, R. G., PEARSON, J. D. & MANN, G. E. 1994. Discrimination between citrulline and arginine transport in activated murine macrophages: inefficient synthesis of NO from recycling of citrulline to arginine. *Br J Pharmacol,* 112**,** 487-92.

BAZZONI, G. 2003. The JAM family of junctional adhesion molecules. *Curr Opin Cell Biol,* 15**,** 525-30.

BECHMANN, I., GALEA, I. & PERRY, V. H. 2007. What is the blood-brain barrier (not)? *Trends Immunol,* 28**,** 5-11.

BEDFORD, M. T. & RICHARD, S. 2005. Arginine methylation an emerging regulator of protein function. *Mol Cell,* 18**,** 263-72.

BEGLEY, D. J. 2004. ABC transporters and the blood-brain barrier. *Curr Pharm Des,* 10**,** 1295-312.

BELLOFATTO, V., FAIRLAMB, A. H., HENDERSON, G. B. & CROSS, G. A. 1987. Biochemical changes associated with alpha-difluoromethylornithine uptake and resistance in Trypanosoma brucei. *Mol Biochem Parasitol,* 25**,** 227-38.

BENAIM, G., LOPEZ-ESTRANO, C., DOCAMPO, R. & MORENO, S. N. 1993. A calmodulin-stimulated Ca2+ pump in plasma-membrane vesicles from Trypanosoma brucei; selective inhibition by pentamidine. *Biochem J,* 296 (Pt 3)**,** 759-63.

BENZ, P. M., BLUME, C., MOEBIUS, J., OSCHATZ, C., SCHUH, K., SICKMANN, A., WALTER, U., FELLER, S. M. & RENNE, T. 2008. Cytoskeleton assembly at endothelial cell-cell contacts is regulated by alphaII-spectrin-VASP complexes. *J Cell Biol,* 180**,** 205-19.

BEREZOWSKI, V., MIECZ, D., MARSZALEK, M., BROER, A., BROER, S., CECCHELLI, R. & NALECZ, K. A. 2004. Involvement of OCTN2 and B0,+ in the transport of carnitine through an in vitro model of the blood-brain barrier. *J Neurochem,* 91**,** 860-72.

BERNACKI, J., DOBROWOLSKA, A., NIERWINSKA, K. & MALECKI, A. 2008. Physiology and pharmacological role of the blood-brain barrier. *Pharmacol Rep,* 60**,** 600-22.

BESLER, C., HEINRICH, K., MAKRIDES, V., RIWANTO, M., STEIN, S., VERREY, F., LUSCHER, T. & LANDMESSER, U. 2010. HDL Stimulates Endothelial CAT-1 Expression and L-Arginine Uptake: A Novel Mechanism Leading to Endothelial-Protective Effects of HDL That is Profoundly Altered in Patients With Coronary Disease. *Circulation,* 122:A19862.

BHARDWAJ, A., NORTHINGTON, F. J., CARHUAPOMA, J. R., FALCK, J. R., HARDER, D. R., TRAYSTMAN, R. J. & KOEHLER, R. C. 2000. P-450 epoxygenase and NO synthase inhibitors reduce cerebral blood flow response to N-methyl-D-aspartate. *Am J Physiol Heart Circ Physiol,* 279**,** H1616-24.

BISSER, S., N'SIESI, F. X., LEJON, V., PREUX, P. M., VAN NIEUWENHOVE, S., MIAKA MIA BILENGE, C. & BUSCHER, P. 2007. Equivalence trial of melarsoprol and nifurtimox monotherapy and combination therapy for the treatment of second-stage Trypanosoma brucei gambiense sleeping sickness. *J Infect Dis,* 195**,** 322-9.

BODE-BOGER, S. M., SCALERA, F. & IGNARRO, L. J. 2007. The L-arginine paradox: Importance of the L-arginine/asymmetrical dimethylarginine ratio. *Pharmacol Ther,* 114**,** 295-306.

BOGER, R. H. 2003. The emerging role of asymmetric dimethylarginine as a novel cardiovascular risk factor. *Cardiovasc Res,* 59**,** 824-33.

BOGER, R. H. 2004. Asymmetric dimethylarginine, an endogenous inhibitor of nitric oxide synthase, explains the "L-arginine paradox" and acts as a novel cardiovascular risk factor. *J Nutr,* 134**,** 2842S-2847S; discussion 2853S.

BOGER, R. H. 2007. The pharmacodynamics of L-arginine. *J Nutr,* 137**,** 1650S-1655S.

BOGER, R. H., BODE-BOGER, S. M., SZUBA, A., TSAO, P. S., CHAN, J. R., TANGPHAO, O., BLASCHKE, T. F. & COOKE, J. P. 1998. Asymmetric dimethylarginine (ADMA): a novel risk factor for endothelial dysfunction: its role in hypercholesterolemia. *Circulation,* 98**,** 1842-7.

BOGER, R. H. & RON, E. S. 2005. L-Arginine improves vascular function by overcoming deleterious effects of ADMA, a novel cardiovascular risk factor. *Altern Med Rev,* 10**,** 14-23.

BOGER, R. H., SYDOW, K., BORLAK, J., THUM, T., LENZEN, H., SCHUBERT, B., TSIKAS, D. & BODE-BOGER, S. M. 2000. LDL cholesterol upregulates synthesis of asymmetrical dimethylarginine in human endothelial cells: involvement of S-adenosylmethionine-dependent methyltransferases. *Circ Res,* 87**,** 99-105.

BOGLE, R. G., MACALLISTER, R. J., WHITLEY, G. S. & VALLANCE, P. 1995. Induction of NG-monomethyl-L-arginine uptake: a mechanism for differential inhibition of NO synthases? *Am J Physiol,* 269**,** C750-6.

BORST, P., EVERS, R., KOOL, M. & WIJNHOLDS, J. 2000. A family of drug transporters: the multidrug resistance-associated proteins. *J Natl Cancer Inst,* 92**,** 1295-302.

BOUTEILLE, B., OUKEM, O., BISSER, S. & DUMAS, M. 2003. Treatment perspectives for human African trypanosomiasis. *Fundam Clin Pharmacol,* 17**,** 171-81.

BROER, A., WAGNER, C. A., LANG, F. & BROER, S. 2000. The heterodimeric amino acid transporter 4F2hc/y+LAT2 mediates arginine efflux in exchange with glutamine. *Biochem J,* 349 Pt 3**,** 787-95.

BROER, S. 2008. Amino acid transport across mammalian intestinal and renal epithelia. *Physiol Rev,* 88**,** 249-86.

BROUNS, R., MARESCAU, B., POSSEMIERS, I., SHEORAJPANDAY, R. & DE DEYN, P. P. 2009. Dimethylarginine levels in cerebrospinal fluid of hyperacute ischemic stroke patients are associated with stroke severity. *Neurochem Res,* 34**,** 1642-9.

BRUGGEMANN, E. P., GERMANN, U. A., GOTTESMAN, M. M. & PASTAN, I. 1989. Two different regions of P-glycoprotein [corrected] are photoaffinity-labeled by azidopine. *J Biol Chem,* 264**,** 15483-8.

BRUN, R., BLUM, J., CHAPPUIS, F. & BURRI, C. 2010. Human African trypanosomiasis. *Lancet,* 375**,** 148-59.

BULAU, P., ZAKRZEWICZ, D., KITOWSKA, K., LEIPER, J., GUNTHER, A., GRIMMINGER, F. & EICKELBERG, O. 2007. Analysis of methylarginine metabolism in the cardiovascular system identifies the lung as a major source of ADMA. *Am J Physiol Lung Cell Mol Physiol,* 292**,** L18-24.

BURNETT, A. L. 1995. Nitric oxide control of lower genitourinary tract functions: a review. *Urology,* 45**,** 1071-83.

BURRI, C. & BRUN, R. 2003. Eflornithine for the treatment of human African trypanosomiasis. *Parasitol Res,* 90 Supp 1**,** S49-52.

CALABRESE, V., MANCUSO, C., CALVANI, M., RIZZARELLI, E., BUTTERFIELD, D. A. & STELLA, A. M. 2007. Nitric oxide in the central nervous system: neuroprotection versus neurotoxicity. *Nat Rev Neurosci,* 8**,** 766-75.

CAMPBELL, N. & REECE, J. 2002. Biology Sixth Edition. Chapter 41, page 853.

CARDOUNEL, A. J., CUI, H., SAMOUILOV, A., JOHNSON, W., KEARNS, P., TSAI, A. L., BERKA, V. & ZWEIER, J. L. 2007. Evidence for the pathophysiological role of endogenous methylarginines in regulation of endothelial NO production and vascular function. *J Biol Chem,* 282**,** 879-87.

CARDOUNEL, A. J. & ZWEIER, J. L. 2002. Endogenous methylarginines regulate neuronal nitric-oxide synthase and prevent excitotoxic injury. *J Biol Chem,* 277**,** 33995-4002.

CARL, S. M., LINDLEY, D. J., COURAUD, P. O., WEKSLER, B. B., ROMERO, I., MOWERY, S. A. & KNIPP, G. T. 2010. ABC and SLC transporter expression and pot substrate characterization across the human CMEC/D3 blood-brain barrier cell line. *Mol Pharm,* 7**,** 1057-68.

CECCHELLI, R., BEREZOWSKI, V., LUNDQUIST, S., CULOT, M., RENFTEL, M., DEHOUCK, M. P. & FENART, L. 2007. Modelling of the blood-brain barrier in drug discovery and development. *Nat Rev Drug Discov,* 6**,** 650-61.

CECCHELLI, R., DEHOUCK, B., DESCAMPS, L., FENART, L., BUEE-SCHERRER, V. V., DUHEM, C., LUNDQUIST, S., RENTFEL, M., TORPIER, G. & DEHOUCK, M. P. 1999. In vitro model for evaluating drug transport across the blood-brain barrier. *Adv Drug Deliv Rev,* 36**,** 165-178.

CHAPPUIS, F., PITTET, A., BOVIER, P. A., ADAMS, K., GODINEAU, V., HWANG, S. Y., MAGNUS, E. & BUSCHER, P. 2002. Field evaluation of the CATT/Trypanosoma brucei gambiense on blood-impregnated filter papers for diagnosis of human African trypanosomiasis in southern Sudan. *Trop Med Int Health,* 7**,** 942-8.

CHECCHI, F., FILIPE, J. A., HAYDON, D. T., CHANDRAMOHAN, D. & CHAPPUIS, F. 2008. Estimates of the duration of the early and late stage of gambiense sleeping sickness. *BMC Infect Dis,* 8**,** 16.

CHECCHI, F., PIOLA, P., AYIKORU, H., THOMAS, F., LEGROS, D. & PRIOTTO, G. 2007. Nifurtimox plus Eflornithine for late-stage sleeping sickness in Uganda: a case series. *PLoS Negl Trop Dis,* 1**,** e64.

CHEN, C. A., DRUHAN, L. J., VARADHARAJ, S., CHEN, Y. R. & ZWEIER, J. L. 2008. Phosphorylation of endothelial nitric-oxide synthase regulates superoxide generation from the enzyme. *J Biol Chem,* 283**,** 27038-47.

CHEN, Y., XU, X., SHENG, M., ZHANG, X., GU, Q. & ZHENG, Z. 2009. PRMT-1 and DDAHs-induced ADMA upregulation is involved in ROS- and RAS-mediated diabetic retinopathy. *Exp Eye Res,* 89**,** 1028-34.

CHEN, Y. H., XU, X., SHENG, M. J., ZHENG, Z. & GU, Q. 2011. Effects of asymmetric dimethylarginine on bovine retinal capillary endothelial cell proliferation, reactive oxygen species production, permeability, intercellular adhesion molecule-1, and occludin expression. *Mol Vis,* 17**,** 332-40.

CHEN, Z. S. & TIWARI, A. K. 2011. Multidrug resistance proteins (MRPs/ABCCs) in cancer chemotherapy and genetic diseases. *FEBS J,* 278**,** 3226-45.

CHISHTY, M., BEGLEY, D. J., ABBOTT, N. J. & REICHEL, A. 2004. Interaction of nucleoside analogues with nucleoside transporters in rat brain endothelial cells. *J Drug Target,* 12**,** 265-72.

CHRISSOBOLIS, S., MILLER, A. A., DRUMMOND, G. R., KEMP-HARPER, B. K. & SOBEY, C. G. 2011. Oxidative stress and endothelial dysfunction in cerebrovascular disease. *Front Biosci,* 16**,** 1733-45.

CHRISTENSEN, H. N. & ANTONIOLI, J. A. 1969. Cationic amino acid transport in the rabbit reticulocyte. Na+-dependent inhibition of Na+-independent transport. *J Biol Chem,* 244**,** 1497-504.

CHRISTENSEN, H. N. & HANDLOGTEN, M. E. 1969. Reactions of neutral amino acids plus Na(+) with a cationic amino acid transport system. *FEBS Lett,* 3**,** 14-17.

CHRISTENSEN, H. N., HANDLOGTEN, M. E. & THOMAS, E. L. 1969. Na plus-facilitated reactions of neutral amino acids with a cationic amino acid transport system. *Proc Natl Acad Sci U S A,* 63**,** 948-55.

CISTERNINO, S., MERCIER, C., BOURASSET, F., ROUX, F. & SCHERRMANN, J. M. 2004. Expression, up-regulation, and transport activity of the multidrug-resistance protein Abcg2 at the mouse blood-brain barrier. *Cancer Res,* 64**,** 3296-301.

CLARKSON, A. B., JR., BIENEN, E. J., BACCHI, C. J., MCCANN, P. P., NATHAN, H. C., HUTNER, S. H. & SJOERDSMA, A. 1984. New drug combination for experimental late-stage African trypanosomiasis: DL-alpha-difluoromethylornithine (DFMO) with suramin. *Am J Trop Med Hyg,* 33**,** 1073-7.

CLARKSON, P., ADAMS, M. R., POWE, A. J., DONALD, A. E., MCCREDIE, R., ROBINSON, J., MCCARTHY, S. N., KEECH, A., CELERMAJER, D. S. & DEANFIELD, J. E. 1996. Oral L-arginine improves endothelium-dependent dilation in hypercholesterolemic young adults. *J Clin Invest,* 97**,** 1989-94.

CLOSS, E. I., ALBRITTON, L. M., KIM, J. W. & CUNNINGHAM, J. M. 1993. Identification of a low affinity, high capacity transporter of cationic amino acids in mouse liver. *J Biol Chem,* 268**,** 7538-44.

CLOSS, E. I., BASHA, F. Z., HABERMEIER, A. & FORSTERMANN, U. 1997a. Interference of L-arginine analogues with L-arginine transport mediated by the y+ carrier hCAT-2B. *Nitric Oxide,* 1**,** 65-73.

CLOSS, E. I., BOISSEL, J. P., HABERMEIER, A. & ROTMANN, A. 2006. Structure and function of cationic amino acid transporters (CATs). *J Membr Biol,* 213**,** 67-77.

CLOSS, E. I., GRAF, P., HABERMEIER, A., CUNNINGHAM, J. M. & FORSTERMANN, U. 1997b. Human cationic amino acid transporters hCAT-1, hCAT-2A, and hCAT-2B: three related carriers with distinct transport properties. *Biochemistry,* 36**,** 6462-8.

CLOSS, E. I., SCHELD, J. S., SHARAFI, M. & FORSTERMANN, U. 2000. Substrate supply for nitric-oxide synthase in macrophages and endothelial cells: role of cationic amino acid transporters. *Mol Pharmacol,* 57**,** 68-74.

CLOSS, E. I., SIMON, A., VEKONY, N. & ROTMANN, A. 2004. Plasma membrane transporters for arginine. *J Nutr,* 134**,** 2752S-2759S; discussion 2765S-2767S.

COMERFORD, K. M., LAWRENCE, D. W., SYNNESTVEDT, K., LEVI, B. P. & COLGAN, S. P. 2002. Role of vasodilator-stimulated phosphoprotein in PKA-induced changes in endothelial junctional permeability. *FASEB J,* 16**,** 583-5.

COORAY, H. C., BLACKMORE, C. G., MASKELL, L. & BARRAND, M. A. 2002. Localisation of breast cancer resistance protein in microvessel endothelium of human brain. *Neuroreport,* 13**,** 2059-63.

CORDON-CARDO, C., O'BRIEN, J. P., CASALS, D., RITTMAN-GRAUER, L., BIEDLER, J. L., MELAMED, M. R. & BERTINO, J. R. 1989. Multidrug-resistance gene (P-glycoprotein) is expressed by endothelial cells at blood-brain barrier sites. *Proc Natl Acad Sci U S A,* 86**,** 695-8.

CREAGER, M. A., GALLAGHER, S. J., GIRERD, X. J., COLEMAN, S. M., DZAU, V. J. & COOKE, J. P. 1992. L-arginine improves endothelium-dependent vasodilation in hypercholesterolemic humans. *J Clin Invest,* 90**,** 1248-53.

CUCULLO, L., COURAUD, P. O., WEKSLER, B., ROMERO, I. A., HOSSAIN, M., RAPP, E. & JANIGRO, D. 2008. Immortalized human brain endothelial cells and flow-based vascular modeling: a marriage of convenience for rational neurovascular studies. *J Cereb Blood Flow Metab,* 28**,** 312-28.

CULOTTA, E. & KOSHLAND, D. E., JR. 1992. NO news is good news. *Science,* 258**,** 1862-5.

CZEREDYS, M., MYSIOREK, C., KULIKOVA, N., SAMLUK, L., BEREZOWSKI, V., CECCHELLI, R. & NALECZ, K. A. 2008. A polarized localization of amino acid/carnitine transporter B(0,+) (ATB(0,+)) in the blood-brain barrier. *Biochem Biophys Res Commun,* 376**,** 267-70.

DAHLIN, A., ROYALL, J., HOHMANN, J. G. & WANG, J. 2009. Expression profiling of the solute carrier gene family in the mouse brain. *J Pharmacol Exp Ther,* 329**,** 558-70.

DAMPER, D. & PATTON, C. L. 1976a. Pentamidine transport and sensitivity in brucei-group trypanosomes. *J Protozool,* 23**,** 349-56.

DAMPER, D. & PATTON, C. L. 1976b. Pentamidine transport in Trypanosoma brucei-kinetics and specificity. *Biochem Pharmacol,* 25**,** 271-6.

DANEMAN, R., ZHOU, L., KEBEDE, A. A. & BARRES, B. A. 2010. Pericytes are required for blood-brain barrier integrity during embryogenesis. *Nature,* 468**,** 562-6.

DANIEWSKA-MICHALSKA, D., MOTYL, T., GELLERT, R., KUKULSKA, W., PODGURNIAK, M., OPECHOWSKA-PACOCHA, E. & OSTROWSKI, K. 1993. Efficiency of hemodialysis of pyrimidine compounds in patients with chronic renal failure. *Nephron,* 64**,** 193-7.

DAUCHY, S., MILLER, F., COURAUD, P. O., WEAVER, R. J., WEKSLER, B., ROMERO, I. A., SCHERRMANN, J. M., DE WAZIERS, I. & DECLEVES, X. 2009. Expression and transcriptional regulation of ABC transporters and cytochromes P450 in hCMEC/D3 human cerebral microvascular endothelial cells. *Biochem Pharmacol,* 77**,** 897-909.

DAVIDS, M., RICHIR, M. C., VISSER, M., ELLGER, B., VAN DEN BERGHE, G., VAN LEEUWEN, P. A. & TEERLINK, T. 2011. Role of dimethylarginine dimethylaminohydrolase activity in regulation of tissue and plasma concentrations of asymmetric dimethylarginine in an animal model of prolonged critical illness. *Metabolism*.

DAVSON, H. & OLDENDORF, W. H. 1967. Symposium on membrane transport. Transport in the central nervous system. *Proc R Soc Med,* 60**,** 326-9.

DAYOUB, H., RODIONOV, R. N., LYNCH, C., COOKE, J. P., ARNING, E., BOTTIGLIERI, T., LENTZ, S. R. & FARACI, F. M. 2008. Overexpression of dimethylarginine dimethylaminohydrolase

inhibits asymmetric dimethylarginine-induced endothelial dysfunction in the cerebral circulation. *Stroke,* 39**,** 180-4.

DE KONING, H. P. 2001. Transporters in African trypanosomes: role in drug action and resistance. *Int J Parasitol,* 31**,** 512-22.

DEELEY, R. G., WESTLAKE, C. & COLE, S. P. 2006. Transmembrane transport of endo- and xenobiotics by mammalian ATP-binding cassette multidrug resistance proteins. *Physiol Rev,* 86**,** 849-99.

DEHOUCK, M. P., JOLLIET-RIANT, P., BREE, F., FRUCHART, J. C., CECCHELLI, R. & TILLEMENT, J. P. 1992. Drug transfer across the blood-brain barrier: correlation between in vitro and in vivo models. *J Neurochem,* 58**,** 1790-7.

DEHOUCK, M. P., MERESSE, S., DELORME, P., FRUCHART, J. C. & CECCHELLI, R. 1990. An easier, reproducible, and mass-production method to study the blood-brain barrier in vitro. *J Neurochem,* 54**,** 1798-801.

DEJANA, E. 2004. Endothelial cell-cell junctions: happy together. *Nat Rev Mol Cell Biol,* 5**,** 261-70.

DEJANA, E., ORSENIGO, F. & LAMPUGNANI, M. G. 2008. The role of adherens junctions and VE-cadherin in the control of vascular permeability. *J Cell Sci,* 121**,** 2115-22.

DEMEULE, M., REGINA, A., JODOIN, J., LAPLANTE, A., DAGENAIS, C., BERTHELET, F., MOGHRABI, A. & BELIVEAU, R. 2002. Drug transport to the brain: key roles for the efflux pump P-glycoprotein in the blood-brain barrier. *Vascul Pharmacol,* 38**,** 339-48.

DENIZOT, F. & LANG, R. 1986. Rapid colorimetric assay for cell growth and survival. Modifications to the tetrazolium dye procedure giving improved sensitivity and reliability. *J Immunol Methods,* 89**,** 271-7.

DESCAMPS, L., DEHOUCK, M. P., TORPIER, G. & CECCHELLI, R. 1996. Receptor-mediated transcytosis of transferrin through blood-brain barrier endothelial cells. *Am J Physiol,* 270**,** H1149-58.

DEVES, R., ANGELO, S. & ROJAS, A. M. 1998. System y+L: the broad scope and cation modulated amino acid transporter. *Exp Physiol,* 83**,** 211-20.

DEVES, R. & BOYD, C. A. 1998. Transporters for cationic amino acids in animal cells: discovery, structure, and function. *Physiol Rev,* 78**,** 487-545.

DEVES, R., CHAVEZ, P. & BOYD, C. A. 1992. Identification of a new transport system (y+L) in human erythrocytes that recognizes lysine and leucine with high affinity. *J Physiol,* 454**,** 491-501.

DOCAMPO, R. & MORENO, S. N. 2003. Current chemotherapy of human African trypanosomiasis. *Parasitol Res,* 90 Supp 1**,** S10-3.

DONELSON, J. E., HILL, K. L. & EL-SAYED, N. M. 1998. Multiple mechanisms of immune evasion by African trypanosomes. *Mol Biochem Parasitol,* 91**,** 51-66.

DOYLE, L. A., YANG, W., ABRUZZO, L. V., KROGMANN, T., GAO, Y., RISHI, A. K. & ROSS, D. D. 1998. A multidrug resistance transporter from human MCF-7 breast cancer cells. *Proc Natl Acad Sci U S A,* 95**,** 15665-70.

DRUHAN, L. J., FORBES, S. P., POPE, A. J., CHEN, C. A., ZWEIER, J. L. & CARDOUNEL, A. J. 2008. Regulation of eNOS-derived superoxide by endogenous methylarginines. *Biochemistry,* 47**,** 7256-63.

DUVERNOY, H. M. & RISOLD, P. Y. 2007. The circumventricular organs: an atlas of comparative anatomy and vascularization. *Brain Res Rev,* 56**,** 119-47.

EBONG, E. E., MACALUSO, F. P., SPRAY, D. C. & TARBELL, J. M. 2011. Imaging the endothelial glycocalyx in vitro by rapid freezing/freeze substitution transmission electron microscopy. *Arterioscler Thromb Vasc Biol,* 31**,** 1908-15.

ELAHIAN, F., KALALINIA, F. & BEHRAVAN, J. 2010. Evaluation of indomethacin and dexamethasone effects on BCRP-mediated drug resistance in MCF-7 parental and resistant cell lines. *Drug Chem Toxicol,* 33**,** 113-9.

ENANGA, B., KEITA, M., CHAUVIERE, G., DUMAS, M. & BOUTEILLE, B. 1998. Megazol combined with suramin: a chemotherapy regimen which reversed the CNS pathology in a model of human African trypanosomiasis in mice. *Trop Med Int Health,* 3**,** 736-41.

ENGELHARDT, B. & COISNE, C. 2011. Fluids and barriers of the CNS establish immune privilege by confining immune surveillance to a two-walled castle moat surrounding the CNS castle. *Fluids Barriers CNS,* 8**,** 4.

ENNIS, S. R. & BETZ, A. L. 1986. Sucrose permeability of the blood-retinal and blood-brain barriers. Effects of diabetes, hypertonicity, and iodate. *Invest Ophthalmol Vis Sci,* 27**,** 1095-102.

EREZ, A., NAGAMANI, S. C., SHCHELOCHKOV, O. A., PREMKUMAR, M. H., CAMPEAU, P. M., CHEN, Y., GARG, H. K., LI, L., MIAN, A., BERTIN, T. K., BLACK, J. O., ZENG, H., TANG, Y., REDDY, A. K., SUMMAR, M., O'BRIEN, W. E., HARRISON, D. G., MITCH, W. E., MARINI, J. C., ASCHNER, J. L., BRYAN, N. S. & LEE, B. 2011. Requirement of argininosuccinate lyase for systemic nitric oxide production. *Nat Med*.

ERICKSON, K. K., SUNDSTROM, J. M. & ANTONETTI, D. A. 2007. Vascular permeability in ocular disease and the role of tight junctions. *Angiogenesis,* 10**,** 103-17.

ERLANDSEN, S. L., KRISTICH, C. J., DUNNY, G. M. & WELLS, C. L. 2004. High-resolution visualization of the microbial glycocalyx with low-voltage scanning electron microscopy: dependence on cationic dyes. *J Histochem Cytochem,* 52**,** 1427-35.

ESTEVEZ, R., CAMPS, M., ROJAS, A. M., TESTAR, X., DEVES, R., HEDIGER, M. A., ZORZANO, A. & PALACIN, M. 1998. The amino acid transport system y+L/4F2hc is a heteromultimeric complex. *FASEB J,* 12**,** 1319-29.

EUGENIN, E. A., CLEMENTS, J. E., ZINK, M. C. & BERMAN, J. W. 2011. Human immunodeficiency virus infection of human astrocytes disrupts blood-brain barrier integrity by a gap junction-dependent mechanism. *J Neurosci,* 31**,** 9456-65.

EYAL, S., HSIAO, P. & UNADKAT, J. D. 2009. Drug interactions at the blood-brain barrier: fact or fantasy? *Pharmacol Ther,* 123**,** 80-104.

FARACI, F. M., BRIAN, J. E., JR. & HEISTAD, D. D. 1995. Response of cerebral blood vessels to an endogenous inhibitor of nitric oxide synthase. *Am J Physiol,* 269**,** H1522-7.

FARRELL, C. L. & PARDRIDGE, W. M. 1991. Blood-brain barrier glucose transporter is asymmetrically distributed on brain capillary endothelial lumenal and ablumenal membranes: an electron microscopic immunogold study. *Proc Natl Acad Sci U S A,* 88**,** 5779-83.

FASLER-KAN, E., SUENDERHAUF, C., BARTENEVA, N., POLLER, B., GYGAX, D. & HUWYLER, J. 2010. Cytokine signaling in the human brain capillary endothelial cell line hCMEC/D3. *Brain Res,* 1354**,** 15-22.

FEHM, H. L., KERN, W. & PETERS, A. 2006. The selfish brain: competition for energy resources. *Prog Brain Res,* 153**,** 129-40.

FELDMAN, S. & WEIDENFELD, J. 2004. Involvement of endogeneous glutamate in the stimulatory effect of norepinephrine and serotonin on the hypothalamo-pituitary-adrenocortical axis. *Neuroendocrinology,* 79**,** 43-53.

FLAM, B. R., HARTMANN, P. J., HARRELL-BOOTH, M., SOLOMONSON, L. P. & EICHLER, D. C. 2001. Caveolar localization of arginine regeneration enzymes, argininosuccinate synthase, and lyase, with endothelial nitric oxide synthase. *Nitric Oxide,* 5**,** 187-97.

FLETCHER, N. F., WILSON, G. K., MURRAY, J., HU, K., LEWIS, A., REYNOLDS, G. M., STAMATAKI, Z., MEREDITH, L. W., ROWE, I. A., LUO, G., LOPEZ-RAMIREZ, M. A., BAUMERT, T. F.,

WEKSLER, B., COURAUD, P. O., KIM, K. S., ROMERO, I. A., JOPLING, C., MORGELLO, S., BALFE, P. & MCKEATING, J. A. 2011. Hepatitis C Virus Infects the Endothelial Cells of the Blood-Brain Barrier. *Gastroenterology*.

FORBES, S. P., DRUHAN, L. J., GUZMAN, J. E., PARINANDI, N., ZHANG, L., GREEN-CHURCH, K. B. & CARDOUNEL, A. J. 2008. Mechanism of 4-HNE mediated inhibition of hDDAH-1: implications in no regulation. *Biochemistry,* 47**,** 1819-26.

FORSTER, C., BUREK, M., ROMERO, I. A., WEKSLER, B., COURAUD, P. O. & DRENCKHAHN, D. 2008. Differential effects of hydrocortisone and TNFalpha on tight junction proteins in an in vitro model of the human blood-brain barrier. *J Physiol,* 586**,** 1937-49.

FRANK, R. N., DUTTA, S. & MANCINI, M. A. 1987. Pericyte coverage is greater in the retinal than in the cerebral capillaries of the rat. *Invest Ophthalmol Vis Sci,* 28**,** 1086-91.

FURUSE, M., HIRASE, T., ITOH, M., NAGAFUCHI, A., YONEMURA, S. & TSUKITA, S. 1993. Occludin: a novel integral membrane protein localizing at tight junctions. *J Cell Biol,* 123**,** 1777-88.

GAILLARD, P. J. & DE BOER, A. G. 2000. Relationship between permeability status of the blood-brain barrier and in vitro permeability coefficient of a drug. *Eur J Pharm Sci,* 12**,** 95-102.

GANONG, W. F. 2000. Circumventricular organs: definition and role in the regulation of endocrine and autonomic function. *Clin Exp Pharmacol Physiol,* 27**,** 422-7.

GARCIA-BOURNISSEN, F., ALTCHEH, J., PANCHAUD, A. & ITO, S. 2010. Is use of nifurtimox for the treatment of Chagas disease compatible with breast feeding? A population pharmacokinetics analysis. *Arch Dis Child,* 95**,** 224-8.

GARCIA-NOGALES, P., ALMEIDA, A. & BOLANOS, J. P. 2003. Peroxynitrite protects neurons against nitric oxide-mediated apoptosis. A key role for glucose-6-phosphate dehydrogenase activity in neuroprotection. *J Biol Chem,* 278**,** 864-74.

GARTHWAITE, J., CHARLES, S. L. & CHESS-WILLIAMS, R. 1988. Endothelium-derived relaxing factor release on activation of NMDA receptors suggests role as intercellular messenger in the brain. *Nature,* 336**,** 385-8.

GEHRIG, S. & EFFERTH, T. 2008. Development of drug resistance in Trypanosoma brucei rhodesiense and Trypanosoma brucei gambiense. Treatment of human African trypanosomiasis with natural products (Review). *Int J Mol Med,* 22**,** 411-9.

GIACOIA, G. P. 1995. Nitric oxide: a selective pulmonary vasodilator. *South Med J,* 88**,** 33-41.

GIBBS, J. E. & THOMAS, S. A. 2002. The distribution of the anti-HIV drug, 2'3'-dideoxycytidine (ddC), across the blood-brain and blood-cerebrospinal fluid barriers and the influence of organic anion transport inhibitors. *J Neurochem,* 80**,** 392-404.

GIRI, C. P., SHIMA, K., TALL, B. D., CURTIS, S., SATHYAMOORTHY, V., HANISCH, B., KIM, K. S. & KOPECKO, D. J. 2012. Cronobacter spp. (previously Enterobacter sakazakii) invade and translocate across both cultured human intestinal epithelial cells and human brain microvascular endothelial cells. *Microb Pathog,* 52**,** 140-7.

GOMEZ-PINILLA, F. 2008. Brain foods: the effects of nutrients on brain function. *Nat Rev Neurosci,* 9**,** 568-78.

GONNERT, R. & BOCK, M. 1972. The effect of nifurtimox on Trypanosoma cruzi in tissue cultures. *Arzneimittelforschung,* 22**,** 1582-6.

GRAB, D. J. & KENNEDY, P. G. 2008. Traversal of human and animal trypanosomes across the blood-brain barrier. *J Neurovirol,* 14**,** 344-51.

GRILLO, M. A. & COLOMBATTO, S. 2004. Arginine revisited: minireview article. *Amino Acids,* 26**,** 345-51.

GU, X., ZHANG, J., BRANN, D. W. & YU, F. S. 2003. Brain and retinal vascular endothelial cells with extended life span established by ectopic expression of telomerase. *Invest Ophthalmol Vis Sci,* 44**,** 3219-25.

GUIX, F. X., URIBESALGO, I., COMA, M. & MUNOZ, F. J. 2005. The physiology and pathophysiology of nitric oxide in the brain. *Prog Neurobiol,* 76**,** 126-52.

HABERKORN, A. 1979. The effect of nifurtimox on experimental infections with trypanosomatidae other than Trypanosoma cruzi. *Zentralbl Bakteriol Orig A,* 244**,** 331-8.

HABERKORN, A. & GONNERT, R. 1972. Animal experimental investigation into the activity of nifurtimox against Trypanosoma cruzi. *Arzneimittelforschung,* 22**,** 1570-82.

HAEFLIGER, I. O., ZSCHAUER, A. & ANDERSON, D. R. 1994. Relaxation of retinal pericyte contractile tone through the nitric oxide-cyclic guanosine monophosphate pathway. *Invest Ophthalmol Vis Sci,* 35**,** 991-7.

HARIK, S. I., KALARIA, R. N., ANDERSSON, L., LUNDAHL, P. & PERRY, G. 1990. Immunocytochemical localization of the erythroid glucose transporter: abundance in tissues with barrier functions. *J Neurosci,* 10**,** 3862-72.

HASEGAWA, K., WAKINO, S., TANAKA, T., KIMOTO, M., TATEMATSU, S., KANDA, T., YOSHIOKA, K., HOMMA, K., SUGANO, N., KURABAYASHI, M., SARUTA, T. & HAYASHI, K. 2006. Dimethylarginine dimethylaminohydrolase 2 increases vascular endothelial growth factor expression through Sp1 transcription factor in endothelial cells. *Arterioscler Thromb Vasc Biol,* 26**,** 1488-94.

HASELOFF, R. F., BLASIG, I. E., BAUER, H. C. & BAUER, H. 2005. In search of the astrocytic factor(s) modulating blood-brain barrier functions in brain capillary endothelial cells in vitro. *Cell Mol Neurobiol,* 25**,** 25-39.

HATANAKA, T., HARAMURA, M., FEI, Y. J., MIYAUCHI, S., BRIDGES, C. C., GANAPATHY, P. S., SMITH, S. B., GANAPATHY, V. & GANAPATHY, M. E. 2004. Transport of amino acid-based prodrugs by the Na+- and Cl(-) -coupled amino acid transporter ATB0,+ and expression of the transporter in tissues amenable for drug delivery. *J Pharmacol Exp Ther,* 308**,** 1138-47.

HATANAKA, T., NAKANISHI, T., HUANG, W., LEIBACH, F. H., PRASAD, P. D., GANAPATHY, V. & GANAPATHY, M. E. 2001. Na+ - and Cl- -coupled active transport of nitric oxide synthase inhibitors via amino acid transport system B(0,+). *J Clin Invest,* 107**,** 1035-43.

HATHERELL, K., COURAUD, P. O., ROMERO, I. A., WEKSLER, B. & PILKINGTON, G. J. 2011. Development of a three-dimensional, all-human in vitro model of the blood-brain barrier using mono-, co-, and tri-cultivation Transwell models. *J Neurosci Methods,* 199**,** 223-9.

HATZOGLOU, M., FERNANDEZ, J., YAMAN, I. & CLOSS, E. 2004. Regulation of cationic amino acid transport: the story of the CAT-1 transporter. *Annu Rev Nutr,* 24**,** 377-99.

HAWKINS, B. T. & DAVIS, T. P. 2005. The blood-brain barrier/neurovascular unit in health and disease. *Pharmacol Rev,* 57**,** 173-85.

HAWKINS, B. T. & EGLETON, R. D. 2008. Pathophysiology of the blood-brain barrier: animal models and methods. *Curr Top Dev Biol,* 80**,** 277-309.

HAWKINS, R. A., O'KANE, R. L., SIMPSON, I. A. & VINA, J. R. 2006. Structure of the blood-brain barrier and its role in the transport of amino acids. *J Nutr,* 136**,** 218S-26S.

HEALY, D. P. & WILK, S. 1993. Localization of immunoreactive glutamyl aminopeptidase in rat brain. II. Distribution and correlation with angiotensin II. *Brain Res,* 606**,** 295-303.

HEDIGER, M. A., ROMERO, M. F., PENG, J. B., ROLFS, A., TAKANAGA, H. & BRUFORD, E. A. 2004. The ABCs of solute carriers: physiological, pathological and therapeutic implications of human membrane transport proteinsIntroduction. *Pflugers Arch,* 447**,** 465-8.

HERVE, F., GHINEA, N. & SCHERRMANN, J. M. 2008. CNS delivery via adsorptive transcytosis. *AAPS J,* 10**,** 455-72.

HIRANO, T., OOKUBO, K., KASHIWAZAKI, K., TAJIMA, H., YOSHINO, G. & ADACHI, M. 2000. Vascular endothelial markers, von Willebrand factor and thrombomodulin index, are specifically elevated in type 2 diabetic patients with nephropathy: comparison of primary renal disease. *Clin Chim Acta,* 299**,** 65-75.

HOFFMANN, A., BREDNO, J., WENDLAND, M., DERUGIN, N., OHARA, P. & WINTERMARK, M. 2011. High and Low Molecular Weight Fluorescein Isothiocyanate (FITC)-Dextrans to Assess Blood-Brain Barrier Disruption: Technical Considerations. *Transl Stroke Res,* 2**,** 106-111.

HOGLUND, P. J., NORDSTROM, K. J., SCHIOTH, H. B. & FREDRIKSSON, R. 2011. The solute carrier families have a remarkably long evolutionary history with the majority of the human families present before divergence of Bilaterian species. *Mol Biol Evol,* 28**,** 1531-41.

HSUCHOU, H., KASTIN, A. J., TU, H., JOAN ABBOTT, N., COURAUD, P. O. & PAN, W. 2010. Role of astrocytic leptin receptor subtypes on leptin permeation across hCMEC/D3 human brain endothelial cells. *J Neurochem,* 115**,** 1288-98.

HUANG, Y., KANG, B. N., TIAN, J., LIU, Y., LUO, H. R., HESTER, L. & SNYDER, S. H. 2007. The cationic amino acid transporters CAT1 and CAT3 mediate NMDA receptor activation-dependent changes in elaboration of neuronal processes via the mammalian target of rapamycin mTOR pathway. *J Neurosci,* 27**,** 449-58.

HUBER, J. D., EGLETON, R. D. & DAVIS, T. P. 2001. Molecular physiology and pathophysiology of tight junctions in the blood-brain barrier. *Trends Neurosci,* 24**,** 719-25.

IADECOLA, C. 2004. Neurovascular regulation in the normal brain and in Alzheimer's disease. *Nat Rev Neurosci,* 5**,** 347-60.

ITEN, M., METT, H., EVANS, A., ENYARU, J. C., BRUN, R. & KAMINSKY, R. 1997. Alterations in ornithine decarboxylase characteristics account for tolerance of Trypanosoma brucei rhodesiense to D,L-alpha-difluoromethylornithine. *Antimicrob Agents Chemother,* 41**,** 1922-5.

JANIGRO, D., WEST, G. A., NGUYEN, T. S. & WINN, H. R. 1994. Regulation of blood-brain barrier endothelial cells by nitric oxide. *Circ Res,* 75**,** 528-38.

JEGANATHAN, S., SANDERSON, L., DOGRUEL, M., RODGERS, J., CROFT, S. & THOMAS, S. A. 2011. The distribution of nifurtimox across the healthy and trypanosome-infected murine blood-brain and blood-CSF barriers. *J Pharmacol Exp Ther,* 336**,** 506-15.

JENNINGS, F. W. 1993. Combination chemotherapy of CNS trypanosomiasis. *Acta Trop,* 54**,** 205-13.

JENNINGS, F. W., GICHUKI, C. W., KENNEDY, P. G., RODGERS, J., HUNTER, C. A., MURRAY, M. & BURKE, J. M. 1997. The role of the polyamine inhibitor eflornithine in the neuropathogenesis of experimental murine African trypanosomiasis. *Neuropathol Appl Neurobiol,* 23**,** 225-34.

JOHNSON, M. D. & ANDERSON, B. D. 1996. Localization of purine metabolizing enzymes in bovine brain microvessel endothelial cells: an enzymatic blood-brain barrier for dideoxynucleosides? *Pharm Res,* 13**,** 1881-6.

JONES, A. R. & SHUSTA, E. V. 2007. Blood-brain barrier transport of therapeutics via receptor-mediation. *Pharm Res,* 24**,** 1759-71.

KAGEYAMA, T., NAKAMURA, M., MATSUO, A., YAMASAKI, Y., TAKAKURA, Y., HASHIDA, M., KANAI, Y., NAITO, M., TSURUO, T., MINATO, N. & SHIMOHAMA, S. 2000. The 4F2hc/LAT1 complex transports L-DOPA across the blood-brain barrier. *Brain Res,* 879**,** 115-21.

KAJIMOTO, H., KAI, H., AOKI, H., YASUOKA, S., ANEGAWA, T., AOKI, Y., UEDA, S., OKUDA, S. & IMAIZUMI, T. 2012. Inhibition of eNOS phosphorylation mediates endothelial dysfunction in renal failure: new effect of asymmetric dimethylarginine. *Kidney Int*.

KAKOKI, M., KIM, H. S., ARENDSHORST, W. J. & MATTSON, D. L. 2004. L-Arginine uptake affects nitric oxide production and blood flow in the renal medulla. *Am J Physiol Regul Integr Comp Physiol,* 287**,** R1478-85.

KANEKO, S., ANDO, A., OKUDA-ASHITAKA, E., MAEDA, M., FURUTA, K., SUZUKI, M., MATSUMURA, M. & ITO, S. 2007. Ornithine transport via cationic amino acid transporter-1 is involved in ornithine cytotoxicity in retinal pigment epithelial cells. *Invest Ophthalmol Vis Sci,* 48**,** 464-71.

KARLSSON, M., THORN, H., PARPAL, S., STRALFORS, P. & GUSTAVSSON, J. 2002. Insulin induces translocation of glucose transporter GLUT4 to plasma membrane caveolae in adipocytes. *FASEB J,* 16**,** 249-51.

KARUNAKARAN, S., RAMACHANDRAN, S., COOTHANKANDASWAMY, V., ELANGOVAN, S., BABU, E., PERIYASAMY-THANDAVAN, S., GURAV, A., GNANAPRAKASAM, J. P., SINGH, N., SCHOENLEIN, P. V., PRASAD, P. D., THANGARAJU, M. & GANAPATHY, V. 2011. SLC6A14 (ATB0,+) protein, a highly concentrative and broad specific amino acid transporter, is a novel and effective drug target for treatment of estrogen receptor-positive breast cancer. *J Biol Chem,* 286**,** 31830-8.

KARUNAKARAN, S., UMAPATHY, N. S., THANGARAJU, M., HATANAKA, T., ITAGAKI, S., MUNN, D. H., PRASAD, P. D. & GANAPATHY, V. 2008. Interaction of tryptophan derivatives with SLC6A14 (ATB0,+) reveals the potential of the transporter as a drug target for cancer chemotherapy. *Biochem J,* 414**,** 343-55.

KAVANAUGH, M. P., WANG, H., BOYD, C. A., NORTH, R. A. & KABAT, D. 1994. Cell surface receptor for ecotropic host-range mouse retroviruses: a cationic amino acid transporter. *Arch Virol Suppl,* 9**,** 485-94.

KAWANO, K., MASUDA, H., YANO, M., KIHARA, K., SUGIMOTO, A. & AZUMA, H. 2006. Altered nitric oxide synthase, arginase and ornithine decarboxylase activities, and polyamine synthesis in response to ischemia of the rabbit detrusor. *J Urol,* 176**,** 387-93.

KENNEDY, P. G. 2004. Human African trypanosomiasis of the CNS: current issues and challenges. *J Clin Invest,* 113**,** 496-504.

KETABI-KIYANVASH, N., HEROLD-MENDE, C., KASHFI, F., CALDEIRA, S., TOMMASINO, M., HAEFELI, W. E. & WEISS, J. 2007. NKIM-6, a new immortalized human brain capillary endothelial cell line with conserved endothelial characteristics. *Cell Tissue Res,* 328**,** 19-29.

KIELSTEIN, A., TSIKAS, D., GALLOWAY, G. P. & MENDELSON, J. E. 2007. Asymmetric dimethylarginine (ADMA)--a modulator of nociception in opiate tolerance and addiction? *Nitric Oxide,* 17**,** 55-9.

KIELSTEIN, J. T., DONNERSTAG, F., GASPER, S., MENNE, J., KIELSTEIN, A., MARTENS-LOBENHOFFER, J., SCALERA, F., COOKE, J. P., FLISER, D. & BODE-BOGER, S. M. 2006a. ADMA increases arterial stiffness and decreases cerebral blood flow in humans. *Stroke,* 37**,** 2024-9.

KIELSTEIN, J. T., IMPRAIM, B., SIMMEL, S., BODE-BOGER, S. M., TSIKAS, D., FROLICH, J. C., HOEPER, M. M., HALLER, H. & FLISER, D. 2004. Cardiovascular effects of systemic nitric oxide synthase inhibition with asymmetrical dimethylarginine in humans. *Circulation,* 109**,** 172-7.

KIELSTEIN, J. T. & KIELSTEIN, A. 2009. ADMA and the brain: an unfolding story. *Am J Hypertens,* 22**,** 240.

KIELSTEIN, J. T., SALPETER, S. R., BODE-BOEGER, S. M., COOKE, J. P. & FLISER, D. 2006b. Symmetric dimethylarginine (SDMA) as endogenous marker of renal function--a meta-analysis. *Nephrol Dial Transplant,* 21**,** 2446-51.

KIM, J. W., CLOSS, E. I., ALBRITTON, L. M. & CUNNINGHAM, J. M. 1991. Transport of cationic amino acids by the mouse ecotropic retrovirus receptor. *Nature,* 352**,** 725-8.

KIM, J. W. & CUNNINGHAM, J. M. 1993. N-linked glycosylation of the receptor for murine ecotropic retroviruses is altered in virus-infected cells. *J Biol Chem,* 268**,** 16316-20.

KIRKHAM, M. & PARTON, R. G. 2005. Clathrin-independent endocytosis: new insights into caveolae and non-caveolar lipid raft carriers. *Biochim Biophys Acta,* 1746**,** 349-63.

KNIPP, M. 2006. How to control NO production in cells: N(omega),N(omega)-dimethyl-L-arginine dimethylaminohydrolase as a novel drug target. *Chembiochem,* 7**,** 879-89.

KONISHI, H., SYDOW, K. & COOKE, J. P. 2007. Dimethylarginine dimethylaminohydrolase promotes endothelial repair after vascular injury. *J Am Coll Cardiol,* 49**,** 1099-105.

KOOIJMANS, S. A., SENYSCHYN, D., MEZHISELVAM, M. M., MORIZZI, J., CHARMAN, S. A., WEKSLER, B., ROMERO, I. A., COURAUD, P. O. & NICOLAZZO, J. A. 2012. The involvement of a na(+)- and cl(-)-dependent transporter in the brain uptake of amantadine and rimantadine. *Mol Pharm,* 9**,** 883-93.

KOVAC, A., ERICKSON, M. A. & BANKS, W. A. 2011. Brain microvascular pericytes are immunoactive in culture: cytokine, chemokine, nitric oxide, and LRP-1 expression in response to lipopolysaccharide. *J Neuroinflammation,* 8**,** 139.

KRAUSE, C. D., YANG, Z. H., KIM, Y. S., LEE, J. H., COOK, J. R. & PESTKA, S. 2007. Protein arginine methyltransferases: evolution and assessment of their pharmacological and therapeutic potential. *Pharmacol Ther,* 113**,** 50-87.

KRISTENSSON, K., NYGARD, M., BERTINI, G. & BENTIVOGLIO, M. 2010. African trypanosome infections of the nervous system: parasite entry and effects on sleep and synaptic functions. *Prog Neurobiol,* 91**,** 152-71.

KUEPFER, I., HHARY, E. P., ALLAN, M., EDIELU, A., BURRI, C. & BLUM, J. A. 2011. Clinical presentation of T.b. rhodesiense sleeping sickness in second stage patients from Tanzania and Uganda. *PLoS Negl Trop Dis,* 5**,** e968.

KUSCH-PODDAR, M., DREWE, J., FUX, I. & GUTMANN, H. 2005. Evaluation of the immortalized human brain capillary endothelial cell line BB19 as a human cell culture model for the blood-brain barrier. *Brain Res,* 1064**,** 21-31.

LAJER, M., TARNOW, L., JORSAL, A., TEERLINK, T., PARVING, H. H. & ROSSING, P. 2008. Plasma concentration of asymmetric dimethylarginine (ADMA) predicts cardiovascular morbidity and mortality in type 1 diabetic patients with diabetic nephropathy. *Diabetes Care,* 31**,** 747-52.

LANAS, A. 2008. Role of nitric oxide in the gastrointestinal tract. *Arthritis Res Ther,* 10 Suppl 2**,** S4.

LEIPER, J. & NANDI, M. 2011. The therapeutic potential of targeting endogenous inhibitors of nitric oxide synthesis. *Nat Rev Drug Discov,* 10**,** 277-91.

LEIPER, J., NANDI, M., TORONDEL, B., MURRAY-RUST, J., MALAKI, M., O'HARA, B., ROSSITER, S., ANTHONY, S., MADHANI, M., SELWOOD, D., SMITH, C., WOJCIAK-STOTHARD, B., RUDIGER, A., STIDWILL, R., MCDONALD, N. Q. & VALLANCE, P. 2007. Disruption of methylarginine metabolism impairs vascular homeostasis. *Nat Med,* 13**,** 198-203.

LEIPER, J. & VALLANCE, P. 1999. Biological significance of endogenous methylarginines that inhibit nitric oxide synthases. *Cardiovasc Res,* 43**,** 542-8.

LEIPER, J. & VALLANCE, P. 2006. New tricks from an old dog: nitric oxide-independent effects of dimethylarginine dimethylaminohydrolase. *Arterioscler Thromb Vasc Biol,* 26**,** 1419-20.

LEIPER, J. M., SANTA MARIA, J., CHUBB, A., MACALLISTER, R. J., CHARLES, I. G., WHITLEY, G. S. & VALLANCE, P. 1999. Identification of two human dimethylarginine dimethylaminohydrolases with distinct tissue distributions and homology with microbial arginine deiminases. *Biochem J,* 343 Pt 1**,** 209-14.

LEO, A., HANSCH, C. & ELKINS, D. 1971. Partition Coefficients and Their Uses. *Chemical Reviews,* 71**,** 525-+.

LESLIE, E. M., DEELEY, R. G. & COLE, S. P. 2005. Multidrug resistance proteins: role of P-glycoprotein, MRP1, MRP2, and BCRP (ABCG2) in tissue defense. *Toxicol Appl Pharmacol,* 204**,** 216-37.

LI, C., HUANG, W., HARRIS, M. B., GOOLSBY, J. M. & VENEMA, R. C. 2005. Interaction of the endothelial nitric oxide synthase with the CAT-1 arginine transporter enhances NO release by a mechanism not involving arginine transport. *Biochem J,* 386**,** 567-74.

LI, H., CYBULSKY, M. I., GIMBRONE, M. A., JR. & LIBBY, P. 1993. Inducible expression of vascular cell adhesion molecule-1 by vascular smooth muscle cells in vitro and within rabbit atheroma. *Am J Pathol,* 143**,** 1551-9.

LIEBNER, S., CZUPALLA, C. J. & WOLBURG, H. 2011. Current concepts of blood-brain barrier development. *Int J Dev Biol,* 55**,** 467-76.

LIN, K. Y., ITO, A., ASAGAMI, T., TSAO, P. S., ADIMOOLAM, S., KIMOTO, M., TSUJI, H., REAVEN, G. M. & COOKE, J. P. 2002. Impaired nitric oxide synthase pathway in diabetes mellitus: role of asymmetric dimethylarginine and dimethylarginine dimethylaminohydrolase. *Circulation,* 106**,** 987-92.

LIPPOLDT, A., LIEBNER, S., ANDBJER, B., KALBACHER, H., WOLBURG, H., HALLER, H. & FUXE, K. 2000. Organization of choroid plexus epithelial and endothelial cell tight junctions and regulation of claudin-1, -2 and -5 expression by protein kinase C. *Neuroreport,* 11**,** 1427-31.

LIU, F., SHI, J., TANIMUKAI, H., GU, J., GRUNDKE-IQBAL, I., IQBAL, K. & GONG, C. X. 2009. Reduced O-GlcNAcylation links lower brain glucose metabolism and tau pathology in Alzheimer's disease. *Brain,* 132**,** 1820-32.

LIU, N. Q., LOSSINSKY, A. S., POPIK, W., LI, X., GUJULUVA, C., KRIEDERMAN, B., ROBERTS, J., PUSHKARSKY, T., BUKRINSKY, M., WITTE, M., WEINAND, M. & FIALA, M. 2002. Human immunodeficiency virus type 1 enters brain microvascular endothelia by macropinocytosis dependent on lipid rafts and the mitogen-activated protein kinase signaling pathway. *J Virol,* 76**,** 6689-700.

LORRAIN, D. S. & HULL, E. M. 1993. Nitric oxide increases dopamine and serotonin release in the medial preoptic area. *Neuroreport,* 5**,** 87-9.

LOSCALZO, J. & WELCH, G. 1995. Nitric oxide and its role in the cardiovascular system. *Prog Cardiovasc Dis,* 38**,** 87-104.

LU, C. W., XIONG, Y. & HE, P. 2007. Dimethylarginine dimethylaminohydrolase-2 overexpression improves impaired nitric oxide synthesis of endothelial cells induced by glycated protein. *Nitric Oxide,* 16**,** 94-103.

LUNDMAN, P., ERIKSSON, M. J., STUHLINGER, M., COOKE, J. P., HAMSTEN, A. & TORNVALL, P. 2001. Mild-to-moderate hypertriglyceridemia in young men is associated with endothelial dysfunction and increased plasma concentrations of asymmetric dimethylarginine. *J Am Coll Cardiol,* 38**,** 111-6.

LUTJE, V., SEIXAS, J. & KENNEDY, A. 2010. Chemotherapy for second-stage Human African trypanosomiasis. *Cochrane Database Syst Rev,* 8**,** CD006201.

MAAS, R., BOGER, R. H., SCHWEDHELM, E., CASAS, J. P., LOPEZ-JARAMILLO, P., SERRANO, N. & DIAZ, L. A. 2004. Plasma concentrations of asymmetric dimethylarginine (ADMA) in Colombian women with pre-eclampsia. *JAMA,* 291**,** 823-4.

MALEK, A. M. & IZUMO, S. 1996. Mechanism of endothelial cell shape change and cytoskeletal remodeling in response to fluid shear stress. *J Cell Sci,* 109 (Pt 4)**,** 713-26.

MANN, G. E., PEARSON, J. D., SHERIFF, C. J. & TOOTHILL, V. J. 1989. Expression of amino acid transport systems in cultured human umbilical vein endothelial cells. *J Physiol,* 410**,** 325-39.

MANN, G. E., YUDILEVICH, D. L. & SOBREVIA, L. 2003. Regulation of amino acid and glucose transporters in endothelial and smooth muscle cells. *Physiol Rev,* 83**,** 183-252.

MASER, P. & KAMINSKY, R. 1998. Identification of three ABC transporter genes in Trypanosoma brucei spp. *Parasitol Res,* 84**,** 106-11.

MASOCHA, W., ROTTENBERG, M. E. & KRISTENSSON, K. 2007. Migration of African trypanosomes across the blood-brain barrier. *Physiol Behav,* 92**,** 110-4.

MASON, B. L., PARIANTE, C. M. & THOMAS, S. A. 2008. A revised role for P-glycoprotein in the brain distribution of dexamethasone, cortisol, and corticosterone in wild-type and ABCB1A/B-deficient mice. *Endocrinology,* 149**,** 5244-53.

MASUDA, H., GOTO, M., TAMAOKI, S. & AZUMA, H. 1999. Accelerated intimal hyperplasia and increased endogenous inhibitors for NO synthesis in rabbits with alloxan-induced hyperglycaemia. *Br J Pharmacol,* 126**,** 211-8.

MATSSON, P., PEDERSEN, J. M., NORINDER, U., BERGSTROM, C. A. & ARTURSSON, P. 2009. Identification of novel specific and general inhibitors of the three major human ATP-binding cassette transporters P-gp, BCRP and MRP2 among registered drugs. *Pharm Res,* 26**,** 1816-31.

MCBRIDE, A. E. & SILVER, P. A. 2001. State of the arg: protein methylation at arginine comes of age. *Cell,* 106**,** 5-8.

MCDERMOTT, J. R. 1976. Studies on the catabolism of Ng-methylarginine, Ng, Ng-dimethylarginine and Ng, Ng-dimethylarginine in the rabbit. *Biochem J,* 154**,** 179-84.

MCDONALD, K. K., ZHARIKOV, S., BLOCK, E. R. & KILBERG, M. S. 1997. A caveolar complex between the cationic amino acid transporter 1 and endothelial nitric-oxide synthase may explain the "arginine paradox". *J Biol Chem,* 272**,** 31213-6.

MERINO, G., ALVAREZ, A. I., PULIDO, M. M., MOLINA, A. J., SCHINKEL, A. H. & PRIETO, J. G. 2006. Breast cancer resistance protein (BCRP/ABCG2) transports fluoroquinolone antibiotics and affects their oral availability, pharmacokinetics, and milk secretion. *Drug Metab Dispos,* 34**,** 690-5.

MERINO, G., JONKER, J. W., WAGENAAR, E., VAN HERWAARDEN, A. E. & SCHINKEL, A. H. 2005. The breast cancer resistance protein (BCRP/ABCG2) affects pharmacokinetics, hepatobiliary excretion, and milk secretion of the antibiotic nitrofurantoin. *Mol Pharmacol,* 67**,** 1758-64.

MIECZ, D., JANUSZEWICZ, E., CZEREDYS, M., HINTON, B. T., BEREZOWSKI, V., CECCHELLI, R. & NALECZ, K. A. 2008. Localization of organic cation/carnitine transporter (OCTN2) in cells forming the blood-brain barrier. *J Neurochem,* 104**,** 113-23.

MINAGAR, A. & ALEXANDER, J. S. 2003. Blood-brain barrier disruption in multiple sclerosis. *Mult Scler,* 9**,** 540-9.

MINER, S. E., AL-HESAYEN, A., KELLY, S., BENSON, T., THIESSEN, J. J., YOUNG, V. R. & PARKER, J. D. 2004. L-arginine transport in the human coronary and peripheral circulation. *Circulation,* 109**,** 1278-83.

MINN, A., LECLERC, S., HEYDEL, J. M., MINN, A. L., DENIZCOT, C., CATTARELLI, M., NETTER, P. & GRADINARU, D. 2002. Drug transport into the mammalian brain: the nasal pathway and its specific metabolic barrier. *J Drug Target,* 10**,** 285-96.

MIYAJIMA, M., KUSUHARA, H., FUJISHIMA, M., ADACHI, Y. & SUGIYAMA, Y. 2011. Organic anion transporter 3 mediates the efflux transport of an amphipathic organic anion,

dehydroepiandrosterone sulfate, across the blood-brain barrier in mice. *Drug Metab Dispos,* 39**,** 814-9.

MKRTCHYAN, H., SCHELER, S., KLEIN, I., FAHR, A., COURAUD, P. O., ROMERO, I. A., WEKSLER, B. & LIEHR, T. 2009. Molecular cytogenetic characterization of the human cerebral microvessel endothelial cell line hCMEC/D3. *Cytogenet Genome Res,* 126**,** 313-7.

MOCHIZUKI, S., ONO, J., YADA, T., OGASAWARA, Y., MIYASAKA, T., KIMOTO, M., KASHIHARA, N. & KAJIYA, F. 2005. Systemic nitric oxide production rate during hemodialysis and its relationship with nitric oxide-related factors. *Blood Purif,* 23**,** 317-24.

MOENS, F., DE WILDE, M. & NGATO, K. 1984. [Clinical trial of nifurtimox in human African trypanosomiasis]. *Ann Soc Belg Med Trop,* 64**,** 37-43.

MOLLER, P., ALVESTRAND, A., BERGSTROM, J., FURST, P. & HELLSTROM, K. 1983. Electrolytes and free amino acids in leg skeletal muscle of young and elderly women. *Gerontology,* 29**,** 1-8.

MOLLER, P., BERGSTROM, J., ERIKSSON, S., FURST, P. & HELLSTROM, K. 1979. Effect of aging on free amino acids and electrolytes in leg skeletal muscle. *Clin Sci (Lond),* 56**,** 427-32.

MONCADA, S., PALMER, R. M. & HIGGS, E. A. 1991. Nitric oxide: physiology, pathophysiology, and pharmacology. *Pharmacol Rev,* 43**,** 109-42.

MOOKERJEE, R. P., DALTON, R. N., DAVIES, N. A., HODGES, S. J., TURNER, C., WILLIAMS, R. & JALAN, R. 2007. Inflammation is an important determinant of levels of the endogenous nitric oxide synthase inhibitor asymmetric dimethylarginine (ADMA) in acute liver failure. *Liver Transpl,* 13**,** 400-5.

MORRIS, S. M., JR. 1992. Regulation of enzymes of urea and arginine synthesis. *Annu Rev Nutr,* 12**,** 81-101.

MORRIS, S. M., JR. 2002. Regulation of enzymes of the urea cycle and arginine metabolism. *Annu Rev Nutr,* 22**,** 87-105.

MOUSAVI, S. A., MALEROD, L., BERG, T. & KJEKEN, R. 2004. Clathrin-dependent endocytosis. *Biochem J,* 377**,** 1-16.

MPIA, B. & PEPIN, J. 2002. Combination of eflornithine and melarsoprol for melarsoprol-resistant Gambian trypanosomiasis. *Trop Med Int Health,* 7**,** 775-9.

MULDER, C., WAHLUND, L. O., BLOMBERG, M., DE JONG, S., VAN KAMP, G. J., SCHELTENS, P. & TEERLINK, T. 2002. Alzheimer's disease is not associated with altered concentrations of the nitric oxide synthase inhibitor asymmetric dimethylarginine in cerebrospinal fluid. *J Neural Transm,* 109**,** 1203-8.

MULENGA, C., MHLANGA, J. D., KRISTENSSON, K. & ROBERTSON, B. 2001. Trypanosoma brucei brucei crosses the blood-brain barrier while tight junction proteins are preserved in a rat chronic disease model. *Neuropathol Appl Neurobiol,* 27**,** 77-85.

MURAKAMI, H., MURAKAMI, R., KAMBE, F., CAO, X., TAKAHASHI, R., ASAI, T., HIRAI, T., NUMAGUCHI, Y., OKUMURA, K., SEO, H. & MUROHARA, T. 2006. Fenofibrate activates AMPK and increases eNOS phosphorylation in HUVEC. *Biochem Biophys Res Commun,* 341**,** 973-8.

MURUGANANDAM, A., HERX, L. M., MONETTE, R., DURKIN, J. P. & STANIMIROVIC, D. B. 1997. Development of immortalized human cerebromicrovascular endothelial cell line as an in vitro model of the human blood-brain barrier. *FASEB J,* 11**,** 1187-97.

NADZIEJKO, C. E. & REICHBERG, S. B. 1984. Inhibition of Sodium-Independent Amino-Acid-Transport by Dexamethasone in Rat Hepatoma-Cells. *Journal of Biological Chemistry,* 259**,** 394-398.

NAGASAWA, K., CHIBA, H., FUJITA, H., KOJIMA, T., SAITO, T., ENDO, T. & SAWADA, N. 2006. Possible involvement of gap junctions in the barrier function of tight junctions of brain and lung endothelial cells. *J Cell Physiol,* 208**,** 123-32.

NARANG, V. S., FRAGA, C., KUMAR, N., SHEN, J., THROM, S., STEWART, C. F. & WATERS, C. M. 2008. Dexamethasone increases expression and activity of multidrug resistance transporters at the rat blood-brain barrier. *Am J Physiol Cell Physiol,* 295**,** C440-50.

NEUWELT, E. A., BAUER, B., FAHLKE, C., FRICKER, G., IADECOLA, C., JANIGRO, D., LEYBAERT, L., MOLNAR, Z., O'DONNELL, M. E., POVLISHOCK, J. T., SAUNDERS, N. R., SHARP, F., STANIMIROVIC, D., WATTS, R. J. & DREWES, L. R. 2011. Engaging neuroscience to advance translational research in brain barrier biology. *Nat Rev Neurosci,* 12**,** 169-82.

NGUYEN, T. V., SMITH, D. E. & FLEISHER, D. 2007. PEPT1 enhances the uptake of gabapentin via trans-stimulation of b0,+ exchange. *Pharm Res,* 24**,** 353-60.

NI, Z., BIKADI, Z., ROSENBERG, M. F. & MAO, Q. 2010. Structure and function of the human breast cancer resistance protein (BCRP/ABCG2). *Curr Drug Metab,* 11**,** 603-17.

NICHOLSON, B., SAWAMURA, T., MASAKI, T. & MACLEOD, C. L. 1998. Increased Cat3-mediated cationic amino acid transport functionally compensates in Cat1 knockout cell lines. *J Biol Chem,* 273**,** 14663-6.

NIESSEN, C. M. 2007. Tight junctions/adherens junctions: basic structure and function. *J Invest Dermatol,* 127**,** 2525-32.

NIJVELDT, R. J., SIROEN, M. P., TEERLINK, T. & VAN LEEUWEN, P. A. 2004. Elimination of asymmetric dimethylarginine by the kidney and the liver: a link to the development of multiple organ failure? *J Nutr,* 134**,** 2848S-2852S; discussion 2853S.

NIJVELDT, R. J., TEERLINK, T., SIROEN, M. P., VAN LAMBALGEN, A. A., RAUWERDA, J. A. & VAN LEEUWEN, P. A. 2003. The liver is an important organ in the metabolism of asymmetrical dimethylarginine (ADMA). *Clin Nutr,* 22**,** 17-22.

NILIUS, B. & DROOGMANS, G. 2001. Ion channels and their functional role in vascular endothelium. *Physiol Rev,* 81**,** 1415-59.

NOK, A. J. 2003. Arsenicals (melarsoprol), pentamidine and suramin in the treatment of human African trypanosomiasis. *Parasitol Res,* 90**,** 71-9.

NORGALL, S., PAPOUTSI, M., ROSSLER, J., SCHWEIGERER, L., WILTING, J. & WEICH, H. A. 2007. Elevated expression of VEGFR-3 in lymphatic endothelial cells from lymphangiomas. *BMC Cancer,* 7**,** 105.

NOTSU, Y., NABIKA, T., BOKURA, H., SUYAMA, Y., KOBAYASHI, S., YAMAGUCHI, S. & MASUDA, J. 2009. Evaluation of asymmetric dimethylarginine and homocysteine in microangiopathy-related cerebral damage. *Am J Hypertens,* 22**,** 257-62.

NOZAWA, T., MINAMI, H., SUGIURA, S., TSUJI, A. & TAMAI, I. 2005. Role of organic anion transporter OATP1B1 (OATP-C) in hepatic uptake of irinotecan and its active metabolite, 7-ethyl-10-hydroxycamptothecin: in vitro evidence and effect of single nucleotide polymorphisms. *Drug Metab Dispos,* 33**,** 434-9.

O'KANE, R. L., VINA, J. R., SIMPSON, I., ZARAGOZA, R., MOKASHI, A. & HAWKINS, R. A. 2006. Cationic amino acid transport across the blood-brain barrier is mediated exclusively by system y+. *Am J Physiol Endocrinol Metab,* 291**,** E412-9.

ODIIT, M., KANSIIME, F. & ENYARU, J. C. 1997. Duration of symptoms and case fatality of sleeping sickness caused by Trypanosoma brucei rhodesiense in Tororo, Uganda. *East Afr Med J,* 74**,** 792-5.

OGAWA, T., KIMOTO, M. & SASAOKA, K. 1987a. Occurrence of a new enzyme catalyzing the direct conversion of NG,NG-dimethyl-L-arginine to L-citrulline in rats. *Biochem Biophys Res Commun,* 148**,** 671-7.

OGAWA, T., KIMOTO, M., WATANABE, H. & SASAOKA, K. 1987b. Metabolism of NG,NG-and NG,N'G-dimethylarginine in rats. *Arch Biochem Biophys,* 252**,** 526-37.

OGONOWSKI, A. A., KAESEMEYER, W. H., JIN, L., GANAPATHY, V., LEIBACH, F. H. & CALDWELL, R. W. 2000. Effects of NO donors and synthase agonists on endothelial cell uptake of L-Arg and superoxide production. *Am J Physiol Cell Physiol,* 278**,** C136-43.

OLDENDORF, W. H. & BROWN, W. J. 1975. Greater number of capillary endothelial cell mitochondria in brain than in muscle. *Proc Soc Exp Biol Med,* 149**,** 736-8.

OLDENDORF, W. H., CORNFORD, M. E. & BROWN, W. J. 1976. The large apparent metabolic work capacity of the blood-brain barrier. *Trans Am Neurol Assoc,* 101**,** 157-60.

OLDENDORF, W. H. & SZABO, J. 1976. Amino acid assignment to one of three blood-brain barrier amino acid carriers. *Am J Physiol,* 230**,** 94-8.

OMIDI, Y., CAMPBELL, L., BARAR, J., CONNELL, D., AKHTAR, S. & GUMBLETON, M. 2003. Evaluation of the immortalised mouse brain capillary endothelial cell line, b.End3, as an in vitro blood-brain barrier model for drug uptake and transport studies. *Brain Res,* 990**,** 95-112.

PAL, A., HALL, B. S. & FIELD, M. C. 2002. Evidence for a non-LDL-mediated entry route for the trypanocidal drug suramin in Trypanosoma brucei. *Mol Biochem Parasitol,* 122**,** 217-21.

PALLOSHI, A., FRAGASSO, G., PIATTI, P., MONTI, L. D., SETOLA, E., VALSECCHI, G., GALLUCCIO, E., CHIERCHIA, S. L. & MARGONATO, A. 2004. Effect of oral L-arginine on blood pressure and symptoms and endothelial function in patients with systemic hypertension, positive exercise tests, and normal coronary arteries. *Am J Cardiol,* 93**,** 933-5.

PALM, F., ONOZATO, M. L., LUO, Z. & WILCOX, C. S. 2007. Dimethylarginine dimethylaminohydrolase (DDAH): expression, regulation, and function in the cardiovascular and renal systems. *Am J Physiol Heart Circ Physiol,* 293**,** H3227-45.

PALMERI, D., VAN ZANTE, A., HUANG, C. C., HEMMERICH, S. & ROSEN, S. D. 2000. Vascular endothelial junction-associated molecule, a novel member of the immunoglobulin superfamily, is localized to intercellular boundaries of endothelial cells. *J Biol Chem,* 275**,** 19139-45.

PAN, G., GIRI, N. & ELMQUIST, W. F. 2007. Abcg2/Bcrp1 mediates the polarized transport of antiretroviral nucleosides abacavir and zidovudine. *Drug Metab Dispos,* 35**,** 1165-73.

PARATHATH, S. R., PARATHATH, S. & TSIRKA, S. E. 2006. Nitric oxide mediates neurodegeneration and breakdown of the blood-brain barrier in tPA-dependent excitotoxic injury in mice. *J Cell Sci,* 119**,** 339-49.

PARDRIDGE, W. M. 1977. Unidirectional influx of glutamine and other neutral amino acids into liver of fed and fasted rat in vivo. *Am J Physiol,* 232**,** E492-6.

PARDRIDGE, W. M. 1998. Blood-brain barrier carrier-mediated transport and brain metabolism of amino acids. *Neurochem Res,* 23**,** 635-44.

PARDRIDGE, W. M. 1999. Blood-brain barrier biology and methodology. *J Neurovirol,* 5**,** 556-69.

PARDRIDGE, W. M. 2002. Drug and gene targeting to the brain with molecular Trojan horses. *Nat Rev Drug Discov,* 1**,** 131-9.

PARDRIDGE, W. M. 2005. The blood-brain barrier: bottleneck in brain drug development. *NeuroRx,* 2**,** 3-14.

PARDRIDGE, W. M., BOADO, R. J. & FARRELL, C. R. 1990. Brain-type glucose transporter (GLUT-1) is selectively localized to the blood-brain barrier. Studies with quantitative western blotting and in situ hybridization. *J Biol Chem,* 265**,** 18035-40.

PAREPALLY, J. M., MANDULA, H. & SMITH, Q. R. 2006. Brain uptake of nonsteroidal anti-inflammatory drugs: ibuprofen, flurbiprofen, and indomethacin. *Pharm Res,* 23**,** 873-81.

PEPIN, J. & MILORD, F. 1994. The treatment of human African trypanosomiasis. *Adv Parasitol,* 33**,** 1-47.

PEPIN, J., MILORD, F., KHONDE, A., NIYONSENGA, T., LOKO, L. & MPIA, B. 1994. Gambiense trypanosomiasis: frequency of, and risk factors for, failure of melarsoprol therapy. *Trans R Soc Trop Med Hyg,* 88**,** 447-52.

PEPIN, J., MILORD, F., MPIA, B., MEURICE, F., ETHIER, L., DEGROOF, D. & BRUNEEL, H. 1989. An open clinical trial of nifurtimox for arseno-resistant Trypanosoma brucei gambiense sleeping sickness in central Zaire. *Trans R Soc Trop Med Hyg,* 83**,** 514-7.

PERKINS, C. P., MAR, V., SHUTTER, J. R., DEL CASTILLO, J., DANILENKO, D. M., MEDLOCK, E. S., PONTING, I. L., GRAHAM, M., STARK, K. L., ZUO, Y., CUNNINGHAM, J. M. & BOSSELMAN, R. A. 1997. Anemia and perinatal death result from loss of the murine ecotropic retrovirus receptor mCAT-1. *Genes Dev,* 11**,** 914-25.

PHILIP, K. A., DASCOMBE, M. J., FRASER, P. A. & PENTREATH, V. W. 1994. Blood-brain barrier damage in experimental African trypanosomiasis. *Ann Trop Med Parasitol,* 88**,** 607-16.

PHILLIPS, M. A., COFFINO, P. & WANG, C. C. 1987. Cloning and sequencing of the ornithine decarboxylase gene from Trypanosoma brucei. Implications for enzyme turnover and selective difluoromethylornithine inhibition. *J Biol Chem,* 262**,** 8721-7.

POLLER, B., GUTMANN, H., KRAHENBUHL, S., WEKSLER, B., ROMERO, I., COURAUD, P. O., TUFFIN, G., DREWE, J. & HUWYLER, J. 2008. The human brain endothelial cell line hCMEC/D3 as a human blood-brain barrier model for drug transport studies. *J Neurochem,* 107**,** 1358-68.

POPE, A. J., KARUPPIAH, K. & CARDOUNEL, A. J. 2009. Role of the PRMT-DDAH-ADMA axis in the regulation of endothelial nitric oxide production. *Pharmacol Res,* 60**,** 461-5.

POTSCHKA, H., BALTES, S. & LOSCHER, W. 2004. Inhibition of multidrug transporters by verapamil or probenecid does not alter blood-brain barrier penetration of levetiracetam in rats. *Epilepsy Res,* 58**,** 85-91.

PRIOTTO, G., FOGG, C., BALASEGARAM, M., ERPHAS, O., LOUGA, A., CHECCHI, F., GHABRI, S. & PIOLA, P. 2006. Three drug combinations for late-stage Trypanosoma brucei gambiense sleeping sickness: a randomized clinical trial in Uganda. *PLoS Clin Trials,* 1**,** e39.

PRIOTTO, G., KASPARIAN, S., MUTOMBO, W., NGOUAMA, D., GHORASHIAN, S., ARNOLD, U., GHABRI, S., BAUDIN, E., BUARD, V., KAZADI-KYANZA, S., ILUNGA, M., MUTANGALA, W., POHLIG, G., SCHMID, C., KARUNAKARA, U., TORREELE, E. & KANDE, V. 2009. Nifurtimox-eflornithine combination therapy for second-stage African Trypanosoma brucei gambiense trypanosomiasis: a multicentre, randomised, phase III, non-inferiority trial. *Lancet,* 374**,** 56-64.

PRIOTTO, G., KASPARIAN, S., NGOUAMA, D., GHORASHIAN, S., ARNOLD, U., GHABRI, S. & KARUNAKARA, U. 2007. Nifurtimox-eflornithine combination therapy for second-stage Trypanosoma brucei gambiense sleeping sickness: a randomized clinical trial in Congo. *Clin Infect Dis,* 45**,** 1435-42.

PSYCHOGIOS, N., HAU, D. D., PENG, J., GUO, A. C., MANDAL, R., BOUATRA, S., SINELNIKOV, I., KRISHNAMURTHY, R., EISNER, R., GAUTAM, B., YOUNG, N., XIA, J., KNOX, C., DONG, E., HUANG, P., HOLLANDER, Z., PEDERSEN, T. L., SMITH, S. R., BAMFORTH, F., GREINER, R., MCMANUS, B., NEWMAN, J. W., GOODFRIEND, T. & WISHART, D. S. 2011. The human serum metabolome. *PLoS One,* 6**,** e16957.

RAMSAUER, M., KRAUSE, D. & DERMIETZEL, R. 2002. Angiogenesis of the blood-brain barrier in vitro and the function of cerebral pericytes. *FASEB J,* 16**,** 1274-6.

RASEROKA, B. H. & ORMEROD, W. E. 1986. The trypanocidal effect of drugs in different parts of the brain. *Trans R Soc Trop Med Hyg,* 80**,** 634-41.

RAWAL, N., RAJPUROHIT, R., LISCHWE, M. A., WILLIAMS, K. R., PAIK, W. K. & KIM, S. 1995. Structural specificity of substrate for S-adenosylmethionine:protein arginine N-methyltransferases. *Biochim Biophys Acta,* 1248**,** 11-8.

REDZIC, Z. 2011. Molecular biology of the blood-brain and the blood-cerebrospinal fluid barriers: similarities and differences. *Fluids Barriers CNS,* 8**,** 3.

REES, D. D., PALMER, R. M., SCHULZ, R., HODSON, H. F. & MONCADA, S. 1990. Characterization of three inhibitors of endothelial nitric oxide synthase in vitro and in vivo. *Br J Pharmacol,* 101**,** 746-52.

RICHIR, M. C., BOUWMAN, R. H., TEERLINK, T., SIROEN, M. P., DE VRIES, T. P. & VAN LEEUWEN, P. A. 2008. The prominent role of the liver in the elimination of asymmetric dimethylarginine (ADMA) and the consequences of impaired hepatic function. *JPEN J Parenter Enteral Nutr,* 32**,** 613-21.

ROBENEK, H. & SEVERS, N. J. 2008. Recent advances in freeze-fracture electron microscopy: the replica immunolabeling technique. *Biol Proced Online,* 10**,** 9-19.

ROBERTS, R. L., FINE, R. E. & SANDRA, A. 1993. Receptor-mediated endocytosis of transferrin at the blood-brain barrier. *J Cell Sci,* 104 (Pt 2)**,** 521-32.

RODIONOV, R. N., MURRY, D. J., VAULMAN, S. F., STEVENS, J. W. & LENTZ, S. R. 2010. Human alanine-glyoxylate aminotransferase 2 lowers asymmetric dimethylarginine and protects from inhibition of nitric oxide production. *J Biol Chem,* 285**,** 5385-91.

ROSENBAUM, C., ROHRS, S., MULLER, O. & WALDMANN, H. 2005. Modulation of MRP-1-mediated multidrug resistance by indomethacin analogues. *J Med Chem,* 48**,** 1179-87.

ROTMANN, A., SIMON, A., MARTINE, U., HABERMEIER, A. & CLOSS, E. I. 2007. Activation of classical protein kinase C decreases transport via systems y+ and y+L. *Am J Physiol Cell Physiol,* 292**,** C2259-68.

SANCHEZ DEL PINO, M. M., PETERSON, D. R. & HAWKINS, R. A. 1995. Neutral amino acid transport characterization of isolated luminal and abluminal membranes of the blood-brain barrier. *J Biol Chem,* 270**,** 14913-8.

SANDERSON, L., DOGRUEL, M., RODGERS, J., BRADLEY, B. & THOMAS, S. A. 2008. The blood-brain barrier significantly limits eflornithine entry into Trypanosoma brucei brucei infected mouse brain. *J Neurochem,* 107**,** 1136-46.

SANDERSON, L., DOGRUEL, M., RODGERS, J., DE KONING, H. P. & THOMAS, S. A. 2009. Pentamidine movement across the murine blood-brain and blood-cerebrospinal fluid barriers: effect of trypanosome infection, combination therapy, P-glycoprotein, and multidrug resistance-associated protein. *J Pharmacol Exp Ther,* 329**,** 967-77.

SANDERSON, L., KHAN, A. & THOMAS, S. 2007. Distribution of suramin, an antitrypanosomal drug, across the blood-brain and blood-cerebrospinal fluid interfaces in wild-type and P-glycoprotein transporter-deficient mice. *Antimicrob Agents Chemother,* 51**,** 3136-46.

SANDOVAL, K. E. & WITT, K. A. 2008. Blood-brain barrier tight junction permeability and ischemic stroke. *Neurobiol Dis,* 32**,** 200-19.

SANDS, M., KRON, M. A. & BROWN, R. B. 1985. Pentamidine: a review. *Rev Infect Dis,* 7**,** 625-34.

SAUER, S. W., OPP, S., MAHRINGER, A., KAMINSKI, M. M., THIEL, C., OKUN, J. G., FRICKER, G., MORATH, M. A. & KOLKER, S. 2010. Glutaric aciduria type I and methylmalonic aciduria: simulation of cerebral import and export of accumulating neurotoxic dicarboxylic acids in in vitro models of the blood-brain barrier and the choroid plexus. *Biochim Biophys Acta,* 1802**,** 552-60.

SAUNDERS, N. R., EK, C. J., HABGOOD, M. D. & DZIEGIELEWSKA, K. M. 2008. Barriers in the brain: a renaissance? *Trends Neurosci,* 31**,** 279-86.

SBAA, E., FRERART, F. & FERON, O. 2005. The double regulation of endothelial nitric oxide synthase by caveolae and caveolin: a paradox solved through the study of angiogenesis. *Trends Cardiovasc Med,* 15**,** 157-62.

SCHERBAKOV, N., SANDEK, A., MARTENS-LOBENHOFFER, J., KUNG, T., TURHAN, G., LIMAN, T., EBINGER, M., VON HAEHLING, S., BODE-BOGER, S. M., ENDRES, M. & DOEHNER, W. 2012. Endothelial dysfunction of the peripheral vascular bed in the acute phase after ischemic stroke. *Cerebrovasc Dis,* 33**,** 37-46.

SCHINKEL, A. H. & JONKER, J. W. 2003. Mammalian drug efflux transporters of the ATP binding cassette (ABC) family: an overview. *Adv Drug Deliv Rev,* 55**,** 3-29.

SCHMIDT, K., KLATT, P. & MAYER, B. 1994. Uptake of nitric oxide synthase inhibitors by macrophage RAW 264.7 cells. *Biochem J,* 301 (Pt 2)**,** 313-6.

SCHMIDT, K., LIST, B. M., KLATT, P. & MAYER, B. 1995. Characterization of neuronal amino acid transporters: uptake of nitric oxide synthase inhibitors and implication for their biological effects. *J Neurochem,* 64**,** 1469-75.

SCHNEEBERGER, E. E. & LYNCH, R. D. 2004. The tight junction: a multifunctional complex. *Am J Physiol Cell Physiol,* 286**,** C1213-28.

SCHNITZER, J. E., OH, P. & MCINTOSH, D. P. 1996. Role of GTP hydrolysis in fission of caveolae directly from plasma membranes. *Science,* 274**,** 239-42.

SCHRAM, M. T., CHATURVEDI, N., SCHALKWIJK, C., GIORGINO, F., EBELING, P., FULLER, J. H. & STEHOUWER, C. D. 2003. Vascular risk factors and markers of endothelial function as determinants of inflammatory markers in type 1 diabetes: the EURODIAB Prospective Complications Study. *Diabetes Care,* 26**,** 2165-73.

SELLEY, M. L. 2003. Increased concentrations of homocysteine and asymmetric dimethylarginine and decreased concentrations of nitric oxide in the plasma of patients with Alzheimer's disease. *Neurobiol Aging,* 24**,** 903-7.

SHEPRO, D. & MOREL, N. M. 1993. Pericyte physiology. *FASEB J,* 7**,** 1031-8.

SHIN, K., FOGG, V. C. & MARGOLIS, B. 2006. Tight junctions and cell polarity. *Annu Rev Cell Dev Biol,* 22**,** 207-35.

SHIN, S., MOHAN, S. & FUNG, H. L. 2011. Intracellular L-arginine concentration does not determine NO production in endothelial cells: implications on the "L-arginine paradox". *Biochem Biophys Res Commun,* 414**,** 660-3.

SHIN, W. W., FONG, W. F., PANG, S. F. & WONG, P. C. 1985. Limited blood-brain barrier transport of polyamines. *J Neurochem,* 44**,** 1056-9.

SIMARRO, P. P., DIARRA, A., RUIZ POSTIGO, J. A., FRANCO, J. R. & JANNIN, J. G. 2011. The human African trypanosomiasis control and surveillance programme of the World Health Organization 2000-2009: the way forward. *PLoS Negl Trop Dis,* 5**,** e1007.

SIMARRO, P. P., FRANCO, J., DIARRA, A., POSTIGO, J. A. & JANNIN, J. 2012. Update on field use of the available drugs for the chemotherapy of human African trypanosomiasis. *Parasitology***,** 1-5.

SIMIONESCU, M., GHINEA, N., FIXMAN, A., LASSER, M., KUKES, L., SIMIONESCU, N. & PALADE, G. E. 1988. The cerebral microvasculature of the rat: structure and luminal surface properties during early development. *J Submicrosc Cytol Pathol,* 20**,** 243-61.

SIMON, A., PLIES, L., HABERMEIER, A., MARTINE, U., REINING, M. & CLOSS, E. I. 2003. Role of neutral amino acid transport and protein breakdown for substrate supply of nitric oxide synthase in human endothelial cells. *Circ Res,* 93**,** 813-20.

SIMPSON, I. A., APPEL, N. M., HOKARI, M., OKI, J., HOLMAN, G. D., MAHER, F., KOEHLER-STEC, E. M., VANNUCCI, S. J. & SMITH, Q. R. 1999. Blood-brain barrier glucose transporter: effects of hypo- and hyperglycemia revisited. *J Neurochem,* 72**,** 238-47.

SIMPSON, I. A., CARRUTHERS, A. & VANNUCCI, S. J. 2007. Supply and demand in cerebral energy metabolism: the role of nutrient transporters. *J Cereb Blood Flow Metab,* 27**,** 1766-91.

SIROEN, M. P., TEERLINK, T., NIJVELDT, R. J., PRINS, H. A., RICHIR, M. C. & VAN LEEUWEN, P. A. 2006. The clinical significance of asymmetric dimethylarginine. *Annu Rev Nutr,* 26**,** 203-28.

SISO, S., JEFFREY, M. & GONZALEZ, L. 2010. Sensory circumventricular organs in health and disease. *Acta Neuropathol,* 120**,** 689-705.

SLOAN, J. L., GRUBB, B. R. & MAGER, S. 2003. Expression of the amino acid transporter ATB 0+ in lung: possible role in luminal protein removal. *Am J Physiol Lung Cell Mol Physiol,* 284**,** L39-49.

SLOAN, J. L. & MAGER, S. 1999. Cloning and functional expression of a human Na(+) and Cl(-)-dependent neutral and cationic amino acid transporter B(0+). *J Biol Chem,* 274**,** 23740-5.

SMITH, C. L., ANTHONY, S., HUBANK, M., LEIPER, J. M. & VALLANCE, P. 2005. Effects of ADMA upon gene expression: an insight into the pathophysiological significance of raised plasma ADMA. *PLoS Med,* 2**,** e264.

SMITH, M., OMIDI, Y. & GUMBLETON, M. 2007. Primary porcine brain microvascular endothelial cells: biochemical and functional characterisation as a model for drug transport and targeting. *J Drug Target,* 15**,** 253-68.

SMITH, M. W. & GUMBLETON, M. 2006. Endocytosis at the blood-brain barrier: from basic understanding to drug delivery strategies. *J Drug Target,* 14**,** 191-214.

SOFRONIEW, M. V. & VINTERS, H. V. 2010. Astrocytes: biology and pathology. *Acta Neuropathol,* 119**,** 7-35.

SPECTOR, R. 2009. Nutrient transport systems in brain: 40 years of progress. *J Neurochem,* 111**,** 315-20.

SPERANDEO, M. P., BORSANI, G., INCERTI, B., ZOLLO, M., ROSSI, E., ZUFFARDI, O., CASTALDO, P., TAGLIALATELA, M., ANDRIA, G. & SEBASTIO, G. 1998. The gene encoding a cationic amino acid transporter (SLC7A4) maps to the region deleted in the velocardiofacial syndrome. *Genomics,* 49**,** 230-6.

SPINDLER, V., SCHLEGEL, N. & WASCHKE, J. 2010. Role of GTPases in control of microvascular permeability. *Cardiovasc Res,* 87**,** 243-53.

STAMATOVIC, S. M., KEEP, R. F., WANG, M. M., JANKOVIC, I. & ANDJELKOVIC, A. V. 2009. Caveolae-mediated internalization of occludin and claudin-5 during CCL2-induced tight junction remodeling in brain endothelial cells. *J Biol Chem,* 284**,** 19053-66.

STANEK, A., GADOWSKA-CICHA, A., GAWRON, K., WIELKOSZYNSKI, T., ADAMEK, B., CIESLAR, G., WICZKOWSKI, A. & SIERON, A. 2008. Role of nitric oxide in physiology and pathology of the gastrointestinal tract. *Mini Rev Med Chem,* 8**,** 1549-60.

STOLL, J., WADHWANI, K. C. & SMITH, Q. R. 1993. Identification of the cationic amino acid transporter (System y+) of the rat blood-brain barrier. *J Neurochem,* 60**,** 1956-9.

STRAZIELLE, N. & GHERSI-EGEA, J. F. 2005. Factors affecting delivery of antiviral drugs to the brain. *Rev Med Virol,* 15**,** 105-33.

STRIJDOM, H., CHAMANE, N. & LOCHNER, A. 2009. Nitric oxide in the cardiovascular system: a simple molecule with complex actions. *Cardiovasc J Afr,* 20**,** 303-10.

STUHLINGER, M. C., TSAO, P. S., HER, J. H., KIMOTO, M., BALINT, R. F. & COOKE, J. P. 2001. Homocysteine impairs the nitric oxide synthase pathway: role of asymmetric dimethylarginine. *Circulation,* 104**,** 2569-75.

SUD, N., WELLS, S. M., SHARMA, S., WISEMAN, D. A., WILHAM, J. & BLACK, S. M. 2008. Asymmetric dimethylarginine inhibits HSP90 activity in pulmonary arterial endothelial cells: role of mitochondrial dysfunction. *Am J Physiol Cell Physiol,* 294**,** C1407-18.

SUZUKI, M., SUZUKI, H., SUGIMOTO, Y. & SUGIYAMA, Y. 2003. ABCG2 transports sulfated conjugates of steroids and xenobiotics. *J Biol Chem,* 278**,** 22644-9.

SYDOW, K. & MUNZEL, T. 2003. ADMA and oxidative stress. *Atheroscler Suppl,* 4**,** 41-51.

SYDOW, K., SCHWEDHELM, E., ARAKAWA, N., BODE-BOGER, S. M., TSIKAS, D., HORNIG, B., FROLICH, J. C. & BOGER, R. H. 2003. ADMA and oxidative stress are responsible for endothelial dysfunction in hyperhomocyst(e)inemia: effects of L-arginine and B vitamins. *Cardiovasc Res,* 57**,** 244-52.

TADDEI, A., GIAMPIETRO, C., CONTI, A., ORSENIGO, F., BREVIARIO, F., PIRAZZOLI, V., POTENTE, M., DALY, C., DIMMELER, S. & DEJANA, E. 2008. Endothelial adherens junctions control tight junctions by VE-cadherin-mediated upregulation of claudin-5. *Nat Cell Biol,* 10**,** 923-34.

TAI, L. M., LOUGHLIN, A. J., MALE, D. K. & ROMERO, I. A. 2009a. P-glycoprotein and breast cancer resistance protein restrict apical-to-basolateral permeability of human brain endothelium to amyloid-beta. *J Cereb Blood Flow Metab,* 29**,** 1079-83.

TAI, L. M., LOUGHLIN, A. J., MALE, D. K. & ROMERO, I. A. 2009b. P-glycoprotein and breast cancer resistance protein restrict apical-to-basolateral permeability of human brain endothelium to amyloid-beta. *J Cereb Blood Flow Metab*.

TAI, L. M., REDDY, P. S., LOPEZ-RAMIREZ, M. A., DAVIES, H. A., MALE, D. K., LOUGHLIN, A. J. & ROMERO, I. A. 2009c. Polarized P-glycoprotein expression by the immortalised human brain endothelial cell line, hCMEC/D3, restricts apical-to-basolateral permeability to rhodamine 123. *Brain Res,* 1292**,** 14-24.

TAIN, Y. L. & BAYLIS, C. 2007. Determination of dimethylarginine dimethylaminohydrolase activity in the kidney. *Kidney Int,* 72**,** 886-9.

TAMAI, I., SENMARU, M., TERASAKI, T. & TSUJI, A. 1995. Na(+)- and Cl(-)-dependent transport of taurine at the blood-brain barrier. *Biochem Pharmacol,* 50**,** 1783-93.

TEERLINK, T., LUO, Z., PALM, F. & WILCOX, C. S. 2009. Cellular ADMA: regulation and action. *Pharmacol Res,* 60**,** 448-60.

THIEL, V. E. & AUDUS, K. L. 2001. Nitric oxide and blood-brain barrier integrity. *Antioxid Redox Signal,* 3**,** 273-8.

THOMPSON, J. P. & DEBINSKI, W. 1999. Mutants of interleukin 13 with altered reactivity toward interleukin 13 receptors. *J Biol Chem,* 274**,** 29944-50.

TODA, N., AYAJIKI, K. & OKAMURA, T. 2009. Cerebral blood flow regulation by nitric oxide: recent advances. *Pharmacol Rev,* 61**,** 62-97.

TODA, N. & OKAMURA, T. 2003. The pharmacology of nitric oxide in the peripheral nervous system of blood vessels. *Pharmacol Rev,* 55**,** 271-324.

TORRENTS, D., ESTEVEZ, R., PINEDA, M., FERNANDEZ, E., LLOBERAS, J., SHI, Y. B., ZORZANO, A. & PALACIN, M. 1998. Identification and characterization of a membrane protein (y+L amino acid transporter-1) that associates with 4F2hc to encode the amino acid transport activity y+L. A candidate gene for lysinuric protein intolerance. *J Biol Chem,* 273**,** 32437-45.

TOUSOULIS, D., BOGER, R. H., ANTONIADES, C., SIASOS, G., STEFANADI, E. & STEFANADIS, C. 2007. Mechanisms of disease: L-arginine in coronary atherosclerosis--a clinical perspective. *Nat Clin Pract Cardiovasc Med,* 4**,** 274-83.

TOWBIN, H., STAEHELIN, T. & GORDON, J. 1979. Electrophoretic transfer of proteins from polyacrylamide gels to nitrocellulose sheets: procedure and some applications. *Proc Natl Acad Sci U S A,* 76**,** 4350-4.

TRAN, C. T., FOX, M. F., VALLANCE, P. & LEIPER, J. M. 2000. Chromosomal localization, gene structure, and expression pattern of DDAH1: comparison with DDAH2 and implications for evolutionary origins. *Genomics,* 68**,** 101-5.

TRAN, C. T., LEIPER, J. M. & VALLANCE, P. 2003. The DDAH/ADMA/NOS pathway. *Atheroscler Suppl,* 4**,** 33-40.

TRIPATHY, D., YIN, X., SANCHEZ, A., LUO, J., MARTINEZ, J. & GRAMMAS, P. 2010. Cerebrovascular expression of proteins related to inflammation, oxidative stress and neurotoxicity is altered with aging. *J Neuroinflammation,* 7**,** 63.

TSIKAS, D., BOGER, R. H., SANDMANN, J., BODE-BOGER, S. M. & FROLICH, J. C. 2000. Endogenous nitric oxide synthase inhibitors are responsible for the L-arginine paradox. *FEBS Lett,* 478**,** 1-3.

UTEPBERGENOV, D. I., MERTSCH, K., SPORBERT, A., TENZ, K., PAUL, M., HASELOFF, R. F. & BLASIG, I. E. 1998. Nitric oxide protects blood-brain barrier in vitro from hypoxia/reoxygenation-mediated injury. *FEBS Lett,* 424**,** 197-201.

UTTARA, B., SINGH, A. V., ZAMBONI, P. & MAHAJAN, R. T. 2009. Oxidative stress and neurodegenerative diseases: a review of upstream and downstream antioxidant therapeutic options. *Curr Neuropharmacol,* 7**,** 65-74.

VALLANCE, P. & LEIPER, J. 2002. Blocking NO synthesis: how, where and why? *Nat Rev Drug Discov,* 1**,** 939-50.

VALLANCE, P., LEONE, A., CALVER, A., COLLIER, J. & MONCADA, S. 1992a. Accumulation of an endogenous inhibitor of nitric oxide synthesis in chronic renal failure. *Lancet,* 339**,** 572-5.

VALLANCE, P., LEONE, A., CALVER, A., COLLIER, J. & MONCADA, S. 1992b. Endogenous dimethylarginine as an inhibitor of nitric oxide synthesis. *J Cardiovasc Pharmacol,* 20 Suppl 12**,** S60-2.

VAN NIEUWENHOVE, S. 1992. Advances in sleeping sickness therapy. *Ann Soc Belg Med Trop,* 72 Suppl 1**,** 39-51.

VAN WINKLE, L. J. & CAMPIONE, A. L. 1990. Functional changes in cation-preferring amino acid transport during development of preimplantation mouse conceptuses. *Biochim Biophys Acta,* 1028**,** 165-73.

VAN WINKLE, L. J., CHRISTENSEN, H. N. & CAMPIONE, A. L. 1985. Na+-dependent transport of basic, zwitterionic, and bicyclic amino acids by a broad-scope system in mouse blastocysts. *J Biol Chem,* 260**,** 12118-23.

VAN ZWIETEN, E. J., RAVID, R., SWAAB, D. F. & VAN DE WOUDE, T. 1988. Immunocytochemically stained vasopressin binding sites on blood vessels in the rat brain. *Brain Res,* 474**,** 369-73.

VANDER BORGHT, S., VAN PELT, J., VAN MALENSTEIN, H., CASSIMAN, D., RENARD, M., VERSLYPE, C., LIBBRECHT, L. & ROSKAMS, T. A. 2008. Up-regulation of breast cancer resistance protein expression in hepatoblastoma following chemotherapy: A study in patients and in vitro. *Hepatol Res,* 38**,** 1112-21.

VANWERT, A. L., GIONFRIDDO, M. R. & SWEET, D. H. 2010. Organic anion transporters: discovery, pharmacology, regulation and roles in pathophysiology. *Biopharm Drug Dispos,* 31**,** 1-71.

VARATHARAJAN, L. & THOMAS, S. A. 2009. The transport of anti-HIV drugs across blood-CNS interfaces: summary of current knowledge and recommendations for further research. *Antiviral Res,* 82**,** A99-109.

VEKONY, N., WOLF, S., BOISSEL, J. P., GNAUERT, K. & CLOSS, E. I. 2001. Human cationic amino acid transporter hCAT-3 is preferentially expressed in peripheral tissues. *Biochemistry,* 40**,** 12387-94.

VERREY, F., CLOSS, E. I., WAGNER, C. A., PALACIN, M., ENDOU, H. & KANAI, Y. 2004. CATs and HATs: the SLC7 family of amino acid transporters. *Pflugers Arch,* 447**,** 532-42.

VINCENT, I. M., CREEK, D., WATSON, D. G., KAMLEH, M. A., WOODS, D. J., WONG, P. E., BURCHMORE, R. J. & BARRETT, M. P. 2010. A molecular mechanism for eflornithine resistance in African trypanosomes. *PLoS Pathog,* 6**,** e1001204.

WAGNER, C. A., LANG, F. & BROER, S. 2001. Function and structure of heterodimeric amino acid transporters. *Am J Physiol Cell Physiol,* 281**,** C1077-93.

WANBY, P., TEERLINK, T., BRUDIN, L., BRATTSTROM, L., NILSSON, I., PALMQVIST, P. & CARLSSON, M. 2006. Asymmetric dimethylarginine (ADMA) as a risk marker for stroke and TIA in a Swedish population. *Atherosclerosis,* 185**,** 271-7.

WANG, C. C. 1995. Molecular mechanisms and therapeutic approaches to the treatment of African trypanosomiasis. *Annu Rev Pharmacol Toxicol,* 35**,** 93-127.

WANG, D., GILL, P. S., CHABRASHVILI, T., ONOZATO, M. L., RAGGIO, J., MENDONCA, M., DENNEHY, K., LI, M., MODLINGER, P., LEIPER, J., VALLANCE, P., ADLER, O., LEONE, A., TOJO, A., WELCH, W. J. & WILCOX, C. S. 2007. Isoform-specific regulation by N(G),N(G)-dimethylarginine dimethylaminohydrolase of rat serum asymmetric dimethylarginine and vascular endothelium-derived relaxing factor/NO. *Circ Res,* 101**,** 627-35.

WANG, D., STRANDGAARD, S., BORRESEN, M. L., LUO, Z., CONNORS, S. G., YAN, Q. & WILCOX, C. S. 2008. Asymmetric dimethylarginine and lipid peroxidation products in early autosomal dominant polycystic kidney disease. *Am J Kidney Dis,* 51**,** 184-91.

WANG, D., STRANDGAARD, S., IVERSEN, J. & WILCOX, C. S. 2009. Asymmetric dimethylarginine, oxidative stress, and vascular nitric oxide synthase in essential hypertension. *Am J Physiol Regul Integr Comp Physiol,* 296**,** R195-200.

WANG, J., SIM, A. S., WANG, X. L. & WILCKEN, D. E. 2006. L-arginine regulates asymmetric dimethylarginine metabolism by inhibiting dimethylarginine dimethylaminohydrolase activity in hepatic (HepG2) cells. *Cell Mol Life Sci,* 63**,** 2838-46.

WANG, L. Y., ZHANG, D. L., ZHENG, J. F., ZHANG, Y., ZHANG, Q. D. & LIU, W. H. 2011a. Apelin-13 passes through the ADMA-damaged endothelial barrier and acts on vascular smooth muscle cells. *Peptides,* 32**,** 2436-43.

WANG, Q., LIANG, B., SHIRWANY, N. A. & ZOU, M. H. 2011b. 2-Deoxy-D-glucose treatment of endothelial cells induces autophagy by reactive oxygen species-mediated activation of the AMP-activated protein kinase. *PLoS One,* 6**,** e17234.

WATSON, C. P., DOGRUEL, M., MIHOREANU, L., BEGLEY, D. J., WEKSLER, B. B., COURAUD, P. O., ROMERO, I. A. & THOMAS, S. A. 2012. The transport of nifurtimox, an anti-trypanosomal drug, in an in vitro model of the human blood-brain barrier: evidence for involvement of breast cancer resistance protein. *Brain Res,* 1436**,** 111-21.

WEISS, J., ROSE, J., STORCH, C. H., KETABI-KIYANVASH, N., SAUER, A., HAEFELI, W. E. & EFFERTH, T. 2007. Modulation of human BCRP (ABCG2) activity by anti-HIV drugs. *J Antimicrob Chemother,* 59**,** 238-45.

WEKSLER, B. B., SUBILEAU, E. A., PERRIERE, N., CHARNEAU, P., HOLLOWAY, K., LEVEQUE, M., TRICOIRE-LEIGNEL, H., NICOTRA, A., BOURDOULOUS, S., TUROWSKI, P., MALE, D. K., ROUX, F., GREENWOOD, J., ROMERO, I. A. & COURAUD, P. O. 2005. Blood-brain barrier-specific properties of a human adult brain endothelial cell line. *FASEB J,* 19**,** 1872-4.

WHITE, M. F. 1985. The transport of cationic amino acids across the plasma membrane of mammalian cells. *Biochim Biophys Acta,* 822**,** 355-74.

WHITE, M. F. & CHRISTENSEN, H. N. 1982. Cationic amino acid transport into cultured animal cells. II. Transport system barely perceptible in ordinary hepatocytes, but active in hepatoma cell lines. *J Biol Chem,* 257**,** 4450-7.

WHITE, M. F., GAZZOLA, G. C. & CHRISTENSEN, H. N. 1982. Cationic amino acid transport into cultured animal cells. I. Influx into cultured human fibroblasts. *J Biol Chem,* 257**,** 4443-9.

WHITEMAN, M., HOOPER, D. C., SCOTT, G. S., KOPROWSKI, H. & HALLIWELL, B. 2002. Inhibition of hypochlorous acid-induced cellular toxicity by nitrite. *Proc Natl Acad Sci U S A,* 99**,** 12061-6.

WHO 2009. Secretariat Progress Report [Control of African trypanosomiasis]. *(http://apps.who.int/gb/ebwha/pdf_files/EB126/B126_38-en.pdf)*.

WHO, D. O. C. O. N. T. D. O. 2010. Human African trypanosomiasis: number of new cases drops to historically low level in 50 years. *http://www.who.int/neglected_diseases/integrated_media/integrated_media_hat_june_2010/en/index.html*.

WIESINGER, H. 2001. Arginine metabolism and the synthesis of nitric oxide in the nervous system. *Prog Neurobiol,* 64**,** 365-91.

WILHELM, I., FAZAKAS, C. & KRIZBAI, I. A. 2011. In vitro models of the blood-brain barrier. *Acta Neurobiol Exp (Wars),* 71**,** 113-28.

WILKINSON, I. B., QASEM, A., MCENIERY, C. M., WEBB, D. J., AVOLIO, A. P. & COCKCROFT, J. R. 2002. Nitric oxide regulates local arterial distensibility in vivo. *Circulation,* 105**,** 213-7.

WILLIAMS, S. A., ABBRUSCATO, T. J., HRUBY, V. J. & DAVIS, T. P. 1996. Passage of a delta-opioid receptor selective enkephalin, [D-penicillamine2,5] enkephalin, across the blood-brain and the blood-cerebrospinal fluid barriers. *J Neurochem,* 66**,** 1289-99.

WOJCIAK-STOTHARD, B., TORONDEL, B., TSANG, L. Y., FLEMING, I., FISSLTHALER, B., LEIPER, J. M. & VALLANCE, P. 2007. The ADMA/DDAH pathway is a critical regulator of endothelial cell motility. *J Cell Sci,* 120**,** 929-42.

WOJCIAK-STOTHARD, B., TORONDEL, B., ZHAO, L., RENNE, T. & LEIPER, J. M. 2009. Modulation of Rac1 activity by ADMA/DDAH regulates pulmonary endothelial barrier function. *Mol Biol Cell,* 20**,** 33-42.

WOJTAL, K. A., DE VRIES, E., HOEKSTRA, D. & VAN IJZENDOORN, S. C. 2006. Efficient trafficking of MDR1/P-glycoprotein to apical canalicular plasma membranes in HepG2 cells requires PKA-RIIalpha anchoring and glucosylceramide. *Mol Biol Cell,* 17**,** 3638-50.

WOLBURG, H. & LIPPOLDT, A. 2002. Tight junctions of the blood-brain barrier: development, composition and regulation. *Vascul Pharmacol,* 38**,** 323-37.

WOLBURG, H., NOELL, S., MACK, A., WOLBURG-BUCHHOLZ, K. & FALLIER-BECKER, P. 2009. Brain endothelial cells and the glio-vascular complex. *Cell Tissue Res,* 335**,** 75-96.

WOLBURG, H., WOLBURG-BUCHHOLZ, K., KRAUS, J., RASCHER-EGGSTEIN, G., LIEBNER, S., HAMM, S., DUFFNER, F., GROTE, E. H., RISAU, W. & ENGELHARDT, B. 2003. Localization of claudin-3 in tight junctions of the blood-brain barrier is selectively lost during experimental autoimmune encephalomyelitis and human glioblastoma multiforme. *Acta Neuropathol,* 105**,** 586-92.

WOLF, S., JANZEN, A., VEKONY, N., MARTINE, U., STRAND, D. & CLOSS, E. I. 2002. Expression of solute carrier 7A4 (SLC7A4) in the plasma membrane is not sufficient to mediate amino acid transport activity. *Biochem J,* 364**,** 767-75.

XIAO, S., WAGNER, L., MAHANEY, J. & BAYLIS, C. 2001. Uremic levels of urea inhibit L-arginine transport in cultured endothelial cells. *Am J Physiol Renal Physiol,* 280**,** F989-95.

YAMAOKA, J., KABASHIMA, K., KAWANISHI, M., TODA, K. & MIYACHI, Y. 2002. Cytotoxicity of IFN-gamma and TNF-alpha for vascular endothelial cell is mediated by nitric oxide. *Biochem Biophys Res Commun,* 291**,** 780-6.

YAMAUCHI, A., DOHGU, S., NISHIOKU, T., SHUTO, H., NAITO, M., TSURUO, T., SAWADA, Y. & KATAOKA, Y. 2007. An inhibitory role of nitric oxide in the dynamic regulation of the blood-brain barrier function. *Cell Mol Neurobiol,* 27**,** 263-70.

YAMAUCHI, K., SAKURAI, H., KIMURA, T., WIRIYASERMKUL, P., NAGAMORI, S., KANAI, Y. & KOHNO, N. 2009. System L amino acid transporter inhibitor enhances anti-tumor activity of cisplatin in a head and neck squamous cell carcinoma cell line. *Cancer Lett,* 276**,** 95-101.

YANG, Z. C., WANG, K. S., WU, Y., ZOU, X. Q., XIANG, Y. Y., CHEN, X. P. & LI, Y. J. 2009. Asymmetric dimethylarginine impairs glucose utilization via ROS/TLR4 pathway in adipocytes: an effect prevented by vitamin E. *Cell Physiol Biochem,* 24**,** 115-24.

YEMISCI, M., GURSOY-OZDEMIR, Y., VURAL, A., CAN, A., TOPALKARA, K. & DALKARA, T. 2009. Pericyte contraction induced by oxidative-nitrative stress impairs capillary reflow despite successful opening of an occluded cerebral artery. *Nat Med,* 15**,** 1031-7.

YERAMIAN, A., MARTIN, L., SERRAT, N., ARPA, L., SOLER, C., BERTRAN, J., MCLEOD, C., PALACIN, M., MODOLELL, M., LLOBERAS, J. & CELADA, A. 2006. Arginine transport via cationic amino acid transporter 2 plays a critical regulatory role in classical or alternative activation of macrophages. *J Immunol,* 176**,** 5918-24.

YIN, W. H., CHEN, J. W., TSAI, C., CHIANG, M. C., YOUNG, M. S. & LIN, S. J. 2005. L-arginine improves endothelial function and reduces LDL oxidation in patients with stable coronary artery disease. *Clin Nutr,* 24**,** 988-97.

YOO, J. H. & LEE, S. C. 2001. Elevated levels of plasma homocyst(e)ine and asymmetric dimethylarginine in elderly patients with stroke. *Atherosclerosis,* 158**,** 425-30.

YUN, O., PRIOTTO, G., TONG, J., FLEVAUD, L. & CHAPPUIS, F. 2010. NECT is next: implementing the new drug combination therapy for Trypanosoma brucei gambiense sleeping sickness. *PLoS Negl Trop Dis,* 4**,** e720.

ZHANG, P., HU, X., XU, X., CHEN, Y. & BACHE, R. J. 2011. Dimethylarginine dimethylaminohydrolase 1 modulates endothelial cell growth through nitric oxide and Akt. *Arterioscler Thromb Vasc Biol,* 31**,** 890-7.

ZHARIKOV, S. I., SIGOVA, A. A., CHEN, S., BUBB, M. R. & BLOCK, E. R. 2001. Cytoskeletal regulation of the L-arginine/NO pathway in pulmonary artery endothelial cells. *Am J Physiol Lung Cell Mol Physiol,* 280**,** L465-73.

ZOCCALI, C. 2006a. Asymmetric dimethylarginine (ADMA): a cardiovascular and renal risk factor on the move. *J Hypertens,* 24**,** 611-9.

ZOCCALI, C. 2006b. Asymmetric dimethylarginine in end-stage renal disease patients: a biomarker modifiable by calcium blockade and angiotensin II antagonism? *Kidney Int,* 70**,** 2053-5.

ZOCCALI, C., MAAS, R., CUTRUPI, S., PIZZINI, P., FINOCCHIARO, P., CAMBARERI, F., PANUCCIO, V., MARTORANO, C., SCHULZE, F., ENIA, G., TRIPEPI, G. & BOGER, R. 2007. Asymmetric dimethyl-arginine (ADMA) response to inflammation in acute infections. *Nephrol Dial Transplant,* 22**,** 801-6.

ZOUGBEDE, S., MILLER, F., RAVASSARD, P., REBOLLO, A., CICERON, L., COURAUD, P. O., MAZIER, D. & MORENO, A. 2011. Metabolic acidosis induced by Plasmodium falciparum intraerythrocytic stages alters blood-brain barrier integrity. *J Cereb Blood Flow Metab,* 31**,** 514-26.

ZUZACK, J. S., TASCA, R. J. & DIZIO, S. M. 1985. Neutral amino acid transport in embryonal carcinoma cells. *J Cell Physiol,* 122**,** 379-86.

Appendices

Appendix 1

Normal accumulation buffer stocks:

BUFFER	**Conc.**	**Volume (µl)**	**Weight (g)**
NaCl	5M	675	
Hepes	1M	250	
KCl	1M	135	
$CaCl_2$ ($CaCl_2 \cdot 2H_2O$)	1M	37.5	
$MgCl_2$ ($MgCl_2 \cdot 6H_2O$)	1M	30	
TOTAL		1127.5	
Glucose			0.0045
Sterile dH_2O		23872.5	
TOTAL		25000	

Accumulation buffer consisting of sterile distilled water (dH_2O), 135mM NaCl, 10mM HEPES, 5.4mM KCL, 1.5mM $CaCl_2$, 1.2mM $MgCl_2$, 1.1mM glucose, all sterile filtered with a 0.2µm filter and purchased from Sigma Aldrich Company Ltd, Poole, UK and adjusted to pH 7.4 with 1M HCL.

Appendix 2

TGN Lysis buffer stock for cell lysates:

In a 50 ml Falcon;

2.5 ml 1M Tris

1.5 ml 5M NaCl

5 ml Glycerol

5 ml 0.5M glycerophosphate

0.5 ml Tween 20

0.1 ml NP-40 (Nonident P 40)

Fill up with dd water (35.4 ml) to get a total of 50mls and mix well.

Store in 5ml aliquots at -20°C (5mls per bijou)

TGN lysis buffer (50mM Tris, 150mM NaCl, 10% glycerol, 50mM glycerophosphate B, 1% Tween-20, 0.2% NP-40, all purchased from Sigma Aldrich Company Ltd, Poole, UK.

Appendix 3

Polyacrylamide gel stock solutions (adapted from Rachel Brown's protocol with permission):

1.5 M Tris-HCl, pH 8.8 – stored at 4°C

54.4 g Tris base (Sigma Aldrich Company Ltd, Poole, UK)

150ml dH_2O

Adjust to pH 8.8 with 1M HCl. Make to 300ml with dH_2O and store at 4°C.

0.5 M Tris-HCl, pH 6.8 – stored at 4°C

6 g Tris Base

~60ml dH_2O

Adjust to pH 6.8 with 1M HCl. Make to 100ml with dH_2O and store at 4°C.

10% APS (Sigma Aldrich Company Ltd, Poole, UK) made fresh each time – 0.1g in 1ml PBS

10% SDS (Sigma Aldrich Company Ltd, Poole, UK) 10g in 100ml dH_2O. Stored at RT.

10% separating gel recipe:

Materials	10%
dH_2O	4.426 ml
1.5 M Tris-HCl	2.5 ml
10% SDS	100µl
Acryl/Bis (40% stock solution from Merck Chemical Ltd, Nottingham, UK)	2.87 ml
10% APS	100µl
TEMED (Sigma Aldrich Company Ltd, Poole, UK)	4µl
Total Volume	**10 ml**

The above amount was enough for two separating gels on Biorad Mini-PROTEAN 3 cells.

4% stacking gel recipe:

Materials	4%
dH_2O	3.182 ml
0.5 M Tris-HCl	1.25 ml
10% SDS	50µl
Acryl/Bis	488µl
10% APS	25µl
TEMED	5µl
Total Volume	**5 ml**

The above amount was enough for two separate stacking gels on Biorad Mini-PROTEAN 3 cells.

10x Running Buffer, pH 8.3 - stored at 4°C

29.0 g Tris Base

144.0 g Glycine (Sigma Aldrich Company Ltd, Poole, UK)

10.0 g SDS (Sigma Aldrich Company Ltd, Poole, UK)

to 1 L with dH_2O

Dilute to 1x for running gels in dH_2O.

Transfer Buffer, pH 8.1-8.5 - stored at 4°C

3.025 g Tris base

14.4 g Glycine

100 ml Methanol (Sigma Aldrich Company Ltd, Poole, UK)

Add dH_2O to final volume of 1 L. pH to 8.1-8.5 and de-gas prior to first use.

PBS-Tween – 1 tablet (Merck Chemical Ltd, Nottingham, UK) in 1 L of dH_2O, automatically pH 7.4 - stored at 4°C.

Appendix 4

Na^+ and Cl^- free accumulation buffer:

BUFFER	**Conc.**	**Volume (µl)**	**Weight (g)**
Sucrose	1M	6000	
Hepes	1M	250	
$C_6H_{11}KO_7$ (Potassium-D gluconate)	1M	100	
$CaSO_4$	1M	70	
$MgSO_4 \cdot 7H_2O$	1M	25	
TOTAL		**6445**	
Glucose			0.0045
Sterile dH_2O		**18555**	
TOTAL		**25000**	

Appendix 5

PNGase F protocol.

1. Combine 1-20µg of glycoprotein, 1µl of 10X Glycoprotein Denaturing Buffer and H_2O (if necessary) to make a 10µl total reaction volume.
2. Denature glycoprotein by heating reaction at 100°C for 10 minutes in heat block.
3. Make a total reaction volume of 20µl by adding 2µl 10X G7 Reaction Buffer, 2µl 10% NP40, dH_2O and 1-2µl PNGaseF.
4. Incubate reaction at 37°C for 1 hour.

Nifurtimox publication 2012

BRAIN RESEARCH 1436 (2012) 111–121

Available online at www.sciencedirect.com

SciVerse ScienceDirect

www.elsevier.com/locate/brainres

BRAIN RESEARCH

Research Report

The transport of nifurtimox, an anti-trypanosomal drug, in an *in vitro* model of the human blood–brain barrier: Evidence for involvement of breast cancer resistance protein

Christopher P. Watson[a], Murat Dogruel[a], Larisa Mihoreanu[a], David J. Begley[a], Babette B. Weksler[b], Pierre O. Couraud[c,d,e], Ignacio A. Romero[f], Sarah A. Thomas[a,*]

[a]King's College London, Institute of Pharmaceutical Science, Waterloo, London, UK
[b]Weill Medical College of Cornell University, New York, NY, USA
[c]INSERM, U1016, Institut Cochin, Paris, France
[d]Cnrs, UMR8104, Paris, France
[e]Univ Paris Descartes, Paris, France
[f]The Open University, Department of Life Sciences, Walton Hall, Milton Keynes, UK

ARTICLE INFO

Article history:
Accepted 28 November 2011
Available online 4 December 2011

Keywords:
Human African trypanosomiasis
Blood–brain barrier
Nifurtimox
Eflornithine
Breast cancer resistance protein

ABSTRACT

Human African trypanosomiasis (HAT) is a parasitic disease affecting sub-Saharan Africa. The parasites are able to traverse the blood–brain barrier (BBB), which marks stage 2 (S2) of the disease. Delivery of anti-parasitic drugs across the BBB is key to treating S2 effectively and the difficulty in achieving this goal is likely to be a reason why some drugs require highly intensive treatment regimes to be effective. This study aimed to investigate not only the drug transport mechanisms utilised by nifurtimox at the BBB, but also the impact of nifurtimox–eflornithine combination therapy (NECT) and other anti-HAT drug combination therapies (CTs) on radiolabelled-nifurtimox delivery in an *in vitro* model of drug accumulation and the human BBB, the hCMEC/D3 cell line. We found that nifurtimox appeared to use several membrane transporters, in particular breast-cancer resistance protein (BCRP), to exit the BBB cells. The addition of eflornithine caused no change in the accumulation of nifurtimox, nor did the addition of clinically relevant doses of the other anti-HAT drugs suramin, nifurtimox or melarsoprol, but a significant increase was observed with the addition of pentamidine. The results provide evidence that anti-HAT drugs are interacting with membrane transporters at the human BBB and suggest that combination with known transport inhibitors could potentially improve their efficacy.

* Corresponding author at: King's College London, Institute of Pharmaceutical Science, Franklin-Wilkins Building, 150 Stamford Street, Waterloo, London SE1 9NH, UK. Fax: +44 207 848 4781.
E-mail address: sarah.thomas@kcl.ac.uk (S.A. Thomas).

Abbreviations: BBB, blood–brain barrier; BCRP, breast cancer resistance protein; CT, combination therapy; HAT, human African trypanosomiasis; NECT, nifurtimox–eflornithine combination therapy; S1, stage 1 of human African trypanosomiasis; S2, stage 2 of human African trypanosomiasis

0006-8993/$ – see front matter © 2011 Elsevier B.V. All rights reserved.
doi:10.1016/j.brainres.2011.11.053